Mammalian RAD23 homologs: multifunctional proteins in DNA repair and development

Thesis

To obtain the degree of doctor from the Erasmus University Rotterdam
on the authority of the Rector Magnificus Prof.dr.ir. J. H. van Bemmel
according to the decision of the Doctorate Board.

The public defence shall be held on
Wednesday, 12th September 2001 at 15.45 hrs.

by

吳美燕

Mei Yin Ng
born in Hong Kong

Doctoral Committee

Supervisors
Prof.dr. J. H. J. Hoeijmakers
Prof.dr. D. Bootsma

Other members
Prof.dr. J. A. Grootegoed
Prof.dr. B. A. Oostra
Dr. L. H. F. Mullenders

Co-supervisor
Dr. G. T. J. van der Horst

Cover design and illustrations
Tony C. C. Cheung

Lay-out
Inês Chaves

© J.M.Y. Ng. 2001

The work presented in this thesis was performed at the MGC-Department of Cell Biology & Genetics, Centre for Biomedical Genetics, Erasmus University Rotterdam, The Netherlands.

Mammalian RAD23 homologs: multifunctional proteins in DNA repair and development

De RAD23 homologen in zoogdieren:
multifunctionele eiwitten in DNA herstel en ontwikkeling

Proefschrift

Ter verkrijging van de graad van doctor
aan de Erasmus Universiteit Rotterdam
op gezag van de Rector Magnificus Prof.dr.ir. J. H. van Bemmel
en volgens besluit van het College voor Promoties.

De openbare verdediging zal plaatsvinden op
woensdag 12 september 2001 om 15:45 uur

door

吳美燕

Mei Yin Ng
geboren te Hong Kong

Promotiecommissie

Promotoren
Prof.dr. J. H. J. Hoeijmakers
Prof.dr. D. Bootsma

Overige leden
Prof.dr. J. A. Grootegoed
Prof.dr. B. A. Oostra
Dr. L. H. F. Mullenders

Copromotor
Dr. G. T. J. van der Horst

Grafisch ontwerp en illustraties
Tony C. C. Cheung

Lay-out
Inês Chaves

© J.M.Y. Ng. 2001

Dit proefschrift kwam tot stand binnen de vakgroep Celbiologie & Genetica van de faculteit der Geneeskunde en Gezondheidswetenschappen van de Erasmus Universiteit Rotterdam. De vakgroep maakt deel uit van het Medisch Genetisch Centrum Zuid-West Nederland en de onderzoeksschool Center for Biomedical Genetics.

Learn as if you would live forever,
but live as if you would die tomorrow.

給爸爸和媽媽

For **Tony**

Contents

Abbreviations

aa	amino acid
ATP	adenosine triphosphate
BER	base excision repair
BRCA1	breast cancer susceptibility gene 1
CEN2	centrin 2/caltractin 1
CS	Cockayne syndrome
CSA and CSB	Cockayne syndrome A and B proteins
CPD	cyclobutane pyrimidine dimer
(c)DNA	(copy) deoxyribonucleic acid
E.coli	*Escherichia coli*
EGFP	enhanced green fluorescent protein variant
ERCC	human excision repair cross complementing gene
FRAP	fluorescence redistribution after photobleaching
GFP	green fluorescent protein
GGR or GG-NER	global genome (nucleotide excision) repair
HA	histidine-hemagglutinin
hHR23A and B	human homolog of *S.cerevisiae* repair proteins RAD23 A and B
mHR23A and B	mouse homolog of *S.cerevisiae* repair proteins RAD23 A and B
(m)RNA	(messenger) ribonucleic acid
MEFs	mouse embryonic fibroblasts
MMR	mismatch repair
NER	nucleotide excision repair
PCNA	proliferating cell nuclear antigen
Pol δ/ε	polymerase δ/ε
6-4 PP	(6-4) pyrimidine-pyrimidone photoproduct
RAD23	*Saccharomyces cerevisiae* DNA repair protein RAD23
RNAP II	RNA polymerase II
RPA	replication factor A
S.cerevisiae	*Saccharomyces cerevisiae*
S.pombe	*Saccharomyces pombe*
ssDNA	single-stranded DNA
TCR or TC-NER	transcription-coupled (nucleotide excision) repair
TFIIH	transcription factor IIH
TTD	trichothiodystrophy
UBA	ubiquitin-associated domain
UbL	ubiquitin-like domain
UDS	unscheduled DNA synthesis
UV	ultraviolet light
(UV)DDB	(UV-light) DNA damage binding protein
XAB2	XPA binding protein 2
XP	xeroderma pigmentosum
XPA to XPG	xeroderma pigmentosum groups A to G

Chapter

I

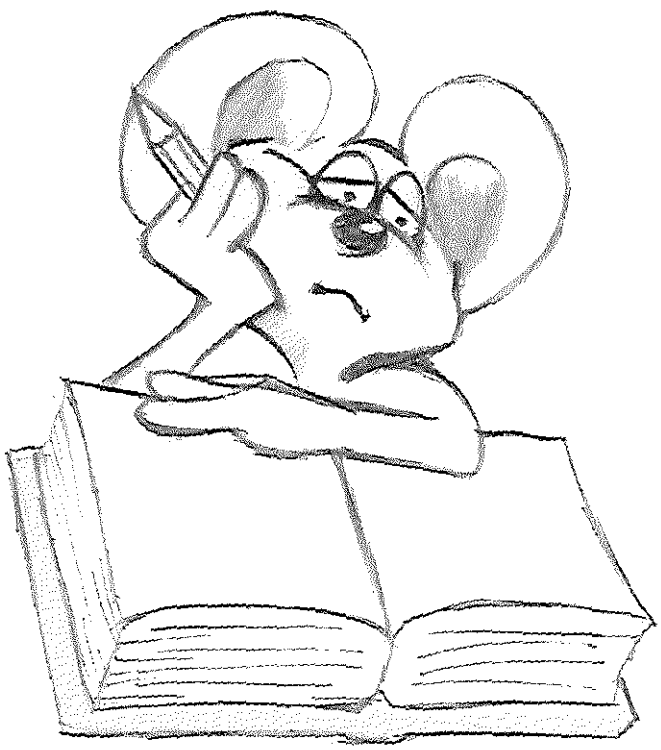

I.1 Introduction

Preservation of an intact genome is of utmost importance to all living organisms. However, the integrity of DNA, the carrier of genetic information required for proper functioning of cellular processes, is continuously challenged. Cells must overcome endogenous (metabolic) and exogenous (environmental) threats, as well as the intrinsic instability of chemical bonds in DNA itself (e.g. deamination and depurination). Oxidative stress, ultraviolet (UV) light, ionizing radiation (X-rays), and numerous chemicals induce a wide variety of lesions in the DNA. DNA damage can affect cellular processes and can have severe consequences for human health. Its direct effect at the cellular level is inhibition of vital processes like transcription and replication resulting in cell cycle arrest. Accumulation of lesions in DNA above certain thresholds can lead either to (programmed) cell death by apoptosis or to permanent alterations in the genetic code (mutations). These mutations can in turn cause changes in metabolic processes, inborn defects or overall functional decline contributing to premature aging. Mutations, specifically in proto-oncogenes and tumor suppressor genes, are directly responsible for tumor initiation and subsequent progression of the multistep process of carcinogenesis.

To guard the vital genetic information and prevent the harmful consequences of DNA damage, an intricate network of genome caretaking systems has evolved (schematically depicted in Figure 1). Multiple DNA repair processes and cell cycle control mechanisms constitute an important component of this genome protection network. For a comprehensive review of DNA damage and the intricate network of DNA repair systems in general, the interested reader is referred to Friedberg, Walker, and Siede (1995) and Hoeijmakers (2001).

I.2 DNA repair mechanisms

The progression from DNA damage to mutagenesis and ultimately carcinogenesis can be interrupted if a cell is able to recognize and efficiently remove or correct the DNA damage. DNA double strand breaks induced by ionizing radiation, stalled replication forks or incomplete recombination events can be repaired by homologous recombination or non-homologous end-joining (Kanaar et al. 1998; van Gent et al. 2001). Incorporations of inappropriate nucleotides and small (1-5 nucleotides) insertions/deletions introduced during DNA replication are repaired by mismatch repair (MMR). Chemically adducted DNA is repaired by excision of the lesion via base excision repair (BER) or nucleotide excision repair (NER). BER corrects base

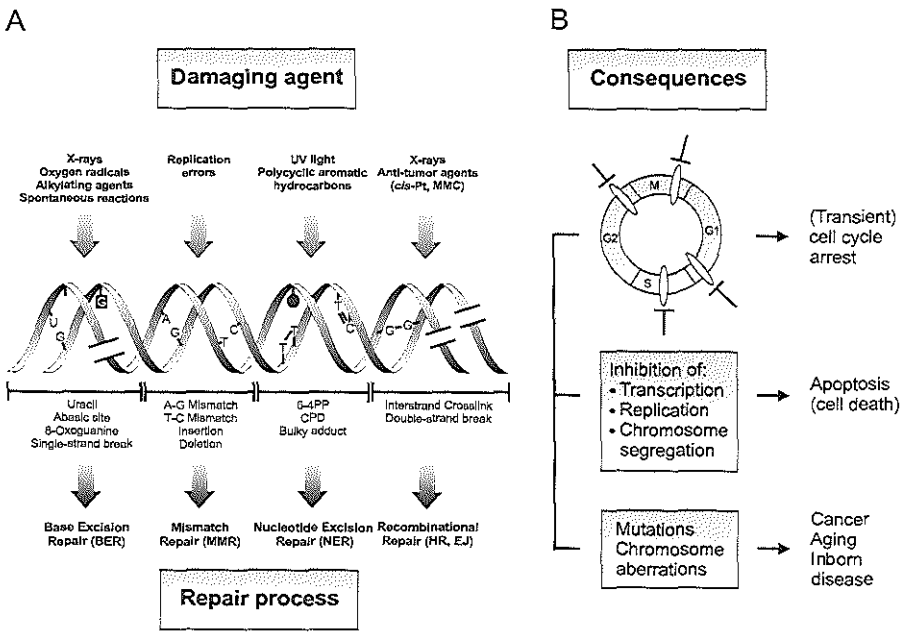

Figure 1. DNA damage, repair mechanisms and consequences. **(A)** Common DNA damaging agents (top); examples of DNA lesions induced by these agents (middle); and most relevant DNA repair mechanism responsible for the removal of lesions (bottom). **(B)** Acute effects of DNA damage on cell cycle progression, leading to transient arrest in the G1, S, G2, and M phases (top), and on DNA metabolism (middle). Long-term consequences of DNA injury (bottom) include permanent changes in the DNA sequence (point mutations affecting single genes or chromosome aberrations which may involve multiple genes) and their biological effects. Abbreviations: *cis*-Pt and MMC, cisplatin and mitomycin C, respectively (both DNA-crosslinking agents); 6-4PP and CPD, 6-4 photoproduct and cyclobutane pyrimidine dimer, respectively (both induced by UV light); HR, homologous recombination; EJ, end joining. Adapted from De Laat (PhD thesis 1998) and Hoeijmakers (2001).

alterations induced by endogenous or exogenous oxidative events, ionizing radiation and small alkylating agents (Seeberg et al. 1995). Examples of potentially mutagenic BER-lesions are 8-oxoguanine, O^6-methylguanine, deaminated methylated cytosine and thymine glycol. Accumulating evidence implicates unrepaired BER lesions in the aging process of somatic cells (Martin et al. 1996). NER, the repair mechanism studied in this thesis, is responsible for the removal of numerous helix-distorting DNA lesions, among which UV-induced cis-syn-cyclobutane pyrimidine dimers (CPDs) and pyrimidine (6-4) pyrimidone photoproducts (6-4PPs) are extensively

studied (de Laat et al. 1999). The NER system, which will be described in more detail in the next chapter, excises the damage as a short, single strand DNA fragment and replaces it with a newly synthesized DNA coded for by the strand opposite the lesion. Other important consequences of DNA damage include arrest of cell cycle progression at specific points in G1, S, G2, and M phases, to allow repair of the lesions before damage is fixed into mutations. Finally, when the damage is too severe to be adequately repaired, the cell may undergo apoptosis or enter an irreversible senescence-like state (Kastan 1997).

The importance of DNA repair is highlighted by the clinical features of three inherited human syndromes caused by a deficiency in NER: xeroderma pigmentosum (XP), Cockayne syndrome (CS), and trichothiodystrophy (TTD) (emphasized in the next chapter and also reviewed in Bootsma et al. 2001). Extreme sensitivity to sunlight is the hallmark of all three syndromes. In addition, distinctive features characterize each disorder. XP patients show mainly UV-induced cutaneous symptoms (including photosensitivity, pigmentation abnormalities) and predisposition to skin cancer, and carcinogen-induced internal tumors (Kraemer et al. 1984). In some cases accelerated neurologic degeneration due to increased neuronal death is observed. In contrast, CS and TTD patients do not exhibit an obvious cancer predisposition, but suffer from severe physical and mental abnormalities. Sulfur-deficient brittle hair and dystrophic nails, and ichthyosis (scaling of the skin) are the additional typical traits of TTD.

I.3 Aim of the thesis

The work described in this thesis aims to provide insight into the molecular mechanism of NER in mammals, particularly the function of the mammalian RAD23 repair proteins, HR23A and HR23B. Specific attention was given to (i) investigation of the relationship of HR23A/B with other repair factors, most notably XPC, (ii) generation and functional characterization of *HR23A* and *HR23B* knockout mice, (iii) involvement of HR23A/B in development, and (iv) aspects of HR23A/B within the ubiquitin/proteasome protein degradation system.

Chapter II reviews the current literature on mammalian NER mechanisms and the clinical symptoms associated with XP, CS and TTD. In addition, NER-deficient mouse models and the phenotypical consequence of the role of NER proteins in DNA repair, transcription and other cellular processes are discussed. **Chapter III** describes the functional redundancy

of the mammalian RAD23 proteins in stimulating the repair activity of XPC *in vitro*. **Chapter IV** focuses on the primary damage recognition protein complex XPC-HR23B in global genome repair. The generation and characterization of the mouse models for *HR23A* and *HR23B* are presented in **Chapters V** and **VI**.

I.4 References

Bootsma D, Kraemer KH, Cleaver JE, and Hoeijmakers JHJ (2001). Nucleotide excision repair syndromes: xeroderma pigmentosum, Cockayne syndrome, and trichothiodystrophy. *In:* Scriver CR, Beaudet, AL, Sly, WS, Valle, D Vogelstein and Kinzler (eds) The Metabolic and Molecular Bases of Inherited Disease, McGraw-Hill Book Co, New York *1*, 677-703.

de Laat WL, Jaspers NG, and Hoeijmakers JHJ (1999). Molecular mechanism of nucleotide excision repair. Genes Dev *13*, 768-785.

Friedberg EC, Walker GC, and Siede W (1995). DNA repair and mutagenesis. ASM Press, Washington DC.

Hoeijmakers JHJ (2001). Genome maintenance mechanisms for preventing cancer. Nature *411*, 366-374.

Kanaar R, Hoeijmakers JHJ, and van Gent DC (1998). Molecular mechanisms of DNA double strand break repair. Trends Cell Biol *8*, 483-489.

Kastan MB (1997). Checkpoint controls and cancer. Plantview, NY: Cold Spring Harbor Laboratory Press.

Kraemer KH, Lee MM, and Scotto J (1984). DNA repair protects against cutaneous and internal neoplasia: evidence from xeroderma pigmentosum. Carcinogenesis *5*, 511-514.

Martin GM, Austad SN, and Johnson TE (1996). Genetic analysis of ageing: role of oxidative damage and environmental stresses. Nat Genet *13*, 25-34.

Seeberg E, Eide L, and Bjoras M (1995). The base excision repair pathway. Trends Biochem Sci *20*, 391-397.

van Gent DC, Hoeijmakers JHJ, and Kanaar R (2001). Chromosomal stability and the DNA double-stranded break connection. Nat Rev Genet *2*, 196-206.

Chapter

II

II.1 Introduction

Nucleotide excision repair (NER) functions to maintain the integrity of the genome and thereby avoid cellular dysfunctioning including cancer. This mechanism to remove DNA damage is evolutionary conserved throughout eukaryotes, with basic similarities even extending to prokaryotes. It counteracts the deleterious effects of a plethora of structurally unrelated DNA lesions, including damage induced by sunlight and cigarette smoke. Some of the lesions eliminated by NER are CPDs and 6-4PPs, which are the two major types of damage induced by the shortwave UV-B component (290-320 nm) of sunlight in human skin (Friedberg et al. 1995). This explains why patients with inherited deficiencies in the NER process display marked hypersensitivity to sun exposure. Other substrates for NER include bulky chemical adducts (caused e.g. by polycyclic aromatic hydrocarbons like N-2-acetylaminofluorene-AAF (2-AAF) and benzo[a]pyrene (B[a]P) found in tobacco smoke, car exhaust fumes and industrial pollution) and intrastrand crosslinks (generated e.g. by anticancer drugs such as cisplatin and psoralens). Recently, oxygen free-radical-induced helix distorting 5',8-purine cyclodeoxynucleotides have also been identified as important substrates for NER (Kuraoka et al. 2000). The common feature of the wide spectrum of lesions repaired by NER is a significant distortion of the DNA helix. Both helical distortion and alteration of DNA chemistry are necessary for recognition by the NER machinery (Hess et al. 1997). NER has also been implicated as a back-up system for BER in the repair of smaller base damages induced by alkylating and oxidizing agents which are usually less distorting (Satoh et al. 1993; Satoh and Lindahl 1994). The high versatility of the NER mechanism explains how a variety of endogenous and exogenous genotoxic agents may contribute to the large spectrum of clinical symptoms associated with defects in one of the NER components.

II.2 Mammalian NER proteins and molecular mechanisms

In NER, DNA lesions are removed by a multistep "cut and patch"-like reaction mechanism. The NER process involves about 20-30 proteins (presented in Figure 1) and consists of several successive steps of DNA damage recognition, local opening of the DNA double helix, and incision of the damaged strand on either side of the lesion. After excision of the damage-containing oligonucleotide the resulting gap is filled by DNA repair synthesis, followed by strand ligation (Aboussekhra et al. 1995; de Laat et al. 1999; Wood 1999).

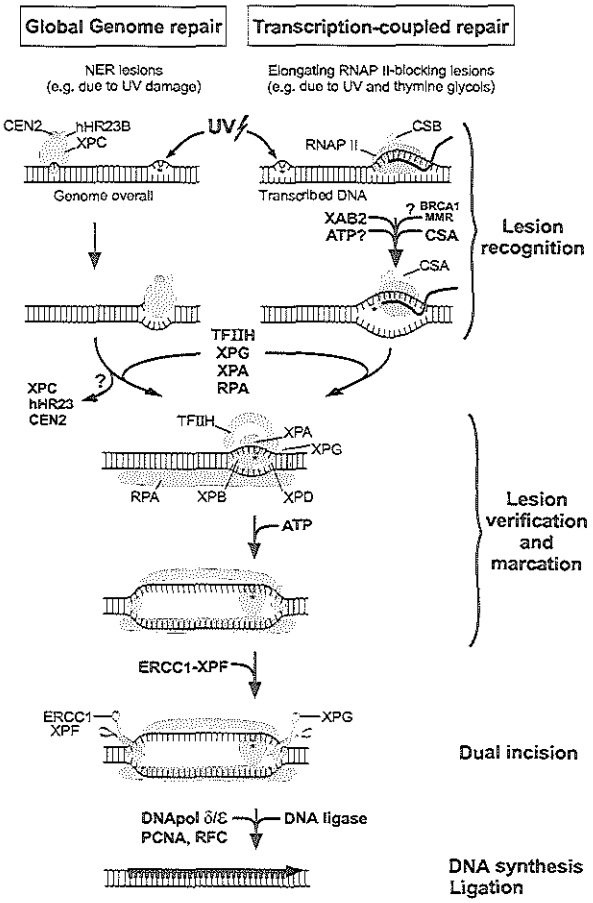

Figure 1. Model for mechanism of global genome nucleotide excision repair (NER) and transcription-coupled repair. Helix-distorting NER lesions are identified by the initial damage detector XPC-hHR23B-CEN2 in global genome repair (GGR), leading to partial opening of the DNA helix. Elongating RNA polymerase II (RNAP II) initiates transcription-coupled repair (TCR). CSA, CSB, XAB2, and probably other (co)factors (such as MMR (Leadon and Avrutskaya 1998) and BRCA1 (Gowen et al. 1998)) participate in the further processing of stalled RNAP II making the damage accessible to repair and subsequent resumption of transcription. The subsequent stages of GGR and TCR may be identical. The coordinated action of TFIIH, XPG, XPA, and RPA mediates the formation of an unwound intermediate around the lesion. XPB and XPD helicase components of TFIIH catalyze ATP-dependent unwinding, whereas XPA and RPA stabilize the open complex and position the other factors. The presence of XPG is required for the stabilization of a fully opened complex. Dual incision is performed by ERCC1-XPF and XPG structure-specific endonucleases, which cleave the damaged strand 5' and 3' of the lesion, respectively. The lesion is released as part of a ~30mer oligonucleotide. Gap filling DNA synthesis by the replication machinery followed by ligation completes the NER. * indicates a DNA lesion. III in bold indicates newly synthesized DNA. Model adapted from De Laat (PhD thesis 1998) and Hoeijmakers (2001).

Eukaryotic NER involves at least two distinct subpathways for damage detection: global genome repair (GGR or GG-NER) and transcription-coupled repair (TCR or TC-NER). The GG-NER subpathway safeguards the entire genome. Its efficiency is lesion-dependent; for instance, the highly helix-distorting 6-4PPs are repaired 5-fold faster than CPDs in human cells *in vivo* (Mitchell and Nairn 1989). In contrast, TC-NER preferentially accounts for the fast removal of damage in the transcribed strand of active genes. TC-NER is necessary to release blocks to RNA polymerase II (RNAP II) driven transcription (Bohr et al. 1985; Mellon et al. 1987). Unlike GG-NER, the TC-NER subpathway eliminates different lesions at similar rates (van Hoffen et al. 1995) and may contribute to the rapid recovery of transcriptional activity after DNA damage (Hanawalt and Mellon 1993; Friedberg 1996). Both GG-NER and TC-NER are mechanistically the same, except for the initial damage recognition step.

The biological relevance of mammalian NER has been well documented, because several human genetic disorders, including XP, CS, and TTD, are associated with impaired NER activity. XP is due to a mutation in one of seven genes (designated *XPA* to *XPG*). CS is caused by a defect in the *CSA* or *CSB* genes, and TTD by a defect in the *TTDA* gene. In addition, specific mutations in three XP genes (*XPB*, *XPD*, and *XPG*) can cause a combination of XP and CS, whereas mutations in *XPB* and *XPD* can also give rise to the photosensitive form of TTD (for review, see Bootsma et al. 2001). Unlike most forms of XP and TTD which are deficient in both subpathways of NER, patients belonging to XP group C and group E have defective GG-NER, whereas TC-NER still functions normally (Venema et al. 1990b and 1991; Hwang et al. 1999; Tang et al. 2000). In contrast, defective TC-NER, but functional GG-NER is specifically associated with CS (van Hoffen et al. 1995; Venema et al. 1990a). In addition, complementation analysis has revealed another class of XP patients (XP-variant). A mutation in the responsible gene (*XPV*) does not cause impairment of NER but leads to defective postreplication repair (which is a damage-tolerance mechanism). *XPV* was recently cloned and was identified as the gene encoding hRad30A, which is the damage-specific DNA polymerase η involved in translesion synthesis (Masutani et al. 1999).

The key NER genes have been identified and the core reaction has been reconstituted *in vitro* using purified proteins and DNA substrates containing site-specific or random damage (Aboussekhra et al. 1995; Wood 1999; de Laat et al 1999). In short: the molecular mechanism of NER involves two major steps: (i) lesion recognition and incision of the DNA strand containing the lesion and (ii) gap filling replicative DNA synthesis to

restore the undamaged DNA. In mammalian cells, six core components are necessary for damage recognition and dual incision in *in vitro* GG-NER reactions: the XPC-hHR23B complex, XPA, the heterotrimeric RPA protein (additionally involved in DNA replication and recombination), the multiprotein transcription factor IIH (TFIIH, with dual involvement in basal transcription initiation and in NER), and the endonucleases XPG and ERCC1-XPF (ERCC1 stands for excision repair cross complementation group 1) (see Figure 1). In the gap filling step of DNA repair synthesis, replication factor C (RFC), proliferating cell nuclear antigen (PCNA), RPA, DNA polymerase δ or ε holoenzyme, and DNA ligase I are involved (Araujo et al. 2000). Table 1 lists all mammalian NER genes cloned to date and summarizes their main properties. These steps are discussed *in extenso* below.

II.2.1 Damage recognition (XPC-hHR23B and probably XPE)

The GG-NER reaction primarily starts with recognition of the DNA injury. This initial, damage-recognizing step is mediated by the XPC-hHR23B protein complex (which consists of the XP group C gene product and the human homolog of the *Saccharomyces cerevisiae* RAD23B protein (Masutani et al. 1994; Shivji et al. 1994). The complex formation is required for efficient repair activity of XPC *in vitro* (Sugasawa et al. 1996 and 1997; Batty et al. 2000), at least in part due to the stabilization of XPC by hHR23B (Araki et al. 2001). The heterodimer has high affinity for both single- and double-stranded undamaged DNA but even higher affinity when DNA lesions are present (Masutani et al. 1994; Shivji et al. 1994). XPC-hHR23B is the only NER factor shown to make stable footprints around a lesion, such as 6-4PP (Sugasawa et al. 1998). Since locally melted DNA precludes the need for XPC-hHR23B (Mu and Sancar 1997), the XPC-hHR23B complex is thought to increase single-strandedness at the site of the DNA injury, so that other NER core proteins can bind (reviewed in de Laat et al. 1999; Wood 1999; Wood et al. 2001). After binding DNA, XPC-hHR23B recruits the entire repair protein machinery to the injury (Sugasawa et al. 1998 and also discussed in Chapter 4; Yokoi et al. 2000; Volker et al. 2001). In a subset of XPE patients, the NER deficiency is caused by a mutation in the UV-damaged DNA binding protein (UV-DDB). Cells from these patients lack UV-DDB activity (Chu and Chang 1988; Keeney et al. 1992). The UV-DDB protein is composed of two subunits: p125 (or DDB1) and p48 (or DDB2, carrying the causative XPE mutations). UV-DDB is not essential for NER *in vitro* (Aboussekhra et al. 1995; Rapic

Table 1. Main properties of cloned human NER genes

Gene*	Chromosome Location	Protein Size (aa)	Yeast Homolog	Protein Properties
XPA	9q34	273	*RAD14*	Zn^{2+}-finger, binds different types of damaged DNA, transient interaction with ERCC1, RPA and TFIIH complex.
XPB (ERCC3)	2q21	782	*RAD25*	3' → 5' DNA helicase, subunit of TFIIH, essential for transcription initiation.
XPC	3p25.1	940	*RAD4*	Complexed with hHR23B, strong damage-specific DNA binding, involved in global genome repair only, initiator of global genome repair.
XPD (ERCC2)	19q13.3 §	760	*RAD3*	5' → 3' DNA helicase, subunit of TFIIH, essential for transcription initiation.
XPE	11p11-12	427	Identified ¶	Binds UV-damaged DNA, causative mutations identified in p48, WD-repeat containing protein, complexed with p125 UV-DDB protein.
XPF (ERCC4)	16p13.1-13.2	~905	*RAD1*	Also identical to ERCC11, complex with ERCC1 makes 5' incision, Y structure-specific endonuclease, dual function in recombination.
XPG (ERCC5)	13q32.3-33.1	1186	*RAD2*	Y structure-specific endonuclease, makes 3' incision.
CSA (ERCC8)	5	396	*RAD28*	5 WD-repeats, involved in transcription-coupled repair only.
CSB (ERCC6)	10q11	1493	*RAD26*	DNA-dependent ATPase, involved in transcription-coupled repair only, present in (elongating) RNA polymerase II complex.
ERCC1	19q13.3 §	297	*RAD10*	Partial homology to *E.coli* NER protein UvrC and many nucleases, complex with XPF makes 5' incision Y structure-specific endonuclease, dual function in recombination.
hHR23A	19p13.1	363	*RAD23*	Ubiquitin-like N-terminus, 2 ubiquitin-associated domains.
hHR23B	9q32-33	409	*RAD23*	As hHR23A, fraction of hHR23B complexed with XPC, complex binds ssDNA and is involved in global genome repair only.
p62 ^{TFIIH}	11p14-15.1	548	*TFB1*	Subunit of TFIIH, essential for transcription initiation.
p52 ^{TFIIH}	6p21.3	513	*TFB2*	Subunit of TFIIH, essential for transcription initiation.
p44 ^{TFIIH}	5q1.3	395	*SSL1*	DNA-binding Zn^{2+}-finger, subunit of TFIIH, essential for transcription initiation.
P34 ^{TFIIH}	12	303	*TFB4*	Zn^{2+}-finger, subunit of TFIIH, essential for transcription initiation.

* Not included in this table are the genes encoding proteins involved in the DNA synthesis step of the NER reaction, such as the proteins PCNA, RPA, RFC, DNA ligase; aa: amino acids; § The *ERCC1* and *XPD (ERCC2)* genes are located less than 20 kb apart; ¶ A yeast gene encoding a product with clear overall homology to the XPE protein has been identified in the yeast genome database. In addition, a second human gene with significant similarity to *XPE* has been discovered (Van der Spek and Hoeijmakers, unpublished results). Table adapted from Bootsma *et al.* (2001).

Otrin et al. 1998). This heterodimer may assist in damage recognition of lesions for which XPC-hHR23B has a low binding affinity, such as CPDs (Keeney et al. 1993; Hwang et al. 1999), or it may facilitate DNA repair in the context of chromatin structure (Otrin et al. 1997; Datta et al. 2001). However, the precise role for UV-DDB in DNA repair remains unknown.

XPA, like XPC, preferentially binds damaged DNA (Jones and Wood 1993), particularly in a single-stranded context (Buschta-Hedayat et al. 1999). XPA is known to also bind to RPA, TFIIH and ERCC1-XPF endonuclease (Nagai et al. 1995; Park et al. 1995; Saijo et al. 1996; Araujo et al. 2000). Recently it has been shown that XPA is involved in the post-recognition steps of the NER pathway, to verify the presence of damage and to organize the binding of the repair machinery with the assistance of the single-strand DNA binding protein complex RPA (Sugasawa et al. 1998; Volker et al. 2001).

II.2.2 Steps specific for GG-NER (XPC-hHR23B) and TC-NER (RNAP II, CSA and CSB)

XPC-hHR23B and probably UV-DDB (XPE) are the only repair proteins that are specifically involved in GG-NER but are dispensable for TC-NER. The XPC protein has low, but significant sequence homology with the yeast RAD4 protein (Legerski and Peterson 1992; Masutani et al. 1994). However, *rad4* null mutants, in contrast to *XPC* mutants, are defective in both GG-NER and TC-NER (Verhage et al. 1994). This may reflect a fundamental difference between mammals and yeast.

The hHR23B protein sequence includes an N-terminal ubiquitin-like domain (Masutani et al. 1994). Other proteins that contain this ubiquitin-like domain are thought to function as chaperones. Hence this domain may perform a similar function in assembling the XPC-hHR23B complex. Thus far, none of the known human NER syndromes has been associated with mutations in the *hHR23B* gene. A simple explanation might be that the highly homologous hHR23A protein (with 57% identity and 76% similarity) can substitute for hHR23B function. Consistent with that hypothesis, both hHR23 proteins are functionally interchangeable in their ability to form a complex with XPC and stimulate its repair activity *in vitro* (Sugasawa et al. 1997, see also Chapter III). However, in contrast to this hypothesis, *in vivo* XPC-hHR23B complexes predominate and only trace amounts of hHR23A copurify with XPC (Araki 2001). Instead of functional redundancy, another way to explain the lack of NER-disorder related mutations in the human HR23 genes is that the gene products are essential

(Chapters V and VI). In line with this, the 60 amino acid XPC-binding domain of hHR23B is sufficient for XPC stimulation (Masutani 1997). Furthermore, only a fraction of the cellular hHR23B is complexed with XPC at any given time; the majority of hHR23B exists in a free form *in vivo*, like hHR23A (van der Spek et al. 1996; Sugasawa et al. 1996). Together, these observations suggest that the hHR23 proteins have additional functions outside NER and it is possible that these functions are essential to life.

In TC-NER, it is believed that the elongating RNAP II complex encounters a lesion and activates the TCR pathway in a CSA/CSB-dependent manner (Hanawalt 1994). The CSA and CSB proteins may function to facilitate recruitment of repair factors and make the lesions accessible by displacing the stalled polymerase. After damage recognition by RNAP II, the lesion is removed by the core NER reaction (see Figure 1). The CSA protein contains a consensus sequence of five so-called WD-repeats, which appear to have more of a regulatory rather than a catalytic function. WD-repeats are common to proteins involved in multiprotein complexes which play diverse roles in cellular metabolism, including cell cycle regulation, RNA processing and gene regulation (Henning et al. 1995). CSB (or ERCC6) is a member of the SWI/SNF family of DNA-dependent ATPases which have been implicated in a wide range of nuclear processes, including transcription regulation, chromatin remodeling, and diverse DNA repair processes like NER, postreplication and recombination repair (Troelstra et al. 1992; Eisen et al. 1995). *In vitro*, CSA, CSB and the p44 subunit of TFIIH show interactions (Henning et al. 1995). CSA associates with XAB2 (XPA binding protein 2), a protein involved in TC-NER and in transcription (Nakatsu et al. 2000). In addition, CSB and RNAP II interact *in vivo* (van Gool et al. 1997a), consistent with a role for CS proteins in processing of a stalled RNAP II complex. However, the precise function of CSA and CSB in TC-NER remains unclear. Besides their role in NER, the CS proteins may act to bridge DNA repair systems (e.g. TCR and BER) (van Oosterwijk et al. 1996; Cooper et al. 1997; Le Page et al. 2000) .

II.2.3 Open complex formation and lesion demarcation (XPA, RPA, XPB, XPD and XPG)

The next common step in NER is the formation of an open complex, which requires local unwinding of the DNA helix and demarcation of the lesion. This is an ATP-dependent process (Evans et al. 1997a). XPC-hHR23B and TFIIH are essential at the earliest step of helix opening (Evans et al. 1997a). The helicases of the TFIIH complex mediate the ATP-dependent melting of

the DNA around the lesion. DNA unwinding by the XPB and XPD helicase subunits of TFIIH may be facilitated by RPA (Wold 1997). In NER, RPA probably binds to the single-stranded region of the undamaged strand with a defined polarity and stabilizes the structure (de Laat et al. 1998). The optimal binding patch of RPA is 30 nucleotides (Kim et al. 1992), which is similar to the size of the fully opened repair complex (~25 nucleotides) and the size of the released damage-containing oligonucleotide (Huang and Sancar 1994). XPA and XPG are also required for the formation of the open complex. XPG likely has a structural function by stabilizing the preincision complex, since its nuclease activity is not needed for opening (Evans et al. 1997b; Mu et al. 1997).

The basal transcription factor TFIIH is a nine-subunit, multifunctional protein complex harboring helicase and protein kinase activities. The p89 and p80 subunits correspond to the previously identified XPB and XPD NER helicases (Schaeffer et al. 1993; Schaeffer et al. 1994), and are essential for NER (Evans et al. 1997b; Winkler et al. 2000). They contain ATPase-dependent 3' → 5' (XPB) and 5' → 3' (XPD) DNA unwinding activity. TFIIH is essential for local unwinding of the DNA helix around the lesion in NER (Evans et al. 1997b) and in the transcription initiation by RNAP II at the promoter (Holstege et al. 1996). In line with the crucial role of TFIIH in basal transcription, inactivation of the *XPB* and *XPD* genes in the mouse is incompatible with life (de Boer et al. 1998b; Weeda et al. manuscript in preparation). XPB has an essential function in transcription initiation, and its helicase activity is required for promoter opening and stimulatory for promoter escape (Bradsher et al. 2000; Tirode et al. 1999). In contrast, XPD catalytic activity is dispensable for *in vitro* transcription (Tirode et al. 1999; Winkler et al. 2000) and was shown to play a structural role in promoter escape (Bradsher et al. 2000). Additional TFIIH components include cyclin dependent kinase Cdk7, cyclin H and MAT1, together constituting the cdk-activating kinase (CAK) complex associated with TFIIH. The CAK complex is able to phosphorylate cyclin-dependent kinases (CDKs) involved in cell cycle regulation, and is essential for phosphorylation of the C-terminal domain of RNAP II during transcription initiation (Nigg 1995; Svejstrup et al. 1995). Although the CAK complex is associated with TFIIH, it occurs also in a free form and is not essential for NER *in vitro* (Svejstrup et al. 1995; Mu et al. 1996; Araujo et al. 2000). In addition to a role in NER and transcription, TFIIH interacts directly with p53 (tumor suppressor gene involved in checkpoint control) (Leveillard et al. 1996; O'Donovan et al. 1994), suggesting that TFIIH is also involved in cell cycle regulation and apoptosis.

II.2.4 Dual incision (ERCC1-XPF and XPG)

After local unwinding and demarcation of the lesion, a single strand fragment of DNA 24-32 nucleotides long and containing the damage, is excised. This process requires the structure-specific endonuclease activities of XPG at the 3' side of the open complex (O'Donovan et al. 1994) followed by the ERCC1/XPF complex 5' to the damage (Sijbers et al. 1996). Both structure-specific nucleases cleave at the junctions between duplex and single-stranded DNA in a partially melted DNA. The 3' incision by XPG is made first and can be detected in the absence of ERCC1-XPF (Mu et al. 1996). In contrast, ERCC1/XPF requires the physical presence, but not the catalytic activity of XPG to perform the 5' incision, suggesting an additional structural role for XPG (Mu et al. 1997; Wakasugi et al. 1997). In theory, both nucleases can incise the undamaged strand. However, the cleavage activity of ERCC1-XPF is coordinated by RPA, which plays an important role in positioning both nucleases. The 3' side of RPA stimulates ERCC1-XPF whereas the 5'-oriented end inhibits endonuclease specificity of ERCC1-XPF (de Laat et al. 1998). Although RPA and XPG interact directly, RPA alone is not sufficient to confer strand specificity to XPG (de Laat et al. 1998). The strong interaction between XPG and TFIIH (Iyer et al. 1996) may instead serve to confer strand selectivity to XPG-mediated cleavage (de Laat et al. 1999).

II.2.5 Gap filling and ligation (RPA, RFC, PCNA, pol δ/ε, and DNA ligase I)

The final step in the NER reaction is gap filling of the excised patch by DNA synthesis. This step is often used to measure NER activity *in vitro* and *in vivo* (i.e. unscheduled DNA synthesis (UDS)). Gap filling synthesis requires the mammalian DNA replication factors RPA, RFC, PCNA, and DNA polymerase δ and ε for an efficient repair synthesis (Nichols and Sancar 1992; Shivji et al. 1992 and 1995). PCNA stimulates DNA polymerase δ and/or ε in DNA replication. DNA synthesis is followed by sealing of the remaining nick by ligation of the newly synthesized DNA, most likely by DNA ligase I, since mutations in the gene causes UV-hypersensitivity (Barnes et al. 1992).

II.3 NER in living cells

In order to study the NER reaction *in vivo*, confocal laser-scanning microscopy has been recently adapted to the measurement of the mobility

of repair factors in single living cells. This novel approach is based on the analysis of functional NER proteins fused to green fluorescence protein (GFP, cloned from the jellyfish *Aequorea vitoria*) stably expressed in human fibroblasts (Houtsmuller et al. 1999). GFP-tagged molecules can be monitored for long periods of time because of the photostability of GFP. The GFP protein tag rarely affects the function and localization of the fusion protein. Experiments with GFP-tagged molecules demonstrated that most proteins move freely within the compartments of the cell by ATP-independent diffusion (Partikian et al. 1998). There is no clear size limit for free diffusion *in vivo*, because even large protein complexes such as the proteasome can move freely through the cytoplasm and the nucleus (Reits et al. 1997). Thus, utilization of GFP tags enables the application of fluorescence redistribution after photobleaching (FRAP) technology. In FRAP, fluorescent molecules in a small area of the cell are irreversibly photobleached by a high-powered focused laser beam (Houtsmuller et al. 1999; Reits and Neefjes 2001). FRAP experiments permit measurement of the mobility of a fluorescent molecule in a defined compartment of the cell. Furthermore, FRAP can also be used to address a number of questions regarding protein localization, activity, protein interactions, conformational changes and cell cycle fluctuations.

The mobility of the fusion protein ERCC1-GFP-XPF in the nucleus was studied using FRAP. In the absence of DNA damage, the ERCC1-GFP-XPF complex was found to diffuse rapidly in the nucleus with a diffusion coefficient (12 ± 5 square micrometers per second) consistent with its molecular weight, arguing against the idea that ERCC1 is part of a NER holocomplex (Svejstrup et al. 1995). UV-induced DNA damage caused a fraction of the ERCC1-GFP-XPF molecules to become temporarily immobilized, likely due to engagement of the complex in repair events. After 4 minutes, the complex regained the mobility characteristic for ERCC1 in undamaged cells. On the basis of these data, a model was proposed in which individual NER proteins assemble at the site of DNA damage rather than being organized in a preassembled NER supercomplex ("repairosome"). The same model was supported by studies of Volker and coworkers (2001) with the novel technique of local UV-irradiation combined with fluorescent antibody labeling. Moreover, ERCC1-GFP-XPF seems to identify the damaged site not by a processive mechanism (DNA-scanning) but in a distributive fashion by diffusion and collision with the other repair components (Houtsmuller et al. 1999). However, it is not known whether DNA damage detection in GG-NER by XPC-hHR23B (Sugasawa et al. 1998) occurs via a processive mechanism. In TC-NER, damage detection by RNAP

II (Hanawalt et al. 1994) is by its nature processive, and actual repair in this NER subpathway could take place at the nuclear matrix where transcription also occurs (Mullenders et al. 1984; Jackson et al. 1994).

II.4 Connection between NER and p53

In addition to the direct involvement of NER factors in transcription, NER is tightly connected to cell cycle progression via p53-dependent and p53-independent pathways following the accumulation of (UV-induced) DNA damage (Levine 1997). To complicate matters further, the p53 protein may play a role in modulating DNA repair (Ford et al. 1998). Moreover, p53 physically interacts with some of the NER components (Wang et al. 1995 and 1996). DNA damage interfering with RNAP II driven transcription triggers p53 response (Ljungman et al. 1999). This in turn is believed to cause temporary cell cycle arrest, allowing the cell time to repair the DNA damage before replication (Kastan et al. 1991). If the DNA damage is too severe and p53 accumulation is sustained, the cell undergoes apoptosis (Lowe et al. 1993). To further study the roles of NER and *p53*-deficiency in mutagenesis and tumorigenesis, mice with a completely defective NER can be crossed with *p53* knockout mice (Jacks et al. 1994). An example of this approach (i.e. $XPA^{-/-}$ mice (de Vries et al. 1995) crossed with *p53*-deficient mice) is described in section II.6.

II.5 Human NER deficiency syndromes

In humans, NER constitutes a major defense mechanism against the carcinogenic effects of sunlight. The biological consequences of a defect in one of the NER proteins are apparent from three rare autosomal recessive photosensitive diseases: XP, CS and TTD. Several of the NER proteins participate in nuclear processes outside NER. For example, all genes associated with TTD (*XPB*, *XPD*, and *TTDA* (Vermeulen et al. 2000)) are also implicated in basal transcription. The ERCC1-XPF complex has a dual involvement in repair of interstrand crosslinks probably via mitotic recombination. The notion of function sharing has important implications for the clinical consequences of inherited mutations in the NER proteins. The spectrum of clinical symptoms differs considerably between the three human NER syndromes (summarized in Table 2 and also reviewed in Bootsma et al. 2001) and many of the peculiar abnormalities of CS and TTD

Table 2. Main clinical symptoms of human NER syndromes

Clinical symptoms	*XP*[#]	*XP/CS*	*CS*	*TTD*
Cutaneous				
Photosensitivity	++	++	+*	+*
Pigmentation abnormalities	++	+	-	-
Skin cancer	++	+	-	-
Brittle hair and nails	-	-	-	+
Icthyosis	-	-	-	+
Developmental				
Growth defect	-	+	+	+
Hypogonadism	-	+	+	+
Neurologic				
Progressive mental degeneration	+/-	+	+	+
Degeneration				
Wizened face	-	+	+	+
Primary defect:				
Neuronal loss	+	-	-	-
Neurodysmyelination	+	+	+	+
Cellular				
UDS (% of control)	5-50%	5-50%	Normal	5-50%
UV-sensitivity	++	++	+	+/±

#Does not include the XP-Variant form.
*Also CS and TTD patients exist without photosensitivity and NER defect.
Table adapted from Bootsma *et al.* (2001).

are difficult to attribute directly to defective NER, e.g. the neurologic abnormalities due to dysmyelination and the brittle hair seen in TTD. Ultraviolet sensitive (UVS) syndrome is yet another clinical disorder distinct from XP, CS, and XP-V. Similar to NER patients, subjects with UVS do have a sun-sensitive skin (Itoh et al. 1995). UV-exposure causes an irreversible inhibition of transcription in UVS cells, however, the level of UDS is normal. These features are grossly reminiscent of CS and some XPD patients (Jaspers and Bootsma, unpublished results). The available observations support the notion that the XP, CS, and TTD syndromes are biochemically intimately connected and may be part of a broad clinical continuum. Mouse models of NER deficiencies have been generated (discussed in the next section), which provide excellent tools for understanding the complex relationship between DNA repair defects and their clinical consequences.

II.5.1 Xeroderma pigmentosum (XP)

Parchment skin (xeroderma) and freckles (pigmentosum) are the prominent cutaneous hallmarks of XP patients. These manifestations are strikingly restricted to sun-exposed areas of their skin. Typically, sun exposure of XP patients causes a progressive degenerative alteration of the skin and eyes (Bootsma et al. 2001), beginning as early as the age of 2 years (Kraemer 1997). Furthermore, XP is associated with an elevated frequency (>1000-fold) of sunlight-induced skin cancers, which are also largely confined to sun-exposed areas like the face, neck, head and even the tip of the tongue. XP patients mainly develop basal cell or squamous cell carcinomas (SCCs, seen in at least 45% of all XP patients, many of whom often have multiple primary neoplasms), and less frequently melanomas (5% of patients). The mean age of onset for skin neoplasms is 8 years, which is about 50 years earlier than in the general population (Kraemer 1997). The main cause of death in XP individuals is neoplasia, which reduces the lifespan by approximately 30 years. XP patients also have a 10- to 20-fold increased risk of developing several types of internal cancers before the age of 20 years (Kraemer et al. 1984). Abnormalities in the immune system, detected in XP patients (but not in CS and TTD), are likely to contribute to the development of (skin) tumors (Morison et al. 1985; Mariani et al. 1992).

A fraction of XP patients (~18%) displays progressive neurologic degeneration secondary to a loss of neurons. This feature seems to be related to the significance of the NER defect. For example XPC patients, who only have GG-NER defect, usually do not develop neurologic abnormalities, and if so, symptoms appear much later in life compared to TC-NER-defective XPD and completely NER-deficient XPA patients (Bootsma et al. 2001). A possible explanation for the onset of neurologic abnormalities in XP individuals is that defective DNA repair of endogenous, oxidative NER lesions in neurons triggers cell death (Kuraoka et al. 2000).

The genetic heterogeneity of XP patients is accompanied by heterogeneity in severity of the repair defect and of the consequent symptoms. The most severely affected patients are XPA, XPB, XPD and XPG individuals. The two most common forms of XP are XPA and XPC (Bootsma et al. 2001). The group of XPD patients is the most heterogeneous, with a level of residual repair synthesis between 15 and >50% (Matsumura et al. 1998). Furthermore, XPF patients are moderately UV-sensitive and show intermediate repair synthesis, indicative of mutations that lead to poor but not complete abolishment of NER. This could be due to the anticipated dual function of the ERCC1-XPF complex in NER and recombination repair (Davies et al. 1995; De Silva et al. 2000). A null allele for ERCC1 or XPF and

the consequential defect in crosslink repair are predicted to be incompatible with life. All XP patients of complementation groups A to G are defective in both NER subpathways, with the exception of XPC and XPE whose NER defect is limited to GG-NER (Hwang et al. 1998; Venema et al. 1990b). The susceptibility to sunburn of XPC patients is no different from normal individuals, indicating that TC-NER alone is sufficient to prevent this acute response to UV-exposure (Berg et al. 2000; van Oosten et al. 2000). *XPC* cells have a residual UDS level of 15-30% due to functional TC-NER and are therefore less sensitive to UV than *XPA* or *XPD* cells (Bootsma et al. 2001). Patients in the XP-variant group have mild to severe skin symptoms and usually display a normal functioning central nervous system. Unlike classical XP, XPV patients show a normal level of NER activity but lack the capacity to efficiently replicate damaged DNA leading to error prone replication and a hypermutable phenotype. This phenotype, together with the increased frequencies of genomic rearrangements observed in *XPV* cells (Limoli et al. 2000), may cause the elevated sun-induced carcinogenesis seen in these patients.

II.5.2 Cockayne syndrome (CS)

CS is a very pleiotropic disorder characterized by cutaneous photosensitivity (with or without thin or dry skin and hair), severe postnatal growth failure (cachectic dwarfism), mental retardation, and progressive neurologic dysfunction (extensively reviewed in Nance and Berry 1992; Bootsma et al. 2001). CS cells are sensitive to a number of DNA-damaging agents (including UV) due to a defect in TC-NER. In contrast to patients suffering from the prototype NER-deficient disorder XP, CS individuals are not predisposed to skin cancer. Other common CS symptoms include sensorineural hearing loss, progressive ocular abnormalities (such as pigmentary retinopathy and/or cataracts), wizened bird-like faces, impaired sexual development, skeletal abnormalities (typically resulting in short stature), dental caries, kyphosis (hunchback), and premature osteoporosis (demineralization). The progressive neurological degeneration has a very early onset in CS individuals (beginning around 2 years of age) and is caused by dysmyelination. The mean age of death in CS is 12.5 years and mainly secondary to pneumonia, which in turn could be due to the generally poor condition of the patients (Nance and Berry 1992).

Clearly, CS clinical symptoms are much more severe than the classical XP condition and go beyond photosensitivity. Photosensitivity and other XP-like features (such as pigmentation abnormalities and

predisposition to skin cancer) can be attributed to the NER defect. However, the severe developmental and neurological manifestations of CS can not be explained by NER (Bootsma and Hoeijmakers 1993; Vermeulen et al. 1994b), implicating additional functions for the CS proteins outside NER (van Gool et al. 1997b). The transcriptional engagement of CSA and CSB (analogous to XPB and XPD) suggests that transcription deficiency, perhaps induced by DNA damage, also contributes to the clinical picture. In some cases, CS features are found in combination with XP, due to specific mutations in the *XPB*, *XPD*, or *XPG* genes. Cells from CSA, CSB, and XPG individuals with severe CS symptoms are slightly sensitive to ionizing radiation in addition to UV-light (Leadon and Cooper 1993). It is hypothesized that inefficient TCR of oxidative lesions (e.g. thymine glycol) which block transcription underlies this ionizing radiation sensitivity (Cooper et al. 1997) although ionizing radiation is a poor inhibition of transcription in general. This indicates an additional role of CSA, CSB, and XPG in coupling arrested transcription with both BER and NER (reviewed in Citterio et al. 2000), and suggests a general repair-transcription coupling deficiency as the major cause of the extensive variations in symptoms and severity of the CS phenotype. The developmental defects and the premature aging-related symptoms of CS can be attributed to the incomplete repair of endogenous oxidative damage (Martin et al. 1996; Cooper et al. 1997), which in turn causes cellular malfunction and/or induction of apoptosis. The defective TCR in CS cells enhances their p53-dependent apoptotic response, contributing to the elimination of cells that potentially carry oncogenic mutations. This explains the lack of cancer predisposition in CS after UV-exposure (Yamaizumi and Sugano 1994; Ljungman and Zhang 1996; Ljungman et al. 1999; McKay et al. 1999; Conforti et al. 2000). Numerous other CS-like patients have been identified, for example CAMFAK (for cataracts, microcephaly, failure to thrive, kyphoscoliosis) and COFS (cerebro-oculofacial syndrome), but these patients fail to exhibit pronounced photosensitivity in spite of the fact that cells of the patients display defective recovery of RNA synthesis (Colella et al. 1999; Bootsma et al. 2001), suggesting the possibility of a partial transcription defect without the accompanying TC-NER defect of CS.

II.5.3 Trichothiodystrophy (TTD)

TTD is caused by a neurectodermal dysplasia, which causes a collection of symptoms referred to by the acronym PIBIDS: photosensitivity, ichthyosis, brittle hairs, intellectual impairment, decreased fertility, and short stature.

Skeletal abnormalities are also frequently observed, including a peculiar bird-like face, a receding chin, and retardation of skeletal age. Moreover, axial osteosclerosis (abnormal hardening of the bone), peripheral osteoporosis (McCuaig et al. 1993), and kyphosis (Norwood 1964) have been reported. The striking ectodermal symptoms (brittle hair and dystrophic nails) are unique for TTD. However, the remainder of the clinical features are strikingly similar to CS, including the absence of cancer predisposition (de Boer and Hoeijmakers 2000; Bootsma et al. 2001). The photosensitivity in TTD patients is due to a defect in NER caused by a mutation in one of three genes: *XPB*, *XPD* or *TTDA*. The NER defect in all but two of 20 studied UV-sensitive TTD families can be assigned to the XPD complementation group (Stefanini et al. 1993a and 1993b; Vermeulen et al. 1994a). Despite the NER defect, the pigmentation abnormalities are relatively mild compared to classical XP (Itin and Pittelkow 1990; Botta et al. 1998). The typical brittleness of TTD hair is caused by a substantial reduction in the content of hair-specific cysteine-rich matrix proteins that provide the hair shaft with its natural strength by crosslinking the keratin filaments (Gillespie and Marshall 1983). Growth retardation (cachectic dwarfism) in TTD patients is a very heterogeneous clinical symptom and - when severe - can be associated with death in early childhood. TTD, like CS, is considered to be a repair/transcription syndrome (Vermeulen et al. 1994b). Mutations in *XPD* may not only affect the NER function but also cripple transcription by TFIIH, accounting for the typical TTD and CS phenotypes. Consistent with this idea, all causative mutations in *XPD* have been found to be disease-specific (Winkler and Hoeijmakers 1998; de Boer and Hoeijmakers 2000). Recently, the phenotype of two unrelated TTDA patients was directly attributed to a limiting amount of TFIIH, probably secondary to a mutation in a gene determining the complex stability. A reduced TFIIH level has an effect on its repair function and also on its role in basal transcription (Vermeulen et al. 2000).

II.6 Mouse models for genetic defects in NER

In recent years, mouse strains carrying defined mutations in repair genes, have been generated in order to study the syndromes caused by a defect in NER. Via conventional gene targeting methodologies, inactivated alleles or specific mutations (mimicking patient-specific gene alterations) were introduced by homologous recombination into the genome of totipotent embryonic stem cells, thereby creating gene knockout and specific mutant mouse models for *XP*, *CS*, and *TTD* (outlined in Table 3). The use of this

genetic technique will have a major impact on understanding clinical and fundamental features of human NER syndromes and ultimately cancer in general. Phenotypic characterization of the mouse models can help to answer questions about the role of the specific gene in NER and the consequences of NER deficiency *in vivo*. In addition, these models may provide clues about novel phenotypes related to NER defects that correspond to human syndromes in which the causative gene is yet unknown. Crossing animals with different genetic lesions allows *in vivo* investigation of the possible interplay between NER and other mechanisms implicated in genetic (in)stability, such as complementary repair pathways, cell cycle control, and apoptosis. Finally, since the NER system targets a very wide spectrum of DNA lesions, mice deficient in this pathway will be a valuable and sensitive model for allowing assessment of the genotoxic effect of known and unknown compounds. However, several factors should be taken into account when studying NER-deficient mouse models. First, there are some important differences in the activity of NER between mouse and man. For instance, CPDs (but not 6-4PPs and some chemical adducts) are removed much less efficient from the non-transcribed strand of transcriptionally active genes in rodents than in man (Bohr et al. 1985). However, this difference does not appear to have dramatic consequences in the model phenotypes since repair parameters (such as UDS, recovery of RNA synthesis after UV-irradiation and sensitivity to UV-light) in mouse embryonic fibroblasts (MEFs) derived from the mutant mice correlate very well with those of human patient fibroblasts (see Table 3). However, in contrast to human cells, the selective repair of DNA lesions in the transcribed strand in rodent cells leads to a strong bias of mutations arising from lesions in the poorly repaired non-transcribed strand. Second, there is a substantial difference in the life span between mouse and man and many of the clinical features of the NER-deficient syndromes are age-dependent. For example, the accelerated neurodegeneration seen in XPA human patients evolves over the course of several years (longer than the life span of a mouse (see below)). Third, there is phenotypic diversity amongst the various genetic backgrounds of mutant mice (e.g. in a given genetic background approximately half of the *XPA*-deficient mouse embryos died in the midfetal stage (with signs of anemia (de Vries et al. 1995)), while in another background the mice were born at the expected Mendelian frequency (Nakane et al. 1995). Recent evidence indicates that the genetic background influences not only embryonic lethality but also the life span of NER-deficient mice to a considerable extent. For example, the maximal life

Table 3. Properties of NER mouse models and corresponding human syndromes

	Mouse	UV-sensitivity*		UDS (%)*		Skin Cancer		Relevant clinical symptoms or differences with human
Gene	Mutation	Man	Mouse	Man	Mouse	Man	Mouse	Syndrome
XPA	KO	+/−	+/+	<5	<5	++	++	Neurodegeneration as in man is not apparent in mouse.
XPB	KO	n.a.	n.a.	n.a.	n.a.	n.a.	n.a.	Embryonic lethal;
XPB	Truncation	++	−/−	~10%	~10%	+/++	n.d.	No severe phenotype in mouse.
XPC	KO	−	+	15-30	30	++	++	MED in wildtype range.
XPD	KO	n.a.	n.a.	n.a.	n.a.	n.a.	n.a.	Embryonic lethal.
XPD	TTD point mutation	+/-	+/-	25	25	-	+	Like human TTD, except neurodysmyelination.
CSB	Truncation	++	−/−	Normal	Normal	-	+	CS symptoms mildly present. Mild growth retardation. Retinal degeneration. Cancer prone.
CSA	KO	++	++	Normal	Normal	-	n.d.	As CSB.
ERCC1	KO Truncation	n.a.	+/+	n.a.	<5	n.a.	n.d.	Runted growth, early death through liver/kidney dysfunction. Signs of premature aging. No human syndrome.
mHR23A	KO	n.a.	Normal	n.a.	Normal	n.a.	n.d.	No apparent phenotype. No human syndrome.
mHR23B	KO	n.a.	Normal	n.a.	Normal	n.a.	n.d.	No human syndrome. Intrauterine or premature death. Growth retardation. Male sterility. Facial dysmorphology. UV-sensitivity and reduced UDS (as XPC) of *mHR23A/B* DKO E8.5 MEFs. DKO mice are not viable.

*UV-sensitivity and UDS (unscheduled DNA synthesis) of cultured MEFs (mouse embryonic fibroblasts) and of skin; Abbreviations: KO (knockout); DKO (double knockout); n.a. (not applicable); n.d. (not determined); E8.5 (embryonic day 8.5); MED (minimal UV-dose required to induce erythema/edema). Table adapted from De Boer and Hoeijmakers (1999).

span of *ERCC1*-deficient mice is extended to several months in a FVB strain as compared to a C57BL/6 background (Weeda et al. 1997).

II.6.1 Damage recognition and verification proteins

XPA

The mouse homolog of the human *XPA* gene was cloned (Tanaka et al. 1989; van Oostrom et al. 1994) and a mouse model for the totally NER-deficient XPA (*XPA*$^{-/-}$ mice) was generated independently in two laboratories (de Vries et al. 1995; Nakane et al. 1995). *XPA*$^{-/-}$ MEFs display all the

characteristics of a total NER deficiency. In contrast to XPA patients, *XPA*$^{-/-}$ mice appear physiologically normal, are fertile, and show no enhanced mortality up to the age of 18 months (reviewed in de Vries and van Steeg 1996). A slightly increased incidence of spontaneous liver carcinomas and lymphomas is found in older *XPA*-deficient mice (de Vries et al. 1997; van Steeg et al. 1998), but no clear spontaneous neurological abnormalities are observed. However, following experimental brain trauma, *XPA*-deficient mice show delayed recovery of neuromotor defects and cognitive dysfunction (Tomasevic et al. 2000) .

XPA$^{-/-}$ mice provide an excellent model for the susceptibility of human XPA patients to skin cancer. Daily exposure of *XPA*-deficient mice to UV-B leads to hyperkeratosis and erythema (sunburn) on the UV-exposed skin even after relatively low doses (200 J/m^2). The erythema is followed by a high incidence of skin tumors, primarily SCCs (de Vries et al. 1995; Nakane et al. 1995). Daily exposure to UV-B (32 or 80 J/m^2) causes skin tumors in 100% of hairless *XPA*$^{-/-}$ mice after a short latency period (Berg et al. 1997). A shift from SCCs in wildtype hairless mice to papillomas in *XPA*-deficient hairless mice is correlated with a shift in cancer-susceptibility genes (*p53* versus *Ras*) mutated in the tumors (de Vries et al. 1998). In addition to the effects of UV-light on the skin, hyperplasia and SCCs in the cornea of *XPA*-deficient mice are observed (de Vries et al. 1998). This mimics the corneal abnormalities seen in human XPA patients. A short-term effect of UV-B-exposure is also suppression of the immune system. This feature is prominent in XPA patients and *XPA*-deficient mice (Kripke 1990 and 1991) and is likely to play an important role in the development of UV-B-induced cutaneous malignancies (Glover et al. 1994). Elevated UV-induced inflammation and immune suppression (Miyauchi-Hashimoto et al. 1996) as well as a suppression of natural killer cell activity are found in *XPA*-deficient mice (Miyauchi-Hashimoto et al. 1999). The latter phenomenon is also observed in XPA, but not in CS or TTD patients (Morison et al. 1985; Mariani et al. 1992). In accordance with this finding, systemic immunomodulation is only observed in UV-irradiated mice if both NER subpathways are compromised (Garssen et al. 2000). *In vivo*, UV-irradiation causes an acute inflammatory reaction in the skin, characterized by cutaneous vasodilatation (erythema), followed by an increase in the vascular permeability with exudation of fluid (edema). Examination of mice with different NER genotypes exposed to the minimal UV-dose required to induce erythema/edema (MED) suggests a role of persistent UV-photoproducts in transcriptionally active DNA in triggering the cascade that leads to erythema and edema in the irradiated skin. The MED of *XPA*$^{-/-}$ mice

is 10-fold lower than for wildtype mice (150 J/m^2 versus 1500 J/m^2) (Berg et al. 1998; Garssen et al. 2000). Defective TC-NER in *XPA*$^{-/-}$ cells causes an irreversible block of RNA synthesis, which contributes directly to the occurrence of UV-induced erythema and edema (Berg et al. 1998) and apoptosis (Ljungman and Zhang 1996). Consistent with this, epidermal cells of hairless *XPA*$^{-/-}$ mice are extremely prone to UV-induced apoptosis (van Oosten et al. 2000).

Topical treatment of *XPA*$^{-/-}$ mice with the chemical carcinogen dimethyl-benz[a]anthracene (DMBA) results in acute skin effects like acanthosis and epidermal hyperplasia, and chronic effects such as an increased incidence of papillomas (de Vries et al. 1995; Nakane et al. 1995). *XPA*-deficient mice also have a predisposition to chemically-induced internal carcinogenesis (reviewed in van Steeg et al. 1998 and 2000). Oral treatment of *XPA*-deficient mice with a subchronical dose of B[a]P results in an increased level of lymphomas in knockout mice compared to wildtype mice (de Vries et al. 1997). In *XPA*$^{-/-}$/*p53*$^{+/-}$ double mutant mice, lymphomas develop much earlier and with higher frequency compared to their single mutant counterparts (van Oostrom et al. 1999). Intratracheal treatment of *XPA*$^{-/-}$ mice with B[a]P leads to enhanced frequency of pulmonary adenomas and lung carcinomas (Ide et al. 2000). Oral exposure to 2-AAF and 2-amino-l-methyl-phenylimidazo[4.5-b]pyridine (PhIP) causes increased incidence of liver tumors in female mice and bladder cancer in male mice (2-AAF) and intestinal adenomas and lymphomas (PhIP) (van Steeg et al. 1998 and 2000). Since carcinogenesis is accelerated in *XPA*$^{-/-}$ mice, this animal model might contribute towards identifying the role of individual carcinogens in tissue-specific cancer initiation and progression (van Steeg et al. 1998 and 2000).

XPC

Two independent *XPC* knockout mouse models were developed (Sands et al. 1995; Cheo et al. 1997). The mice are viable and develop normally similar to *XPA*-deficient mice. No increased incidence of spontaneous tumors is observed in *XPC*-deficient animals up to one year of age (Sands et al. 1995; Cheo et al. 1997; Friedberg et al. 1999 and 2000). UV-B irradiation of the mice results in acute effects to the skin (i.e. hyperkeratosis and erythema), followed by a high incidence of skin- and eye tumors. The minimal UV-dose required to induce acute effects in *XPC*-deficient mice is 1500 J/m^2, which is comparable to that of wildtype mice (Berg et al. 1998 and 2000; Garssen et al. 2000). In accordance, nine XPC patients showed MED within the normal range of healthy humans (Kondo et al. 1992). Since in mice there is

much less repair of CPD than in man, the difference in repair between the wildtype and *XPC*$^{-/-}$ mice is smaller when compared to the repair state in normal humans and XPC patients. In accordance, UV-exposed keratinocytes of *XPC*$^{-/-}$ mice do not display an enhanced apoptotic response compared to the wildtype mice (Ananthaswamy et al. 1999; van Oosten et al. 2000). Together, these data suggest that a GG-NER deficiency causes skin cancer susceptibility but does not influence the sensitivity to acute effects of UV-B irradiation. *XPC*$^{+/-}$ mice show an increased predisposition to UV-B radiation-induced skin cancers compared to wildtype mice, indicating that haplo-insufficiency of the *XPC* gene may be operating in mice and is a risk factor for UV-B induced skin cancer (Cheo et al. 2000). *XPC/p53* double knockout embryos show neural tube defects. Furthermore, solar keratosis and skin cancer predisposition are significantly increased in double knockout mice compared to *XPC* single knockout animals (Cheo et al. 1996). The mouse homolog of the human BER gene *HAP1/REF1/APE*, *Apex*, is a redox protein that encodes the major apurinic/apyrimidinic endonuclease activity in mouse cells and regulates p53 activation (Meira et al. 1997). *XPC*$^{-/-}$*/Apex*$^{+/-}$ mice show a further increase in UV-induced cancer susceptibility when compared to *XPC*$^{-/-}$*/Apex*$^{+/+}$ mice (Friedberg et al. 1999; Meira et al. 1997 and 2001). Double mutant mice of *XPC* and *Msh2* (involved in MMR) are viable and exhibit an enhanced predisposition to UV-induced skin cancer compared to *XPC*$^{-/-}$ mice, probably directly attributable to the general mutator-phenotype seen in *MMR*-deficient mice (Friedberg and Meira 2000). A significantly higher incidence of chemically-induced liver and lung tumors is observed in *XPC*$^{-/-}$ mice compared to wildtype and heterozygous littermates after treatment with 2-AAF or N-OH-AAF (Cheo et al. 1999). But in *XPC*$^{-/-}$ mice a *p53*$^{+/-}$ status further accelerates progression of AAF-induced liver tumors. Furthermore, a higher incidence of spontaneous testicular tumors is reported in *XPC/p53* double knockout mice compared to *XPC*$^{+/+}$*/p53*$^{-/-}$ mice (Cheo et al. 1999). *XPC/XPA* double knockout mice are completely NER-deficient and are phenotypically similar to *XPA* single knockout mice (Friedberg and Meira 2000; van der Horst et al. manuscript in preparation).

Human RAD23 homologs *hHR23A* and *hHR23B* (highlighted in Chapters V and VI)

Each of the hHR23A and hHR23B proteins can form a complex with XPC, and thereby function in damage recognition in GG-NER. *mHR23A* and *mHR23B* knockout mice were recently generated in our laboratory and are described extensively in Chapters V and VI. *mHR23A*$^{-/-}$ mice (see Chapter

VI) are viable, develop normally, and display no characteristics of an overt NER defect (at least up to 16 months). In contrast, *mHR23B*$^{-/-}$ mice (see Chapter V) are viable but severely runted at birth. Furthermore, *mHR23B*$^{-/-}$ animals are born at 10-fold decreased frequency than expected. Perinatal death of *mHR23B* knockout mice is common. Intrauterine death is associated with a total absence of vascularization (anemia) or profuse internal hemorrhage as well as edema and craniofacial abnormalities. Placental defects are also observed in *mHR23B*$^{-/-}$ embryos due to impaired vascularization of the placental labyrinth. This limits the maternal-fetal exchange of gases, and transport of nutrients to the fetus. Animals that survive this critical stage display severe growth retardation, male sterility (due to the complete absence of spermatogenesis), facial dysmorphology and ocular inflammation. *mHR23B*$^{-/-}$ female mice are fertile, albeit at a reduced level. The dramatic phenotype of *mHR23B*$^{-/-}$ mice is very different from any of the human NER syndromes or mouse models, and strongly suggests that mHR23B is essential for proper mouse development. Furthermore, the immense difference between the phenotype of *mHR23B*$^{-/-}$ and *mHR23A*$^{-/-}$ mice can likely be attributed to the fact that mHR23A can only partly compensate for the loss of mHR23B.

Cells of both *mHR23A* and *mHR23B* single knockout mice are UV-resistant, suggesting that in NER the two proteins share common activities and are therefore functionally redundant. This conclusion is in line with the results of *in vitro* repair studies (Sugasawa et al. 1997; see also in Chapter III). *mHR23A/B* double knockout embryos (see Chapter VI) die before day 13.5 of embryonic development (E13.5). Importantly, total *mHR23A/B*-deficient MEFs from E8.5 could be isolated and were found to be as UV-sensitive as the *XPC*$^{-/-}$ cells. Other DNA repair parameters tested also reveal a striking similarity between *mHR23A/B*-deficient and *XPC*$^{-/-}$ cells, strongly suggesting that a total *mHR23A/B*-deficiency leads to an *XPC*-like UV-sensitivity. Interestingly, the XPC protein level is significantly decreased in *mHR23A/B*-deficient cells, indicating that XPC is unstable in the absence of both mammalian RAD23 proteins. Stable cotransfection of cDNAs encoding GFP-tagged *XPC (XPC-GFP)* and/or *hHR23B* into *mHR23A*$^{-/-}$/*B*$^{-/-}$ cells rescued the UV-sensitivity. The observation that the single *mHR23B*$^{-/-}$ and *mHR23A*$^{-/-}$/*B*$^{-/-}$ phenotypes are so much more severe than the *XPC*$^{-/-}$ phenotype implicates that the mammalian RAD23 proteins have additional functions outside NER but that mHR23A cannot compensate for all the activities of mHR23B.

In view of XPC and its strong relation with the mammalian RAD23 proteins, *mHR23A/XPC* and *mHR23B/XPC* knockout mice were generated

and appeared viable (Ng et al. unpublished data). Neither *mHR23A*$^{-/-}$/*XPC*$^{-/-}$ nor *mHR23B*$^{-/-}$/*XPC*$^{-/-}$ MEFs showed an additional increase in UV-sensitivity, and the levels of UDS and RNA synthesis recovery were similar to those of single *XPC*$^{-/-}$ cells. However, in contrast to *mHR23A*$^{-/-}$/*XPC*$^{-/-}$ mice which are healthy without gross abnormalities apart from a GG-NER defect, *mHR23B*$^{-/-}$/*XPC*$^{-/-}$ mutants are phenotypically similar to single *mHR23B* knockout animals. These findings support the idea that, in addition to a role in excision repair, mHR23 proteins are involved in another pathway. In view of the amino acid sequences and other properties, the additional role of mHR23 proteins is most likely associated with the ubiquitin/proteasome protein degradation pathway. The connection between NER and the ubiquitin system is discussed in more detail in the next section, and in Chapters V and VI.

II.6.2 DNA unwinding proteins

TFIIH subunits *XPB* and *XPD*

The TFIIH complex has a second function outside NER, which complicates the clinical effect of a mutation in the genes involved. The second function is initiation of basal transcription of all structural genes transcribed by RNAP II. This is one of the most fundamental processes in the cell. Complete inactivation of such a function is most probably lethal, explaining the rarity of mutants in TFIIH genes. An *XPB* mouse model with a truncation at the position corresponding to the frameshift in the human *XPB* gene of a XP/CS patient was recently generated and is viable (Friedberg and Meira 2000; Weeda et al. manuscript in preparation). Furthermore, the mouse *XPB* mutant cells are UV-sensitive and NER-deficient.

The function of the XPD protein is, just like XPB, essential in basal transcription, and only subtle XPD mutations are found in XP, XP/CS and TTD patients. Consistent with this, the *XPD* mutant mouse model in which the DNA helicase domains IV-VI are deleted is not viable and shows preimplantation lethality at the two-cell stage when normal embryonic transcription begins (de Boer et al. 1998b). However, mice carrying in both *XPD* alleles the causative point mutation of a TTD patient (designated *XPD*^{TTD} mouse) are viable (de Boer et al. 1998a). Moreover, *XPD*^{TTD} mice mimic to a remarkable extent the clinical symptoms of the human patients, including brittle hair, developmental problems, reduced life span, and skin abnormalities. *XPD*^{TTD} cells have reduced NER capacity and are mildly sensitive to UV and DMBA. In accordance with this, *XPD*^{TTD} mice exhibit a

modest increase in inflammation and hyperplasia of the skin secondary to UV exposure. Differentiation of skin keratinocytes is impaired. *XPD*^{TTD} mice have a slightly reduced MED compared to wildtype and *XPC*$^{-/-}$ mice (1200 J/m^2 versus 1500 J/m^2) but not as low as in *XPA*$^{-/-}$ mice, consistent with the idea that TC-NER is only partially affected in *XPD*^{TTD} mice (de Boer et al. 1999; Garssen et al. 2000). Whereas TTD patients do not show elevated cancer incidence, *XPD*^{TTD} mice display a clear susceptibility to UV- and DMBA-induced skin carcinogenesis (although this is not as pronounced as in the totally NER-deficient *XPA*$^{-/-}$ mice) confirming the idea that a defect in DNA repair in general predisposes to cancer (de Boer et al. 1999).

The phenotype of *XPD*^{TTD} mice is dramatically exaggerated if the defect is crossed into a totally NER-deficient background, i.e. *XPD*^{TTD}/*XPA*$^{-/-}$. The double mutant mice are growth retarded and die prematurely just after weaning (de Boer et al. manuscript in preparation). In contrast, the combination of a GG-NER and TTD defect in *XPC*/*XPD*^{TTD} double mutant mice fails to show a strong synergism when compared to *XPD*^{TTD} single mutant mice. Apparently, the residual TCR capacity in *XPC*/*XPD*^{TTD} double knockout mice is sufficient to sustain life. Given the involvement of the XPD and CSB proteins in transcription initiation and elongation respectively, we hypothesize that the premature aging features in CS and TTD originate from a subtle transcription defect that worsens with increasing accumulation of unrepaired DNA damage in active genes. The generation of mouse models with an *XP*-type or *XP/CS*-type mutation in the *XPD* gene is in progress.

II.6.3 Incision proteins

XPG

The phenotypic heterogeneity of human XPG patients is reflected by the different *XPG*-deficient mouse models. *XPG*-deficient mice generated by deletion of exon 3 of the mouse *XPG* gene, exhibit postnatal growth failure and undergo premature death (Harada et al. 1999), similar to the severe CS features in human XPG/CS patients. Primary *XPG*$^{-/-}$ MEFs display premature senescence and exhibit early onset of immortalization and accumulation of p53 (Harada et al. 1999), which is consistent with XPG having an additional function in genome stabilization besides its role in NER. In contrast, deletion of exon 15 of the mouse *XPG* gene resulted in mice that develop normally (Friedberg and Meira 2000). Cells of these mice are moderately NER-defective and UV-sensitive.

XPF

The mouse *XPF* gene has recently been isolated and characterized (Shannon et al. 2000). The predicted mouse XPF protein is 86% homologous to the human XPF protein. XPF mRNA levels are specifically elevated in adult mouse testis. Moreover, elevated levels of XPF and ERCC1 mRNAs were found in meiotic and early post-meiotic spermatogenic cells, which may point to a role for the encoded protein ERCC1-XPF in meiotic recombination. However, *XPF*-deficient mice have not yet been generated (Friedberg and Meira 2000).

ERCC1

ERCC1 gene was the first human NER gene cloned (Westerveld et al. 1984), but is not implicated in any of the known XP, CS or TTD complementation groups. No human syndrome attributable to a mutation in *ERCC1* is yet known (van Duin et al. 1989), suggesting that complete gene inactivation in humans is incompatible with life. However, a functional knockout mutation of the *ERCC1* gene in mice is viable, but most *ERCC1*-deficient embryos die *in utero* or perinatally. The few mutants that survived are severely runted and usually die before weaning i.e. within 4 weeks of birth (Weeda et al. 1997; McWhir et al. 1993). One of the causes of early postnatal death is liver malfunction. Aneuploidy and elevated levels of the tumor suppressor proteins p53 and p21 are detected in hepatocytes, suggesting the presence of early DNA damage-induced cell cycle arrest (McWhir et al. 1993). Other hallmarks include aneuploid nuclei in kidney, ferritin deposition in spleen, and increased levels of p53 in brain and kidney (Weeda et al. 1997). The mutant mice have no subcutaneous fat but their neurologic status appears normal. As expected, *ERCC1*-deficient MEFs show almost no repair activity after exposure to UV-light, and are hypersensitive to UV and chemical genotoxins that are substrates for NER. In addition, the MEFs are sensitive to crosslinking agents, presumably as a consequence of an additional defect in one of the recombination pathways (Dronkert et al. manuscript in press). Some symptoms seemed to be less severe in the mouse model in which the encoded protein contains a C-terminal seven amino-acids truncation (Weeda et al. 1997). Both *ERCC1* mutant mouse models exhibit additional symptoms that point to a premature replicative senescence in liver and kidney cells as well as increased spontaneous transformation of MEFs *in vitro* that is not observed in cells of mice with a defect in NER only (Weeda et al. 1997). This early onset of cell cycle arrest and polyploidy in liver and kidney is most likely caused by an accumulation of unremoved DNA damage of which some might be normally repaired by ERCC1-dependent

recombination (Mu and Sancar 1997; Sargent et al. 1997; Melton et al. 1998; Nunez et al. 2000). The signs of premature senescence observed in *ERCC1*-deficient mice suggest that accumulation of unrepaired DNA damage contributes to early aging. Cutaneous application of DMBA at a dose easily tolerated by *XPA* knockout mice (Nakane et al. 1995) caused *ERCC1*$^{-/-}$ animals to die within 3 days, revealing an extreme sensitivity to genotoxins (Weeda et al. 1997).

Apart from the UV sensitivity, the phenotype of *ERCC1*$^{-/-}$ mice is very different from any of the human NER syndromes. The lack of similarity between the mouse and the human NER mutants may in part reflect species differences, but the feature also may be compounded by the dual functionality of the ERCC1 protein. A comparison of the characteristics of *ERCC1* mutant mice with that of *XPA* knockout mice (also harboring a complete NER defect) will be very instructive. *ERCC1* knockout mice are considered suitable candidate mice to study the genotoxic effects of crosslinking agents. However, given their extremely reduced life span (McWhir et al. 1993; Weeda et al. 1997), an approach to develop a conditional mutant mouse (see Chapter VII) is essential.

II.6.4 TC-NER-specific proteins

CSB

A truncation mutation of a CSB patient was mimicked in the mouse genome (van der Horst et al. 1997). Similar to the human syndrome, *CSB*-deficient mice were born at Mendelian frequency and exhibit all of the CS repair characteristics: UV-sensitivity, specific loss of TC-NER, normal GG-NER, and inability to resume RNA synthesis after UV-exposure. Other CS-like clinical features such as growth failure and neurological dysfunction are only present in a mild form in the mouse model. Although neurodysmyelination was not observed, the behavior of the mice in various tests (behavioral and motor coordination) points to some neurological impairment. The MED of *CSB*-deficient mice is equal to that of *XPA* knockout animals (i.e. 150 J/m^2), which is 10-fold lower than observed for TCR-proficient mice (*XPC*$^{-/-}$ and wildtype mice) (Berg et al. 2000; Garssen et al. 2000). The apoptotic response in epidermal cells is also similar to that in *XPA*$^{-/-}$ mice (van Oosten et al. 2000). In contrast to CS patients, *CSB*-deficient mice appear prone to skin cancer when exposed to UV-light or to DMBA (van der Horst et al. 1997). This can be explained by a more efficient GG-NER pathway for some lesions (i.e. CPDs) in humans compared to mice.

Remarkably, when an additional GG-NER defect was bred into *CSB*-deficient mice, a strong augmentation of the CS phenotype was observed. The *CSB/XPA* and *CSB/XPC* double mutant mice exhibit very severe growth retardation (75% less of wildtype mice), suffer from neurological problems (unable to walk), and die before weaning (around day 18). These observations suggest that a CS defect becomes exaggerated in the absence of GG-NER, pointing to an accumulation of endogenous damage as a contributing factor to the CS symptoms (van Gool et al. 1997b). The fact that *CSB/XPA* and *CSB/XPC* double mutant mice display a phenotype more severe than single *XPA* knockout animals (with a complete NER defect) argues that CSB has additional functions beyond its role in NER. Cells of combined *CS/XP* mice are totally defective in NER and show an *XPA*-like UV-sensitivity (van Gool et al. 1997b; van der Horst et al. manuscript in preparation). In view of the involvement of mHR23 in NER, *CSB/mHR23A* double knockout mice were generated, and were found to display a normal phenotype. *CSB/mHR23A* double mutant MEFs do not have an additional NER defect on top that seen in single $CSB^{-/-}$ cells (Ng et al. unpublished data), further suggesting the existence of functional redundancy between the two mammalian RAD23 proteins in NER. Given that XPC and hHR23B are tightly complexed, crossing *CSB* and *mHR23B* knockout animals will be of interest in the near future.

CSA

CSA-deficient mice were generated very recently (van der Horst et al. manuscript in preparation). Animals were shown TC-NER deficient, photosensitive and UV-induced skin cancer prone, and as such form a phenocopy of $CSB^{-/-}$ animals. Like *CSB/XPC* double mutant mice, *CSA/XPC* double knockout animals die before weaning. $CSA^{-/-}/XPC^{+/-}$ mice are viable, but display increased incidence of skin cancer after UV-B exposure compared to either single mutants (van der Horst et al. manuscript in preparation). Thus, inactivation of TC-NER uncovers XPC haploinsufficiency with respect to UV-induced cancer predisposition. This finding is in line with the increased spontaneous mutation frequency observed in aging $XPC^{+/-}$ animals (Wijnhoven et al. 2001).

II.7 Connection between NER and the ubiquitin system

II.7.1 Interaction between RAD23 and ubiquitin

Interestingly, the developmental abnormalities detected in *mHR23B*$^{-/-}$ mice (Chapter V) and the lethality in *mHR23A/B* double knockout animals (Chapter VI) are absent in *XPC* and other NER-deficient mouse models. This strongly suggests that mHR23B has an important separate function, which furthermore can not be fully complemented by mHR23A. The RAD23 homologs share a number of well-conserved domains, including an N-terminal ubiquitin-like (UbL-like, ~80 amino acids in length) sequence, and two copies of a highly conserved ubiquitin-associated domain (UBA, ~50 amino acids long) one in the middle and one at the C-terminus of the proteins (schematically represented in Figure 2). These domains are not found in any other NER proteins. The UbL-like domain shares 23% sequence identity with ubiquitin, which is a very conserved polypeptide, composed of 76 amino acids and present in all cells. Ubiquitin functions as a protein tag marking its targets for non-lysosomal proteolytic degradation or for refolding. Ubiquitination plays a regulatory role in numerous cellular processes, including homeostasis, stress response, organelle biosynthesis, protein translocation across membranes, and DNA repair (reviewed in Ciechanover et al. 2000). All of these roles depend upon the covalent coupling of ubiquitin to cellular substrates, resulting in mono- or poly-ubiquitination via a complex enzymatic pathway (depicted in Figure 3 and discussed in section II.7.2). Poly-ubiquitination signals the proteolytic breakdown of substrate proteins by the proteasome, whereas mono-ubiquitination may serve other functions.

Studies in yeast and in mammals have shown that the strongly conserved UbL-like domain of RAD23 is required for maximal efficiency of NER (Watkins et al. 1993). In addition, the domain mediates interaction between RAD23 and the 26S proteasome (Schauber et al. 1998; Hiyama et al. 1999), suggesting a role for RAD23 in protein degradation via the ubiquitin/proteasome pathway. Consistent with this finding, the entire amino acid sequence of this region is strictly conserved between mouse and human, including lysine 48, which in ubiquitin is required for poly-ubiquitination (Chau et al. 1989). Conservation of this residue further suggests the possibility of covalent attachment of ubiquitin to RAD23.
The UBA domain is evolutionarily conserved from yeast to humans and is found in all eukaryotes (Hofmann and Bucher 1996). Although, UBA

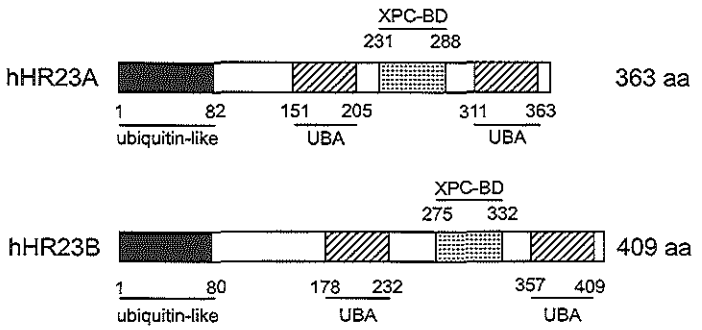

Figure 2. Schematic representation of functional domains in the two human homologs of *S. cerevisiae* RAD23 NER proteins: hHR23A and hHR23B. Both proteins share 57% identity and 76% similarity in amino acid (aa) sequence. Abbreviations: UBA, ubiquitin-associated domain; XPC-BD, XPC-binding domain for XPC stimulation.

domains are present in many enzymes and proteins that are involved in pathways utilizing ubiquitination, DNA repair, and cell signaling via protein kinases, their cellular function is not completely understood. Such an UBA domain constitutes a large hydrophobic patch at a protein's surface, that may serve as a binding site for other proteins. The UBA domain also includes numerous conserved residues that contribute to the stabilization of the overall structure of the domain by promoting its intra- and inter-α-helical interactions (Dieckmann et al. 1998). The most C-terminal UBA domain of HR23 was recently shown to interact with the human BER protein 3-methyladenine DNA glycosylase (MPG, Miao et al. 2000). Based on this observation it was proposed that the *hHR23* gene products act as universal DNA damage recognition accessory proteins. Previously, it was also found that the human immunodeficiency virus (HIV-1) Vpr protein binds specifically to the C-terminal UBA of hHR23 (Withers-Ward et al. 1997). It is therefore possible that HIV-1 Vpr may compete with MPG, XPC, and other proteins for binding to hHR23, thereby affecting BER, and/or NER, and/or other processes. This permits further speculation that the interaction of HIV-1 Vpr with the hHR23 UBA domain may be important in HIV-induced cell cycle arrest and/or apoptosis (Withers-Ward et al. 2000). Furthermore, the UBA domain could be involved in the interaction of RAD23 with the 19S complex (see below) of the proteasome resulting in an alteration of the NER activity (Russell et al. 1999; Ortolan et al. 2000; Gillette et al. 2001). Thus, a link between NER and the 19S complex of the

26S proteasome mediated by RAD23 seems well established but the functional implications remain obscure.

The characterization of the mammalian cells deficient in RAD23 activity led to the discovery that XPC stability depends on the presence of mHR23 proteins (discussed in Chapter VI) and that DNA damage is able to further stabilize the XPC protein in a transient fashion. These findings establish the main function of the RAD23 proteins in NER, which is to regulate the first step of the GG-NER pathway. The discovered role of mHR23 in protein stabilization provides an explanation of the unusual phenotype of the *mHR23B* mice and the lethality of the double mutant, and may have important implications for the other partners of HR23 proteins.

II.7.2 The ubiquitin system

Degradation of cellular proteins is a highly complex, temporally controlled, and tightly regulated process that plays major roles in a broad array of basic pathways during cell life and death. The ubiquitin proteolytic system is involved in physiological regulation of many cellular processes, including cell cycle progression, modulation of the immune and inflammatory responses, development, cell differentiation, signal transduction, spermatogenesis, and repair. These complex processes are controlled via degradation or processing of a single or a subset of proteins. Ubiquitin-mediated degradation of a protein involves two distinct and successive steps: (i) conjugation of multiple ubiquitin molecules to the substrate, and (ii) degradation of the tagged protein by the 26S proteasome complex (see Figure 3 for a scheme of the ubiquitin/proteasome pathway). For recent comprehensive reviews of the mechanisms of the ubiquitin/proteasome system, the interested reader is referred to Laney and Hochstrasser (1999), Kornitzer and Ciechanover (2000), and Ciechanover et al. (2000).

The 26S proteasome consists of two different subunits: the 19S regulatory complex and the 20S catalytic core (Varshavsky 1997). The 19S complex consists of at least 17 proteins, which can bind substrate-linked multiubiquitin chains, unfold the attached proteins and translocate the polypeptide chains into the 20S catalytic core. A key feature of the 19S complex is the presence of the six so-called homologous AAA ATPases that are thought to unfold substrate proteins in an ATP-dependent manner. However, it is not clear if the intact 26S proteasome is necessary for all proteasomal functions or whether the 19S complex can function on its own independently of the 20S core.

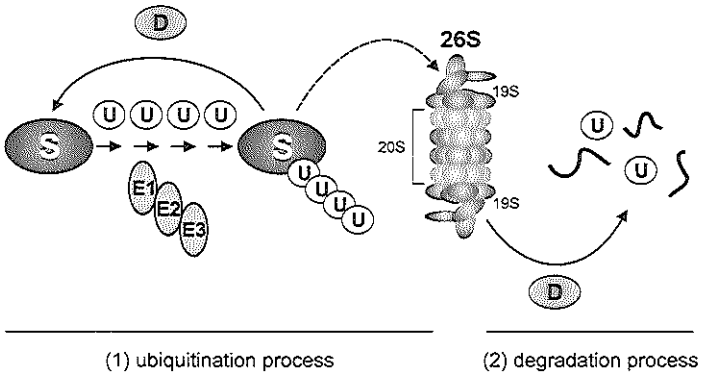

Figure 3. The ubiquitin/proteasome pathway. **(1)** Conjugation of ubiquitin (U) to the target protein substrate (S) generally requires the successive actions of three different enzymes: the ubiquitin-activating enzymes E1, the ubiquitin-conjugating enzymes E2, and the ligating enzymes E3. These enzymes are depicted as a single complex, but this is hypothetical. The subsequent E1, E2, and E3 activities couple the C-terminal carboxyl group of ubiquitin to a lysine residue of the substrate giving rise to a mono-ubiquitinated protein. Further ubiquitination of the mono-ubiquitin moiety results in a polyubiquitinated protein. **(2)** Degradation of the polyubiquitinated proteins are recognized by the 26S proteasome complex (composed of two 19S regulatory particles attached at each side to the 20S catalytic core), and intact ubiquitin is released from the peptide fragments by the action of deubiquitinating enzymes (D), most likely of the ubiquitin carboxyl-terminal hydrolases and ubiquitin-specific processing proteases. Model adapted from Baarends and coworkers (2000).

An important question concerns the identity of the mechanisms that underlie the high degree of specificity of the system: why are some proteins extremely stable while others are short-lived? Substrate recognition is governed by a large family of ubiquitin ligases that identify the substrates, bind them and catalyze their ubiquitination (Hochstrasser 2000; Jackson et al. 2000). But time and spatial regulation remain poorly understood. For instance, although many components of the ubiquitin/proteasome system are located in the nucleus and the cytosol, targets of the system are known to include membrane-anchored and even ER lumenal proteins. These proteins are thought to be "retro-transported" to the cytosol, ubiquitinated, and degraded by the proteasome (reviewed in Bonifacino and Weissman 1998; Plemper and Wolf 1999).

With the multitude of substrates available for targeting as well as processes involved, it is not surprising that aberrations in the pathway were recently implicated in the pathogenesis of many diseases, including certain malignancies and neurodegeneration. For example, Angelman's syndrome is

associated with a defect in the ubiquitin-protein ligase E3 enzyme E6-AP (Kishino et al. 1997). Other examples of neurodegenerative diseases are Alzheimer, Parkinson, and Creutzfeld-Jacob (reviewed in Mayer et al. 1996). Protein aggregates in ubiquitin- and proteasome-positive intranuclear inclusion bodies are found in Huntington disease and spinocerebellar ataxias (Cummings et al. 1998; Davies et al. 1997).

II.7.3 Interplay between spermatogenesis and the ubiquitin system

Since numerous proteins are regulated through ubiquitination, it is not surprising that general inhibition of the ubiquitin system frequently results in a rapid dysregulation of multiple cellular processes, and subsequently in apoptosis. Ubiquitination of histones is also observed in histone removal from chromatin during spermatogenesis (Agell et al. 1983; Nickel et al. 1987) and is a general phenomenon found in mammalian cell types. However, depending upon certain cell type-specific activities of the ubiquitin system, even a partial inhibition of ubiquitination may be lethal in some cells. For example, the turnover of nuclear proteins during the post-meiotic histone-to-protamine transition in male germ cells probably requires massive breakdown of histones and transition proteins, and thus places high demands on the ubiquitination machinery and proteasome.

In the mouse, quite a number of targeted gene mutations have been reported to lead to male infertility. With respect to the role of ubiquitination in spermatogenesis, inactivation of the mouse *HR6B* gene (encoding a mammalian homolog of the *S.cerevisiae* RAD6 ubiquitin-conjugating enzyme, involved in postreplication repair and damage-induced mutagenesis (Koken et al. 1991)) fails to cause a phenotype in the mouse with the exception of male-limited infertility (Roest et al. 1996). In *HR6B* knockout mice, both meiotic and post-meiotic germ cell development are affected, although the major consequences occur during spermatid nuclear condensation (Roest et al. 1996; Grootegoed et al. 1998). Surprisingly, mutations in the mouse *HR6A* gene (encoding the second mammalian homolog of *S.cerevisiae* RAD6) affect early embryonic development (maternal factor infertility), whereas *HR6A* knockout males are completely fertile (Roest et al. 1996; Grootegoed et al. 1998). Additional knockout mouse models with a gametogenic failure suggest that the ubiquitination machinery is also important for gametogenesis (Baarends et al. 2000). Most likely, different phases of mammalian spermatogenesis require different specialized activities of the ubiquitin system (Baarends et al. 2000).

Yeast RAD23 mRNA is induced fivefold during the meiotic prophase, coinciding with recombination (Madura and Prakash 1990). However, it is not known whether meiotic recombination is affected in these mutants since *rad23* mutants undergo sporulation and produce viable spores. The feature of meiotic-specific induction of RAD23 expression may be a preserved property of the gene, perhaps pointing to an involvement in meiotic recombination. Disruption of *mHR23B* in the mouse causes defective spermatogenesis, resulting in absence of developing germ cells and a Sertoli-cell-only phenotype. Further studies show that failure of spermatogenesis in *mHR23B*$^{-/-}$ animals occurs between E15.5 and day 15 after birth. The action of mHR23B may be involved in development of a normal population of gonocytes (precursors of spermatogonia), which is capable to support initiation of spermatogenesis. In addition, or alternatively, mHR23B may be required for the subsequent initiation phase of spermatogenesis which involves spermatogonial proliferation and differentiation, and entry into the meiotic prophase (see Chapter V for more detail).

II.8 References

Aboussekhra A, Biggerstaff M, Shivji MK, Vilpo JA, Moncollin V, Podust VN, Protic M, Hubscher U, Egly JM, and Wood RD (1995). Mammalian DNA nucleotide excision repair reconstituted with purified protein components. Cell *80*, 859-868.

Agell N, Chiva M, and Mezquita C (1983). Changes in nuclear content of protein conjugate histone H2A-ubiquitin during rooster spermatogenesis. FEBS Lett *155*, 209-212.

Ananthaswamy HN, Ouhtit A, Evans RL, Gorny A, Khaskina P, Sands AT, and Conti CJ (1999). Persistence of p53 mutations and resistance of keratinocytes to apoptosis are associated with the increased susceptibility of mice lacking the *XPC* gene to UV carcinogenesis. Oncogene *18*, 7395-7398.

Araki M, Masutani C, Takemura M, Uchida A, Sugasawa K, Kondoh J, Ohkuma Y, and Hanaoka F (2001). Centrosome protein centrin 2/caltractin 1 is part of the xeroderma pigmentosum group C complex that initiates global genome nucleotide excision repair. J Biol Chem *18665-18672*, 27.

Araujo SJ, Tirode F, Coin F, Pospiech H, Syvaoja JE, Stucki M, Hubscher U, Egly JM, and Wood RD (2000). Nucleotide excision repair of DNA with recombinant human proteins: definition of the minimal set of factors, active forms of TFIIH, and modulation by CAK. Genes Dev *14*, 349-359.

Baarends WM, van der Laan R, and Grootegoed JA (2000). Specific aspects of the ubiquitin system in spermatogenesis. J Endocrinol Invest *23*, 597-604.

Barnes DE, Tomkinson AE, Lehmann AR, Webster AD, and Lindahl T (1992). Mutations in the *DNA ligase* I gene of an individual with immunodeficiencies and cellular hypersensitivity to DNA-damaging agents. Cell *69*, 495-503.

Batty D, Rapic Otrin V, Levine AS, and Wood RD (2000). Stable binding of human XPC complex to irradiated DNA confers strong discrimination for damaged sites. J Mol Biol *300*, 275-290.

Berg RJ, de Vries A, van Steeg H, and de Gruijl FR (1997). Relative susceptibilities of *XPA* knockout mice and their heterozygous and wildtype littermates to UVB-induced skin cancer. Cancer Res *57*, 581-584.

Berg RJ, Rebel H, van der Horst GTJ, van Kranen HJ, Mullenders LHF, van Vloten WA, and de Gruijl FR (2000). Impact of global genome repair versus transcription-coupled repair on ultraviolet carcinogenesis in hairless mice. Cancer Res *60*, 2858-2863.

Berg RJ, Ruven HJ, Sands AT, de Gruijl FR, and Mullenders LHF (1998). Defective global genome repair in *XPC* mice is associated with skin cancer susceptibility but not with sensitivity to UVB induced erythema and edema. J Invest Dermatol *110*, 405-409.

Bohr VA, Smith CA, Okumoto DS, and Hanawalt PC (1985). DNA repair in an active gene: removal of pyrimidine dimers from the *DHFR* gene of CHO cells is much more efficient than in the genome overall. Cell *40*, 359-369.

Bonifacino JS, and Weissman AM (1998). Ubiquitin and the control of protein fate in the secretory and endocytic pathways. Annu Rev Cell Dev Biol *14*, 19-57.

Bootsma D, and Hoeijmakers JHJ (1993). DNA repair. Engagement with transcription. Nature *363*, 114-115.

Bootsma D, Kraemer KH, Cleaver JE, and Hoeijmakers JHJ (2001). Nucleotide excision repair syndromes: xeroderma pigmentosum, Cockayne syndrome, and trichothiodystrophy. *In:* Scriver CR, Beaudet, AL, Sly, WS, Valle, D Vogelstein and Kinzler (eds) The Metabolic and Molecular Bases of Inherited Disease, McGraw-Hill Book Co, New York *1*, 677-703.

Botta E, Nardo T, Broughton BC, Marinoni S, Lehmann AR, and Stefanini M (1998). Analysis of mutations in the *XPD* gene in Italian patients with trichothiodystrophy: site of mutation correlates with repair deficiency, but gene dosage appears to determine clinical severity. Am J Hum Genet *63*, 1036-1048.

Bradsher J, Coin F, and Egly JM (2000). Distinct roles for the helicases of TFIIH in transcript initiation and promoter escape. J Biol Chem *275*, 2532-2538.

Buschta-Hedayat N, Buterin T, Hess MT, Missura M, and Naegeli H (1999). Recognition of nonhybridizing base pairs during nucleotide excision repair of DNA. Proc Natl Acad Sci U S A *96*, 6090-6095.

Chau V, Tobias JW, Bachmair A, Marriott D, Ecker DJ, Gonda DK, and Varshavsky A (1989). A multiubiquitin chain is confined to specific lysine in a targeted short-lived protein. Science *243*, 1576-1583.

Cheo DL, Burns DK, Meira LB, Houle JF, and Friedberg EC (1999). Mutational inactivation of the xeroderma pigmentosum group C gene confers predisposition to 2-acetylaminofluorene-induced liver and lung cancer and to spontaneous testicular cancer in *Trp53-/-* mice. Cancer Res *59*, 771-775.

Cheo DL, Meira LB, Burns DK, Reis AM, Issac T, and Friedberg EC (2000). Ultraviolet B radiation-induced skin cancer in mice defective in the *Xpc*, *Trp53*, and *Apex* (*HAP1*) genes: genotype-specific effects on cancer predisposition and pathology of tumors. Cancer Res *60*, 1580-1584.

Cheo DL, Meira LB, Hammer RE, Burns DK, Doughty AT, and Friedberg EC (1996). Synergistic interactions between XPC and p53 mutations in double-mutant mice: neural tube abnormalities and accelerated UV radiation-induced skin cancer. Curr Biol *6*, 1691-1694.

Cheo DL, Ruven HJ, Meira LB, Hammer RE, Burns DK, Tappe NJ, van Zeeland A A, Mullenders LHF, and Friedberg EC (1997). Characterization of defective nucleotide excision repair in *XPC* mutant mice. Mutat Res *374*, 1-9.

Chu G, and Chang E (1988). Xeroderma pigmentosum group E cells lack a nuclear factor that binds to damaged DNA. Science *242*, 564-567.

Ciechanover A, Orian A, and Schwartz AL (2000). Ubiquitin-mediated proteolysis: biological regulation via destruction. Bioessays *22*, 442-451.

Citterio E, Vermeulen W, and Hoeijmakers JHJ (2000). Transcriptional healing. Cell *101*, 447-450.

Colella S, Nardo T, Mallery D, Borrone C, Ricci R, Ruffa G, Lehmann AR, and Stefanini M (1999). Alterations in the CSB gene in three Italian patients with the severe form of Cockayne syndrome (CS) but without clinical photosensitivity. Hum Mol Genet *8*, 935-941.

Conforti G, Nardo T, D'Incalci M, and Stefanini M (2000). Proneness to UV-induced apoptosis in human fibroblasts defective in transcription coupled repair is associated with the lack of Mdm2 transactivation. Oncogene *19*, 2714-2720.

Cooper PK, Nouspikel T, Clarkson SG, and Leadon SA (1997). Defective transcription-coupled repair of oxidative base damage in Cockayne syndrome patients from XP group G. Science *275*, 990-993.

Cummings CJ, Mancini MA, Antalffy B, DeFranco DB, Orr HT, and Zoghbi HY (1998). Chaperone suppression of aggregation and altered subcellular proteasome localization imply protein misfolding in SCA1. Nat Genet *19*, 148-154.

Datta A, Bagchi S, Nag A, Shiyanov P, Adami GR, Yoon T, and Raychaudhuri P (2001). The p48 subunit of the damaged-DNA binding protein DDB associates with the CBP/p300 family of histone acetyltransferase. Mutat Res *486*, 89-97.

Davies AA, Friedberg EC, Tomkinson AE, Wood RD, and West SC (1995). Role of the Rad1 and Rad10 proteins in nucleotide excision repair and recombination. J Biol Chem *270*, 24638-24641.

Davies SW, Turmaine M, Cozens BA, DiFiglia M, Sharp AH, Ross CA, Scherzinger E, Wanker EE, Mangiarini L, and Bates GP (1997). Formation of neuronal intranuclear inclusions underlies the neurological dysfunction in mice transgenic for the HD mutation. Cell *90*, 537-548.

de Boer J, de Wit J, van Steeg H, Berg RJ, Morreau H, Visser P, Lehmann AR, Duran M, Hoeijmakers JHJ, and Weeda G (1998a). A mouse model for the basal transcription/DNA repair syndrome trichothiodystrophy. Mol Cell *1*, 981-990.

de Boer J, Donker I, de Wit J, Hoeijmakers JHJ, and Weeda G(1998b) Disruption of the mouse xeroderma pigmentosum group D DNA repair/basal transcription gene results in preimplantation lethality. Cancer Res *58*, 89-94.

de Boer J, and Hoeijmakers JHJ (2000). Nucleotide excision repair and human syndromes. Carcinogenesis *21*, 453-460.

de Boer J, van Steeg H, Berg RJ, Garssen J, de Wit J, van Oostrum CT, Beems RB, van der Horst GTJ, van Kreijl CF, de Gruijl FR, and *et al.* (1999). Mouse model for the DNA repair/basal transcription disorder trichothiodystrophy reveals cancer predisposition. Cancer Res *59*, 3489-3494.

de Laat WL, Appeldoorn E, Sugasawa K, Weterings E, Jaspers NG, and Hoeijmakers JHJ (1998). DNA-binding polarity of human replication protein A positions nucleases in nucleotide excision repair. Genes Dev *12*, 2598-2609.

de Laat W, L Jaspers NG, and Hoeijmakers JHJ (1999). Molecular mechanism of nucleotide excision repair. Genes Dev *13*, 768-785.

De Silva IU, McHugh PJ, Clingen PH, and Hartley JA (2000). Defining the roles of nucleotide excision repair and recombination in the repair of DNA interstrand cross-links in mammalian cells. Mol Cell Biol *20*, 7980-7990.

de Vries A, Berg RJ, Wijnhoven S, Westerman A, Wester PW, van Kreijl CF, Capel P J, de Gruijl FR, van Kranen HJ, and van Steeg H (1998). *XPA*-deficiency in hairless mice causes a shift in skin tumor types and mutational target genes after exposure to low doses of UVB. Oncogene *16*, 2205-2212.

de Vries A, Gorgels TG, Berg RJ, Jansen GH, and Van Steeg H (1998). Ultraviolet-B induced hyperplasia and squamous cell carcinomas in the cornea of *XPA*-deficient mice. Exp Eye Res *67*, 53-59.

de Vries A, van Oostrom CT, Dortant PM, Beems RB, van Kreijl CF, Capel PJ, and van Steeg H (1997). Spontaneous liver tumors and benzo[a]pyrene-induced lymphomas in *XPA*-deficient mice. Mol Carcinog *19*, 46-53.

de Vries A, van Oostrom CT, Hofhuis FM, Dortant PM, Berg RJ, de Gruijl FR, Wester PW, van Kreijl CF, Capel PJ, van Steeg H, and *et al.* (1995). Increased susceptibility to ultraviolet-B and carcinogens of mice lacking the DNA excision repair gene *XPA*. Nature *377*, 169-173.

de Vries A, and van Steeg H (1996). *XPA* knockout mice. Semin Cancer Biol *7*, 229-2240.

Dieckmann T, Withers-Ward ES, Jarosinski MA, Liu CF, Chen IS, and Feigon J (1998). Structure of a human DNA repair protein UBA domain that interacts with HIV-1 Vpr. Nat Struct Biol *5*, 1042-1047.

Eisen JA, Sweder KS, and Hanawalt PC (1995). Evolution of the SNF2 family of proteins: subfamilies with distinct sequences and functions. Nucleic Acids Res *23*, 2715-2723.

Evans E, Fellows J, Coffer A, and Wood RD (1997a). Open complex formation around a lesion during nucleotide excision repair provides a structure for cleavage by human XPG protein. Embo J *16*, 625-638.

Evans E, Moggs JG, Hwang JR, Egly JM, and Wood RD (1997b). Mechanism of open complex and dual incision formation by human nucleotide excision repair factors. Embo J *16*, 6559-6573.

Ford JM, Baron EL, and Hanawalt PC (1998). Human fibroblasts expressing the human papillomavirus E6 gene are deficient in global genomic nucleotide excision repair and sensitive to ultraviolet irradiation. Cancer Res *58*, 599-603.

Friedberg EC (1996). Relationships between DNA repair and transcription. Annu Rev Biochem *65*, 15-42.

Friedberg EC, Bond JP, Burns DK, Cheo DL, Greenblatt MS, Meira LB, Nahari D, and Reis AM2000). Defective nucleotide excision repair in *xpc* mutant mice and its association with cancer predisposition. Mutat Res *459*, 99-108.

Friedberg EC, Cheo DL, Meira LB, and Reis AM (1999). Cancer predisposition in mutant mice defective in the *XPC* DNA repair gene. Prog Exp Tumor Res *35*, 37-52.

Friedberg EC, and Meira LB (2000). Database of mouse strains carrying targeted mutations in genes affecting cellular responses to DNA damage. Version 4. Mutat Res *459*, 243-274.

Friedberg EC, Walker GC, and Siede W (1995). DNA repair and mutagenesis. ASM Press, Washington DC.

Garssen J, van Steeg H, de Gruijl F, de Boer J, van der Horst GTJ, van Kranen H, van Loveren H, van Dijk M, Fluitman A, Weeda G, and Hoeijmakers JHJ (2000). Transcription-coupled and global genome repair differentially influence UV-B-induced acute skin effects and systemic immunosuppression. J Immunol *164*, 6199-6205.

Gillespie JM, and Marshall RC (1983). A comparison of the proteins of normal and trichothiodystrophic human hair. J Invest Dermatol *80*, 195-202.

Gillette TG, Huang W, Russell SJ, Reed SH, Johnston SA, and Friedberg EC (2001). The 19S complex of the proteasome regulates nucleotide excision repair in yeast. Genes Dev *15*, 1528-1539.

Glover MT, Niranjan N, Kwan JT, and Leigh IM (1994). Non-melanoma skin cancer in renal transplant recipients: the extent of the problem and a strategy for management. Br J Plast Surg *47*, 86-89.

Gowen LC, Avrutskaya AV, Latour AM, Koller BH, and Leadon SA (1998). BRCA1 required for transcription-coupled repair of oxidative DNA damage. Science *281*, 1009-1012.

Grootegoed JA, Baarends WM, Roest HP, and Hoeijmakers JHJ (1998). Knockout mouse model and gametogenic failure. Mol Cell Endocrinol *145*, 161-166.

Hanawalt PC, and Mellon, I1993). Stranded in an active gene. Curr Biol *3*, 67-69.

Hanawalt PC (1994). Transcription-coupled repair and human disease. Science *266*, 1957-1958.

Hanawalt PC, Donahue BA, and Sweder KS (1994). Repair and transcription. Collision or collusion? Curr Biol *4*, 518-521.

Harada YN, Shiomi N, Koike M, Ikawa M, Okabe M, Hirota S, Kitamura Y, Kitagawa M, Matsunaga T, Nikaido O, and Shiomi T (1999). Postnatal growth failure, short life span, and early

onset of cellular senescence and subsequent immortalization in mice lacking the xeroderma pigmentosum group G gene. Mol Cell Biol *19*, 2366-2372.

Henning KA, Li L, Iyer N, McDaniel LD, Reagan MS, Legerski R, Schultz RA, Stefanini M, Lehmann AR, Mayne LV, and *et al.* (1995). The Cockayne syndrome group A gene encodes a WD repeat protein that interacts with CSB protein and a subunit of RNA polymerase II TFIIH. Cell *82*, 555-564.

Hess MT, Schwitter U, Petretta M, Giese B, and Naegeli H (1997). Bipartite substrate discrimination by human nucleotide excision repair. Proc Natl Acad Sci U S A *94*, 6664-6669.

Hiyama H, Yokoi M, Masutani C, Sugasawa K, Maekawa T, Tanaka K, Hoeijmakers JHJ, and Hanaoka F (1999). Interaction of hHR23 with s5a. The ubiquitin-like domain of hhr23 mediates interaction with s5a subunit of 26s proteasome. J Biol Chem *274*, 28019-28025.

Hochstrasser M (2000). Evolution and function of ubiquitin-like protein-conjugation systems. Nat Cell Biol *2*, E153-E157.

Hofmann K, and Bucher P (1996). The UBA domain: a sequence motif present in multiple enzyme classes of the ubiquitination pathway. Trends Biochem Sci *21*, 172-173.

Holstege FC, van der Vliet PC, and Timmers HT (1996). Opening of an RNA polymerase II promoter occurs in two distinct steps and requires the basal transcription factors IIE and IIH. Embo J *15*, 1666-1677.

Houtsmuller AB, Rademakers S, Nigg AL, Hoogstraten D, Hoeijmakers JHJ, and Vermeulen W (1999). Action of DNA repair endonuclease ERCC1/XPF in living cells. Science *284*, 958-961.

Huang JC, and Sancar A (1994). Determination of minimum substrate size for human excinuclease. J Biol Chem *269*, 19034-19040.

Hwang BJ, Ford JM, Hanawalt PC, and Chu G (1999). Expression of the *p48* xeroderma pigmentosum gene is p53-dependent and is involved in global genomic repair. Proc Natl Acad Sci U S A *96*, 424-428.

Hwang BJ, Toering S, Francke U, and Chu G (1998). p48 Activates a UV-damaged-DNA binding factor and is defective in xeroderma pigmentosum group E cells that lack binding activity. Mol Cell Biol *18*, 4391-4399.

Ide F, Iida N, Nakatsuru Y, Oda H, Tanaka K, and Ishikawa T (2000). Mice deficient in the nucleotide excision repair gene *XPA* have elevated sensitivity to benzo[a]pyrene induction of lung tumors. Carcinogenesis *21*, 1263-1265.

Itin PH, and Pittelkow MR (1990). Trichothiodystrophy: review of sulfur-deficient brittle hair syndromes and association with the ectodermal dysplasias. J Am Acad Dermatol *22*, 705-717.

Itoh T, Fujiwara Y, Ono T, and Yamaizumi M (1995). UVS syndrome, a new general category of photosensitive disorder with defective DNA repair, is distinct from xeroderma pigmentosum variant and rodent complementation group I. Am J Hum Genet *56*, 1267-1276.

Iyer N, Reagan MS, Wu KJ, Canagarajah B, and Friedberg EC (1996). Interactions involving the human RNA polymerase II transcription/nucleotide excision repair complex TFIIH, the nucleotide excision repair protein XPG, and Cockayne syndrome group B (CSB) protein. Biochemistry *35*, 2157-2167.

Jacks T, Remington L, Williams BO, Schmitt EM, Halachmi S, Bronson RT, and Weinberg RA (1994). Tumor spectrum analysis in *p53*-mutant mice. Curr Biol *4*, 1-7.

Jackson DA, Balajee AS, Mullenders LHF, and Cook PR (1994). Sites in human nuclei where DNA damaged by ultraviolet light is repaired: visualization and localization relative to the nucleoskeleton. J Cell Sci *107*, 1745-1752.

Jackson PK, Eldridge AG, Freed E, Furstenthal L, Hsu JY, Kaiser BK, and Reimann JD (2000). The lore of the RINGs: substrate recognition and catalysis by ubiquitin ligases. Trends Cell Biol *10*, 429-439.

Jones CJ, and Wood RD (1993). Preferential binding of the xeroderma pigmentosum group A complementing protein to damaged DNA. Biochemistry *32*, 12096-12104.

Kastan MB, Onyekwere O, Sidransky D, Vogelstein B, and Craig RW (1991). Participation of p53 protein in the cellular response to DNA damage. Cancer Res *51*, 6304-6311.

Keeney S, Chang GJ, and Linn S (1993). Characterization of a human DNA damage binding protein implicated in xeroderma pigmentosum E. J Biol Chem *268*, 21293-21300.

Keeney S, Wein H, and Linn S (1992). Biochemical heterogeneity in xeroderma pigmentosum complementation group E. Mutat Res *273*, 49-56.

Kim C, Snyder RO, and Wold MS (1992). Binding properties of replication protein A from human and yeast cells. Mol Cell Biol *12*, 3050-3059.

Kishino T, Lalande M, and Wagstaff J (1997). UBE3A/E6-AP mutations cause Angelman syndrome. Nat Genet *15*, 70-73.

Koken MH, Reynolds P, Jaspers-Dekker I, Prakash L, Prakash S, Bootsma D, and Hoeijmakers JHJ (1991). Structural and functional conservation of two human homologs of the yeast DNA repair gene *RAD6*. Proc Natl Acad Sci U S A *88*, 8865-8869.

Kondo S, Fukuro S, Nishioka K, and Satoh Y (1992). Xeroderma pigmentosum: recent clinical and photobiological aspects. J Dermatol *19*, 690-695.

Kornitzer D, and Ciechanover A (2000). Modes of regulation of ubiquitin-mediated protein degradation. J Cell Physiol *182*, 1-11.

Kraemer KH (1997). Sunlight and skin cancer: another link revealed. Proc Natl Acad Sci U S A *94*, 11-14.

Kraemer KH, Lee MM, and Scotto J (1984). DNA repair protects against cutaneous and internal neoplasia: evidence from xeroderma pigmentosum. Carcinogenesis *5*, 511-514.

Kripke ML (1990). Effects of UV radiation on tumor immunity. J Natl Cancer Inst *82*, 1392-1396.

Kripke ML (1991). Immunological effects of ultraviolet radiation. J Dermatol *18*, 429-433.

Kuraoka I, Bender C, Romieu A, Cadet J, Wood RD, and Lindahl T (2000). Removal of oxygen free-radical-induced 5',8-purine cyclodeoxynucleosides from DNA by the nucleotide excision-repair pathway in human cells. Proc Natl Acad Sci U S A *97*, 3832-3837.

Laney JD, and Hochstrasser M (1999). Substrate targeting in the ubiquitin system. Cell *97*, 427-430.

Le Page F, Kwoh EE, Avrutskaya A, Gentil A, Leadon SA, Sarasin A, and Cooper PK (2000). Transcription-coupled repair of 8-oxoguanine: requirement for XPG, TFIIH, and CSB and implications for Cockayne syndrome. Cell *101*, 159-171.

Leadon SA, and Avrutskaya AV (1998). Requirement for DNA mismatch repair proteins in the transcription-coupled repair of thymine glycols in Saccharomyces cerevisiae. Mutat Res *407*, 177-187.

Leadon SA, and Cooper PK (1993). Preferential repair of ionizing radiation-induced damage in the transcribed strand of an active human gene is defective in Cockayne syndrome. Proc Natl Acad Sci U S A *90*, 10499-10503.

Legerski R, and Peterson C (1992). Expression cloning of a human DNA repair gene involved in xeroderma pigmentosum group C. Nature *359*, 70-73.

Leveillard T, Andera L, Bissonnette N, Schaeffer L, Bracco L, Egly JM, and Wasylyk B (1996). Functional interactions between p53 and the TFIIH complex are affected by tumour-associated mutations. Embo J *15*, 1615-1624.

Levine AJ (1997). p53, the cellular gatekeeper for growth and division. Cell *88*, 323-331.

Limoli CL, Giedzinski E, Morgan WF, and Cleaver JE (2000). Inaugural article: polymerase eta deficiency in the xeroderma pigmentosum variant uncovers an overlap between the S-phase checkpoint and double-strand break repair. Proc Natl Acad Sci U S A *97*, 7939-7946.

Ljungman M, and Zhang F (1996). Blockage of RNA polymerase as a possible trigger for UV light-induced apoptosis. Oncogene *13*, 823-831.

Ljungman M, Zhang F, Chen F, Rainbow AJ, and McKay BC (1999). Inhibition of RNA polymerase II as a trigger for the p53 response. Oncogene *18*, 583-592.

Lowe SW, Schmitt EM, Smith SW, Osborne BA, and Jacks T (1993). p53 is required for radiation-induced apoptosis in mouse thymocytes. Nature *362*, 847-849.

Madura K, and Prakash S (1990). Transcript levels of the Saccharomyes cerevisiae DNA repair gene RAD23 increase in response to UV light and in meiosis but remain constant in the mitotic cell cycle. Nucleic Acids Res *18*, 4737-4742.

Mariani E, Facchini A, Honorati MC, Lalli E, Berardesca E, Ghetti P, Marinoni S, Nuzzo F, Astaldi Ricotti GC, and Stefanini M (1992). Immune defects in families and patients with xeroderma pigmentosum and trichothiodystrophy. Clin Exp Immunol *88*, 376-382.

Martin G M, Austad SN, and Johnson TE (1996). Genetic analysis of ageing: role of oxidative damage and environmental stresses. Nat Genet *13*, 25-34.

Masutani C, Kusumoto R, Yamada A, Dohmae N, Yokoi M, Yuasa M, Araki M, Iwai S, Takio K, and Hanaoka F (1999). The *XPV* (xeroderma pigmentosum variant) gene encodes human DNA polymerase eta. Nature *399*, 700-704.

Masutani C, Sugasawa K, Yanagisawa J, Sonoyama T, Ui M, Enomoto T, Takio K, Tanaka K, van der Spek PJ, Bootsma D, and *et al.* (1994). Purification and cloning of a nucleotide excision repair complex involving the xeroderma pigmentosum group C protein and a human homolog of yeast RAD23. Embo J *13*, 1831-1843.

Matsumura Y, Nishigori C, Yagi T, Imamura S, and Takebe H (1998). Characterization of molecular defects in xeroderma pigmentosum group F in relation to its clinically mild symptoms. Hum Mol Genet *7*, 969-974.

Mayer RJ, Tipler C, Arnold J, Laszlo L, Al-Khedhairy A, Lowe J, and Landon M (1996). Endosome-lysosomes, ubiquitin and neurodegeneration. Adv Exp Med Biol *389*, 261-269.

McCuaig C, Marcoux D, Rasmussen JE, Werner MM, and Gentner NE (1993). Trichothiodystrophy associated with photosensitivity, gonadal failure, and striking osteosclerosis. J Am Acad Dermatol *28*, 820-826.

McKay BC, Ljungman M, and Rainbow AJ (1999). Potential roles for p53 in nucleotide excision repair. Carcinogenesis *20*, 1389-1396.

McWhir J Selfridge J, Harrison D J, Squires S, and Melton DW (1993). Mice with DNA repair gene *(ERCC-1)* deficiency have elevated levels of p53, liver nuclear abnormalities and die before weaning. Nat Genet *5*, 217-224.

Meira LB, Cheo DL, Hammer RE, Burns DK, Reis A, and Friedberg EC (1997). Genetic interaction between HAP1/REF-1 and p53. Nat Genet *17*, 145.

Meira LB, Reis AM, Cheo DL, Nahari D, Burns DK, and Friedberg EC (2001). Cancer predisposition in mutant mice defective in multiple genetic pathways: uncovering important genetic interactions. Mutat Res *477*, 51-58.

Mellon I, Spivak G, and Hanawalt PC (1987). Selective removal of transcription-blocking DNA damage from the transcribed strand of the mammalian *DHFR* gene. Cell *51*, 241-249.

Melton DW, Ketchen AM, Nunez F, Bonatti-Abbondandolo S, Abbondandolo A, Squires S, and Johnson RT (1998). Cells from ERCC1-deficient mice show increased genome instability and a reduced frequency of S-phase-dependent illegitimate chromosome exchange but a normal frequency of homologous recombination. J Cell Sci *111*, 395-404.

Miao F, Bouziane M, Dammann R, Masutani C, Hanaoka F, Pfeifer GP, and O'Connor TR (2000). 3-methyladenine-DNA glycosylase (MPG protein) interacts with human RAD23 proteins. J Biol Chem *275*, 28433-28438.

Mitchell DL, and Nairn RS (1989). The biology of the (6-4) photoproduct. Photochem Photobiol *49*, 805-819.

Miyauchi-Hashimoto H, Okamoto H, Tanaka K, and Horio T (1999). Ultraviolet radiation-induced suppression of natural killer cell activity is enhanced in xeroderma pigmentosum group A (*XPA*) model mice. J Invest Dermatol *112*, 965-970.

Miyauchi-Hashimoto H, Tanaka K, and Horio T (1996). Enhanced inflammation and immunosuppression by ultraviolet radiation in xeroderma pigmentosum group A (*XPA*) model mice. J Invest Dermatol *107*, 343-348.

Morison WL, Bucana C, Hashem N, Kripke ML, Cleaver JE, and German JL (1985). Impaired immune function in patients with xeroderma pigmentosum. Cancer Res *45*, 3929-3931.

Mu D, Hsu DS, and Sancar A (1996). Reaction mechanism of human DNA repair excision nuclease. J Biol Chem *271*, 8285-8294.

Mu D. and Sancar A (1997). Model for XPC-independent transcription-coupled repair of pyrimidine dimers in humans. J Biol Chem *272*, 7570-7573.

Mu D, Wakasugi M, Hsu DS, and Sancar A (1997). Characterization of reaction intermediates of human excision repair nuclease. J Biol Chem *272*, 28971-28979.

Mullenders LHF, van Kesteren AC, Bussmann CJ, van Zeeland AA, and Natarajan AT (1984). Preferential repair of nuclear matrix associated DNA in xeroderma pigmentosum complementation group C. Mutat Res *141*, 75-82.

Nagai A, Saijo M, Kuraoka I, Matsuda T, Kodo N, Nakatsu Y, Mimaki T, Mino M, Biggerstaff M, Wood RD, and *et al.* (1995). Enhancement of damage-specific DNA binding of XPA by interaction with the ERCC1 DNA repair protein. Biochem Biophys Res Commun *211*, 960-966.

Nakane H, Takeuchi S, Yuba S, Saijo M, Nakatsu Y, Murai H, Nakatsuru Y, Ishikawa T, Hirota S, Kitamura Y, and *et al.* (1995). High incidence of ultraviolet-B or chemical-carcinogen-induced skin tumours in mice lacking the xeroderma pigmentosum group A gene. Nature *377*, 165-168.

Nakatsu Y Asahina H, Citterio E, Rademakers S, Vermeulen W, Kamiuchi S, Yeo JP, Khaw MC, Saijo M, Kodo N, and *et al.* (2000). XAB2, a novel tetratricopeptide repeat protein involved in transcription-coupled DNA repair and transcription. J Biol Chem *275*, 34931-34937.

Nance MA, and Berry SA (1992). Cockayne syndrome: review of 140 cases. Am J Med Genet *42*, 68-84.

Nichols AF, and Sancar A (1992). Purification of PCNA as a nucleotide excision repair protein. Nucleic Acids Res *20*, 2441-2446.

Nickel BE, Roth SY, Cook RG, Allis CD, and Davie JR (1987). Changes in the histone H2A variant H2A.Z and polyubiquitinated histone species in developing trout testis. Biochemistry *26*, 4417-4421.

Nigg EA (1995). Cyclin-dependent protein kinases: key regulators of the eukaryotic cell cycle. Bioessays *17*, 471-480.

Norwood WF (1964). The Marinesco-Sjogren syndrome. J Pediatric *65*, 431-437.

Nunez F, Chipchase MD, Clarke AR, and Melton DW (2000). Nucleotide excision repair gene *(ERCC1)* deficiency causes G(2) arrest in hepatocytes and a reduction in liver binucleation: the role of p53 and p21. Faseb J *14*, 1073-1082.

O'Donovan A, Davies AA, Moggs JG, West SC, and Wood RD (1994). XPG endonuclease makes the 3' incision in human DNA nucleotide excision repair. Nature *371*, 432-435.

Ortolan TG, Tongaonkar P, Lambertson D, Chen L, Schauber C, and Madura K (2000). The DNA repair protein RAD23 is a negative regulator of multi-ubiquitin chain assembly. Nat Cell Biol *2*, 601-608.

Otrin VR, McLenigan M, Takao M, Levine AS, and Protic M (1997). Translocation of a UV-damaged DNA binding protein into a tight association with chromatin after treatment of mammalian cells with UV light. J Cell Sci *110*, 1159-1168.

Park CH, Mu D, Reardon JT, and Sancar A (1995). The general transcription-repair factor TFIIH is recruited to the excision repair complex by the XPA protein independent of the TFIIE transcription factor. J Biol Chem *270*, 4896-4902.

Partikian A, Olveczky B, Swaminathan R, Li Y, and Verkman AS (1998). Rapid diffusion of green fluorescent protein in the mitochondrial matrix. J Cell Biol *140*, 821-829.

Plemper RK, and Wolf DH (1999). Retrograde protein translocation: ERADication of secretory proteins in health and disease. Trends Biochem Sci *24*, 266-270.

Rapic Otrin V, Kuraoka I, Nardo T, McLenigan M, Eker AP, Stefanini M, Levine AS, and Wood RD (1998). Relationship of the xeroderma pigmentosum group E DNA repair defect to the chromatin and DNA binding proteins UV-DDB and replication protein A. Mol Cell Biol *18*, 3182-3190.

Reits EA, Benham AM, Plougastel B, Neefjes J, and Trowsdale J (1997). Dynamics of proteasome distribution in living cells. Embo J *16*, 6087-6094.

Reits EA, and Neefjes JJ (2001). From fixed to FRAP: measuring protein mobility and activity in living cells. Nat Cell Biol *3*, E145-E147.

Roest HP, van Klaveren J, de Wit J, van Gurp CG, Koken MH, Vermey M, van Roijen JH, Hoogerbrugge JW, Vreeburg JT, Baarends WM, and *et al.* (1996). Inactivation of the HR6B ubiquitin-conjugating DNA repair enzyme in mice causes male sterility associated with chromatin modification. Cell *86*, 799-810.

Russell SJ, Reed SH, Huang W, Friedberg EC, and Johnston SA (1999). The 19S regulatory complex of the proteasome functions independently of proteolysis in nucleotide excision repair. Mol Cell *3*, 687-695.

Saijo M, Kuraoka I, Masutani C, Hanaoka F, and Tanaka K (1996). Sequential binding of DNA repair proteins RPA and ERCC1 to XPA in vitro. Nucleic Acids Res *24*, 4719-4724.

Sands AT, Abuin A, Sanchez A, Conti CJ, and Bradley A (1995). High susceptibility to ultraviolet-induced carcinogenesis in mice lacking XPC. Nature *377*, 162-165.

Sargent RG, Rolig RL, Kilburn AE, Adair GM, Wilson JH, and Nairn RS (1997). Recombination-dependent deletion formation in mammalian cells deficient in the nucleotide excision repair gene *ERCC1*. Proc Natl Acad Sci U S A *94*, 13122-13127.

Satoh MS, Jones CJ, Wood RD, and Lindahl T (1993). DNA excision-repair defect of xeroderma pigmentosum prevents removal of a class of oxygen free radical-induced base lesions.Proc Natl Acad Sci U S A *90*, 6335-6339.

Satoh MS, and Lindahl T (1994). Enzymatic repair of oxidative DNA damage.Cancer Res *54*, 1899s-1901s.

Schaeffer L, Moncollin V, Roy R, Staub A, Mezzina M, Sarasin A, Weeda G, Hoeijmakers, JHJ, and Egly JM (1994). The ERCC2/DNA repair protein is associated with the class II BTF2/TFIIH transcription factor. Embo J *13*, 2388-2392.

Schaeffer L, Roy R, Humbert S, Moncollin V, Vermeulen W, Hoeijmakers JHJ, Chambon P, and Egly JM (1993). DNA repair helicase: a component of BTF2 (TFIIH) basic transcription factor. Science *260*, 58-63.

Schauber C, Chen L, Tongaonkar P, Vega I, Lambertson D, Potts W, and Madura K (1998). RAD23 links DNA repair to the ubiquitin/proteasome pathway. Nature *391*, 715-718.

Shannon M, Lamerdin JE, Richardson SL, McCutchen-Maloney SL, Hwang MH, Handel MA, Stubbs L, and Thelen MP (2000). Characterization of the mouse *Xpf* DNA repair gene and differential expression during spermatogenesis. Genomics *62*, 427-435.

Shivji KK, Kenny MK, and Wood RD (1992). Proliferating cell nuclear antigen is required for DNA excision repair. Cell *69*, 367-374.

Shivji MK, Eker AP, and Wood RD (1994). DNA repair defect in xeroderma pigmentosum group C and complementing factor from HeLa cells. J Biol Chem *269*, 22749-22757.

Shivji MK, Podust VN, Hubscher U, and Wood RD (1995). Nucleotide excision repair DNA synthesis by DNA polymerase epsilon in the presence of PCNA, RFC, and RPA. Biochemistry *34*, 5011-5017.

Sijbers AM, de Laat WL, Ariza RR, Biggerstaff M, Wei YF, Moggs JG, Carter KC, Shell BK, Evans E, de Jong MC, and *et al.* (1996). Xeroderma pigmentosum group F caused by a defect in a structure- specific DNA repair endonuclease. Cell *86*, 811-822.

Stefanini M, Lagomarsini P, Giliani S, Nardo T, Botta E, Peserico A, Kleijer WJ, Lehmann AR, and Sarasin A (1993a). Genetic heterogeneity of the excision repair defect associated with trichothiodystrophy. Carcinogenesis *14*, 1101-1105.

Stefanini M, Vermeulen W, Weeda G, Giliani S, Nardo T, Mezzina M, Sarasin A, Harper JI, Arlett CF, Hoeijmakers JH, and *et al.* (1993b). A new nucleotide excision repair gene associated with the disorder trichothiodystrophy. Am J Hum Genet *53*, 817-821.

Sugasawa K, Masutani C, Uchida A, Maekawa T, van der Spek PJ, Bootsma D, Hoeijmakers JHJ, and Hanaoka F (1996). hHR23B, a human RAD23 homolog, stimulates XPC protein in nucleotide excision repair *in vitro*. Mol Cell Biol *16*, 4852-4861.

Sugasawa K, Ng JMY, Masutani C, Iwai S, van der Spek PJ, Eker AP, Hanaoka F, Bootsma D, and Hoeijmakers JHJ (1998). Xeroderma pigmentosum group C protein complex is the initiator of global genome nucleotide excision repair. Mol Cell *2*, 223-232.

Sugasawa K, Ng JMY, Masutani C, Maekawa T, Uchida A, van der Spek PJ, Eker AP, Rademakers S, Visser C, Aboussekhra A, and *et al.* (1997). Two human homologs of RAD23 are functionally interchangeable in complex formation and stimulation of XPC repair activity. Mol Cell Biol *17*, 6924-6931.

Svejstrup JQ, Wang Z, Feaver WJ, Wu X, Bushnell DA, Donahue TF, Friedberg EC, and Kornberg RD (1995). Different forms of TFIIH for transcription and DNA repair: holo-TFIIH and a nucleotide excision repairosome. Cell *80*, 21-28.

Tanaka K, Satokata I, Ogita Z, Uchida T, and Okada Y (1989). Molecular cloning of a mouse DNA repair gene that complements the defect of group A xeroderma pigmentosum. Proc Natl Acad Sci U S A *86*, 5512-5516.

Tang JY, Hwang BJ, Ford JM, Hanawalt PC, and Chu G. (2000). Xeroderma pigmentosum p48 gene enhances global genomic repair and suppresses UV-induced mutagenesis. Mol Cell *5*, 737-744.

Tirode F, Busso D, Coin F, and Egly JM (1999). Reconstitution of the transcription factor TFIIH: assignment of functions for the three enzymatic subunits, XPB, XPD, and cdk7. Mol Cell *3*, 87-95.

Tomasevic G, Laurer HL, Mattiasson G, van Steeg H, Wieloch T, and McIntosh TK (2000). Delayed neuromotor recovery and increased cognitive dysfunction following experimental brain trauma in mice lacking the DNA repair gene *XPA*. In: Chapter 5, Thesis Lund University, Sweden.

Troelstra C, van Gool A, de Wit J, Vermeulen W, Bootsma D, and Hoeijmakers JHJ (1992). ERCC6, a member of a subfamily of putative helicases, is involved in Cockayne's syndrome and preferential repair of active genes. Cell *71*, 939-953.

van der Horst GTJ, van Steeg H, Berg RJ, van Gool AJ, de Wit J, Weeda G, Morreau H, Beems RB, van Kreijl CF, de Gruijl FR, and *et al.* (1997). Defective transcription-coupled repair in Cockayne syndrome B mice is associated with skin cancer predisposition. Cell *89*, 425-435.

van der Spek PJ, Eker A, Rademakers S, Visser C, Sugasawa K, Masutani C, Hanaoka F, Bootsma D, and Hoeijmakers JHJ (1996). XPC and human homologs of RAD23: intracellular localization and relationship to other nucleotide excision repair complexes. Nucleic Acids Res *24*, 2551-2559.

van Duin M, Vredeveldt G, Mayne LV, Odijk H, Vermeulen W, Klein B, Weeda G, Hoeijmakers JHJ, Bootsma D, and Westerveld A (1989). The cloned human DNA excision repair gene *ERCC-1* fails to correct xeroderma pigmentosum complementation groups A through I. Mutat Res *217*, 83-92.

van Gool AJ, Citterio E, Rademakers S, van Os R, Vermeulen W, Constantinou A, Egly JM, Bootsma D, and Hoeijmakers JHJ (1997a). The Cockayne syndrome B protein, involved in transcription-coupled DNA repair, resides in an RNA polymerase II-containing complex. Embo J *16*, 5955-5965.

van Gool AJ, van der Horst GTJ, Citterio E, and Hoeijmakers JHJ (1997b). Cockayne syndrome: defective repair of transcription? Embo J *16*, 4155-4162.

van Hoffen A, Venema J, Meschini R, van Zeeland AA, and Mullenders LHF (1995). Transcription-coupled repair removes both cyclobutane pyrimidine dimers and 6-4 photoproducts with equal efficiency and in a sequential way from transcribed DNA in xeroderma pigmentosum group C fibroblasts. Embo J *14*, 360-367.

van Oosten M, Rebel H, Friedberg EC, van Steeg H, van der Horst GTJ, van Kranen HJ, Westerman A, van Zeeland AA, Mullenders LHF, and de Gruijl FR (2000). Differential role of transcription-coupled repair in UVB-induced G2 arrest and apoptosis in mouse epidermis. Proc Natl Acad Sci U S A *97*, 11268-11273.

van Oosterwijk MF, Versteeg A, Filon R, van Zeeland AA, and Mullenders LHF (1996). The sensitivity of Cockayne's syndrome cells to DNA-damaging agents is not due to defective transcription-coupled repair of active genes. Mol Cell Biol *16*, 4436-4444.

van Oostrom CT, Boeve M, van Den Berg J, de Vries A, Dolle ME, Beems RB, van Kreijl CF, Vijg J, and van Steeg H (1999). Effect of heterozygous loss of p53 on benzo[a]pyrene-induced mutations and tumors in DNA repair-deficient *XPA* mice. Environ Mol Mutagen *34*, 124-130.

van Oostrom CT, de Vries A, Verbeek SJ, van Kreijl CF, and van Steeg H. (1994). Cloning and characterization of the mouse *XPAC* gene. Nucleic Acids Res *22*, 11-14.

van Steeg H, Klein H, Beems RB, and van Kreijl CF (1998). Use of DNA repair-deficient XPA transgenic mice in short-term carcinogenicity testing. Toxicol Pathol *26*, 742-749.

van Steeg H, Mullenders LHF, and Vijg J (2000). Mutagenesis and carcinogenesis in nucleotide excision repair-deficient *XPA* knock out mice. Mutat Res *450*, 167-180.

Varshavsky A (1997). The ubiquitin system. Trends Biochem Sci *22*, 383-387.

Venema J, Mullenders LHF, Natarajan AT, van Zeeland AA, and Mayne LV (1990a). The genetic defect in Cockayne syndrome is associated with a defect in repair of UV-induced DNA damage in transcriptionally active DNA. Proc Natl Acad Sci U S A *87*, 4707-4711.

Venema J, van Hoffen A, Karcagi V, Natarajan AT, van Zeeland AA, and Mullenders LHF (1991). Xeroderma pigmentosum complementation group C cells remove pyrimidine dimers selectively from the transcribed strand of active genes. Mol Cell Biol *11*, 4128-4134.

Venema J, van Hoffen A, Natarajan AT, van Zeeland AA, and Mullenders LHF (1990b). The residual repair capacity of xeroderma pigmentosum complementation group C fibroblasts is highly specific for transcriptionally active DNA. Nucleic Acids Res *18*, 443-448.

Verhage R, Zeeman AM, de Groot N, Gleig F, Bang DD, van de Putte P, and Brouwer J (1994). The *RAD7* and *RAD16* genes, which are essential for pyrimidine dimer removal from the silent mating type loci, are also required for repair of the nontranscribed strand of an active gene in *Saccharomyces cerevisiae*. Mol Cell Biol *14*, 6135-6142.

Vermeulen W, Bergmann E, Auriol J, Rademakers S, Frit P, Appeldoorn E, Hoeijmakers JHJ, and Egly JM (2000). Sublimiting concentration of TFIIH transcription/DNA repair factor causes TTD-A trichothiodystrophy disorder. Nat Genet *26*, 307-313.

Vermeulen W, Scott RJ, Rodgers S, Muller HJ, Cole J, Arlett CF, Kleijer WJ, Bootsma D, Hoeijmakers JHJ, and Weeda G (1994a). Clinical heterogeneity within xeroderma pigmentosum associated with mutations in the DNA repair and transcription gene *ERCC3*. Am J Hum Genet *54*, 191-200.

Vermeulen W, van Vuuren AJ, Chipoulet M, Schaeffer L, Appeldoorn E, Weeda G, Jaspers NG, Priestley A, Arlett CF, Lehmann AR, and *et al.* (1994b). Three unusual repair deficiencies associated with transcription factor BTF2(TFIIH): evidence for the existence of a transcription syndrome. Cold Spring Harb Symp Quant Biol *59*, 317-329.

Volker M, Moné MJ, Karmakar P, Hoffen A, SchulW, Vermeulen W, Hoeijmakers JHJ, van Driel R, Zeeland AA, and Mullenders LHF (2001). Sequential assembly of the nucleotide excision repair factors *in vivo*. Mol Cell *8*, 213-224.

Wakasugi M, Reardon JT, and Sancar A (1997). The non-catalytic function of XPG protein during dual incision in human nucleotide excision repair. J Biol Chem *272*, 16030-16034.

Wang XW, Vermeulen W, Coursen JD, Gibson M, Lupold SE, Forrester K, Xu G, Elmore L, Yeh H, Hoeijmakers JHJ, and Harris CC (1996). The XPB and XPD DNA helicases are components of the p53-mediated apoptosis pathway. Genes Dev *10*, 1219-1232.

Wang XW, Yeh H, Schaeffer L, Roy R, Moncollin V, Egly JM, Wang Z, Freidberg EC, Evans MK, Taffe BG, and *et al.* (1995). p53 modulation of TFIIH-associated nucleotide excision repair activity. Nat Genet *10*, 188-195.

Watkins JF, Sung P, Prakash L, and Prakash S (1993). The Saccharomyces cerevisiae DNA repair gene RAD23 encodes a nuclear protein containing a ubiquitin-like domain required for biological function. Mol Cell Biol *13*, 7757-7765.

Weeda G, Donker I, de Wit J, Morreau H, Janssens R, Vissers CJ, Nigg A, van Steeg H, Bootsma D, and Hoeijmakers JHJ (1997). Disruption of mouse *ERCC1* results in a novel repair syndrome with growth failure, nuclear abnormalities and senescence. Curr Biol *7*, 427-439.

Westerveld A, Hoeijmakers JHJ, van Duin M, de Wit J, Odijk H, Pastink A, Wood RD, and Bootsma D (1984). Molecular cloning of a human DNA repair gene. Nature *310*, 425-429.

White J, and Stelzer E (1999). Photobleaching GFP reveals protein dynamics inside live cells. Trends Cell Biol *9*, 61-65.

Wijnhoven SW, Kool HJ, Mullenders LHF, Slater R, van Zeeland AA, and Vrieling H (2001). DMBA-induced toxic and mutagenic responses vary dramatically between NER-deficient *Xpa*, *Xpc* and *Csb* mice. Carcinogenesis *22*, 1099-1106.

Winkler GS, Araujo SJ, Fiedler U, Vermeulen W, Coin F, Egly JM, Hoeijmakers JHJ, Wood RD, Timmers HT, and Weeda G (2000). TFIIH with inactive XPD helicase functions in transcription initiation but is defective in DNA repair. J Biol Chem *275*, 4258-4266.

Winkler GS, and Hoeijmakers, JHJ (1998). From a DNA helicase to brittle hair. Nat Genet *20*, 106-107.

Withers-Ward ES, Jowett JB, Stewart SA, Xie YM, Garfinkel A, Shibagaki Y, Chow SA, Shah N, Hanaoka F, Sawitz DG, and *et al.* (1997). Human immunodeficiency virus type 1 Vpr interacts with HHR23A, a cellular protein implicated in nucleotide excision DNA repair. J Virol *71*, 9732-9742.

Withers-Ward, ES, Mueller, TD, Chen, IS, and Feigon J (2000). Biochemical and structural analysis of the interaction between the UBA(2) domain of the DNA repair protein HHR23A and HIV-1 Vpr. Biochemistry *39*, 14103-14112.

Wold MS (1997). Replication protein A: a heterotrimeric, single-stranded DNA-binding protein required for eukaryotic DNA metabolism. Annu Rev Biochem *66*, 61-92.

Wood RD (1999). DNA damage recognition during nucleotide excision repair in mammalian cells. Biochimie *81*, 39-44.

Wood RD, Mitchell M, Sgouros J, and Lindahl T (2001). Human DNA repair genes. Science *291*, 1284-1289.

Yamaizumi M, and Sugano T (1994). UV-induced nuclear accumulation of p53 is evoked through DNA damage of actively transcribed genes independent of the cell cycle. Oncogene *9*, 2775-2284.

Yokoi M, Masutani C, Maekawa T, Sugasawa K, Ohkuma Y, and Hanaoka F (2000). The xeroderma pigmentosum group C protein complex XPC-HR23B plays an important role in the recruitment of transcription factor IIH to damaged DNA. J Biol Chem *275*, 9870-9875.

Chapter

III

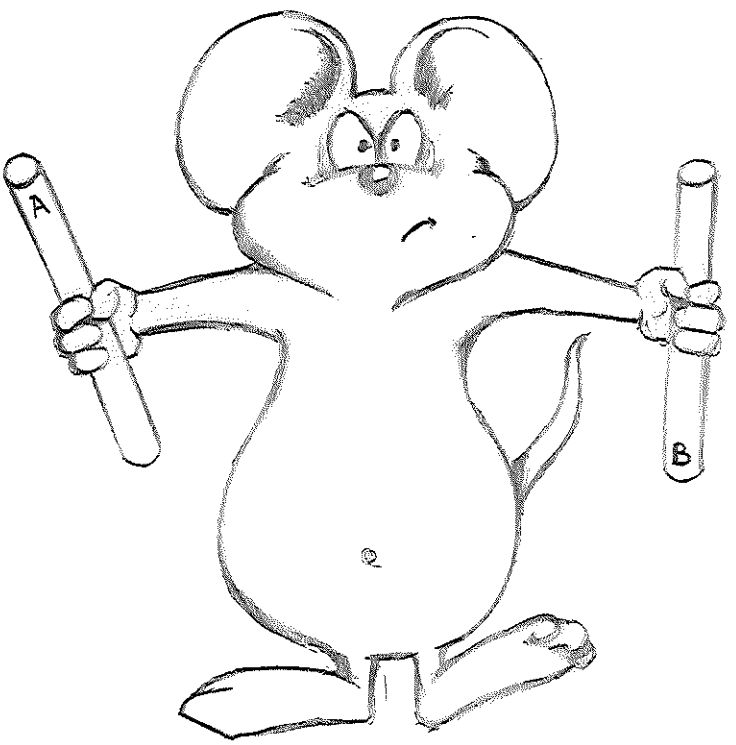

Two Human Homologs of RAD23 Are Functionally Interchangeable in Complex Formation and Stimulation of XPC Repair Activity

Kaoru Sugasawa[1,2], Jessica M. Y. Ng[1] ,Chikahide[3], Takafumi Maekawa[3], Akido Uchida[3], Peter J. van der Spek[1,5], André P. M. Eker[1], Suzanne Rademakers[1], Cecile Visser[1], Abdelilah Aboussekhra[4], Richard D. Wood[4,6], Fumio Hanaoka[2,3], Dirk Bootsma[1] and Jan H. J. Hoeijmakers[1]

[1]Department of Cell Biology and Genetics, Medical Genetic Centre, Erasmus University, P.O. Box 1738, 3000 DR Rotterdam, The Netherlands

[2]Cellular Physiology Laboratory, The Institute of Physical and Chemical Research (RIKEN), 2-1 Hirosawa, Wako, Saitama 351-01, Japan

[3]Institute for Molecular and Cellular Biology, Osaka University, 1-3 Yamada-oka, Suita, Osaka 565, Japan

[4]Imperial Cancer Research Fund, Clare Hall Laboratories, South Mimms, Herts, EN6 3LD, United Kingdom

[5]Present address: N.V. Organon/Akzo Nobel, Target Discovery Unit, P.O. Box 20, 5340 BH Oss, The Netherlands

[6]Present address: Clare Hall Laboratories, University of Pittsburgh Cancer Institute, S867 Scaifihall, Box 100, Pittsburgh, PA, 15260 USA

Summary

XPC-hHR23B protein complex is specifically involved in nucleotide excision repair (NER) of DNA lesions on transcriptionally inactive sequences as well as the non-transcribed strand of active genes. Here we demonstrate that not only highly purified recombinant hHR23B (rhHR23B), but also a second human homolog of the *Saccharomyces cerevisiae* RAD23 repair protein, hHR23A, stimulates the *in vitro* repair activity of recombinant human XPC (rhXPC), revealing functional redundancy between these human RAD23 homologs. Co-precipitation experiments using His-tagged rhHR23 as well as sedimentation velocity analysis showed that both rhHR23 proteins *in vitro* reconstitute a physical complex with rhXPC. Both complexes were more active than free rhXPC, indicating that complex assembly is required for the stimulation. rhHR23B was shown to stimulate an early stage of NER at or prior to incision. Furthermore, both rhHR23 proteins function in a defined NER system reconstituted with purified proteins, indicating direct involvement of hHR23 proteins in the DNA repair reaction via interaction with XPC.

Introduction

Nucleotide excision repair (NER) is the main pathway for cells to remove DNA lesions caused by UV-irradiation as well as various chemical mutagens (Friedberg et al. 1995). The molecular mechanism of NER has been extensively investigated in *Escherichia coli* (van Houten 1990; Liu and Sancar 1992; Grossman and Thiagalingam 1993; Hoeijmakers 1993). Based on studies with this prokaryotic system, the NER reaction could be dissected into several steps: (i) recognition of DNA damage, probably accompanied by chromatin remodelling, (ii) introduction of asymmetric single-strand breaks on both sides of the injury, (iii) removal of the short oligonucleotide containing the lesion, (iv) gap filling DNA synthesis by DNA polymerases, and (v) re-sealing of the resulting nicks by DNA ligase. Although some general features of the eukaryotic NER mechanism are similar to the prokaryotic system, there are many important differences. Only six *E.coli* proteins (i.e. UvrA, UvrB, UvrC, UvrD, DNA polymerase I and DNA ligase) are required to accomplish the core of the NER reaction *in vitro*. The eukaryotic NER system, however, appears to be much more complex, involving at least 20 factors (Hoeijmakers 1994; Wood 1996).

Impaired NER activity has been found to be associated with several rare autosomal recessive human disorders, including xeroderma pigmentosum (XP), Cockayne syndrome (CS) and trichothiodystrophy (TTD) (Bootsma et al. 1997). By cell fusion so far, seven XP (XP-A to G), two CS (CS-

A and B) and three TTD (TTD-A, XP-B and XP-D) NER-deficient complementation groups have been identified. Many mammalian NER genes have been cloned using either mutant fibroblasts from patients or NER-deficient, UV-sensitive Chinese hamster ovary cells (Boulikas 1996). For some of these genes, the possible role in the NER reaction has been suggested on the basis of their amino acid sequence as well as biochemical properties of the isolated gene products. On the other hand, additional factors involved in the mammalian NER have been identified from extensive analyses of cell-free NER systems, and some models for the eukaryotic NER mechanism have been proposed (reviewed in Sancar 1996 and Wood 1996). Several laboratories have recently succeeded in reconstitution of the core of eukaryotic NER reactions with purified proteins (Aboussekhra et al. 1995; Guzder et al. 1995b; Mu et al. 1995).

XPC protein is involved in NER of DNA lesions on transcriptionally inactive sequences as well as the non-transcribed strand of active genes (Venema et al. 1990 and 1991), and is required for *in vitro* NER of many types of DNA lesions (Masutani et al. 1994; Shivji et al.1994). However, certain kinds of lesions could be repaired without XPC *in vitro* (Mu et al. 1996), and the precise role of XPC in the 'global genome repair' NER subpathway remains to be elucidated. Human XPC protein was found to be tightly complexed *in vivo* with hHR23B (*h*uman *H*omolog of *R*AD23), which shows overall homology to yeast NER factor RAD23 (Masutani et al. 1994). Unlike yeast cells, a second RAD23 homolog, designated HR23A, has been identified in human (Masutani et al. 1994) as well as murine cells (van der Spek et al. 1996b). The *RAD23* gene has thus been duplicated during eukaryotic evolution. Indirect immunofluorescence studies revealed that XPC and both hHR23 proteins are predominantly localized in the nucleus (van der Spek et al. 1996). Although XPC protein is bound to hHR23B in a quantitative manner, hHR23B is much more abundant than XPC, so that a majority of hHR23B is present in a free form *in vivo* (Sugasawa et al. 1996; van der Spek et al. 1996). Both the *RAD23* gene duplication and the presence of two forms of hHR23B suggest that the protein may have multiple functions. Despite the overall sequence homology of the two human RAD23 homologs, almost all XPC molecules appear to be complexed *in vivo* with hHR23B, not with hHR23A.

Using a reconstituted *in vitro* NER system devoid of endogenous XPC and hHR23B, we have previously shown that recombinant hHR23B protein (rhHR23B) significantly stimulates the activity of recombinant hXPC protein (rhXPC) (Sugasawa et al. 1996). In the accompanying paper, we determined a domain in hHR23B that is responsible for XPC-binding as well as its

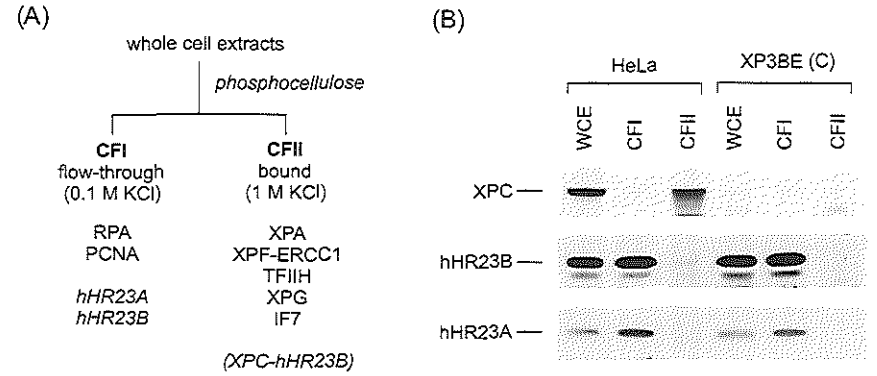

Figure 1. Depletion of endogenous XPC and hHR23B proteins from human whole cell extracts. **(A)** Scheme of phosphocellulose fractionation of human whole cell extracts. **(B)** Whole cell extracts from NER-proficient HeLa cells and XP group C cells (XP3BE) were fractionated on phosphocellulose as illustrated in A. The presence of endogenous XPC, hHR23B and hHR23A proteins in each fraction was examined by immunoblotting using polyclonal antibodies raised against each protein. 40 μg of whole cell extract protein (WCE) and 20 μg protein of CFI and CFII were loaded onto each lane.

stimulatory activity (Masutani et al. 1997). Because the amino acid sequence of this domain is well conserved between the two human RAD23 homologs, the XPC-binding and stimulating activities of hHR23A have been of interest. Here we document and characterize the XPC-stimulating activity of both hHR23 proteins expressed in *E.coli*.

Results

Both hHR23 proteins stimulate the activity of XPC protein in fractionated *XP-C* cell extracts

To detect XPC-stimulating activity of recombinant hHR23B protein, we have previously reported a reconstituted *in vitro* NER system from which endogenous XPC as well as hHR23B were depleted (Sugasawa et al. 1996). This assay system is based on the fact that, when the *XP-C* whole cell extract is fractionated on phosphocellulose as shown in Figure 1A, the bound fraction (CFII) is devoid of both XPC and hHR23B (Figure 1B). Although *XP-C* cells still express hHR23B protein as a free form, all of the hHR23B is recovered in the flow-through fraction (CFI). Immunoblotting analysis revealed that hHR23A is also recovered in CFI and can not be detected in CFII upon the same fractionation, regardless of the presence or absence of XPC expression (Figure 1B). Because two purified NER proteins, replication

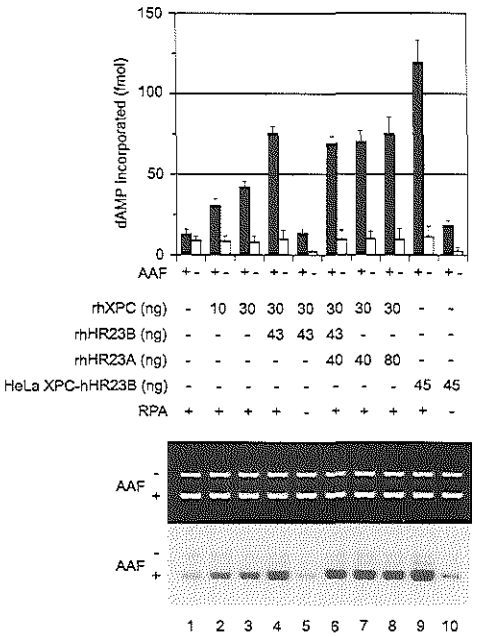

Figure 2. Stimulation of *in vitro* NER reactions by rhHR23 proteins. Plasmid DNA substrates (AAF-damaged and undamaged: each 250 ng) were incubated at 30°C for 90 min with CFII from XP-C cells (100 μg) and indicated purified proteins under standard conditions for *in vitro* NER reactions (see Experimental Procedures). After addition of PCNA (25 ng) and [α-^{32}P]dATP (74 kBq), incubation was continued at 30°C for 15 min. DNA samples were purified, digested with *Bam*HI, and then subjected to agarose gel electrophoresis. Ethidium bromide stained photograph and autoradiogram of the gel are shown. Incorporation of dAMP into each DNA band was calculated and depicted as a graph. The average values and standard errors were calculated from two independent experiments. (*solid bars*) incorporation in damaged plasmid; (*open bars*) incorporation in undamaged control plasmid.

protein A (RPA) and proliferating cell nuclear antigen (PCNA), are sufficient to functionally substitute for CFI in reconstitution of the cell-free NER system (Shivji et al. 1992), both endogenous hHR23 proteins present in the *XP-C* cell extracts can be depleted by this substitution. Thus, reconstitution of NER reactions using the XP-C CFII, purified RPA and PCNA enabled us to test whether the purified recombinant hHR23A could functionally replace hHR23B in this reconstituted system. A two-stage reaction protocol was used for this experiment. A mixture of AAF-damaged and undamaged DNA substrates was incubated with CFII from *XP-C* cells and purified RPA, in the presence or absence of rhXPC, rhHR23B and rhHR23A. During this first incubation, oligonucleotides containing AAF-adducts can be excised from

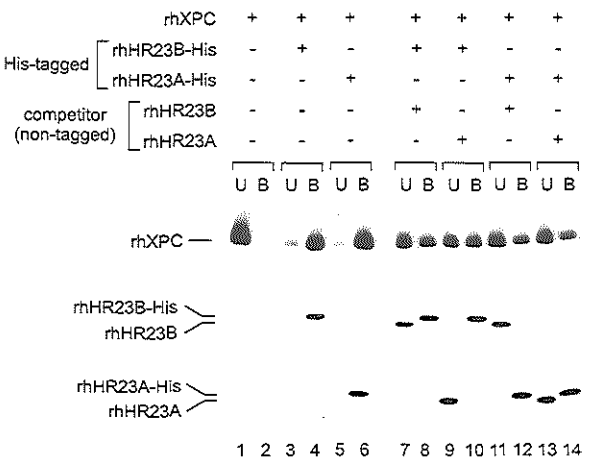

Figure 3. Both rhHR23 proteins bind to rhXPC. rhXPC (0.25 pmol) was incubated on ice for 1 h with various combination of 2.5 pmol each of His-tagged or non-tagged rhHR23 proteins as indicated above lanes. Nickel-chelating Sepharose was added and His-tagged proteins were pulled down by centrifugation after additional 1-h incubation. Unbound (U) and bound (B) materials were subjected to SDS-PAGE (9% polyacrylamide gels). The presence of XPC (*upper panel*), hHR23B (*middle panel*) and hHR23A (*lower panel*) in each fraction was assessed by immunoblotting. For detection of hHR23A and hHR23B, antibodies raised against synthetic polypeptides corresponding to a unique sequence in each protein were used (Masutani et al. 1997).

plasmid DNA substrates, when all incision proteins are present. In the second stage, PCNA and radioactive dATP were added to allow DNA repair synthesis by DNA polymerases and to label repair patches. As shown in Figure 2, rhXPC alone supported DNA repair synthesis up to 3-fold over the background DNA synthesis (lane 3). In the presence of the same amount of rhXPC, addition of non-tagged rhHR23B gave a highly reproducible stimulation of repair synthesis to 6-fold over background (lane 4), although the repair activity was significantly lower than that achieved with the authentic XPC-hHR23B complex purified from HeLa cells (lane 9). As expected, the repair reaction was dependent on the presence of RPA (lanes 5 and 10). Interestingly, rhHR23A could also stimulate the rhXPC activity to a similar extent as rhHR23B (lanes 7 and 8). No further stimulation was observed when both hHR23 proteins were added in one reaction with rhXPC (lane 6). These data suggest that hHR23A can functionally substitute for hHR23B in terms of the XPC-stimulation *in vitro*.

hHR23 proteins stimulate XPC protein via complex formation

To assess complex assembly between rhXPC and rhHR23A, a His-tagged version of recombinant rhHR23 proteins (rhHR23-His) was used to co-precipitate rhXPC with nickel-chelating Sepharose. As shown in Figure 3, rhXPC itself did not bind to the nickel-beads (lanes 1 and 2). In the presence of appropriate amounts of either rhHR23B-His or rhHR23A-His, however, rhXPC was co-precipitated almost completely (lanes 4 and 6), indicating that also rhHR23A is able to form a physical complex with rhXPC. To compare the affinity of the two rhHR23 proteins for rhXPC, non-tagged rhHR23 proteins were included as a competitor in the binding reactions. When equimolar amounts of non-tagged and His-tagged rhHR23B were incubated with rhXPC, about 50% of rhXPC was competed out from rhHR23B-His (lanes 7 and 8). rhHR23A could compete for rhXPC-binding with rhHR23B-His to a similar extent (lanes 9 and 10), indicating that both rhHR23 proteins have comparable affinity for rhXPC. Since non-tagged rhHR23A was hardly co-precipitated with the rhXPC-rhHR23B-His complex (see lane 10), formation of a ternary complex involving rhXPC, rhHR23B and rhHR23A is unlikely. Instead, the two rhHR23 proteins bind to rhXPC in a competitive manner and, most likely, in a 1:1 ratio. Essentially the same results were obtained with rhHR23A-His (lanes 11-14), although slightly more rhXPC was competed out by non-tagged proteins when compared with rhHR23B-His.

The reconstitution of rhXPC-rhHR23 complexes were further analyzed by sedimentation through glycerol gradients. As shown in Figure 4, free rhXPC (panel A) and free rhHR23B (panel B) sedimented with peaks around 5.6S and 2.5S, respectively. When rhXPC was pre-bound to rhHR23B, the position of rhXPC peak was slightly shifted toward the bottom of the gradient, up to around 6.3S (panel C). This is largely consistent with the S value determined for XPC-hHR23B complex purified from HeLa cells (6.2S in Ref. Masutani et al. 1994 and 6.1S in Ref. Shivji et al.1994). In the same gradient, rhHR23B was divided into two peaks: one coinciding with free rhHR23B, and the other with rhXPC, indicating formation of a physical complex between rhXPC and rhHR23B. Similar results were obtained with rhXPC and rhHR23A, as expected (see panels D and E). When the three recombinant proteins were pre-incubated, both rhHR23 proteins were found in complex forms (panel F), in agreement with the results of co-precipitation experiments shown in Figure 3.

To assess whether the complex is responsible for the XPC stimulation, the peak fractions of free rhXPC and rhXPC-rhHR23 complexes were assayed for repair activity. As shown in Figure 5A, these three peak fractions contained a comparable concentration of rhXPC. When the same volume of

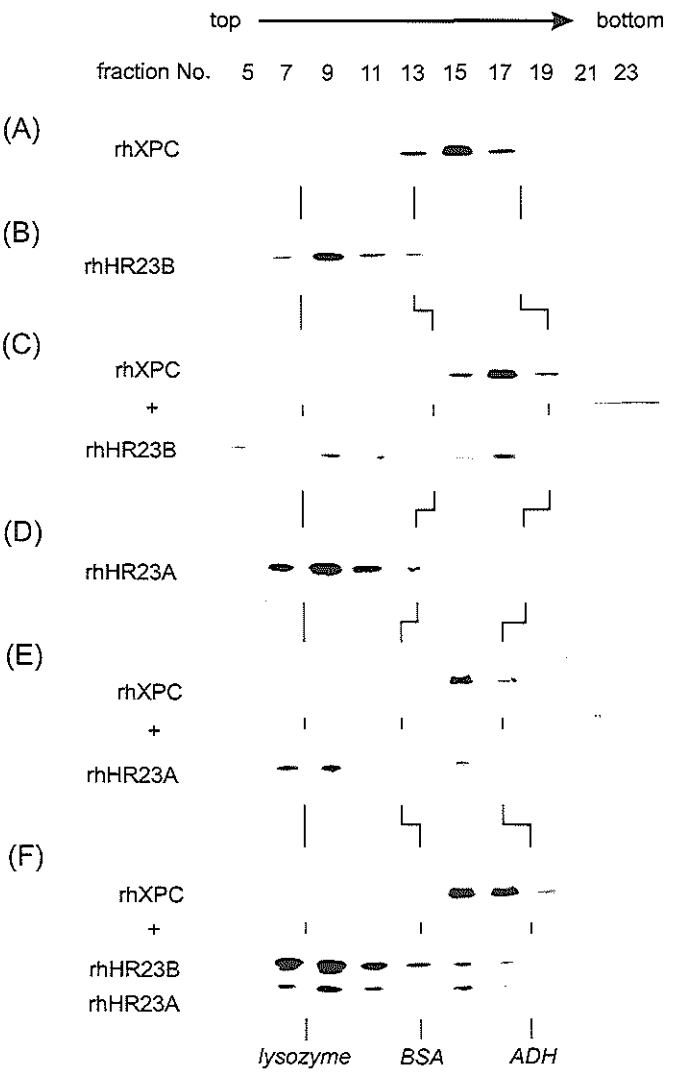

Figure 4. *In vitro* reconstitution of rhXPC-rhHR23 complexes. Indicated protein samples were fractionated through 15-35% glycerol density gradients as described in Experimental Procedures. For mixtures of rhXPC and rhHR23, the samples were pre-incubated on ice for 2 h before being loaded on the gradients. Five microliter of the indicated fractions were subjected to SDS-PAGE (6% acrylamide gel) and the presence of each protein was visualized by immunoblotting using antibodies raised against each protein. The amounts of proteins loaded on each gradient were 7.5 μg (rhXPC), 2 μg (rhHR23B) and 1.7 μg (rhHR23A). Three marker proteins, egg white lysozyme (2.1S), bovine serum albumin (BSA; 4.4S) and yeast alcohol dehydrogenase (ADH; 7.4S), were centrifuged through parallel gradients, and their peak positions are indicated.

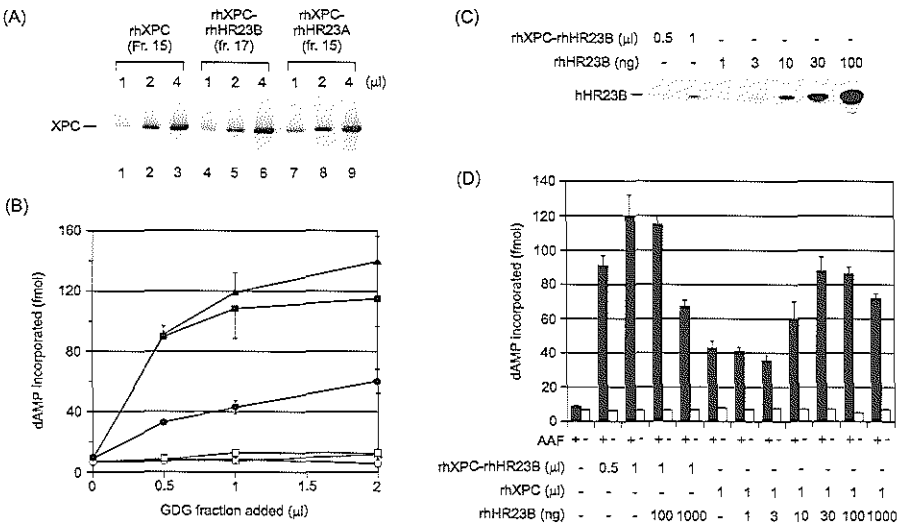

Figure 5. Complex formation with rhHR23 enhances the rhXPC activity. **(A)** The amount of rhXPC in the glycerol density gradient peak fractions of free rhXPC (fraction 15 in Figure 4A), rhXPC-rhHR23B (fraction 17 in Figure 4C) and rhXPC-rhHR23A (fraction 15 in Figure 4E) were compared by immunoblotting. **(B)** The three peak fractions used in A were assayed for XP-C correcting activity in the reconstituted *in vitro* NER system using XP-C CFII and purified RPA. After 90 min incubation at 30°C, PCNA and [α-^{32}P]dATP were added to be incubated for a further 15 min. Radioactivity incorporated in damaged (*closed symbol*) and undamaged (*open symbol*) plasmids was quantified and depicted as a graph. (*circle*) free rhXPC; (*triangle*) rhXPC-rhHR23B; (*square*) rhXPC-rhHR23A. **(C)** The amount of rhHR23B in the peak fraction of rhXPC-rhHR23B was quantified by immunoblotting. **(D)** The glycerol density gradient peak fractions of free rhXPC and rhXPC-rhHR23B complex were assayed in the presence of indicated amounts of rhHR23B under the same conditions as used in B. (*solid bar*) incorporation in damaged plasmid; (*open bar*) incorporation in undamaged plasmid. In B and D, the mean values and standard errors were calculated from 2 to 4 independent experiments.

these fractions was assayed, however, both of the complex fractions showed significantly higher NER activity than free rhXPC (Figure 5B). Thus the activity of rhXPC was enhanced by complex formation with rhHR23 proteins. As shown in Figure 5C, 1 µl of rhXPC-rhHR23B complex fraction contained 3-10 ng of rhHR23B. On the other hand, when rhHR23B was titrated in the presence of 1 µl of free rhXPC fraction, approximately 10 times more (30-100 ng) rhHR23B was needed to obtain maximal stimulation (Figure 5D), likely due to the fact that the efficiency of complex formation is dependent on the concentration of each component. As expected, addition of 100 ng of rhHR23B did not further stimulate the activity of preformed rhXPC-rhHR23B complex, although an excess of 1 µg of rhHR23B markedly inhibited repair reactions. These data indicate that the presence of rhHR23B is not enough

but, instead, complex assembly between XPC and hHR23 proteins is required for the stimulation of XPC activity.

hHR23 proteins stimulate NER in an early stage of the reaction

It has been previously shown that the XPC-hHR23B complex functions at or prior to incisions (Shivji et al.1994). When the XPC complex was included only in the second stage (i.e. DNA repair synthesis stage), repair could be hardly detected. To determine which stages of NER are stimulated by hHR23 proteins, two-stage NER reactions were carried out in the presence of free rhXPC, and rhHR23B was added at various time points. When rhHR23B was present only in the DNA repair synthesis stage, no stimulation was observed (compare lanes 6 and 7 in Figure 6A). Furthermore, when rhHR23B was added at different time points in the first stage of the reaction, the level of DNA repair declined in proportion to incubation time before the addition of rhHR23B (lanes 2 to 5). Thus rhHR23B has to be present in the first stage of incubation to exhibit the XPC-stimulating activity.

To see whether rhHR23B indeed stimulated NER at or prior to incision, DNA repair synthesis was uncoupled from the incision step. After the first incubation, DNA substrates were purified, and the amount of excised DNA damage was subsequently measured by filling the repair gaps with T4 DNA polymerase and radiolabeled dNTPs. As shown in Figure 6B, authentic XPC-hHR23B complex as well as reconstituted recombinant protein complex gave specific repair signals for damaged DNA (lanes 2 and 4) in an RPA-dependent manner (lane 3). Although free rhXPC gave some repair signal in this assay, co-addition of rhHR23B displayed clear stimulatory activity (compare lanes 5 and 6). These results thus demonstrate that hHR23B stimulates some early stages of the NER reaction before DNA repair synthesis.

hHR23 proteins stimulate NER reconstituted with purified proteins

It has been previously reported that damage-dependent incision reactions could be reconstituted *in vitro* with seven purified protein fractions: RPA, XPA, TFIIH, XPC-hHR23B, ERCC1-XPF, XPG, and incision factor 7 (IF7) (Aboussekhra et al. 1995). To test whether hHR23 proteins also show stimulatory activity in this defined NER system, activity of rhXPC was assessed in this system with or without rhHR23 proteins. In this experiment, UV-damaged and undamaged DNA substrates were first incubated with purified incision proteins, and then radioactive dATP and Klenow fragment were added to allow DNA repair synthesis. In the presence of appropriate amounts of other incision proteins, the authentic XPC-hHR23B complex gave

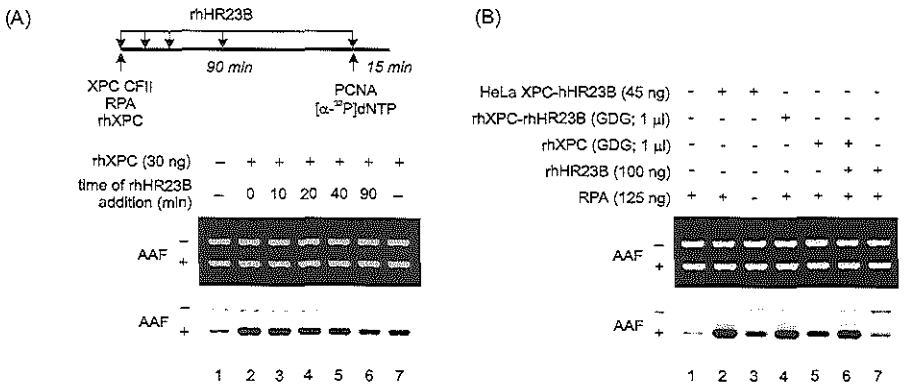

Figure 6. rhHR23B stimulates early stages of NER. **(A)** *In vitro* NER reactions were carried out with XP-C CFII (100 µg protein) and RPA (125 ng) in the presence or absence of rhXPC (30 ng). After first stage reactions at 30°C for 90 min, PCNA (25 ng) and [α-^{32}P]dATP (74 kBq) were added to be incubated further for 15 min. rhHR23B (43 ng) was added at various time points as indicated above each lane. Ethidium bromide stain and autoradiogram of the agarose gel are shown. **(B)** *In vitro* NER reactions were carried out in the presence of XP-C CFII and indicated purified protein fractions. After incubation at 30°C for 90 min, DNAs were purified before being used for DNA synthesis reactions. The DNA synthesis reactions were performed at 37°C for 15 min in mixtures (50 µl) containing 40 mM Hepes-KOH (pH 7.8), 5 mM $MgCl_2$, 0.5 mM dithiothreitol, 20 µM each of dGTP, dCTP and dTTP, 8 µM [α-^{32}P]dATP (74 kBq), bovine serum albumin (18 µg) and T4 DNA polymerase (0.6 units; New England Biolabs). DNAs were purified again, digested with *Bam*HI, and then fractionated by agarose gel electrophoresis.

a considerable repair signal (Figure 7, lane 9). Under the same conditions, rhXPC hardly supported repair reactions (lanes 2 and 3), but addition of either rhHR23B or rhHR23A resulted in strong stimulation of repair (Figure 7, lanes 4, 7 and 8). These repair signals were completely dependent on the presence of TFIIH (lanes 5 and 10), confirming that the signals represented NER reactions. Again, the co-addition of rhHR23A and rhHR23B failed to give a higher repair signal than that achieved by each single rhHR23 protein (lane 6). Finally, the clear effect of hHR23 proteins in the defined NER system made up of purified NER components provides a strong argument against the theoretical possibility that the stimulation of hHR23 proteins was in fact due to titrating out inhibitory factor(s).

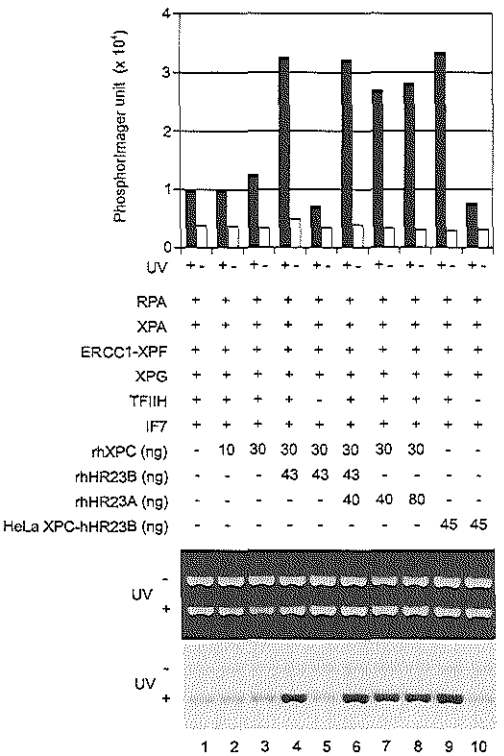

Figure 7. rhHR23 proteins stimulate defined NER reactions reconstituted with purified proteins. Plasmid DNA substrates (UV-damaged and undamaged) were incubated at 30°C for 60 min in the presence of the indicated (+) purified NER proteins. Exo-free *E.coli* DNA polymerase I and [α-^{32}P]dATP were added and incubation was continued at 30°C for 10 min. DNA samples were purified, linearized with *Bam*HI, and separated on a 1% agarose gel. A photograph of the ethidium bromide stained gel and an autoradiogram of the gel are shown. The amounts of purified proteins used were: RPA (250 ng), XPA (45 ng), ERCC1-XPF (10 ng), TFIIH (150 ng), XPG (50 ng), IF7 (500 ng). The gel was exposed to a PhosphorImager (Molecular Dynamics) and the relative radioactivity incorporated in each band was quantified. (*solid bars*) incorporation in damaged plasmid; (*open bars*) incorporation in undamaged plasmid.

Discussion

Functional interchangeability between the two RAD23 homologs

In the accompanying paper, a domain in hHR23B which is responsible for XPC-binding was determined (Masutani et al. 1997). This domain was shown to be required and even sufficient for stimulation of XPC repair activity *in vitro*. Because the amino acid sequence of this domain is well conserved between the two hHR23 proteins, it might be expected that hHR23A also

binds to XPC and stimulates repair activity. In agreement with this, *E.coli*-expressed, highly purified rhHR23A exhibits a similar XPC-stimulating activity as hHR23B (Figure 2). Furthermore, co-precipitation using His-tagged rhHR23 proteins (Figure 3) and the sedimentation velocity experiments (Figure 4) demonstrated that both rhHR23 proteins were capable of forming complexes with rhXPC. This complex assembly could be observed without any other protein fractions or any incubation at relatively high temperature, indicating that special post-translational modifications, such as phosphorylation, of rhHR23 are not necessary for the binding itself. Moreover, neither an energy source such as ATP, nor a divalent cation was required.

The competition experiments shown in Figure 3 revealed that both rhHR23 proteins can bind to rhXPC with comparable affinity under the conditions tested. Recently, possible interaction between XPC and hHR23A has been suggested using the yeast two hybrid system (Li et al. 1997). Furthermore, we have very recently detected trace amounts of hHR23A by immunoblotting in a highly purified XPC protein fraction from HeLa cells, indicating the existence of XPC-hHR23A complex in human cells (our unpublished results). Because the vast majority of XPC is bound to hHR23B, one might expect that rhHR23B shows much higher affinity for rhXPC than rhHR23A. This, however, turned out not to be the case. It is thus still unclear why most of XPC is bound to hHR23B. Although the content of hHR23B in the cells used seems to be higher than hHR23A, the difference is not large enough to explain preferential binding of XPC to hHR23B (our unpublished observations). It is possible that specific modification of hHR23B increases its affinity for XPC or, alternatively, that auxilliary factors specifically target XPC to hHR23B. However, this is not absolutely necessary for the binding itself, as discussed above. Another possibility is that the subcellular localization of the two hHR23 proteins is different. We have recently shown by indirect immunofluorescence analysis that XPC as well as both hHR23 proteins are localized predominantly in the nucleus (van der Spek et al. 1996). From these experiments, however, it was difficult to determine which fraction of these proteins is present in the cytoplasm. One possibility is that a minor amount of hHR23B is localized in the cytoplasm, and preferentially traps newly-synthesized XPC protein before it is transported to the nucleus. Alternatively, the intranuclear localization of hHR23A and hHR23B may be different. Further studies are needed to answer these questions.

Importance of complex assembly for the XPC-stimulation by hHR23 proteins

The correlation between XPC-binding and NER stimulatory activity of various truncated rhHR23B proteins suggests that complex assembly is important for XPC-stimulation (Masutani et al. 1997). Here we demonstrate biochemically that complex assembly enhances the repair activity of rhXPC. Because sedimentation in glycerol gradients incompletely separates rhXPC-rhHR23 complexes from free rhXPC, it was difficult to determine which proportion of rhXPC was complexed with rhHR23s in each glycerol gradient. However, although not all rhXPC molecules may have formed complexes, we still observed a significantly higher activity of the complex fractions than free rhXPC. Furthermore, when free rhXPC was assayed in the presence of various amounts of rhHR23B, a much higher concentration of rhHR23B was needed to obtain maximal stimulation, in comparison with amounts of rhHR23B present in the pre-assembled complex fractions (Figure 5C and D). Since the presence of higher concentrations of rhHR23B should make complex formation more efficient, these data also support the importance of complex assembly for the XPC-stimulation by hHR23 proteins. In addition, Figure 5D shows that the presence of a large excess of rhHR23B is inhibitory. Consequently, maximal stimulation is observed only within a certain range of rhHR23B doses. Thus careful titration of rhHR23B is necessary for observing the stimulatory effect by rhHR23B.

Because the XPC-hHR23B complex was shown to function at an early stage of NER (Shivji et al.1994), it was of interest to determine which stage of NER is stimulated by hHR23 proteins. By carrying out DNA repair synthesis independently from incisions, we demonstrate that the stimulation by hHR23 proteins also takes place at or prior to incisions (Figure 6B). This part of the NER reaction still encompasses multiple steps: damage recognition, local melting of double-stranded DNA, dual incisions and removal of damage-containing oligonucleotides. Yeast RAD23 protein has been previously claimed (Guzder et al. 1995) to mediate physical interactions with Rad14 as well as yeast TFIIH, raising a possibility that RAD23 promotes assembly of higher-order NER protein complexes, like "repairosomes" (Svejstrup et al. 1995). However, similar interactions have not yet been established either *in vivo* or *in vitro* for hHR23 products and other mammalian NER proteins. Further studies are warranted to pinpoint the NER steps in which the hHR23 products exert their function(s).

Stimulation by rhHR23s in the defined NER system

Our rhHR23 proteins showed XPC-stimulating activity also in the defined

NER system reconstituted with purified proteins, which was described by Aboussekhra et al. (1995). Although some of the repair proteins (i.e. IF7, ERCC1-XPF and TFIIH) used in these experiments were not purified to complete homogeneity, these observations strongly argue against a formal possibility that rhHR23s stimulate NER reactions indirectly, e.g. by titrating out some inhibitors present in crude fractions.

The results of the two reconstituted NER systems using XP-C CFII (Figure 2) and the purified proteins (Figure 7) were qualitatively similar, but we noted some quantitative differences as well. For instance, free rhXPC always exhibited some activity when added to the XP-C CFII, whereas the same amount of rhXPC hardly supported repair in the defined NER system (compare lanes 2 and 3, in Figs. 3 and 7). Consequently, the stimulation by rhHR23s appeared to be more pronounced in the defined NER reaction. One possible explanation is that the XP-C CFII used in these studies still contains a trace amount of endogenous hHR23B and/or hHR23A. Alternatively, some repair proteins might be present as higher-order complexes in the CFII fractions, whereas all repair proteins should be free at the beginning of the defined NER reactions. If hHR23 proteins promote such supercomplex assembly by itself or via change in a conformation of XPC, the defined system should be much more dependent on the presence of hHR23. Another possibility is that hHR23 proteins physically stabilize XPC via complex formation. In the defined NER system which contains much lower protein concentrations compared to the crude system, free rhXPC might be more labile and thus depend more on the stabilizing effect of hHR23.

Generally, setting up defined reaction systems composed of multiple purified proteins needs special care: rate-limiting factors depend on the precise ratio of the different purified proteins used. Therefore, to determine the activity of XPC protein, it is important to set up reactions where XPC is rate-limiting. Recently Reardon et al. have reported (Reardon et al. 1996) that rhHR23B had no stimulatory effect in their reconstituted NER system. There are significant differences between the two reaction systems: one detects repair DNA synthesis on randomly damaged plasmid DNA, whereas the other detects dual incision on a singly-damaged DNA substrate. Moreover, our defined NER system requires an extra protein fraction designated IF7, which seems to be dispensable in the other system. Therefore, the discrepancy concerning the stimulation by rhHR23B could be attributed to some intrinsic differences between the two repair systems, including differences in quality of purified proteins used. As discussed above, however, stimulation of XPC might also be overlooked especially in defined NER systems, unless all components are carefully titrated to set up conditions under which XPC is

rate-limiting. It is also important to carefully titrate rhHR23B, because a large excess of rhHR23B turned out to be inhibitory (Figure 5D).

We are generating knock-out mice of *mHR23B* as well as *mHR23A*. Because no natural mutant has been so far available for mammalian RAD23 homologs, these knock-out mice and the derived mutant cells should give important clues to elucidate *in vivo* functions of this set of genes. Analysis of these mice is expected to give more definite answers to the current issues concerning the roles and possible functional redundancy of mammalian RAD23 homologs in NER, and will complement the findings made in *in vitro* studies.

Experimental Procedures

Purification of repair proteins

Recombinant human XPC protein was expressed in an insect cell line, Sf9, by a baculovirus expression system, and purified as described previously (Sugasawa et al. 1996). Non-tagged and His-tagged versions of recombinant hHR23A and hHR23B proteins were expressed in *E.coli* and purified as described in the accompanying paper (Masutani et al. 1997). Recombinant human proliferating cell nuclear antigen (PCNA) was purified from *E.coli* BL21(DE3) harboring pT7-PCNA plasmid (a generous gift from Dr. B. Stillman; Cold Spring Harbor Laboratory) as described (Flen and Stillman 1992). The final Phenyl Sepharose fractions were further loaded on an FPLC Mono Q HR5/5 column equilibrated with buffer A [25 mM Tris-HCl (pH 7.5), 1 mM EDTA, 10% glycerol, 0.01% Triton X-100, 1 mM dithiothreitol, 0.1 mM phenylmethylsulfonyl fluoride (PMSF)] containing 0.2 M NaCl, and eluted with 15 ml of 0.2 to 0.7 M NaCl gradient in buffer A. Peak fractions were stored at –80°C. Human replication protein A (RPA) was also purified from recombinant sources using *E.coli* BL21(DE3) pLysS transformed with p11d-tRPA (kindly provided by Dr. M. Wold; Univ. Iowa) as described (Hendricksen et al. 1994). ERCC1-XPF complex was purified from Chinese hamster group 1 mutant cells (43-3B) transfected with His-tagged human ERCC1 as described previously (Sijbers et al. 1996). XPA, XPG, TFIIH and IF7 were purified as described (Aboussekhra et al. 1995; Gerard et al. 1991). As for TFIIH, the fractions from the second heparin column were used for the reconstituted NER reactions (Hwang et al. 1996).

Preparation and fractionation of whole cell extracts

Lymphoblastoid cells (GM2248B) from an XP-C patient (XP3BE) were grown in suspension with RPMI1640 medium containing 15% fetal calf serum and 20 mM Hepes-NaOH (pH 7.3). Whole cell extracts were prepared as described previously (Manley et al. 1980; Wood et al. 1988). For fractionation, whole cell extracts (~50 mg protein) were loaded onto a phosphocellulose column (φ1.2 x 8 cm) equilibrated with buffer B [25 mM Hepes-KOH (pH 7.8), 1 mM EDTA, 10% glycerol, 0.01% Nonidet P-40, 1 mM dithiothreitol, 0.1 mM PMSF] containing 0.1 M KCl. After an extensive wash with the same buffer, bound proteins were eluted with buffer B containing 1 M KCl. The peak fractions were pooled and dialyzed overnight against buffer containing 25 mM Hepes-KOH (pH 7.9), 0.1 M KCl, 12 mM $MgCl_2$, 1 mM EDTA, 10% glycerol, 20% sucrose and 1 mM dithiothreitol. Insoluble material was removed by centrifugation and the resulting supernatant fraction (column fraction II; CFII) was stored at –80°C.

***In vitro* NER reactions**

Standard reaction mixtures for *in vitro* NER (50 μl) contained the following components: 40 mM Hepes-KOH (pH 7.8), 7 mM $MgCl_2$, 70 mM KCl, 6.8% glycerol, 0.5 mM dithiothreitol, 2 mM ATP, 20 μM each of dGTP, dCTP and dTTP, 8 μM dATP, 23 mM phosphocreatine, 2.5 μg of creatine phosphokinase, 18 μg of bovine serum albumin, 250 ng each of plasmid DNA substrates, pBluescript II KS+ [AAF(*N*-acetyl-2-aminofluorene)- or UV-damaged] and pHM14 (undamaged)], and indicated amounts of fractionated cell extracts and/or purified NER proteins. After incubation performed at 30°C for the indicated time period, 25 ng of PCNA and 74 kBq of [α-^{32}P]dATP (Amersham; ~110 TBq/mmol) were added and further incubated at 30°C for 15 min. For reconstituted NER reactions with purified proteins, exo-free *E.coli* DNA polymerase I (0.025 unit; United States Biochemical) was used to carry out gap filling of DNA incised by the mammalian incision proteins.

Glycerol gradient velocity sedimentation

Stepwise glycerol gradients were made in polyallomer ultracentrifuge tubes (for SW60 rotor; Beckman) by overlaying 340 μl each of 11-step glycerol solution (from 35% to 15%; 2% decrease by each step) in buffer C [25 mM Tris-HCl (pH 7.5), 1 mM EDTA, 0.3 M NaCl, 0.05% Nonidet P-40, 1 mM dithiothreitol, 0.1 mM PMSF]. The gradients were incubated overnight at 4°C before loading samples. Protein samples were put in 50 μl of buffer C containing 10% glycerol and incubated at 4°C for 2 h. After loading samples, the gradients were centrifuged at 2°C for 64 h at 49,000 rpm (Beckman; SW60 rotor). Fractions (160 μl) were taken from the top of the gradients. As marker proteins, egg white lysozyme (2.1S; 30 μg), bovine serum albumin (4.4S; 27 μg) and yeast alcohol dehydrogenase (7.4S; 40 μg) were loaded on parallel gradients and fractionated exactly as described above. Positions of the marker proteins were determined by SDS-PAGE followed by Coomassie Brilliant Blue staining.

Other methods

rhXPC binding assay was carried out as described (Masutani et al. 1997). SDS polyacrylamide gel electrophoresis (SDS-PAGE) was performed as described by Laemmli (1970). For immunoblotting, proteins separated on SDS gels were electrotransferred onto nitrocellulose membrane (Schleicher & Schuell; BA85) at 5 V/cm overnight in blot buffer (25 mM Tris, 193 mM glycine, 0.01% SDS, 15% methanol). XPC, hHR23A and hHR23B proteins were detected using affinity-purified rabbit polyclonal antibodies raised against each protein and alkaline phosphatase-conjugated anti-rabbit IgG. Protein concentration was determined according to the method of Bradford (Bradford 1976), using Coomassie protein assay reagent (Pierce) and bovine serum albumin as a standard.

Acknowledgments

We thank W. de Laat and M. Biggerstaff for the ERCC1-XPF preparation, J.-M. Egly for the TFIIH fraction, and G. J. van der Horst for helpful discussion. This work was financially supported by a Human Frontier Program research grant, by the Medical Genetic Centre, and by the Dutch Scientific Organization (NWO) through the foundation of Medical Scientific Research (contract number 901-01-093). The work was also supported by grants from the Ministry of Education, Science and Culture of Japan, the Biodesign Research Program of the Institute of Physical and Chemical Research (RIKEN), and the Imperial Cancer Research Fund.

References

Aboussekhra, A., M. Biggerstaff, M. K. K. Shivji, J. A. Vilpo, V. Moncollin, V. N. Podust, M. Protic, U. Hübscher, J.-M. Egly, and R. D. Wood. (1995). Mammalian DNA nucleotide excision repair reconstituted with purified protein components. Cell *80*, 859-868.

Bootsma, D., K. H. Kraemer, J. Cleaver, and J. H. J. Hoeijmakers. (1997). Nucleotide excision repair syndromes: xeroderma pigmentosum, Cockayne syndrome and trichothiodystrophy. *In:* C. R. Scriver, A. L. Beaudet, W. S. Sly, and D. Valle (ed.). The Metabolic Basis of Inherited Disease, Eighth Edition, McGraw-Hill Book Co., New York.

Boulikas, T. (1996). Xeroderma pigmentosum and molecular cloning of DNA repair genes. Anticancer Res. *16*, 693-708.

Bradford, M. M. (1976). A rapid and sensitive method for the quantitation of microgram quantities of protein utilizing the principle of protein-dye binding. Anal. Biochem. *72*, 248-254.

Fien, K. and B. Stillman. (1992). Identification of replication factor C from *Saccharomyces cerevisie*: a component of the leading-strand DNA replication complex. Mol. Cell. Biol. *12*, 155-163.

Friedberg, E. C., G. C. Walker, and W. Siede. (1995). DNA Repair and Mutagenesis. ASM Press, Washington, D. C.

Gerard, M., L. Fischer, V. Moncollin, J.-M. Chipoulet, P. Chambon, and J.-M. Egly. (1991). Purification and interaction properties of the human RNA polymerase B(II) general transcription factor BTF2. J. Biol. Chem. 266, 20940-20945.

Grossman, L. and S. Thiagalingam. (1993). Nucleotide excision repair, a tracking mechanism in search of damage. J. Biol. Chem. *268*, 16871-16874.

Guzder, S. N., V. Bailly, P. Sung, L. Prakash, and S. Prakash. (1995). Yeast DNA repair protein RAD23 promotes complex formation between transcription factor TFIIH and DNA damage recognition factor RAD14. J. Biol. Chem. *270*, 8385-8388.

Guzder, S. N., Y. Habraken, P. Sung, L. Prakash, and S. Prakash. (1995). Reconstitution of yeast nucleotide excision repair with purified Rad proteins, replication protein A, and transcription factor TFIIH. J. Biol. Chem. *270*, 12973-12976.

Hendricksen, L. A., C. B. Umbricht, and M. S. Wold. (1994). Recombinant replication protein A: expression, complex formation, and functional cheracterization. J. Biol. Chem. 269, 11121-11132.

Hoeijmakers, J. H. J. (1993). Nucleotide excision repair I: from *E.coli* to yeast. Trends Genet. *9*, 173-177.

Hoeijmakers, J. H. J. (1994). Human nucleotide excision repair syndromes: molecular clues to unexpected intricacies. Eur. J. Cancer *30A*, 1912-1921.

Hwang, J. R., V. Moncollin, W. Vermeulen, T. Seroz, H. van Vuuren, J. H. J. Hoeijmakers, and J.-M. Egly. (1996). A 3'•5' XPB helicase defect in repair/transcription factor TFIIH of xeroderma pigmentosum group B affects both DNA repair and transcription. J. Biol. Chem. *271*, 15898-15904.

Laemmli, U. K. (1970). Cleavage of structural proteins during the assembly of the head of bacteriophage T4. Nature *227*, 680-685.

Li, L., X. Lu, C. Peterson, and R. Legerski. (1997). XPC interacts with both hHR23B and hHR23A *in*

vivo. Mutat. Res. *383*, 197-203.

Liu, J. J. and A. Sancar. (1992). (A)BC exinuclease: the *Escherichia coli* nucleotide excision repair enzyme. Mol. Microbiol. *6*, 2219-2224.

Manley, J. L., A. Fire, A. Cano, P. A. Sharp, and M. L. Gefter. (1980). DNA-dependent transcription of adenovirus genes in a soluble whole-cell extract. Proc. Natl. Acad. Sci. USA *77*, 3855-3859.

Masutani, C., M. Araki, K. Sugasawa, P. J. van der Spek, A. Yamada, A. Uchida, T. Maekawa, D. Bootsma, J. H. J. Hoeijmakers, and F. Hanaoka. (1997). Identification and characterization of XPC-binding domain of hHR23B. Mol. Cell. Biol. submitted for publication.

Masutani, C., K. Sugasawa, J. Yanagisawa, T. Sonoyama, M. Ui, T. Enomoto, K. Takio, K. Tanaka, P. J. van der Spek, D. Bootsma, J. H. J. Hoeijmakers, and F. Hanaoka. (1994). Purification and cloning of a nucleotide excision repair complex involving the xeroderma pigmentosum group C protein and a human homolog of yeast RAD23. EMBO J. *13*, 1831-1843.

Mu, D., D. S. Hsu, and A. Sancar. (1996). Reaction mechanism of human DNA repair excision nuclease. J. Biol. Chem. *271*, 8285-8294.

Mu, D., C. H. Park, T. Matsunaga, D. S. Hsu, J. T. Reardon, and A. Sancar. (1995). Reconstitution of human DNA repair excision nuclease in a highly defined system. J. Biol. Chem. *270*, 2415-2418.

Reardon, J. T., D. Mu, and A. Sancar. (1996). Overproduction, purification, and characterization of the XPC subunit of the human DNA repair excision nuclease. J. Biol. Chem. *271*, 19451-19456.

Sancar, A. (1996). DNA excision repair. Annu. Rev. Biochem. *65*, 43-81.

Shivji, M. K. K., A. P. M. Eker, and R. D. Wood. (1994). DNA repair defect in xeroderma pigmentosum group C and complementing factor from HeLa cells. J. Biol. Chem. *269*, 22749-22757.

Shivji, M. K. K., M. K. Kenny, and R. D. Wood. (1992). Proliferating cell nuclear antigen is required for DNA excision repair. Cell *69*, 367-374.

Sijbers, A. M., W. L. de Laat, R. R. Ariza, M. Biggerstaff, Y. F. Wei, J. G. Moggs, K. C. Carter, B. K. Shell, E. Evans, M. C. de Jong, S. Rademakers, J. de Rooij, N. G. Jaspers, J. H. Hoeijmakers, and R. D. Wood. (1996). Xeroderma pigmentosum group F caused by a defect in a structure-specific DNA repair endonuclease. Cell *86*, 811-822.

Sugasawa, K., C. Masutani, A. Uchida, T. Maekawa, P. J. van der Spek, D. Bootsma, J. H. J. Hoeijmakers, and F. Hanaoka. (1996). hHR23B, a human RAD23 homolog, stimulates XPC protein in nucleotide excision repair *in vitro*. Mol. Cell. Biol. *16*, 4852-4861.

Svejstrup, J. Q., Z. Wang, W. J. Feaver, X. Wu, D. A. Bushnell, T. F. Donahue, E. C. Friedberg, and R. D. Kornberg. (1995). Different forms of TFIIH for transcription and DNA repair: holo-TFIIH and a nucleotide excision repairosome. Cell *80*, 21-28.

van der Spek, P. J., A. Eker, S. Rademakers, C. Visser, K. Sugasawa, C. Masutani, F. Hanaoka, D. Bootsma, and J. H. J. Hoeijmakers. (1996). XPC and human homologs of RAD23: intracellular localization and relationship to other nucleotide excision repair complexes. Nucleic Acids Res. *24*, 2551-2559.

van der Spek, P. J., C. E. Visser, F. Hanaoka, B. Smit, A. Hagemeijer, D. Bootsma, and J. H. J. Hoeijmakers. (1996). Cloning, comparative mapping, and RNA expression of the mouse homologs of

the *Saccharomyces cerevisiae* nucleotide excision repair gene *RAD23*. Genomics *31*, 20-27.

van Houten, B. (1990). Nucleotide excision repair in *Escherichia coli*. Microbiol. Rev. *54*, 18-51.

Venema, J., A. van Hoffen, V. Karcagi, A. T. Natarajan, A. A. van Zeeland, and L. H. F. Mullenders. (1991). Xeroderma pigmentosum complementation group C cells remove pyrimidine dimers selectively from the transcribed strand of active genes. Mol. Cell. Biol. *11*, 4128-4134.

Venema, J., A. van Hoffen, A. T. Natarajan, A. A. van Zeeland, and L. H. F. Mullenders. (1990). The residual repair capacity of xeroderma pigmentosum complementation group C fibroblasts is highly specific for transcriptionally active DNA. Nucleic Acids Res. *18*, 443-448.

Wood, R. D. (1996). DNA repair in eukaryotes. Annu. Rev. Biochem. *65*: 135-167.

Wood, R. D., P. Robins, and T. Lindahl. (1988). Complementation of the xeroderma pigmentosum DNA repair defect in cell-free extracts. Cell *53*, 97-106.

Chapter

IV

Xeroderma Pigmentosum Group C Protein Complex Is the Initiator of Global Genome Nucleotide Excision Repair

Kaoru Sugasawa[1,2], Jessica M. Y. Ng[1], Chikahide Masutani[3], Shigenori Iwai[4], Peter J. van der Spek[1,5], André P. M. Eker[1], Fumio Hanaoka[2,3], Dirk Bootsma[1] and Jan H. J. Hoeijmakers[1]

[1]Department of Cell Biology and Genetics, Medical Genetic Centre, Erasmus University, P.O. Box 1738, 3000 DR Rotterdam, The Netherlands
[2]Cellular Physiology Laboratory, The Institute of Physical and Chemical Research (RIKEN), 2-1 Hirosawa, Wako, Saitama 351-01, Japan
[3]Institute for Molecular and Cellular Biology, Osaka University, 1-3 Yamada-oka, Suita, Osaka 565, Japan
[4]Department of Bioorganic Chemistry, Biomolecular Engineering Research Institute, 6-2-3 Furuedai, Suita, Osaka 565, Japan
[5]Present address: N.V. Organon/Akzo Nobel, Target Discovery Unit, P.O. Box 20, 5340 BH Oss, The Netherlands

Summary

The XPC-HR23B complex is specifically involved in global genome but not in transcription-coupled nucleotide excision repair (NER). Its function is unknown. Using a novel DNA damage recognition-competition assay, we identified XPC-HR23B as the very first damage detector, initiating NER: it acts before the known damage-binding protein XPA. Co-immunoprecipitation and DNase I footprinting show that XPC-HR23B binds to a variety of NER lesions. These results resolve the function of XPC-HR23B, define the first NER stages, and suggest a two-step mechanism of damage recognition involving damage detection by XPC-HR23B followed by damage verification by XPA. This provides a plausible explanation for the extreme damage specificity exhibited by global genome repair. In analogy, in the transcription-coupled NER subpathway RNA polymerase II may take the role of XPC. After this initial subpathway-specific lesion detection, XPA may function as a common damage verifier and adaptor to the core of the NER apparatus.

Introduction

Fundamental problems are associated with the chemical vulnerability of DNA as the carrier of genetic information. A myriad of lesions in DNA is caused by intrinsic instability of chemical bonds and by ubiquitous environmental or endogenous genotoxic agents. DNA damage interferes with the primary DNA functions including transcription and replication, which can lead to acute cell death. In addition, many DNA damaging agents are also mutagens. The biological consequences of mutations and persisting lesions range from the onset of carcinogenesis, genetic disorders, and apoptosis to general cell malfunctioning that may contribute to aging. To cope with these problems, an elaborate cellular defence network has arisen early in evolution, encompassing sophisticated complementary repair pathways and cell cycle checkpoints. Nucleotide excision repair (NER) is one of the most versatile and best studied DNA repair systems, which eliminates a wide variety of DNA damage (Friedberg et al. 1995). Two in part overlapping NER subpathways have been discerned. One process called 'global genome repair' (GGR) operates genome-wide and is able to eliminate NER lesions from all locations in the genome at any moment in the cell cycle. For some types of DNA damage [e.g. UV-induced pyrimidine (6-4) pyrimidone photoproducts (6-4PPs)] this process is very fast and efficient, but for others [e.g. UV-induced cyclobutane pyrimidine dimers (CPDs)] it is much slower and less efficient (Mitchell 1988). Probably because the latter type of lesions obstruct transcription for a too long period of time, an additional repair system has

evolved designated 'transcription-coupled repair' (TCR). This process ensures rapid and efficient clearance of the transcribed strand of active genes from elongation-blocking lesions (Bohr et al. 1985; Mellon et al. 1987; Selby and Sancar 1993). Thus, TCR is an important back-up system for the removal of lesions from active parts of the genome, for which the GGR process is too slow.

Several rare, autosomal recessive human disorders are associated with impaired NER activity. These include xeroderma pigmentosum (XP), Cockayne syndrome (CS) and trichothiodystrophy (TTD), all of which are characterized by sun (UV) hypersensitivity and marked genetical heterogeneity. Cell fusion studies have revealed a large number of genetic complementation groups within these disorders: XP-A to XP-G, CS-A, CS-B, and TTD-A, reflecting different NER genes. These mutants as well as a series of laboratory-generated UV-sensitive hamster cell lines have been a valuable asset for delineating the biological consequences of NER deficiency and for cloning the complementing genes (Bootsma et al. 1998). While the protein products corresponding to some of these NER genes have been identified, mammalian cell-free systems accomplishing NER have been dissected extensively (for recent reviews, see Sancar 1996; Wood 1996). Synergistic progress using the genetical and biochemical approaches culminated in the recent reconstitution of *in vitro* NER with purified protein factors (Aboussekhra et al. 1995; Mu et al. 1995). The NER reaction up to the asymmetric incisions requires at least six protein factors: XPA, XPC-HR23B, ERCC1-XPF, XPG, transcription factor IIH (TFIIH), and replication protein A (RPA). Despite the identification of individual NER components, the precise reaction mechanism including the crucial damage recognition step has not yet been firmly established. The GGR process in particular faces the enormous task to continually survey 5×10^9 bp DNA for trace amounts of a diversity of lesions. Although XPA has been shown to bind a variety of damaged DNAs (Jones and Wood 1993; Asahina et al. 1994) and is implicated in this key NER event, it remains unclear whether XPA can fully account for the lesion specificity required *in vivo*.

In XP-C patients, unlike other NER-deficient complementation groups, only the process of GGR, but not of TCR, is impaired (Venema et al. 1990; Venema et al. 1991). Transfection with a human cDNA expression library resulted in isolation of a partial XPC cDNA which corrects UV-sensitivity of XP-C mutant cells (Legerski and Peterson 1992). Using *in vitro* NER complementation assays, a protein complex containing the *XPC* gene product was purified (Masutani et al. 1994; Shivji et al. 1994). The XPC protein was found to be tightly complexed with HR23B, one of two mammalian homologs

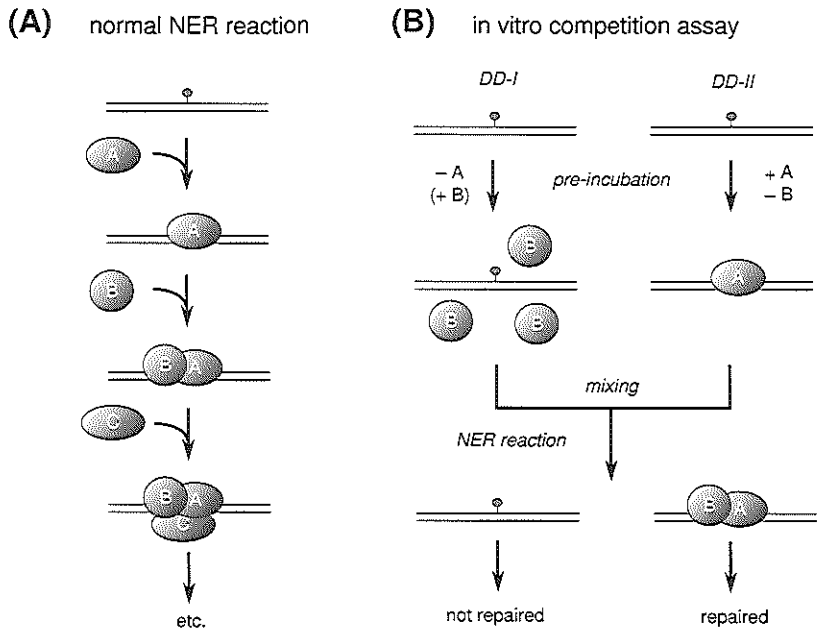

Figure 1. A schematic representation of the damage recognition-competition assay. **(A)** The earliest events of the normal NER process is depicted in a simplified hypothetical model. **(B)** *In vitro* damage recognition-competition assay using two damaged DNAs. See text for details.

of *Saccharomyces cerevisiae* NER factor RAD23. Although the XPC-HR23B complex displays a high affinity for both single- and double-stranded DNA (Masutani et al. 1994; Shivji et al. 1994; Reardon et al. 1996), its function in GGR has remained enigmatic. In the present study, we address the stage at which XPC-HR23B operates, and resolve the function of this GGR-specific NER factor, which has important implications for the crucial mechanism for damage detection, not only in GGR but also in TCR.

Results

Competitive *in vitro* NER assay using two damaged DNA substrates

To examine at which stage XPC-HR23B functions in NER, we designed a competition assay using two damaged DNA substrates, outlined in Figure 1. Ordered assembly of the NER machinery includes as the first step identification of a lesion accomplished by hypothetical factor 'A'. This is then followed by sequential entry of other NER factors (symbolized as 'B' and 'C')

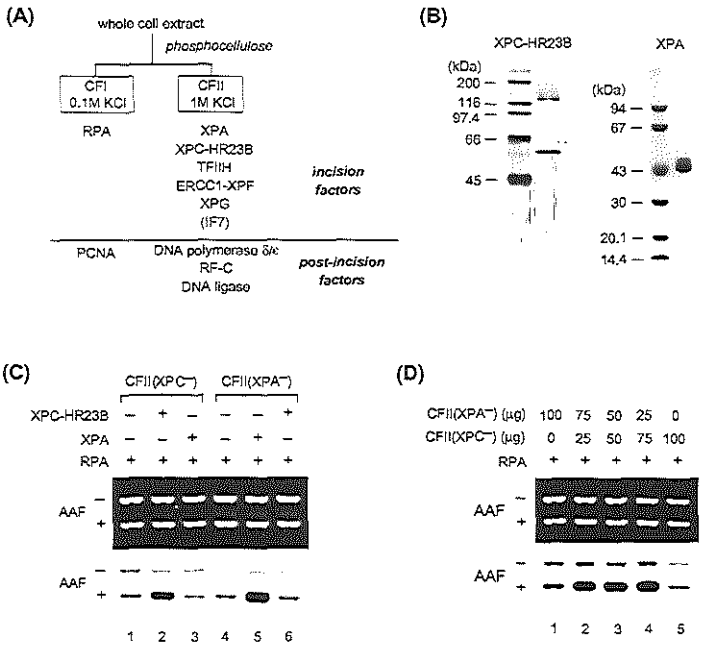

Figure 2. Specificity of fractionated XP cell extracts utilized in the present studies. **(A)** A scheme for phosphocellulose fractionation of whole cell extracts. **(B)** The purified human XPC-HR23B protein complex and the mouse XPA protein were subjected to SDS polyacrylamide gel electrophoresis. Proteins were visualized by silver staining (XPC-HR23B) or by Coomassie Brilliant Blue staining (XPA). **(C and D)** A mixture of AAF-damaged and non-damaged DNAs was incubated at 30°C for 60 min with CFII from XP cells and purified proteins as indicated, under the standard conditions for *in vitro* NER reaction. All reactions contained 100 μg of CFII fractions in total. Amounts of purified proteins used were 45 ng for XPC-HR23B, 20 ng for XPA and 125 ng for RPA. DNA was purified from each reaction, and then the repair gaps were filled by T4 DNA polymerase in the presence of [α-^{32}P]dNTP. The DNA samples were linearized and subjected to agarose gel electrophoresis followed by autoradiography.

involved in processing of the DNA substrate leading to dual incision of the damaged strand (Figure 1A). When two damaged DNA molecules are separately allowed to react with limiting amounts of 'B' resp. 'A', only the 'A-bound DNA' is initially processed further when both DNA molecules are mixed and supplemented with the remaining NER factors (Figure 1B). Although, for this scheme, the initial complex involving 'A' and a lesion has to be sufficiently stable to sequester most of 'A' molecules, the appearance of preferential repair of one of the pre-incubated DNAs provides information on the order of factors required in the NER reaction.

For the pre-incubation of the different damaged DNA substrates in the absence of specific NER factors, we prepared whole cell extracts of different XP cells, each lacking a known NER (XP) factor, which were fractionated over phosphocellulose. The phosphocellulose-bound protein fraction (column fraction II; CFII) contains all essential NER factors required up to the incision stage, except for RPA (Shivji et al. 1992, see also Figure 2A). For the subsequent gap filling repair synthesis, proliferating cell nuclear antigen (PCNA) is required that is also missing from CFII (Shivji et al. 1992). Thus incubation of damaged DNA in the presence of CFII and added RPA (but not PCNA) results in dual incisions around lesions and accumulation of repair gaps, but not repair synthesis. After purifying the DNA substrates, a measure for the number of excised lesions can be obtained by filling the gaps with T4 DNA polymerase and radioactive dNTP. As expected, in the presence of exogenous RPA, CFII from XP-C cells [designated CFII(XPC$^-$)] requires extra addition of XPC-HR23B to accomplish incisions (Figure 2C; lanes 1 and 2). Analogously, intact recombinant mouse XPA protein complemented the defect of incision activity of CFII(XPA$^-$) (lanes 4 and 5). The purity of the purified proteins utilized is documented in Figure 2B. Complementation could be also observed when the two CFIIs were mixed in the presence of RPA (Figure 2D). The addition of XPA to CFII(XPC$^-$) (Figure 2C; lane 3) or the addition of XPC-HR23B to CFII(XPA$^-$) (lane 6) resulted in only a background level of dNTP incorporation. These data indicate that the purified XPA and XPC-HR23B proteins are active and demonstrate the specificity of our mutant CFII preparations. These fractionated extracts and purified proteins were used throughout this study.

Competition between XPA and XPC-HR23B

To distinguish two damaged DNA substrates in *in vitro* NER reactions, closed circular plasmid DNAs of different sizes were treated separately with the same concentration of *N*-acetoxy-2-acetyl-aminofluorene (AAF), mainly inducing *N*-(guanine-8-yl)-AAF adducts that are known substrates of NER. One of the AAF-damaged DNA (DD-I) was first incubated with CFII(XPC$^-$), while the other (DD-II) was with CFII(XPA$^-$). These two mixtures were then combined, and supplemented with RPA to obtain a complete set of incision factors. Non-damaged DNA (ND) was also included as an internal control. The mixture was further incubated for various time periods to examine the time course of incision reactions on each of the damaged DNAs. Unexpectedly, Figure 3 shows that DD-II, which was pre-incubated with CFII(XPA$^-$), was preferentially repaired compared to DD-I (lanes 5-8). Exchange of the two damaged DNAs [i.e. pre-incubation of DD-I with

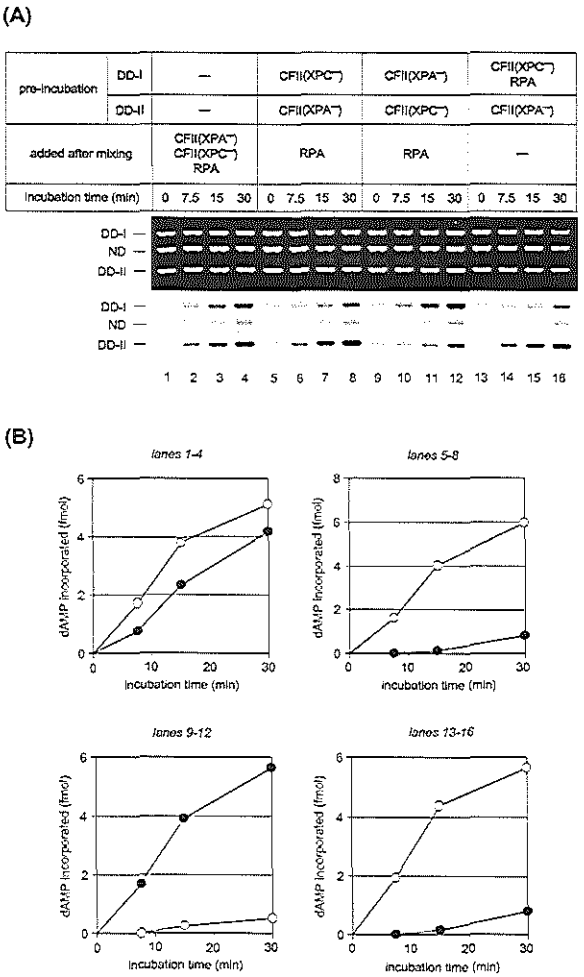

Figure 3. Competitive NER assay using CFIIs from XP-A and XP-C mutant cells. **(A)** Two AAF-damaged DNAs (DD-I and DD-II) were separately pre-incubated at 30°C for 15 min with the indicated protein fractions. After the two reactions were combined, non-damaged DNA (ND) and indicated protein fractions were added. Amounts of protein fractions used were 400 µg for each CFII and 250 ng for RPA. Aliquots of the mixtures were further incubated at 30°C for the indicated periods of time. Repair gaps generated during the second incubations were filled with T4 DNA polymerase and [α-^{32}P]dNTP. The DNA samples were linearized and fractionated by agarose gel electrophoresis. A photograph of the ethidium bromide-stained gel and the corresponding autoradiogram are shown. **(B)** DNA repair synthesis in each damaged DNA was quantitated. Radioactivity incorporated into ND was subtracted as a background from that in damaged DNA bands at each time point. The resulting values were further subtracted by those at the time point of 0 min, and plotted as a time course. Closed circles, DNA repair synthesis in DD-I; open circles, DD-II.

CFII(XPA$^-$) and DD-II with CFII(XPC$^-$)] resulted in a reversed repair bias (lanes 9-12). In both cases, the damaged DNA pre-incubated with CFII(XPC-) was hardly repaired during the initial 15 min incubation (see Figure 3B). Furthermore, in a control incubation, we added RPA as well as both CFII(XPA$^-$) and CFII(XPC$^-$) after the two damaged DNAs were mixed, so that all NER factors were equally available for the two damaged DNAs. Under these conditions, both damaged DNAs were repaired as expected (lanes 1-4). These data indicate that the two damaged DNAs were practically equivalent as substrates for *in vitro* NER, and consequently that the repair biases observed were intrinsic to the CFII fractions.

If XPA binding is the first lesion recognition event which then leads to assembly of all the other NER factors, one can expect that the damaged DNA pre-incubated in the presence of XPA is repaired preferentially. However, the opposite result is found supporting the idea that XPC-HR23B functions at an earlier stage than XPA. It has been reported that interaction with RPA potentiates damage-binding activity of XPA (He et al. 1995). Because virtually all endogenous RPA was removed during phosphocellulose fractionation, extra addition of RPA could be necessary for endogenous XPA in the CFII(XPC$^-$) to bind lesions stably. Therefore, we tested whether the presence of RPA during the pre-incubation influenced the observed repair bias. However, supplementing CFII(XPC$^-$) with purified RPA during the pre-incubation did not alter the repair preference caused by CFII(XPA$^-$) (Figure 3, lanes 13-16). Thus, the XPC-HR23B-containing CFII(XPA$^-$) appears to focus repair to the damage above the XPA-containing CFII(XPC$^-$) regardless of the presence or absence of RPA during pre-incubation.

XPC-HR23B is sequestered by damaged DNA and this induces targeted repair

The previous experiments do not exclude the possibility that other NER factors present in the CFII(XPA$^-$) are necessary even prior to XPC-HR23B for directing the repair machinery to the damaged DNA. To examine whether the XPC-HR23B complex alone is sufficient to induce the repair bias, DD-I was pre-incubated with purified XPC-HR23B, while DD-II was without any proteins. After combining the two reaction mixtures, CFII(XPC$^-$) and RPA were added to complete the NER incision machinery. As shown in Figure 4A (lanes 5-8), DD-I, which was pre-incubated with XPC-HR23B, was repaired better than DD-II. Addition of both CFII(XPC$^-$) and purified XPC-HR23B after mixing the two damaged DNAs, resulted in the absence of any repair bias, as expected (lanes 1-4). Since the XPC-HR23B fraction used was highly purified as shown in Figure 2B (see also Masutani et al. 1994), it is unlikely that the

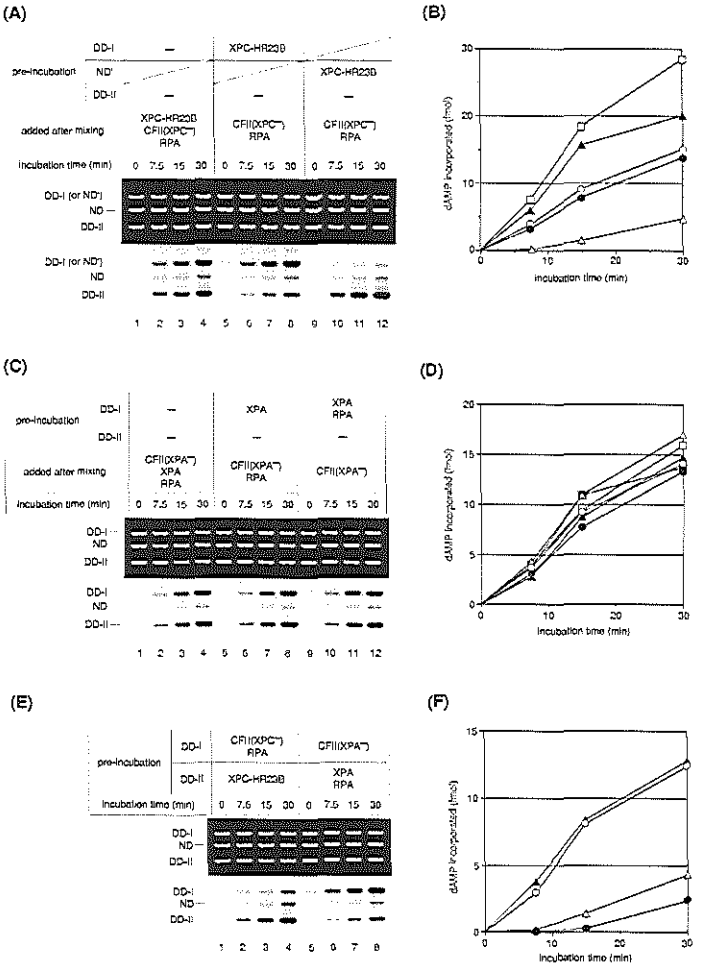

Figure 4. Competition between XPC-HR23B and XPA. **(A, C and E)** Two AAF-damaged DNAs (DD-I and DD-II) or, for lanes 9-12 in panel A, non-damaged version of pBS.XPC• (designated 'ND') were separately pre-incubated at 30•C for 15 min with indicated protein fractions. The two reactions were combined, supplemented with indicated protein fractions as well as non-damaged pHM14 control (ND), and further incubated for various periods of time as indicated. Amounts of protein fractions used were 400 μg for each CFII, 90 ng for XPC-HR23B, 40 ng for XPA and 250 ng for RPA. Repair gaps created in each damaged DNAs were labeled by T4 DNA polymerase. DNA samples were linearized and subjected to agarose gel electrophoresis followed by autoradiography. **(B, D and F)** Radioactivity incorporated in each band in panels A, C and E was quantitated. DNA repair synthesis occurring in each damaged DNA was calculated as done for Figure 3B and depicted as graphs. Closed symbols represent repair of DD-I, while open symbols represent repair of DD-II. Closed circles, open circles: lanes 1-4; Closed triangles, open triangles: lanes 5-8; Closed squares, open squares: lanes 9-12.

presence of minor proteins contaminating the XPC-HR23B was responsible for generation of this repair bias. Furthermore, recombinant XPC-HR23B complex (Sugasawa et al. 1997) was also capable of inducing a similar repair bias (data not shown). Thus the preferential repair of damaged DNA can be induced by pre-incubation with XPC-HR23B alone. Compared to the control incubations (lanes 1-4), the initial repair rate of DD-I was stimulated around 2-fold by pre-incubation with XPC-HR23B, while, conversely, repair of DD-II was significantly inhibited (Figure 4B). Because all the other NER proteins should be available for both damaged DNAs, this repair bias appears to be due to sequestration of XPC-HR23B upon pre-incubation with DD-I. Interestingly, in contrast to damaged DD-I, pre-incubation with non-damaged DNA was unable to reduce subsequent repair of DD-II (Figure 4A and B; lanes 9-12). The above findings show that DNA damage is required for sequestration of XPC-HR23B. Furthermore, during the first 7.5-min incubation, the repair of DD-II was already comparable with that of damaged DNA which was allowed to be pre-incubated with XPC-HR23B (compare lanes 6 and 10 in Figure 4A, and see also Figure 4B), indicating that the sequestration by damaged DNA must be a rapid process.

Similar experiments were carried out with purified XPA and CFII(XPA$^-$). In marked contrast to the pre-incubation with XPC-HR23B, little repair bias was observed when one of the damaged DNAs was pre-incubated with purified XPA (Figure 4C and D; compare lanes 5-8 with lanes 1-4). We also included RPA together with XPA in the pre-incubation, but it failed to cause any preferential repair (lanes 9-12). To investigate the possibility that the absence of a repair bias was due to XPA being present in excess over the number of available lesions in DD-I (and thus still able to bind DD-II after mixing), we performed XPA down titration experiments. When the amount of XPA was reduced to 25 and 50%, no repair bias emerged while total repair of both damaged DNAs was equally suppressed in proportion to the XPA amounts included (data not shown). Apparently, XPA was not stably sequestered by damaged DNA during the pre-incubation, regardless of the presence or absence of RPA.

Although XPA-RPA was not capable of inducing preferential repair, it is not excluded that other combinations of NER factors would have been able to reverse the XPC-HR23B-induced preferential repair. To examine this possibility, DD-II was pre-incubated with purified XPC-HR23B, while DD-I was with CFII(XPC$^-$) and RPA (i.e. containing all the other NER factors). Upon combination of the two mixtures, initial repair still occurred exclusively in DD-II bound to XPC-HR23B (Figure 4E and F; lanes 1-4). Thus the sequestration of XPC-HR23B could not be alleviated by damaged DNA pre-

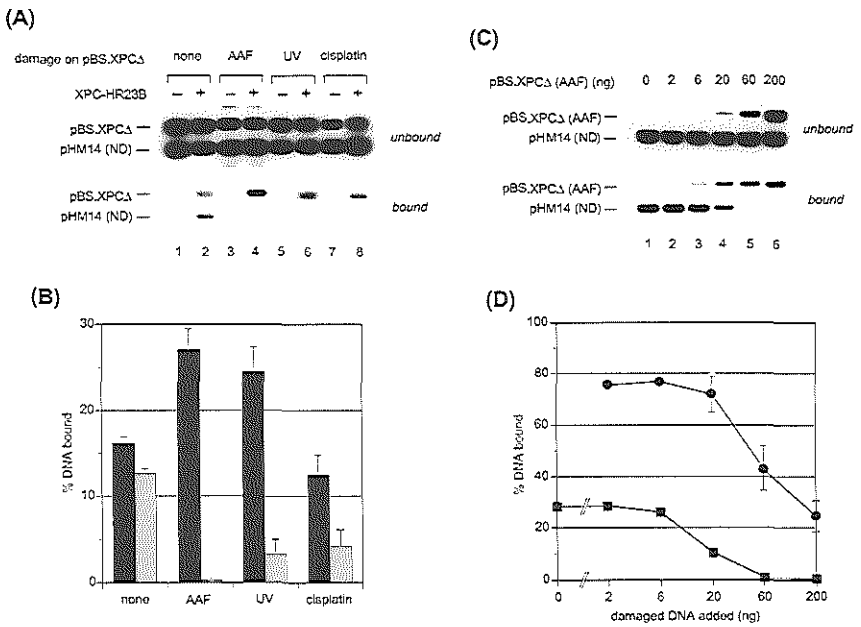

Figure 5. XPC-HR23B preferentially binds to damaged DNAs. **(A)** A mixture of pBS.XPCΔ (non-damaged or damaged with various agents as indicated) and non-damaged pHM14 (200 ng each) was incubated in the presence (+) or absence (-) of 20 ng of XPC-HR23B. Affinity-purified anti-XPC polyclonal antibodies (0.5 μg) were added and precipitated with protein A-Sepharose beads. DNAs in the supernatant (unbound) and precipitate (bound) fractions were purified, linearized and fractionated by agarose gel electrophoresis. The DNAs were transferred onto nylon membrane and visualized by hybridization to ^{32}P-labeled pBKS sequence. **(B)** The percentages of DNA recovered in the bound fractions were quantitated for lanes 2, 4, 6 and 8 in panel A. The mean values and standard errors were calculated from two independent experiments. Solid bars, pBS.XPCΔ; shaded bars, pHM14. **(C)** A mixture of 200 ng of non-damaged pHM14 and varying amounts of AAF-damaged pBS.XPCΔ was incubated with 20 ng of XPC-HR23B, and then immunoprecipitated with anti-XPC antibodies. Linearized DNAs in unbound and bound fractions were subjected to agarose gel electrophoresis followed by Southern blot analysis as done in panel A. **(D)** Quantitation of the result in panel C. The mean values and standard errors were calculated from two independent experiments. (closed circles) AAF-damaged DNA; (closed squares) non-damaged DNA.

incubated with all the other NER proteins: the incision events appeared to be focused on the damaged DNA to which XPC-HR23B was bound. On the other hand, DD-II was pre-incubated with purified XPA and RPA, while DD-I was with CFII(XPA$^-$) (i.e. containing XPC-HR23B). In this case, DD-I was repaired better than DD-II, as expected (lanes 5-8).

XPC-HR23B is a damage-specific DNA binding protein

The above results strongly suggest that XPC-HR23B first binds to DNA lesions and initiates assembly of pre-incision complexes. Although XPC-HR23B has been shown to possess DNA-binding activity, its preference for DNA damage has not yet been documented. Therefore, we examined the damage-specificity of DNA-binding of XPC-HR23B using the same substrates as used in the above experiments. Closed circular plasmid DNA substrates with or without AAF-damage were incubated with XPC-HR23B, which was subsequently precipitated using anti-XPC antibodies. Coprecipitated DNA was purified, fractionated on agarose gels, and visualized by Southern blot hybridization. When a mixture of AAF-damaged and non-damaged DNAs was used, the damaged DNA was coprecipitated with anti-XPC antibodies almost exclusively (Figure 5A, lane 4; see also the quantitative data in Figure 5B). This coprecipitation was completely abolished by omission of XPC-HR23B from the binding reaction (lane 3), indicating that the DNA was precipitated via binding to XPC-HR23B. When the AAF-damaged DNA was replaced by its non-damaged version, XPC-HR23B was bound to both non-damaged DNAs (lanes 1 and 2). Similar preference of XPC-HR23B for damaged DNA was observed, when the DNA was damaged by UV (lanes 5 and 6) or cisplatin (lanes 7 and 8) instead of AAF. These results indicate that XPC-HR23B can bind to DNA even in the absence of lesions and that, when DNA is damaged, XPC-HR23B is recruited to lesions in a specific manner. Moreover, the damage-specific binding properties of XPC-HR23B are not a peculiarity limited to AAF damage, but extend to other lesions that are known NER substrates. To obtain some quantitative impression of the damage preference, a fixed amount (200 ng) of non-damaged DNA was incubated with increasing quantities of AAF-treated DNA in the presence of XPC-HR23B (20 ng; Figure 5C and D). In the absence of damage, in steady state 25-30% of the input non-damaged DNA was bound by XPC-HR23B (lane 1). However, in the presence of AAF-damaged DNA at one-tenth the amount (under these conditions, DNA lesions are still in excess over the XPC molecules), more than half of XPC-HR23B was competed away from the non-damaged DNA (lane 4). Thus, the apparant affinity of XPC-HR23B is at least 10 times higher for the AAF-damaged DNA than for the non-damaged DNA.

To examine whether XPC-HR23B binds directly to DNA damages, DNase I footprinting experiments were carried out. For this purpose, we prepared specific DNA substrates containing a positioned 6-4PP (Figure 6A). When the 3'-end of the damaged strand was labeled and pre-incubated with an increasing amount of XPC-HR23B, a region spanning 15 nucleotides 5' and 20 nucleotides 3' of the lesion was found protected from digestion by

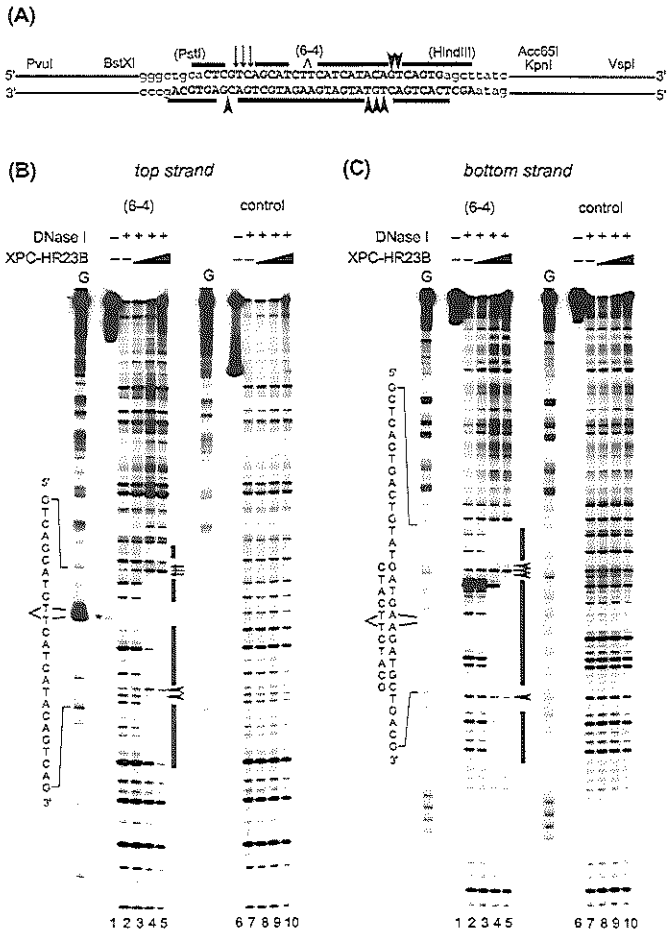

Figure 6. Footprint analysis of XPC-HR23B bound to a UV-induced 6-4PP. **(A)** Defined DNA substrate containing a single 6-4PP. Sequences of the oligonucleotides used for substrate preparation for DNase I footprinting assays are shown by boldfaced letters. **(B and C)** Protection of 6-4PPs against DNase I digestion by XPC-HR23B. DNA fragments containing a site-specific 6-4PP were 3'-labeled at the Acc65I site for the damaged (top) strand (panel B) or at the BstXI site for the non-damaged (bottom) strand (panel C). The labeled DNA fragments were incubated with or without increasing amounts of XPC-HR23B, and then briefly digested by DNase I (or mock-digested). The amounts of XPC-HR23B used were 5 ng (lanes 3 and 8), 10 ng (lanes 4 and 9) and 20 ng (lanes 5 and 10). As markers, the 'G' Maxam-Gilbert sequence ladders were prepared from the same labeled DNA fragments and electrophoresed alongside. The 6-4PP itself is sensitive to piperidine cleavage and gave heavy bands in the Maxam-Gilbert ladders (indicated by asterisks in panel B). In all panels, regions protected and cleavage enhanced by XPC-HR23B binding are indicated by solid lines and arrows, respectively. Arrowheads denote sites accessible to DNase I within the protected regions.

DNase I (Figure 6B). Protection by the XPC-HR23B complex was also observed for the non-damaged strand with bound stretches of 17-18 nucleotides on both sides of the injury (Figure 6C). Several phosphodiester bonds within the protected region remained still accessible to DNase I. Particularly, a couple of cleavage sites in the damaged strand located 8-10 nucleotides 5' of the lesion were weakly enhanced as a result of XPC-HR23B binding. Control DNA substrates lacking damage failed to display any specific protection patterns, indicating damage-specificity of XPC-HR23B binding.

Our findings identify the XPC-HR23B complex as a novel damage binding factor. The damage-dependent sequestration of XPC-HR23B observed in Figure 4 is most likely due to its direct binding to the lesion. If any other combination of NER factors would still be earlier in the NER reaction recruiting XPC-HR23B, we would have observed a reversed repair bias than actually found in Figure 4E (lanes 1-4) where DD-I was incubated with all NER proteins except XPC-HR23B. Hence the focusing of incision events by XPC-HR23B strongly indicates that its binding to the lesion leads to initiation of the repair reaction.

Discussion

Although XPC-HR23B was first purified as a protein factor which corrects defective *in vitro* NER activity of XP-C whole cell extracts (Masutani et al. 1994; Shivji et al. 1994), the positioning of this GGR-specific repair factor in the complex NER reaction has remained mysterious. Our present data demonstrate that the DNA-binding properties of XPC-HR23B are specific for a variety of lesions. In addition, we established that the complex functions at the very first stage of lesion identification in the GGR pathway. This is consistent with a model proposed very recently by Evans et al. (1997), in which TFIIH and XPC-HR23B may be involved in the initial opening of double-stranded DNA around the lesion. In addition, Mu et al. (1997) have recently reported that the first detectable NER intermediate contained the XPC-HR23B complex together with XPA, RPA and TFIIH, also supporting the idea that XPC-HR23B acts at an early stage of NER.

A two-stage damage recognition scheme for GGR?

Our work adds a new damage-recognition protein to the two already known NER factors with preferential affinity for DNA lesions: XPA and UV-DDB/XPE. It has been well documented that XPA preferentially binds DNA containing various NER lesions (Jones and Wood 1993; Asahina et al. 1994; He et al. 1995). XPA shows a much greater affinity for 6-4PPs than for UV-induced

CPDs (Jones and Wood 1993), corresponding with the notion that 6-4PPs are eliminated *in vivo* much more efficiently than CPDs (Mitchell 1988). XP-A null mutant cell lines show an extremely high sensitivity to UV, and the XPA protein contains a DNA-damage binding Zn^{2+}-finger (Tanaka et al. 1990; Morita et al. 1996) as found in the *E.coli* UvrA protein implicated in lesion recognition in prokaryotic NER. Although these findings argued in favour of the idea that XPA is responsible for the lesion recognition step, it has remained unclear whether the damage-specificity of XPA (with or without RPA) is sufficient to account for the very high damage discrimination exhibited by the NER apparatus *in vivo*: the measured association constant of XPA for a heavily UV-irradiated (at 6 kJ/m^2) DNA fragment is about 3×10^6 M^{-1}, which is only 5-fold higher than that for non-irradiated DNA (Jones and Wood 1993). Moreover, interaction of XPA with a single lesion has never been demonstrated by footprint analysis or other methods, as mentioned by Mu et al. (1997) Another damage-binding protein, UV-DDB/XPE, was found to possess a much higher affinity for some lesions than XPA (Reardon et al. 1993; Hwang and Chu 1993). However, UV-DDB seems to play an accessory, but not essential role in the core NER mechanism, because it stimulates *in vitro* NER only 2-fold (Aboussekhra et al. 1995). In contrast to UV-DDB, XPC-HR23B is essential for *in vitro* NER and for GGR *in vivo*. XPC-HR23B was stably sequestered by pre-incubation with damaged DNA, on which incision events were then focused. The results in Figure 4A and B indicate that the lesion binding by XPC-HR23B is a rapid, not rate-limiting step: pre-incubation of XPC-HR23B with non-damaged DNA hardly retarded the repair rate of damaged DNA added later. This explains why the pre-incubation with XPC-HR23B did not result in a dramatic increase in the initial repair rate, but only in a rate proportional to the amount of XPC.

Some lesions can be excised -at least *in vitro*- without the need of XPC-HR23B. These include an artificial, cholesterol-derived adduct (Mu et al. 1996), and a thymine dimer located within an unpaired bubble-like structure (Mu and Sancar 1997). These findings may imply that the XPC complex after binding to a lesion induces a specific conformational change including local opening of DNA, which then allows entry of subsequent NER factors, such as TFIIH, XPA, and RPA (Figure 7). Apparently, the need of XPC-HR23B is bypassed by particular structural features associated with the cholesterol lesion as well as the lesion located in a DNA bubble. Our footprinting analysis using a 6-4PP-containing DNA fragment suggests some interesting structural features of the DNA complexed with XPC-HR23B. Although the XPC-HR23B complex covered a rather long region encompassing the injury, several internal sites were found still accessible to DNase I (Figure 6). Moreover, the

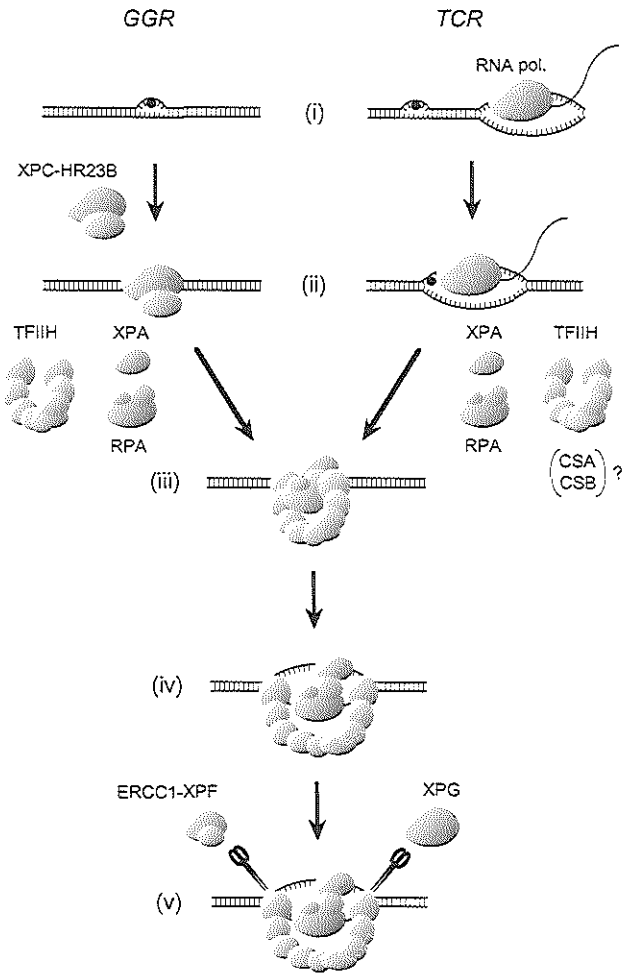

Figure 7. A two-stage damage recognition model for NER. **(i)** A lesion located in the global genome (GGR) or in the transcribed strand of an active gene (TCR). **(ii)** The lesion is first recognized by the XPC-HR23B complex (GGR) or RNA polymerase (TCR). XPC-HR23B may induce some conformational changes of the DNA helix in the vicinity of the lesion, which would favour the subsequent assembly of other NER factors. **(iii)** XPA (possibly together with RPA) participates in the DNA-protein complex to verify the substrate specificity of the lesion. An involvement of TFIIH and initial opening of double-stranded DNA may precede the function of XPA (Evans et al. 1997). It is unknown whether XPC-HR23B is displaced from the lesion or remains bound to it. In TCR, CSA and CSB might be involved in this step. **(iv)** The two DNA helicase subunits of TFIIH may fully open the double-stranded DNA around the lesion. **(v)** Two structure-specific endonucleases, ERCC1-XPF and XPG, make dual incisions at the 5'- and 3'-sites, respectively.

binding of XPC-HR23B also resulted in enhancement of DNase I sensitivity of some phosphodiester bonds in the damaged strand, located 5' to the lesion (see Figure 6A and B). Similar 5'-hypersensitive sites in the damaged strand were observed upon complex formation of the *E.coli* UvrAB repair proteins with various lesions (Van Houten et al. 1987; Voigt et al. 1989; Visse et al. 1991). These sites may enable following NER proteins to participate in the DNA-protein complex.

Using a similar co-immunoprecipitation technique as shown in Figure 5, our XPA preparation was also found to specifically bind AAF-damaged DNA (data not shown). Apparently, however, this direct binding does not lead to productive repair (Figure 4). Therefore, XPA may have to bind damage in a somehow different fashion: a specific protein-protein and/or DNA interaction may be essential for XPA to recognize the lesion productively. This sequential action of two damage-binding proteins may explain the extremely high damage discrimination exhibited by the NER machinery *in vivo*. The problem of tracing numerous types of DNA abnormalities amidst $>10^6$-fold excess of normal nucleotides must be formidable. If the assembly of a specific DNA-protein complex induced by one damage-recognition factor is a prerequisite for the function of the other, one can expect that a much higher damage discrimination could be achievable than with each on its own. The second damage recognition exerted by XPA may provide an oppertunity to verify that the lesion is really a substrate for NER. In addition the XPA protein may help to organize and correctly orient the NER machinery around the DNA injury. Further research using a purified set of NER proteins should elucidate the precise mechanism of early events in GGR, including identification of the XPA function.

Implication for damage recognition in transcription-coupled repair

Although XPC functions specifically in GGR, the findings reported here have also important implications for TCR, the complementary NER subpathway. The principle of sequential damage recognition provides a tempting parallel with the mechanism of lesion detection proposed for TCR. In this process, the equivalent function exerted by XPC-HR23B would be accomplished by RNA polymerase II when it stumbles upon a lesion while transcribing a damaged template (Figure 7). The NER substrate specificity is then checked by XPA (possibly in concert with RPA and TFIIH) that is required for both GGR as well as TCR and thus might play an adaptor role linking the specific components of the two NER subpathways to the common core. Since the principal mechanisms by which the DNA template is screened for intactness by XPC-HR23B and RNA polymerase II are very different, it is to be expected that the

damage recognition profiles of the corresponding NER subpathways are also different. Clearly, the proof of competence exerted by the transcription machinery when copying a DNA strand is probably more rigorous than the test performed by XPC-HR23B. This is the case at least for a number of lesions: TCR efficiently removes several types of damages (e.g. UV-induced CPDs) that are poor substrates for GGR (van Hoffen et al. 1995). In fact, evidence has been obtained that a blocked RNA polymerase may even link multiple DNA repair systems to solve the problem of a damage-induced arrested transcription machinery (Leadon and Cooper 1993; Cooper et al. 1997).

Although the hitherto enigmatic role of XPC-HR23B in NER is clarified by our work, many questions remain unanswered. For instance, which structural features associated with lesions are recognized by XPC-HR23B? A second issue is the fate of XPC-HR23B during the remainder of the NER reaction. It is possible that, soon after the involvement of TFIIH, XPA and/or RPA, the XPC-HR23B complex leaves: the remainder of the NER reaction can at least *in vitro* be conducted without XPC, as shown by the studies using the cholesterol-derived lesion (Mu et al. 1996). Also the notion that TCR takes place without XPC indicates that NER can proceed in the absence of this protein (Mu and Sancar 1997). Future research should shed light on these and other issues.

Experimental Procedures

Plasmid DNA substrates

Plasmid pBS.XPC, which carries the 3.6-kb human XPC cDNA inserted into the NotI site of pBluescript KS+ (pBKS; 3.0 kb) (Masutani et al. 1994), was digested with HindIII and then self-ligated to obtain plasmid pBS.XPCΔ (4.6 kb). Closed circular DNA of this plasmid, as well as pBKS and pHM14 (3.7 kb), was purified from each 2-liter *E.coli* culture. To introduce AAF-damage, pBKS and pBS.XPCΔ were treated as described previosly (van Vuuren et al. 1993). pBS.XPCΔ was also irradiated by UV (450 J/m^2) or treated with cisplatin (a drug/nucleotide ratio = 0.0025) as described (Hansson and Wood 1989). The average number of lesions generated in each preparation was roughly estimated by determining the fraction of DNA that was resistant to digestion by appropriate restriction enzymes: AAF-damaged DNA, ca. one *N*-(guanine-8-yl)-AAF adduct/100 nucleotides; UV-irradiated DNA, 1 thymine dimer (CPD or 6-4PP)/300 nucleotides; cisplatin-treated DNA, 1 d(GpG) intrastrand crosslink/700 nucleotides.

Preparation of protein fractions

Human XPC-HR23B complex was purified from HeLa cells as described previously (Masutani et al. 1994). A heterotrimeric human RPA complex was expressed in *E.coli* BL21(DE3) pLysS transfected with p11d-tRPA (a generous gift from Dr. M. S. Wold), and purified as described (Hendricksen et al. 1994). Mouse XPA protein was expressed in *E.coli* BL21(DE3) pLysS cells, using a pET-8c construct

containing the mouse XPA gene (van Oostrom et al. 1994) kindly provided by Drs. C. F. van Kreyl and H. van Steeg. Consecutive chromatography using heparin-Sepharose CL-6B, Q-Sepharose Fast Flow (both from Pharmacia Biotech), Phospho-Ultrogel A6R (IBF Biotechnics) and Mono Q HR5/5 columns (Pharmacia Biotech) yielded a highly purified XPA preparation. The intact mouse XPA protein was found to be more easily overproduced in *E.coli* than the human counterpart. The complementing activity of the purified XPA protein was checked by microinjection of human XP-A fibroblasts. Whole cell extracts for *in vitro* NER reactions were prepared from lymphoblastoid cell lines derived from XP3BE (GM2248B; group C) or XP7NI (group A) patients as described (Wood et al. 1988). The extracts were fractionated over phosphocellulose as described previously (Sugasawa et al. 1997). Protein concentrations were determined according to the method of Bradford (1976), using bovine serum albumin (BSA) as a standard.

***In vitro* NER reactions**

Standard reaction mixtures for *in vitro* NER (25 μl) contained following components: 40 mM HEPES-KOH (pH 7.8), 9.8 mM $MgCl_2$, 70 mM KCl, 6.8% glycerol, 0.9 mM DTT, 0.4 mM EDTA, 2 mM ATP, 20 μM each of dGTP, dCTP and dTTP, 8 μM dATP, 23 mM phosphocreatine (di-Tris), 1.25 μg of creatine phosphokinase (CrPK), 9 μg of BSA, 125 ng of AAF-damaged pBKS, 125 ng of non-damaged pHM14, and indicated amounts of CFII and purified proteins. For competition experiments, two separate pre-incubations, containing 400 ng each of AAF-damaged pBS.XPC• and pBKS, were carried out at 30°C for 30 min in reaction mixtures lacking at least one NER factor. These two reaction mixtures were combined on ice and supplemented with missing NER factors and non-damaged pHM14 DNA (400 ng), adjusting the final volume of reactions to 100 μl. The mixtures were then aliquoted into four microfuge tubes, and incubated at 30°C for 0, 7.5, 15, and 30 min. Reactions were terminated by addition of EDTA to a final concentration of 20 mM. Purified DNA samples were redissolved in TE buffer [10 mM Tris-HCl (pH 7.5), 1 mM EDTA] and gap filling DNA synthesis reactions were carried out at 37°C for 15 min in 25 μl of mixtures containing 10 mM Tris-HCl (pH 8.0), 5 mM $MgCl_2$, 0.1 M NaCl, 1 mM 2-mercaptoethanol, 20 μM each of dGTP, dCTP and dTTP, 8 μM [α-^{32}P]dATP (~92.5 kBq), 2.5 μg of BSA, and 0.1 unit of T4 DNA polymerase (New England Biolab). DNAs were purified again, linearized with BamHI, and subjected to electrophoresis through 0.8% agarose gels in 1 x TBE buffer containing 0.5 μg/ml of ethidium bromide. The gels were photographed under UV-illumination, dried and autoradiographed with Fuji New RX films and intensifying screens. DNA repair synthesis was quantitated using the PhosphorImager system (Molecular Dynamics).

Damaged DNA binding assay

Purified XPC-HR23B was mixed with 200 ng each of pBS.XPC• (damaged or non-damaged) and non-damaged pHM14 in 25-μl reactions containing 40 mM HEPES-KOH (pH 7.8), 8.8 mM $MgCl_2$, 24 mM KCl, 6.8% glycerol, 0.9 mM DTT, 0.4 mM EDTA, 2 mM ATP, 20 μM each of dGTP, dCTP and dTTP, 8 μM dATP, 23 mM phosphocreatine (di-Tris), 1.25 μg of CrPK, and 9 μg of BSA. After incubation for 30 min at 30°C, 0.5 μg of affinity-purified, polyclonal antibody raised against recombinant human XPC protein (Sugasawa et al. 1996) was added and further incubated on ice for 15 min. A hundred microliter of ice-cold buffer B [25 mM Tris-HCl (pH 7.5), 1 mM EDTA, 0.1 M NaCl, and 0.5% Nonidet P-40] and 25 μl of protein A-Sepharose CL-4B (Pharmacia Biotech; 1:1 suspension in buffer B) were added and kept on ice for 1 h with occasional mixing. After centrifugation, the resulting supernatants were saved as 'unbound' fractions, and the beads were washed three times with 500 μl of ice-cold buffer B. The washed precipitates were suspended in TE buffer containing 1% SDS, and subsequently incubated at 50°C for 30 min. The supernatants were recovered as 'bound' fractions by centrifugation. The purified DNA samples from the unbound and bound fractions were linearized by

BamHI, fractionated through 0.8% agarose gels, and transferred onto Nylon membranes (Hybond-N; Amersham). The blots were hybridized to ^{32}P-labeled pBKS sequences.

DNase I footprinting assay

To prepare DNA substrates for footprinting assays, two non-damaged, synthetic oligonucleotides (30- and 38-mers, sequences of which are shown in Figure 6A) were annealed to each other and cloned between PstI and HindIII sites in pBKS to generate a plasmid, pBS30. The 30-mer oligonucleotide containing a 6-4PP [(6-4)30-mer] was chemically synthesized as described (Iwai et al. 1996). The HindIII-PstI large fragment from pBKS was partially digested by *E.coli* exonuclease III, and then mixed with single-stranded circular DNA derived from pBS30 as well as the 5'-phosphorylated (6-4)30-mer. This mixture was heat-denatured, reannealed and then treated with T4 DNA ligase. Double-stranded closed circular DNA containing a single 6-4PP [pBS(6-4)30] was purified by CsCl-ethidium bromide density gradient centrifugation. A control DNA substrate lacking the lesion [pBS(ND)30] was prepared in the same way, except that the non-damaged 30-mer oligonucleotide was used instead of the (6-4)30-mer.

To label the damaged strand, pBS(6-4)30 was digested by Acc65I and the recessing 3'-end was filled with T7 DNA polymerase (Amersham) in the presence of [α-^{32}P]dCTP. The DNA was further digested by PvuI to obtain a ca. 250-bp fragment containing a 6-4PP. The 3'-end of the non-damaged strand was labeled by sequential treatment of pBS(6-4)30 with BstXI, with T4 DNA polymerase (Takara Shuzo) in the presence of [α-^{32}P]dCTP, and with VspI. For preparing control DNA substrates without 6-4PPs, pBS(ND)30 was treated in the same way. For binding reactions (25 μl), a mixture of 1-2 ng of the ^{32}P-DNA fragment (10,000-20,000 dpm) and 1 ng of poly(dI-dC) was incubated at 30°C for 30 min with various amounts of XPC-HR23B under the same conditions utilized for the damaged DNA binding assay described above. The reactions were chilled on ice, mixed with 25 μl of 5 mM $CaCl_2$, and then digested with 0.004 units of DNase I (Takara Shuzo) at 30°C for 2 min. After the digestion was terminated by addition of 50 μl of stop solution (1% SDS, 20 mM EDTA, 0.2 M NaCl, 100 μg/ml of yeast tRNA). DNA was purified and subjected to denaturing polyacrylamide gel electrophoresis (10% polyacrylamide gel) followed by autoradiography.

Acknowledgements

We thank Gijsbertus T. J. van der Horst, Dik van Gent, Roland Kanaar, and Nicolaas G. J. Jaspers for helpful discussions and advice, and Cécile Visser for preparation of the XPA protein. This work was supported by a Human Frontier Program research grant, by the Medical Genetic Centre, and by the Dutch Scientific Organization (NWO). This work was also supported by grants from the Ministry of Education, Science and Culture of Japan, and by the Biodesign Research Program Grant from RIKEN. K.S. is supported by the President's Special Research Grant from RIKEN and by a grant from the Life Science Foundation of Japan.

References

Aboussekhra, A., Biggerstaff, M., Shivji, M. K. K., Vilpo, J. A., Moncollin, V., Podust, V. N., Protic, M., Hübscher, U., Egly, J.-M., and Wood, R. D. (1995). Mammalian DNA nucleotide excision repair reconstituted with purified protein components. Cell *80*, 859-868.

Asahina, H., Kuraoka, I., Shirakawa, M., Morita, E. H., Miura, N., Miyamoto, I., Ohtsuka, E., Okada, Y., and Tanaka, K. (1994). The XPA protein is a zinc metalloprotein with an ability to recognize

various kinds of DNA damage. Mutat. Res. *315*, 229-237.

Bohr, V. A., Smith, C. A., Okumoto, D. S., and Hanawalt, P. C. (1985). DNA repair in an active gene: removal of pyrimidine dimers from the *DHFR* gene of CHO cells is much more efficient than in the genome overall. Cell *40*, 359-369.

Bootsma, D., Kraemer, K. H., Cleaver, J., and Hoeijmakers, J. H. J. (1998). Nucleotide excision repair syndromes: xeroderma pigmentosum, Cockayne syndrome and trichothiodystrophy. *In:* The Genetic Basis of Human Cancer. B. Vogelstein and K. W. Kinzler, eds. (New York: McGraw-Hill Book Co.), pp. 245-274.

Bradford, M. M. (1976). A rapid and sensitive method for the quantitation of microgram quantities of protein utilizing the principle of protein-dye binding. Anal. Biochem. *72*, 248-254.

Cooper, P. K., Nouspikel, T., Clarkson, S. G., and Leadon, S. A. (1997). Defective transcription-coupled repair of oxidative base damage in Cockayne syndrome patients from XP group G. Science *275*, 990-993.

Evans, E., Moggs, J. G., Hwang, J. R., Egly, J.-M., and Wood, R. D. (1997). Mechanism of open complex and dual incision formation by human nucleotide excision repair factors. EMBO J. *16*, 6559-6573.

Friedberg, E. C., Walker, G. C., and Siede, W. (1995). DNA Repair and Mutagenesis. (Washington, D. C.: ASM Press).

Hansson, J., and Wood, R. D. (1989). Repair synthesis by human cell extracts in DNA damaged by *cis*- and *trans*-diamminedichloroplatinum(II). Nucleic Acids Res. *17*, 8073-8091.

He, Z., Henricksen, L. A., Wold, M. S., and Ingles, C. J. (1995). RPA involvement in the damage-recognition steps of nucleotide excision repair. Nature *374*, 566-569.

Hendricksen, L. A., Umbricht, C. B., and Wold, M. S. (1994). Recombinant replication protein A: expression, complex formation, and functional characterization. J. Biol. Chem. *269*, 11121-11132.

Hwang, B. J., and Chu, G. (1993). Purification and characterization of a human protein that binds to damaged DNA. Biochemistry *32*, 1657-1666.

Iwai, S., Shimizu, M., Kamiya, H., and Ohtsuka, E. (1996). Synthesis of a phosphoramidite coupling unit of the pyrimidine (6-4) pyrimidone photoproduct and its incorporation into oligonucleotides. J. Am. Chem. Soc. *118*, 7642-7643.

Jones, C. J., and Wood, R. D. (1993). Preferential binding of the xeroderma pigmentosum group A complementing protein to damaged DNA. Biochemistry *32*, 12096-12104.

Leadon, S. A., and Cooper, P. K. (1993). Preferential repair of ionizing-radiation induced damage in the transcribed strand of an active human gene is defective in Cockayne syndrome. Proc. Natl. Acad. Sci. USA *90*, 10499-10503.

Legerski, R., and Peterson, C. (1992). Expression cloning of a human DNA repair gene involved in xeroderma pigmentosum group C. Nature *359*, 70-73.

Masutani, C., Sugasawa, K., Yanagisawa, J., Sonoyama, T., Ui, M., Enomoto, T., Takio, K., Tanaka, K., van der Spek, P. J., Bootsma, D., Hoeijmakers, J. H. J., and Hanaoka, F. (1994). Purification and cloning of a nucleotide excision repair complex involving the xeroderma pigmentosum group C protein

and a human homolog of yeast RAD23. EMBO J. *13*, 1831-1843.

Mellon, I., Spivak, G., and Hanawalt, P. (1987). Selective removal of transcription-blocking DNA damage from the transcribed strand of the mammalian *DHFR* gene. Cell *51*, 241-249.

Mitchell, D. L. (1988). The relative cytotoxicity of (6-4) photoproducts and cyclobutane dimers in mammalian cells. Photochem. Photobiol. *48*, 51-57.

Morita, E. H., Ohkubo, T., Kuraoka, I., Shirakawa, M., Tanaka, K., and Morikawa, K. (1996). Implications of the zinc-finger motif found in the DNA-binding domain of the human XPA protein. Genes Cells *1*, 437-442.

Mu, D., Hsu, D. S., and Sancar, A. (1996). Reaction mechanism of human DNA repair excision nuclease. J. Biol. Chem. *271*, 8285-8294.

Mu, D., Park, C. H., Matsunaga, T., Hsu, D. S., Reardon, J. T., and Sancar, A. (1995). Reconstitution of human DNA repair excision nuclease in a highly defined system. J. Biol. Chem. *270*, 2415-2418.

Mu, D., and Sancar, A. (1997). Model for XPC-independent transcription-coupled repair of pyrimidine dimers in humans. J. Biol. Chem. *272*, 7570-7573.

Mu, D., Wakasugi, M., Hsu, D. S., and Sancar, A. (1997). Characterization of reaction intermediates of human excision repair nuclease. J. Biol. Chem. *272*, 28971-28979.

Reardon, J. T., Mu, D., and Sancar, A. (1996). Overproduction, purification, and characterization of the XPC subunit of the human DNA repair excision nuclease. J. Biol. Chem. *271*, 19451-19456.

Reardon, J. T., Nichols, A. F., Keeney, S., Smith, C. A., Taylor, J.-S., Linn, S., and Sancar, A. (1993). Comparative analysis of binding of human damaged DNA-binding protein (XPE) and *Escherichia coli* damage recognition protein (UvrA) to the major ultraviolet photoproducts: T[*c,s*]T, T[*t,s*]T, T[6-4]T, and T[Dewar]T. J. Biol. Chem. *268*, 21301-21308.

Sancar, A. (1996). DNA excision repair. Annu. Rev. Biochem. *65*, 43-81.

Selby, C. P., and Sancar, A. (1993). Molecular mechanism of transcription-repair coupling. Science *260*, 53-58.

Shivji, M. K. K., Eker, A. P. M., and Wood, R. D. (1994). DNA repair defect in xeroderma pigmentosum group C and complementing factor from HeLa cells. J. Biol. Chem. *269*, 22749-22757.

Shivji, M. K. K., Kenny, M. K., and Wood, R. D. (1992). Proliferating cell nuclear antigen is required for DNA excision repair. Cell *69*, 367-374.

Sugasawa, K., Masutani, C., Uchida, A., Maekawa, T., van der Spek, P. J., Bootsma, D., Hoeijmakers, J. H. J., and Hanaoka, F. (1996). hHR23B, a human RAD23 homolog, stimulates XPC protein in nucleotide excision repair *in vitro*. Mol. Cell. Biol. *16*, 4852-4861.

Sugasawa, K., Ng, J. M. Y., Masutani, C., Maekawa, T., Uchida, A., van der Spek, P. J., Eker, A. P. M., Rademakers, S., Visser, C., Aboussekhra, A., Wood, R. D., Hanaoka, F., Bootsma, D., and Hoeijmakers, J. H. J. (1997). Two human homologs of RAD23 are functionally interchangeable in complex formation and stimulation of XPC repair activity. Mol. Cell. Biol. *17*, 6924-6931.

Tanaka, K., Miura, N., Satokata, I., Miyamoto, I., Yoshida, M. C., Satoh, S., Kondo, A., Yasui, A., Okayama, H., and Okada, Y. (1990). Analysis of a human DNA excision repair gene involved in group

A xeroderma pigmentosum and containing a zinc-finger domain. Nature *348*, 73-76.

van Hoffen, A., Venema, J., Meschini, R., van Zeeland, A. A., and Mullenders, L. H. F. (1995). Transcription-coupled repair removes both cyclobutane pyrimidine dimers and 6-4 photoproducts with equal efficiency and in a sequential way from transcribed DNA in xeroderma pigmentosum group C fibroblasts. EMBO J. *14*, 360-367.

Van Houten, B., Gamper, H., Sancar, A., and Hearst, J. E. (1987). DNase I footprint of ABC excinuclease. J. Biol. Chem. *262*, 13180-13187.

van Oostrom, C. T. M., de Vries, A., Verbeek, S. J., van Krijl, C. F., and Versteeg, H. (1994). Cloning and characterization of the mouse *XPAC* gene. Nucleic Acids Res. *22*, 11-14.

van Vuuren, A. J., Appeldoorn, E., Odijk, H., Yasui, A., Jaspers, N. G. J., Bootsma, D., and Hoeijmakers, J. H. J. (1993). Evidence for a repair enzyme complex involving ERCC1 and complementing activities of ERCC4, ERCC11 and xeroderma pigmentosum group F. EMBO J. *12*, 3693-3701.

Venema, J., van Hoffen, A., Karcagi, V., Natarajan, A. T., van Zeeland, A. A., and Mullenders, L. H. F. (1991). Xeroderma pigmentosum complementation group C cells remove pyrimidine dimers selectively from the transcribed strand of active genes. Mol. Cell. Biol. *11*, 4128-4134.

Venema, J., van Hoffen, A., Natarajan, A. T., van Zeeland, A. A., and Mullenders, L. H. F. (1990). The residual repair capacity of xeroderma pigmentosum complementation group C fibroblasts is highly specific for transcriptionally active DNA. Nucleic Acids Res. *18*, 443-448.

Visse, R., de Ruijter, M., Brouwer, J., Brandsma, J. A., and van de Putte, P. (1991). Uvr excision repair protein complex of *Escherichia coli* binds to the convex side of a cisplatin-induced kink in the DNA. J. Biol. Chem. *266*, 7609-7617.

Voigt, J. M., Van Houten, B., Sancar, A., and Topal, M. D. (1989). Repair of O^6-methylguanine by ABC excinuclease of *Escherichia coli in vitro*. J. Biol. Chem. *264*, 5172-5176.

Wood, R. D. (1996). DNA repair in eukaryotes. Annu. Rev. Biochem. *65*, 135-167.

Wood, R. D., Robins, P., and Lindahl, T. (1988). Complementation of the xeroderma pigmentosum DNA repair defect in cell-free extracts. Cell *53*, 97-106.

Chapter

V

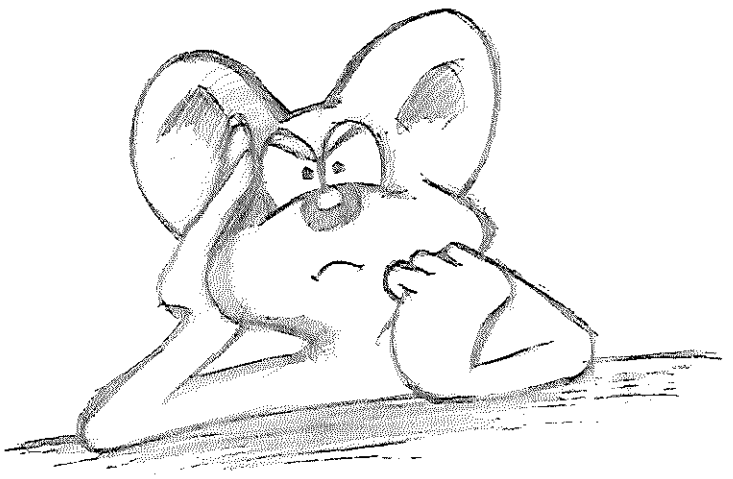

Developmental Defects and Male Sterility in Mice Lacking the Ubiquitin-Like DNA Repair Gene *mHR23B*

Jessica M.Y. Ng[1], Harry Vrieling[3], Kaoru Sugasawa[5,6], Marja P. Ooms[2], J. Anton Grootegoed[2], Jan T.M. Vreeburg[2], Pim Visser[1], Theo G. M. F. Gorgels[1], Rudolph B. Beems[4], Fumio Hanaoka[5,6,7], Jan H.J. Hoeijmakers[1] and Gijsbertus T.J. van der Horst[1]

[1]MGC-Department of Cell Biology & Genetics, Centre for Biomedical Genetics, Erasmus University Rotterdam, P.O. Box 1738, Rotterdam, The Netherlands
[2]Department of Endocrinology & Reproduction, Erasmus University Rotterdam, P.O. Box 1738, Rotterdam, The Netherlands
[3]MGC-Department of Radiation Genetics and Chemical Mutagenesis, Leiden University Medical Center, 2333 AL Leiden, The Netherlands
[4]National Institute of Public Health and the Environment, P.O Box 1, 3720 BA, Bilthoven, The Netherlands
[5]Cellular Physiology Laboratory, RIKEN (The Institute of Physical and Chemical Research), and [6]Core Research for Evolutional Science and Technology, Japan Science and Technology Corporation, Wako, Saitama 351-0198, Japan
[7]Institute for Molecular and Cellular Biology, Osaka University, Suita, Osaka 565-0871, Japan

Summary

mHR23B encodes one of the two mammalian homologs of *S.cerevisiae* RAD23, an ubiquitin-like fusion protein involved in nucleotide exision repair (NER). Part of mHR23B is complexed with the XPC protein and this heterodimer functions as the main damage detector and initiator of global genome NER. While *XPC* defects exist in man and mice, mutants for *mHR23A* and *mHR23B* are not known. Here, we present a mouse model for *mHR23B*. Unlike *XPC*-deficient cells, *mHR23B*$^{-/-}$ mouse embryonic fibroblasts are not UV-sensitive and retain normal repair characteristics. In agreement with *in vitro* repair studies, this indicates that mHR23A can functionally replace mHR23B in NER. Unexpectedly, *mHR23B*$^{-/-}$ mice show impaired embryonic development and a high rate (90%) of intrauterine or neonatal death. Surviving animals display a variety of abnormalities including retarded growth, facial dysmorphology, and male sterility. Such abnormalities are not observed in *XPC* and other NER-deficient mouse mutants and point to a separate function of mHR23B in development. This function may involve regulation of protein stability via the ubiquitin/proteasome pathway and is not or only in part compensated for by mHR23A.

Introduction

Nucleotide excision repair (NER) is the major repair system for the removal of DNA lesions induced by ultraviolet (UV) light and numerous chemical agents (Friedberg et al. 1995; Wood 1996). The "cut-and-patch" type reaction mechanism involves the concerted action of over 25 proteins, sequentially implicated in recognition of DNA damage, unwinding of the DNA around the lesion, excision of a single-stranded piece of DNA containing the damage, and subsequent gap filling DNA synthesis and ligation (de Laat et al. 1999). NER consists of two subpathways. Genome-wide repair is taken care of by the global genome NER (GG-NER) process, acting irrespective of genomic location of the lesion or cell cycle stage. Some lesions however (e.g. UV-induced cyclobutane pyrimidine dimers), are repaired less efficiently by GG-NER. To avoid that such lesions obstruct the vital process of transcription for too long, the transcription-coupled repair (TC-NER) subpathway acts as a fast backup system for clearance of the template strand of actively transcribed genes (Hanawalt 1994 and 2000).

Defective NER is associated with three clinically and genetically heterogeneous human syndromes: xeroderma pigmentosum (XP), Cockayne syndrome (CS) and trichothiodystrophy (TTD) (Bootsma et al. 2001).

Patients suffering from XP (complementation groups XP-A to XP-G) exhibit severe sun (UV) sensitivity, ocular symptoms, and cutaneous abnormalities including a very strong predisposition to develop skin cancer. Most XP patients carry defects in GG-NER and TC-NER, but in the case of XP-C only the GG-NER pathway is affected (Venema et al. 1990 and 1991; van Hoffen et al. 1995).

The XPC protein is essential for GG-NER of various types of DNA damage and is found in a tight complex with hHR23B, one of the two human homologs of the *Saccharomyces cerevisiae* DNA repair protein RAD23 (Masutani et al. 1994). hHR23B stimulates the repair activity of XPC in *in vitro* reconstitution assays with recombinant proteins (Sugasawa et al. 1996). A 56 amino acid segment with a predicted amphiphatic helical structure containing the XPC-binding domain of hHR23B appears sufficient for XPC stimulation. This suggests that hHR23B has a structural rather than a catalytic function (Masutani et al. 1997). A vast majority of XPC protein is bound to hHR23B *in vivo*. However, *in vitro*, hHR23A, the second human homolog of RAD23, can substitute for hHR23B in binding and stimulating XPC. This opens the possibility that both proteins are to some extent functionally interchangeable (van der Spek et al. 1996a; Sugasawa et al. 1997). The XPC-hHR23B complex has been identified as the primary DNA-damage sensor that initiates GG-NER and has *in vivo* and *in vitro* been shown to directly interact with the essential repair/transcription factor TFIIH (Sugasawa et al. 1998; Yokoi et al. 2000). The XPC-hHR23B complex senses different types of damage based on disrupted base paring and stimulates the association of TFIIH with damaged DNA in cell-free extracts (Yokoi et al. 2000; Sugasawa et al. 2001). After the initial subpathway-specific lesion detection, the XPB and XPD helicase subunits of TFIIH open the DNA helix around the lesion. XPA together with the heterotrimeric RPA may function as a common damage verifier before the DNA is incised on both sides of the injury by the XPG and ERCC1/XPF endonucleases (de Laat et al. 1999; Yokoi et al. 2000).

In addition to the XPC-binding domain, yeast and mammalian RAD23 proteins harbor an amino-terminal ubiquitin-like (UbL) moiety and two so-called ubiquitin-associated (UBA) domains (Hofmann and Bucher 1996; Masutani et al. 1997). In yeast, the UbL domain is indispensable for the repair function of RAD23 (Watkins et al. 1993; Mueller and Smerdon 1996). Moreover, hHR23A and hHR23B interact with the S5a subunit of the 26S proteasome, and hHR23A serves as a substrate for E6-associated protein-mediated ubiquitination (Hiyama et al. 1999; Kumar et al. 1999).

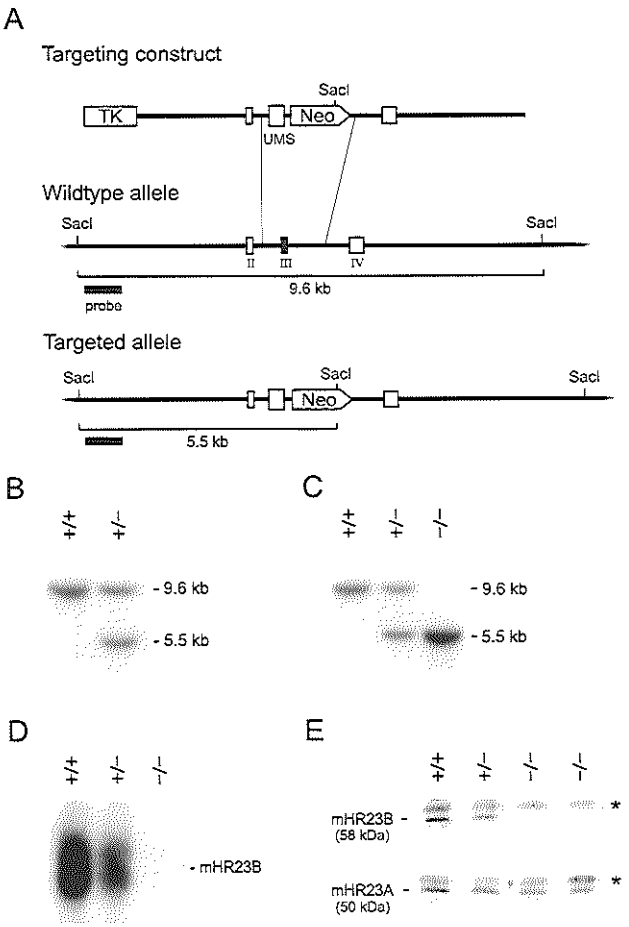

Figure 1. Targeted disruption of the *mHR23B* gene by homologous recombination. **(A)** Genomic organization and disruption strategy for *mHR23B* showing the gene, the targeting construct, and the targeted *mHR23B* allele. Exon III is deleted and the UMS and Neo cassettes are inserted between exon II and exon IV. **(B)** Southern blot analysis of SacI digested DNA from ES cells showing the 9.6 kb and 5.5 kb fragment representing the wildtype and the targeted allele of *mHR23B* respectively. **(C)** Southern blot analysis of SacI digested tail DNA from *mHR23B*$^{+/+}$, *mHR23B*$^{+/-}$, and *mHR23B*$^{-/-}$ mice. **(D)** RNA blot analysis of mHR23B mRNA in cellular extracts from *mHR23B*$^{+/+}$, *mHR23B*$^{+/-}$, and *mHR23B*$^{-/-}$ MEFs using *mHR23B* cDNA as a probe. As a loading control for the amount of RNA, the blot was reprobed with *mHR23A* cDNA (data not shown). **(E)** Immunoblot analysis of mHR23B protein in cellular extracts from *mHR23B*$^{+/+}$, *mHR23B*$^{+/-}$, and *mHR23B*$^{-/-}$ MEFs using polyclonal antibodies against the human HR23B protein (upper panel). Polyclonal antibodies against the human HR23A protein (lower panel) and the human XPC protein (data not shown) were used as a loading control and to check whether mHR23A protein is expressed in *mHR23B* MEFs. The asterisks indicate aspecific crossreacting bands.

These findings strongly suggest that the RAD23 homologs are involved in the ubiquitin/proteasome pathway.

Although hHR23A can functionally replace hHR23B *in vitro* during NER, it is unknown whether and to which extent these two human RAD23 homologs can substitute for each other *in vivo*. Moreover, while for most other NER genes natural and/or laboratory made human and rodent mutant cell lines are available, *HR23*-deficient cell lines have not been described. Thus, to address the biological relevance of mammalian RAD23 homologs and their relationship to XPC in NER, we have inactivated the mouse homolog of HR23B *(mHR23B)* by gene targeting. In the present paper we describe the phenotype of *mHR23B*-deficient mice and cells.

Results

Targeted disruption of the mouse *mHR23B* gene

The mouse *mHR23B* locus was isolated and partly characterized. Deletion of exon III not only removes the sequence encoding amino acid residues 148 to 228 of the mHR23B protein, but also results in a frame shift and accordingly is expected to give rise to a null-allele (Figure 1A). Following transfection of ES cell line E14, properly targeted heterozygous ES cells were obtained at a frequency of 21% (Figure 1B). Two independent ES clones verified for the absence of visible chromosomal abnormalities and additional randomly integrated constructs (data not shown) were used for blastocyst injections. Germ line transmission was obtained for both clones. Heterozygous offspring from matings between chimeric males and C57BL/6 female mice was intercrossed with the aim to generate homozygous mutant *mHR23B* animals (Figure 1C). In parallel, these matings served to isolate mouse embryonic fibroblasts (MEFs) of different genotypes from day 13.5 embryos. The effect of targeted disruption on the expression of the *mHR23B* gene was analyzed in MEFs: neither *mHR23B* mRNA nor mHR23B protein could be detected in *mHR23B*$^{-/-}$ cells by RNA and immunoblot analysis respectively. We conclude that we have created *mHR23B* null-mutants (Figure 1D and E). Homozygous mouse mutants and cell lines from the two independent ES transformants yielded identical results in all subsequent studies indicating that the findings reported below are not due to uncontrolled events that might have occurred in one targeted ES clone, but are the result of *mHR23B* inactivation.

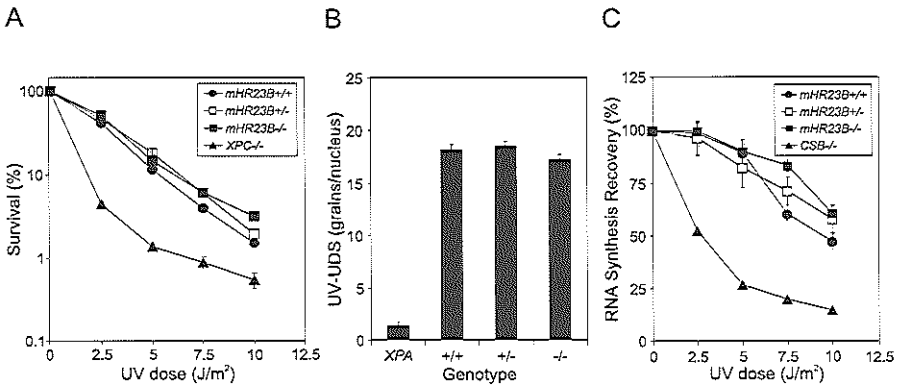

Figure 2. Repair characteristics of *mHR23B*-deficient mouse embryonic fibroblasts. **(A)** UV survival curves of *mHR23B*$^{+/+}$, *mHR23B*$^{+/-}$, and *mHR23B*$^{-/-}$ fibroblast lines. Identical results were obtained with three other cell lines of *mHR23B*$^{+/+}$ and *mHR23B*$^{+/-}$ and with five independent other lines of *mHR23B*$^{-/-}$ MEFs (data not shown). *XPC*$^{-/-}$ fibroblasts were included as negative control. Cells were exposed to different doses of UV (254 nm). After 4-5 days, the number of proliferating cells was estimated from the amount of radioactivity incorporated during a 3 hr pulse with [^{3}H]thymidine. **(B)** Global genome repair (UDS) in *mHR23B*$^{+/+}$, *mHR23B*$^{+/-}$, and *mHR23B*$^{-/-}$ fibroblast lines. Three other lines of *mHR23B*$^{+/+}$ and *mHR23B*$^{+/-}$, and five independent lines of *mHR23B*$^{-/-}$ were tested with consistent results (data not shown). *XPA*$^{-/-}$ fibroblasts were measured to serve as negative control. Cells were irradiated with 16 J/m^2 UV (254 nm) and labelled with [^{3}H]thymidine. Incorporation of radioactivity was measured by autoradiography and grain counting (average of 50 nuclei per cell line: the standard error of the mean is indicated). **(C)** RNA synthesis recovery after UV exposure of *mHR23B*$^{+/+}$, *mHR23B*$^{+/-}$, and *mHR23B*$^{-/-}$ fibroblast lines. Three other lines of *mHR23B*$^{+/+}$ and *mHR23B*$^{+/-}$, and five other independent lines of *mHR23B*$^{-/-}$ were assayed with similar outcome (data not shown). *CSB*$^{-/-}$ fibroblasts were measured as negative control. 16 hours after exposure to different doses of UV (254 nm), the residual RNA synthesis was measured by scintillation counting following a 1 hr pulse labelling with [^{3}H]uridine. For each genotype, comparable results were obtained by grain counting after autoradiography (data not shown).

mHR23B-deficient cells are NER proficient

In view of the role of yeast RAD23 in NER and the tight interaction of mHR23B with XPC (Masutani et al. 1994) we examined cellular survival of wildtype, heterozygous and homozygous *mHR23B* mutant MEFs after exposure to increasing UV-doses. Unexpectedly, UV survival of *mHR23B*$^{+/-}$ and *mHR23B*$^{-/-}$ cells appeared indistinguishable from wildtype (Figure 2A). Moreover, *mHR23B*-deficient MEFs show normal DNA repair synthesis (unscheduled DNA synthesis (UDS): Figure 2B) and recovery of RNA synthesis after UV exposure (Figure 2C), indicating that neither GG-NER

Table 1. Intrauterine and perinatal lethality of *mHR23B* homozygous mutants at different embryonic/fetal stages

Stage	Analyzed	Expected (if Mendelian)	Found	Deviation from Mendelian
E13.5	70	17.5	14	~0
E15.5	72	18.0	9	2x
E18.5	162	40.5	19	2x
Newborn	671	167.8	16	10x

nor TC-NER subpathways were affected. Also in other respects (e.g. morphology, growth rate, etc.) *mHR23B*-deficient MEFs behaved normally. Assuming that a total *mHR23* inactivation would result in a DNA repair deficiency like in yeast (Watkins et al. 1993; Mueller and Smerdon 1996), these data suggest that, mHR23A not only *in vitro*, but also *in vivo* can fully substitute for mHR23B, at least for its function in NER.

mHR23B-deficiency causes impaired embryonic development and intrauterine death

When (phenotypically normal) heterozygous animals were crossed to produce *mHR23B*-deficient mice, the targeted *mHR23B* allele was found to segregate at a ratio far (~10-fold) below Mendelian expectance (Table 1; in total 671 animals analyzed) suggesting that a lack of mHR23B protein causes intrauterine and/or perinatal death. Since *mHR23B*-deficient MEF lines were obtained at an almost Mendelian ratio (data not shown) lethal events must occur after day 13.5 of gestation (E13.5). Analysis of a large series of embryos at different stages of development revealed a near two-fold reduction in the number of viable *mHR23B*-deficient embryos between E13.5 and E15.5 (Table 1). Since at E18.5 still 50% of the *mHR23B*-deficient embryos was alive (and born litters contained only 10% of the expected numbers of knockout animals), 80% of the remaining embryos is assumed to have died immediately prior to, during, or shortly after birth, which is consistent with the observed high number of dead newborn *mHR23B*$^{-/-}$ mice.

mHR23B-deficient embryos (E13.5-E19.5) showed clear signs of growth retardation and were readily recognized by a marked reduction in body size (Figure 3). This is reflected by a reduced body weight, which becomes more pronounced towards term (data not shown). All *mHR23B*$^{-/-}$ embryos alive at stages E13.5-E19.5 appeared pale whereas major blood

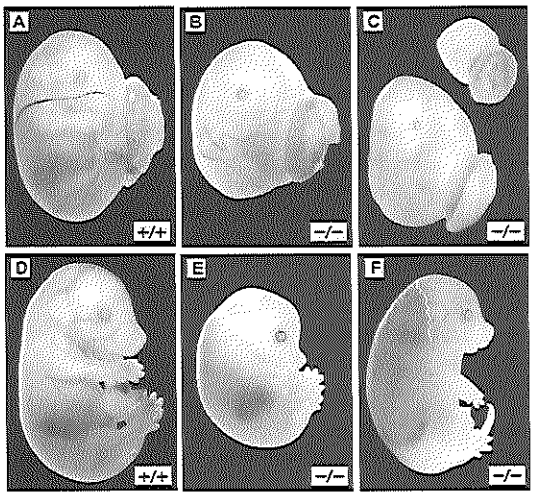

Figure 3. Developmental impairment in *mHR23B*$^{-/-}$ embryos at E15.5. **(A-C)** *mHR23B*$^{+/+}$ (A) and *mHR23B*$^{-/-}$ (B and C) embryos with amniotic/chorionic plates and placentas. **(D-F)** *mHR23B*$^{+/+}$ (D) and *mHR23B*$^{-/-}$ (E and F) embryos without amniotic/chorionic plates and placentas. Embryo of panel A is identical to that of D, and embryo of panel B is identical to that of E. *mHR23B*$^{-/-}$ embryos display retarded growth and impaired vascularization (B and E), intrauterine death (C) and internal bleeding (F).

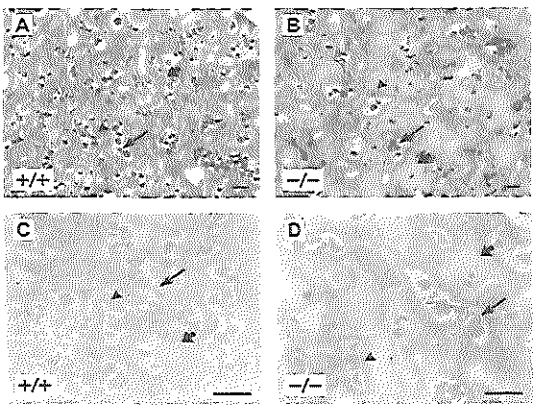

Figure 4. Placental defect in *mHR23B*$^{-/-}$ embryos at E18.5. Histological 1 μm sections **(A and B)** and transmission electron micrographs **(C and D)** of *mHR23B*$^{+/+}$ (A and C) and *mHR23B*$^{-/-}$ (B and D) placentas. *mHR23B*$^{-/-}$ placenta shows swollen throphoblastic cells (small black arrows) and significantly reduced vascularization (blood vessels are indicated by large black arrows and endothelial cells by black arrowheads). Additionally, in contrast to normal placental labyrinth of wildtype, the vascularization and the vascular basement membranes in the mutant placenta seem to be disturbed. Scale bars represent 10 μm (A-D).

vessels were not clearly visible (Figure 3B and E). This suggests that vascularization and/or blood supply was poor. In addition, large numbers of *mHR23B*$^{-/-}$ embryos showed edema (Figure 3F). Also, embryos with interstitial bleeding throughout the body were found (Figure 3F). Moreover, in numerous *mHR23B*-deficient embryos (E13.5-E19.5) the eyelids were not closed and the mouth was widely open, which is a characteristic feature of maceration following embryonic decease. Eyelid closure and fusion normally occur between E15.5 and E16.5 of mouse embryonic development. Widely open mouth normally indicates micrognathia or cleft lip resulting from retarded growth of the mandible.

Preliminary histopathological examination of living *mHR23B*-deficient E15.5 and E18.5 embryos revealed no obvious abnormal architecture of vital organs and tissues, and the reduction in organ weight appeared proportional to the reduction in total body weight. However, in one *mHR23B*-deficient E18.5 embryo we observed an open secondary palate (cleft palate) resulting from imperfect closure of the palatal shelves of the maxilla (in normally developing embryos this is completed at E16; data not shown). Taken together, these data indicate that the mHR23B protein is required for proper embryonic development, and that mHR23A can not or only in part substitute for this function.

Inactivation of *mHR23B* causes a placental defect

In line with the pale appearance of a large number of *mHR23B*-deficient embryos, *mHR23B*$^{-/-}$ placentas at stage E18.5 (n=3) appeared pale and smaller when compared to *mHR23B*$^{+/+}$ and *mHR23B*$^{+/-}$ placentas. Histological examination revealed poor vascularization of mutant placentas, as evident from the reduced number of fetal blood vessels in the labyrinth (Figure 4A and B). Transmission electron microscopy of *mHR23B*$^{-/-}$ placentas (n=3) revealed swollen trophoblastic cells (Figure 4C and D). In addition, altered morphology of the vascular basement membrane of *mHR23B*$^{-/-}$ placentas was observed (Figure 4D). The vascular basement membrane of *mHR23B*$^{-/-}$ placentas was darker and thicker than that of wildtype placentas, which might affect the exchange of gases and transport of nutrients and waste products.

***mHR23B*$^{-/-}$ mice show retarded growth and facial dysmorphology**

Despite the pronounced impact of the *mHR23B*-deficiency on embryonic development, about one tenth of the expected number of homozygous mutant mice were found alive in litters born from heterozygous breeding

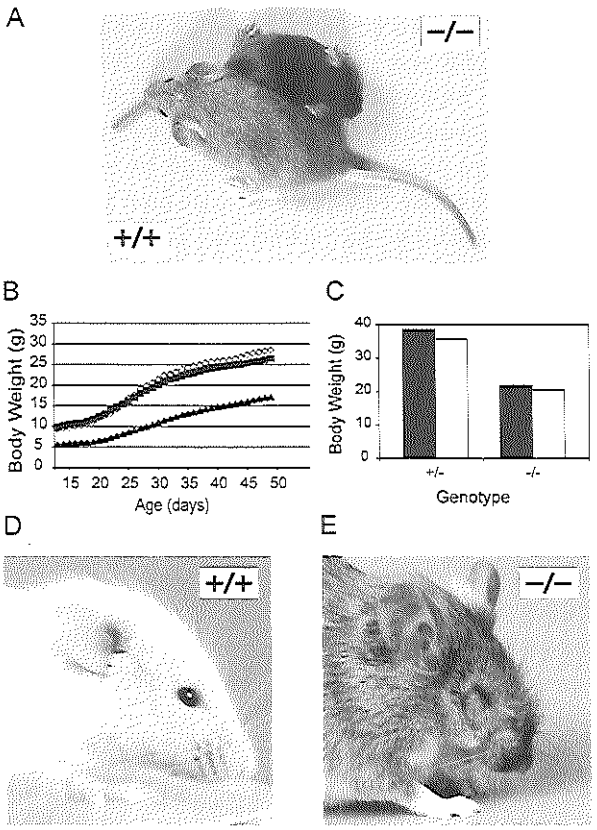

Figure 5. Growth retardation in *mHR23B*$^{-/-}$ mice. **(A)** A 19-day-old wildtype male mouse (brown) and its smaller *mHR23B*$^{-/-}$ (black) littermate. **(B)** Growth curve of *mHR23B* mice: *mHR23B*$^{+/+}$ (n=3 males, open diamonds); *mHR23B*$^{+/-}$ (n=8 (5 males and 3 females), closed squares) and *mHR23B*$^{-/-}$ (n=6 (4 males and 2 females), closed triangles). The average body weights (gram) were followed in time over a period of 5 weeks. **(C)** The average body weights (gram) of 93-day-old *mHR23B*$^{+/-}$ (n=8 (5 males and 3 females)) and *mHR23B*$^{-/-}$ (n=6 (4 males and 2 females)) mice. Males are indicated in black columns and females in white columns. **(D)** Adult *mHR23B*$^{+/+}$ mouse. **(E)** Eyelids are inflamed in adult *mHR23B*$^{-/-}$ mouse and are surrounded by a large amount of tears/eye fluid. The head of *mHR23B*$^{-/-}$ mouse appears irregularly shaped due to hypoplasia of maxilla and mandible.

couples (Table 1). Like *mHR23B*$^{-/-}$ embryos, newborn homozygous mutant mice showed a marked reduction in body size and are readily distinguishable from their heterozygous and wildtype littermates (Figure 5A). After weaning, we did not notice any further loss of *mHR23B*$^{-/-}$ animals. As evident from body weight measurements, *mHR23B*$^{-/-}$ mice display retarded growth, particularly in the last days before weaning (day 21). Up to

7 weeks after birth the average body weight of homozygous mutant males (n=4) and females (n=2) was still approximately 50% lower than that of wildtype (n=3) and heterozygous (n=8) littermates (Figure 5B). This situation remained throughout life (see for body weight at 3 months: Figure 5C). Vital organs were proportionally reduced in size (data not shown). Adult *mHR23B*$^{-/-}$ males and females (up to 1 year and older) lacked fatty tissues, while excessive fat was observed in the abdominal cavity of wildtype mice. However, histopathological examination of the vital organs, sciatic nerve and skeletal muscle from adult *mHR23B*-deficient mice (n=4) failed to reveal any obvious abnormality (data not shown).

mHR23B-deficient mice showed facial dysmorphology. The nose had a blunted shape rather than the tapered appearance characteristic for rodents due to hypoplasia of the maxilla and mandible (Figure 5D and E). In addition, more than one third of the *mHR23B*-deficient mice developed so-called elephant teeth.

mHR23B-deficient mice have ocular pathology

Some 7 to 10 days after birth *mHR23B*-deficient mice started to develop eye pathology, characterized by excessive eye fluid and swelling of the eyelids. Animals refrained from opening the eyes widely. Probably as a result of the continuously drenched eyes, *mHR23B*-deficient mice showed excessive washing activities. These features persisted into adulthood with frequent signs of inflammation in eyelids, that could not be treated by application of eye ointment (Figure 5E). In addition, a large number of *mHR23B*-deficient animals seemed to suffer from itching, as evident from extensive scratching, which was not restricted to the head region but also involved the ears and the neck line. Some *mHR23B*-deficient mice showed corneal opacities (data not shown).

Histological analysis of *mHR23B*-deficient mice (n=6) confirmed conjunctivitis. In addition, in the corner of *mHR23B*-deficient eyes, inflammation cells containing polymorphic nuclei were observed (data not shown). A clear cause of the wet eyes was not detected. The tear-producing glands showed no overt abnormalities. In one *mHR23B*-deficient mouse, however, the number of the conjunctival Goblet cells that produce the mucous layer of the tear film was reduced. The drainage of the tears was checked in one *mHR23B*-deficient animal and appeared normal. Moreover, we failed to observe any abnormalities in other parts of the eye, such as the retina (data not shown).

To examine the possibility of any inflammatory disease, the ratio in IgA, IgG and IgM and white blood cell counts of adult *mHR23B*-deficient

A

B

Average Weights of Body and Sexual Organs in Wildtype and *mHR23B* Knockout Male Mice

	Wildtype*	Knockout**
Body Weight (g)	37.8	18.5
Testes (mg)	221.1	30.4
Epididymides (mg)	79.6	31.5
Seminal Vesicles (mg)	59.5	35.6

* Consisted of 6 (4.5-month-old) mice (+/+ n=3; +/- n=3)
** Consisted of 6 (4.5-month-old) *mHR23B*-/- mice (n=6)

Figure 6. *mHR23B*$^{-/-}$ males display retarded growth of the testis. **(A)** Macrograph of adult wildtype (left) and *mHR23B*$^{-/-}$ (right) testes. Besides reduction in size, blood vessels are not clearly visible in *mHR23B*$^{-/-}$ testes. Scale bar represents 5 mm. **(B)** Average weights of body and sexual organs in wildtype and *mHR23B*$^{-/-}$ male mice.

mice (n=5) was determined, but did not reveal abnormalities, indicating that the immunological system is not compromised (data not shown).

Defective spermatogenesis in *mHR23B*$^{-/-}$ male mice

Attempts to use *mHR23B*-deficient males in breeding protocols with either *mHR23B*$^{-/-}$ or wildtype female mice did not result in pregnancies. Since *mHR23B*$^{-/-}$ males show mating activity (as evident from the presence of copulatory plugs in the female mice), their inability to produce progeny appears related to neither reduced body size (which may affect physical sexual performance) nor hormonal disturbances. Inspection of the reproductive organs of adult *mHR23B*$^{-/-}$ males (3.5-7 months of age; n=11) disclosed a disproportionate reduction in the size of the testes (Figure 6A). Whereas the weight of all internal organs was proportional to the two-fold reduction in body weight, the weight of *mHR23B*$^{-/-}$ testes was about 7-fold reduced. The weight of *mHR23B*$^{-/-}$ epididymides and seminal vesicles was about 2-fold reduced (Figure 6B).

Morphology of seminal vesicles of *mHR23B*-deficient males (n=2) showed no abnormalities. However, histological examination of the testes of

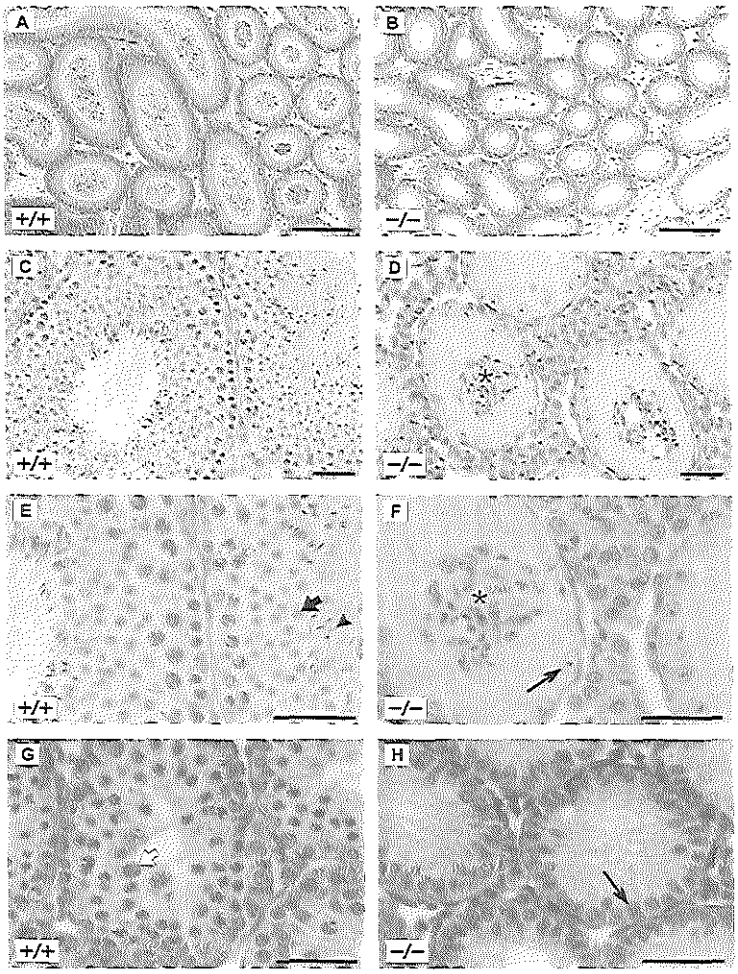

Figure 7. *mHR23B*$^{-/-}$ males show impaired spermatogenesis and dysfunction of Sertoli cells. **(A-F)** Histological examination of 91-day-old caput epididymis (A and B) and testis (C-F) from wildtype (A, C and E (E is a higher magnification of the same section as C)) and *mHR23B*$^{-/-}$ mice (B, D and F (F is a higher magnification of the same section as D)). Epididymis of wildtype mouse (A) is filled with sperm cells, which are absent in the epididymal tubules of *mHR23B*$^{-/-}$ mouse (B). Normal spermatogenesis leading to spermatids (small black arrow) and spermatozoa (black arrowhead) towards the lumen in wildtype testis (C and E), whereas spermatogenesis is impaired in *mHR23B*$^{-/-}$ testes (D and F). Seminiferous tubules of *mHR23B*$^{-/-}$ testis show Sertoli cell nuclei at the normal position near the basal membrane (black arrow) and Sertoli cell clusters (indicated by asterisks) in the lumen. **(G and H)** Histological sections of 15-day-old testis from wildtype (G) and *mHR23B*$^{-/-}$ (H) mice. Tubules of *mHR23B*$^{-/-}$ testis show a Sertoli-cell-only phenotype, with predominant appearance of Sertoli cells (black arrow points to Sertoli cell nucleus) as compared to wildtype testis, with the presence of spermatocytes (small white arrow). Scale bars represent 100 μm (A-H).

mHR23B-deficient males revealed seminiferous tubules with a small diameter, and relatively abundant interstitial tissue in all animals analyzed (n=11; Figure 7). Most striking is the total absence of spermatogenesis, which is in line with absence of sperm cells in the epididymis (Figure 7B). In the tubules, Sertoli cells appear to be the predominant cell type (Figure 7D and F). In the centre of most tubules, we observed a concentration of cells, which are typical of Sertoli cell clusters that represent Sertoli cells detached from the basal membrane of the seminiferous tubule (Figure 7D and F). Such clusters were not observed in wildtype seminiferous tubules, containing all stages of spermatogenesis (Figure 7C and E). Release of Sertoli cells from the basal membrane and clustering in the lumen has been observed in other mouse male sterility models, particularly in the older animals (Russell et al. 1996).

The impairment of spermatogenesis in adult *mHR23B*-deficient mice might reflect a primary defect, resulting in a block at an early or later phase of spermatogenesis. To study this in more detail, a histological analysis was carried out of testis of 15-day-old *mHR23B*$^{-/-}$ animals, when spermatogenesis normally is initiated. Morphology of *mHR23B*-deficient testis revealed no initiation of spermatogenesis, as compared to normal initiation of spermatogenesis, with presence of pachytene spermatocytes, in the wildtype testis. The majority of the tubules of *mHR23B*-deficient testis at 15 days of age showed a Sertoli-cell-only phenotype, although few tubules contained some spermatogonia (Figure 7G and H). Histological examination of an E15.5 *mHR23B*-deficient male revealed normal urogenital morphology of Müllerian duct regression and Wolffian duct development, indicating testicular production of anti-Müllerian hormone (AMH) by Sertoli cells and testosterone by the interstitial Leydig cells. Although testicular histology of E15.5 *mHR23B*-deficient animals displayed normal Sertoli cells, the number of gonocytes (originating from primordial germ cells) seemed to be reduced, compared to wildtype testis (Figure 8A and B).

mHR23B$^{-/-}$ females exhibit reduced fertility

In contrast to *mHR23B* homozygous mutant males, *mHR23B*$^{-/-}$ females (n=5) were fertile. However, compared to *mHR23B*$^{+/+}$ and *mHR23B*$^{+/-}$ females, fertility of the *mHR23B*-deficient females was clearly reduced. Copulatory plugs were found after interbreeding with wildtype or *mHR23B*$^{+/-}$ males, but litters born from the *mHR23B*-deficient females were consistently smaller than normal (1-2 pups/litter only). Histology of *mHR23B*$^{-/-}$ ovaries (n=3) showed a full spectrum of follicular development including Graafian follicles and corpora lutea, indicating normal endocrine

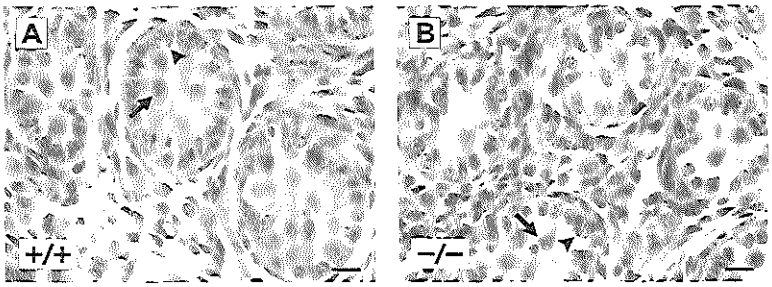

Figure 8. *mHR23B*$^{-/-}$ embryos at E15.5 show impaired development of gonocytes. Histological analysis of the tubules of E15.5 testis from wildtype (A) and *mHR23B*$^{-/-}$ (B) mutants. Sertoli cell nuclei are indicated by black arrowheads. Compared to wildtype testis, tubules of *mHR23B*$^{-/-}$ testis show less gonocytes (black arrows). Scale bars represent 10 μm (A and B).

regulation of ovarian function by follicle-stimulating hormone and luteinizing hormone (data not shown).

Additional findings in *mHR23B*$^{-/-}$ mice

A large proportion of *mHR23B*-deficient mice suffered frequently from inflamed/swollen anus in parallel with ulcers, resulting from rectal prolapse. Also soft oily faeces were found which may point to an intestinal malfunctioning. The skin of *mHR23B*-deficient mice (n=16) appeared thinner than that of wildtype mice. However, morphology of the skin of *mHR23B*-deficient mice (n=4) showed no overt abnormalities as compared with that of the wildtype mice (*mHR23B*$^{+/-}$; n=2). In addition, the levels of subcutaneous fat in *mHR23B*$^{-/-}$ mice were comparable to that of wildtype mice (data not shown). Finally, few *mHR23B*-deficient mice showed abnormal behavior like jumping (n=3) and circling/waltzing (n=1), although definite conclusions await analysis using several behavioral tests with a larger number of animals.

Discussion

mHR23-deficiency does not result in a NER defect

RAD23 is unique among the yeast NER mutants in several respects. Despite an intermediate UV-sensitivity, suggesting partial NER impairment, deletion mutants in both *S.cerevisiae* and *S.pombe* display – paradoxically - no detectable global genome and transcription-coupled repair, indicating that NER is completely disturbed (Verhage et al. 1996; Lombaerts et al. 2000). Within the NER machinery RAD23 is the only component with

multiple connections with the ubiquitin system. The RAD23 protein has an ubiquitin-like N-terminus that is essential for its function in repair *in vivo* (Watkins et al. 1993). The two ubiquitin-associated domains within the protein are very strongly conserved, which underlines their functional importance. The protein interacts physically via its ubiquitin-like domain with components of the 26S proteasome and inhibits multi-ubiquitination *in vitro* (Schauber et al. 1998; Russell et al. 1999). In view of its strong interaction with RAD4, it is likely that the main role of RAD23 in NER is mediated via this repair component. Remarkably, yeast RAD4 and RAD23 appear to be involved in both NER subpathways whereas the mammalian counterpart of RAD4, XPC, is only implicated in GG-NER (Venema et al. 1991; Mueller and Smerdon 1996). Of the two homologs of RAD23 in mammals, hHR23B is the main partner of XPC (Masutani et al. 1994). The XPC-hHR23B heterodimer is identified as the first initiator of damage recognition in global genome repair, and it is also found to stimulate XPC in *in vitro* NER (Sugasawa et al. 1998).

In this study, we have analyzed the function of mHR23B *in vivo* by generating an *mHR23B* knockout mouse model. Surprisingly, in contrast to yeast, no apparent NER-phenotype is detected in *mHR23B*-deficient cells, which are not UV-sensitive and show efficient global genome repair and transcription-coupled repair (Figure 2). These data demonstrate that NER, and in particular the function of *XPC* is not significantly affected by the absence of *mHR23B*. Assuming that analogous to the situation in yeast, the mammalian RAD23 homologs are important for NER, the most plausible interpretation for our findings is that in the absence of mHR23B, the mHR23A protein can functionally replace it, including the binding and stimulation of XPC. This is consistent with the *in vitro* redundancy between the human HR23 homologs in NER (Sugasawa et al. 1997), and supports an *in vivo* function of HR23A in GG-NER. These observations argue against the model that the HR23A protein specifically interacts with a hitherto unidentified second RAD4-like homolog in mammals specific for TC-NER, and that both together would cover the function of the single RAD4 in yeast (Guzder et al. 1998). However, it remains puzzling why in living cells the HR23B protein normally is predominantly associated with XPC, whereas this study suggests that HR23A appears to be equally able to perform this function in NER (van der Spek et al. 1996a; Sugasawa et al. 1996). Therefore, the functional distinction between HR23A and HR23B proteins is still unresolved.

Table 2. Summary of phenotypical analysis of *mHR23B* homozygous mice

Features		Number of mice affected/screened
Reduced body weight		16/16
Eye pathology		16/16
Fertility:	males sterile	11/11
	females reduced fertility	5/5
Facial dysmorphology:	elephant teeth	>6/16
	shape of maxila/mandible	16/16
Other findings:	thin skin	16/16
	rectal prolapse	>5/16
	itching/washing	>3/16
	circling (waltzing)	1/16
	6th toe	1/16

Mice lacking *mHR23B* display a severe, unexpected phenotype

Whereas no apparent NER defect could be detected, *mHR23B*-deficient mice exhibit a severe phenotype, which is quite different from the abnormalities observed in mouse models for other NER genes. A complete *mHR23B*-deficiency causes impaired embryonic development, poor vascularization, growth retardation, male sterility, and facial dysmorphology (see summary in Table 2). In contrast, inactivation of the mammalian *XPC* gene, the other component of the XPC/mHR23B complex, results in a GG-NER defect which is only accompanied by UV-sensitivity and UV-induced skin cancer predisposition (Sands et al. 1995; Cheo et al. 1996). Even a total NER defect as demonstrated by *XPA*-deficient mice allows apparently normal development and life span (de Vries et al. 1995; Nakane et al. 1995).

Mutations in several NER factors can give rise to a spectrum of additional features that at first glance seem not associated with a NER defect. For example, patients with CS show a combination of sun sensitivity, short stature, severe neurologic abnormalities and a characteristic bird-like facies, and TTD patients also have ichthyosis and many symptoms of CS (de Boer and Hoeijmakers 2000; Bootsma et al. 2001). These symptoms are explained by the fact that the corresponding proteins have additional functions outside of the NER context, particularly transcription. For instance, in the case of the *CSA* and *CSB* mutants, sensitivity of the transcription process to a wider range of lesions

hampering transcription may contribute to the severe developmental and neurological complications and premature ageing of CS. Similarly, the dual engagement of the XPB and XPD helicases of TFIIH in both NER and basal transcription initiation may give rise to the typical TTD symptoms (de Boer et al. 1999). However, the CS and TTD symptoms are quite distinct from the abnormalities exhibited by the *mHR23B* mouse mutant. A condition with some resemblance to the phenotype of *mHR23B*-deficiency is Cerebro-Oculo-Facio-Skeletal (COFS) syndrome, which is considered within the same differential diagnosis as CS (Hamel et al. 1996). COFS is a rare birth defect disorder with an autosomal recessive inheritance characterized by a progressive brain and eye defects leading to skeletal and craniofacial abnormalities, postnatal growth deficiency, early death and genital hypoplasia. Further research will be required to determine whether mHR23B is implicated in some form of this disease or in other human disorders. Our work demonstrates that *mHR23B* is essential for normal development of the mouse, and implies an additional function besides its role in GG-NER, which is not or only partially compensated for by mHR23A.

***mHR23B* is essential for growth and development**

The phenotypic abnormalities detected during the intrauterine development of *mHR23B*-deficient mice include prenatal (or early postnatal) death, disturbed growth as well as abnormalities involving improper differentiation of the vascular basement membrane in the placental labyrinth and vascularization. The placenta is essential for embryonic survival beyond E11.5, as it forms vascular connections necessary for maternal-fetal exchange of gases, nutrients and waste products (Cross et al. 1994). Thus, the transport of nutrients to the embryo may be limited in the damaged labyrinth region of homozygous mutant embryos. This may explain a number of abnormal features such as early embryonic death, swollen trophoblast cells, small placenta and poor, delayed development resulting in smaller embryos. *mHR23B*$^{-/-}$ embryos that live beyond E11.5 appear growth retarded. We speculate that these embryos have a placenta with sufficient function to allow survival to term but not normal growth and development. This may also explain the reduction in weight.

***mHR23B*-deficiency is related to an ocular defect and facial dysmorphology**

Mice lacking mHR23B function exhibit wet eyes and inflammation of the eyelids and conjunctiva. We found no gross abnormalities in the tear-producing tissues and also drainage of tears appeared normal. However,

the reduction of conjunctival Goblet cells that was apparent in one of the examined eyes may point to an involvement of vitamin A in this phenotype. Vitamin A is necessary for proper differentiation and maintenance of the mucosal epithelium. Lack of vitamin A causes a depletion of Goblet cells, which alters the composition of the tear film and eventually can lead to xerosis and inflammation of the eye (Huang et al. 1991). Possibly *mHR23B*-deficient mice suffer from vitamin A deficiency in conjunction with disturbed lipid resorption. This would fit with other observations found in *mHR23B*-deficient mice, such as reduced bodyweight, low amount of body fat, and soft, oily faeces probably due to rectal prolapse of which the cause is unknown.

mHR23B-deficient mice also display abnormalities of facial and tooth development. It is possible that the biting/chewing process is disturbed, because of an imperfect positioning of the dental elements in the maxilla and mandible. The facial abnormalities may directly result from subtle developmental defects in the head region. However, reduced growth of the palatal shelves is found in one *mHR23B*$^{-/-}$ embryo. Since the closure of the palate is of critical importance for proper food intake and respiration, this could relate to the death of many *mHR23B*-deficient animals around birth. Therefore, a more systematic analysis of this feature is warranted, to assess the biological significance of this observation.

mHR23B is associated with male sterility

Disruption of *mHR23B* causes defective spermatogenesis, resulting in absence of developing germ cells and a Sertoli-cell-only phenotype. *mHR23A* and *mHR23B* are expressed in all mouse tissues and organs, but both genes show enhanced mRNA levels in testis (van der Spek et al. 1996b), suggesting that loss of the encoded proteins may have specific gonadal consequences. At E15.5, the tubules contain Sertoli cells with a normal histological appearance. The fetal Sertoli cells have produced AMH, as evidenced by Müllerian duct regression. However, the number of gonocytes seemed somewhat reduced. At day 15 after birth, no initiation of spermatogenesis has taken place and many Sertoli cells have become detached from the basal membrane. The results indicate that failure of spermatogenesis in *mHR23B*$^{-/-}$ animals mainly occurs between E15.5 and day 15 after birth. The action of mHR23B may be involved in development of a normal population of gonocytes, which is capable to support initiation of spermatogenesis. In addition, or alternatively, mHR23B may be required for the postnatal initiation phase of spermatogenesis.

It is not clear why *mHR23B*$^{-/-}$ females show decreased fertility, while ovarian histology is normal. The reduced fertility of *mHR23B*$^{-/-}$ females may in part result from the growth retardation.

Other functional involvements of mHR23 proteins outside of NER may link to the ubiquitin proteolytic pathway

Interestingly, the developmental abnormalities detected in *mHR23B*$^{-/-}$ animals are absent in XPC and other NER-deficient mouse mutants. This strongly suggests that mHR23B has a separate important function, which may involve the ubiquitin/proteasome pathway and which cannot be taken over by mHR23A. In fact, studies in yeast and in mammals have shown that RAD23 associates with the 26S proteasome and that hHR23 proteins play a role in cell cycle regulation (Schauber et al. 1998; Hiyama et al. 1999; Kumar et al. 1999). In addition, the function of the two UBA domains in the RAD23 homologs is not known, though they are present in different classes of enzymes involved in ubiquitin-dependent proteolysis (Hofmann and Bucher 1996).

The ubiquitin system is essential in all cells and is involved in modification of protein conformation and in degradation of proteins. Numerous proteins are regulated through ubiquitination and inhibition of the ubiquitin system, therefore frequently results in a rapid dysregulation of multiple cellular processes, and subsequently in apoptosis. The effect of a partial inhibition of ubiquitination is dependent upon the cell type: although lethal to some cells, it is less critical to others. Knockout mouse models with a gametogenic failure suggest that the ubiquitination machinery is important in gametogenesis (Grootegoed et al. 1998; Baarends et al. 2000). During spermatogenesis, dramatic changes in protein composition take place, which will extensively require the ubiquitin/proteasome machinery. Probably, different phases of mammalian spermatogenesis require different specialized activities of the ubiquitin system (Baarends et al. 2000). Mouse models in which genes encoding ubiquitination proteins are mutated result in placental defect, embryonic lethality, abnormal facies, cleft palate, and scratching behavior (Harbers et al. 1996; Pizzuti et al. 1997; Perry et al. 1998).

Taken together, our data suggest that the mammalian HR23 proteins have a broader function outside of NER. To provide further evidence, generation of single knockout *mHR23A* mice and cells is undertaken.

Experimental Procedures

Construction of *mHR23B* targeting vector

Isogenic mouse genomic DNA was isolated from an Ola/129-derived phage lambda library after probing with human *HR23B* cDNA sequences. A 13.6 kb SalI fragment, containing three exons (II-IV), was subcloned into the SalI site of a pUC-vector, designated as pMHR23B1 (16.5 kbp). Following several sub-cloning steps, a 2.5 kb EcoRI fragment (containing exon II) was cloned at the ClaI site and a 4.5 kb NcoI-SacI fragment (containing exon IV) was positioned between the NotI-SacII sites of the targeting vector pmHR23B-E3 (6.9 kb) representing the 5'- and 3'-arm of homology, respectively. Thus, in the targeting vector exon III (amino acids 148 to 228) was replaced with a cassette containing (PGK-promoter driven) neomycin resistance gene and an UMS sequence (described as a transcriptional stop sequence (Heard et al. 1987)). The vector also contained the negative selectable marker HSV-TK (herpes simplex virus thymidine kinase gene).

ES cell culture and transfection

The Ola129-derived ES cell line E14 was electroporated with the *mHR23B* targeting construct and cultured on gelatinized dishes as described (van der Horst et al. 1997). G418 (Geneticin, Gibco) was added 24 hr after electroporation to a final concentration of 200 μg/ml, and the cells were maintained under selection for 6-8 days. Genomic DNA from individual G418-resistent clones was digested with SacI and analyzed by Southern blotting using a genomic PCR fragment (255 bp), isolated between SacI-EcoRI sites (upstream of Exon II), as a probe. Targeted clones, with the correct hybridizing SacI fragments, were subsequently screened with a fragment of the neomycin resistance gene as a probe to confirm proper homologous recombination.

Generation of the *mHR23B*-deficient mice and fibroblasts

Cells of *mHR23B*-targeted clones were karyotyped, and ES cells from two independent clones with 40 chromosomes were injected into 3.5-day-old blastocysts isolated from pregnant C57BL/6 females (van der Horst et al. 1997). Male chimeric mice were mated with C57BL/6 females to obtain heterozygote animals. Germline transmission was observed in the coat colour of the F1 offspring. Heterozygous male and female were interbred to generate *mHR23B*$^{+/+}$, *mHR23B*$^{+/-}$, and *mHR23B*$^{-/-}$ mice. Genotyping was performed by Southern blotting with genomic DNA prepared from tail biopsies of 10-14-day-old born pups. Primary mouse embryonic fibroblasts (at least three independent lines per genotype) were isolated from day 13.5 embryos obtained from matings between *mHR23B*$^{+/-}$ mice (F1). Part of the embryo was used for genotyping. The remaining embryonic tissue was minced using a pair of scissors and immersed in a thin layer of F10/DMEM culture medium (Gibco BRL) supplemented with 15% fetal calf serum, 2mM glutamate, and 50 μg/ml penicillin and streptomycin.

Northern blot analysis

20 μg of total RNA samples were separated on 0.9% agarose gel and transferred to Hybond-N+ membrane (Amersham Pharmacia Biotech). Total RNA was isolated from *mHR23B* MEFs using the acid guanidinium-phenol-chloroform (AGPC)[2] method as described (Chomczynski and Sacchi 1987). RNA blots were hybridized using *mHR23A* and *mHR23B* ^{32}P-labeled cDNA probes.

Protein analysis

Immunoblot analysis of mHR23B protein was performed on fibroblast extracts obtained by sonification (5 x 10^6 cells in 300 μl PBS containing PMSF and CLAP). 80 μg of total cellular protein

per lane was separated on 8% SDS-polyacrylamide gels, blotted to nitrocelluloses (Schleicher & Schuell), and probed with rabbit polyclonal antibodies recognizing mHR23B. Bands were visualized using peroxidase-conjugated secondary antibodies.

DNA repair assays

UV sensitivity was determined as described (Sijbers et al. 1996). MEFs cultures were exposed to different doses of UV-C (254 nm, Philips TUV lamp) and allowed to grow for another 3-5 days, before reaching confluency. The number of proliferating cells was estimated by scintillation counting of the radioactivity incorporated during a 3 hr pulse with [^{3}H]thymidine (5 μCi/ml, specific activity (s.a.): 40-60 Ci/mmole; Amersham). Cell survival was expressed as the ratio of ^{3}H incorporation in irradiated and non-irradiated cells. UV-induced global genome repair was assayed using the UDS method as described (Vermeulen et al. 1994). Cells were exposed to 16 J/m^2 of 254 nm UV light and labelled with [methyl-^{3}H]thymidine (10 μCi/ml, s.a.: 40-60 Ci/mmole). Repair capacity was quantified by grain counting after autoradiography. RNA synthesis recovery after UV irradiation was measured as follows. Cells were labelled with [2-^{14}C]thymidine (0.05 μCi/ml, s.a.: 56 Ci/mmole) for 24 hr, then exposed to different doses of 254 nm UV light, allowed to recover for 16 hr, labelled with [5,6-^{3}H]uridine (10 μCi/ml, s.a.: 47 Ci/mmole) for 1 hr, and processed for scintillation counting. The relative rate of RNA synthesis was expressed as the ratio of radioactivity of UV-irradiated over non-irradiated cells. The method for grain counting after autoradiography was described according to Mayne and Lehman (1982).

Histology and electron microscopical analysis

For histological examination, dissected tissues fixed in Bouin or in 10% neutral buffered formalin were processed and embedded in paraffin. Mounted sections (5-8 μm) were stained with hematoxylin and eosin using routine procedures. For transmission electron microscopy, small pieces of tissue were fixed in buffered 4% paraformaldehyde and postfixed in 1% OsO_4 + $K_3Fe(CN)_6$ (de Bruyn et al. 1973). After dehydration and embedding in Epon, 1μm sections were cut and stained with methylene blue.

Acknowledgements

We thank Dr. C. Vermeij-Keers for discussion of *mHR23B* mutant embryos and Dr. R. Hendriks for ELISA and FACS experiments. This work was partially supported by the Netherlands Organization for Scientific Research (NWO) (SIR 15-2777; TF004 Diseases of the Eldery), NIH grant (AG17242-02), KWF (EUR 98-1774) and the Dutch Foundation "Vereniging Trustfonds Erasmus Universiteit Rotterdam". This work was also supported by grants from the Ministry of Education, Culture, Sports, Science and Technology of Japan, and by the Biodesign Research Program and the Bioarchitect Research Project from RIKEN.

References

Baarends, W.M., van der Laan, R. and Grootegoed, J.A. (2000) Specific aspects of the ubiquitin system in spermatogenesis. J Endocrinol Invest, 23, 597-604.

Bootsma, D., Kraemer, K.H., Cleaver, J.E. and Hoeijmakers, J.H.J. (2001) Nucleotide excision repair syndromes: xeroderma pigmentosum, Cockayne syndrome and trichothiodystrophy. *In:* Scriver C.R., Beaudet, A.L., Sly, W.S., Valle, D. (eds), The Metabolic and Molecular Bases of

Inherited Disease, Eighth Edition, Vol 1, chapter 28, McGraw-Hill Book Co., New York, pp. 677-703.

Cheo, D.L., Meira, L.B., Hammer, R.E., Burns, D.K., Doughty, A.T. and Friedberg, E.C. (1996) Synergistic interactions between *XPC* and *p53* mutations in double-mutant mice: neural tube abnormalities and accelerated UV radiation-induced skin cancer. Curr Biol, 6, 1691-1694.

Chomczynski, P. and Sacchi, N. (1987) Single-step method of RNA isolation by acid guanidinium thiocyanate-phenol-chloroform extraction. Anal Biochem, 162, 156-159.

Cross, J.C., Werb, Z. and Fisher, S.J. (1994) Implantation and the placenta: key pieces of the development puzzle. Science, 266, 1508-1518.

de Boer, J. and Hoeijmakers, J.H.J. (2000) Nucleotide excision repair and human syndromes. Carcinogenesis, 21, 453-460.

de Boer, J., van Steeg, H., Berg, R.J., Garssen, J., de Wit, J., van Oostrum, C.T., Beems, R.B., van der Horst, G.T., van Kreijl, C.F., de Gruijl, F.R., Bootsma, D., Hoeijmakers, J.H.J. and Weeda, G. (1999) Mouse model for the DNA repair/basal transcription disorder trichothiodystrophy reveals cancer predisposition. Cancer Res, 59, 3489-3494.

de Bruijn, W.C. (1973) Glycogen, its chemistry and morphologic appearance in the electron microscope. I. A modified OsO4 fixative which selectively contrasts glycogen. J Ultrastruct Res, 42, 29-50.

de Laat, W.L., Jaspers, N.G. and Hoeijmakers, J.H.J. (1999) Molecular mechanism of nucleotide excision repair. Genes Dev, 13, 768-785.

de Vries, A., van Oostrom, C.T., Hofhuis, F.M., Dortant, P.M., Berg, R.J., de Gruijl, F.R., Wester, P.W., van Kreijl, C.F., Capel, P.J., van Steeg, H. and et al. (1995) Increased susceptibility to ultraviolet-B and carcinogens of mice lacking the DNA excision repair gene *XPA*. Nature, 377, 169-173.

Friedberg, E.C., Walker, G.C. and Siede, W. (1995) DNA repair and mutagenesis. ASM Press. Washington D.C.

Grootegoed, J.A., Baarends, W.M., Roest, H.P. and Hoeijmakers, J.H. (1998) Knockout mouse model and gametogenic failure. Mol Cell Endocrinol, 145, 161-166.

Guzder, S.N., Sung, P., Prakash, L. and Prakash, S. (1998) Affinity of yeast nucleotide excision repair factor 2, consisting of the RAD4 and RAD23 proteins, for ultraviolet damaged DNA. J Biol Chem, 273, 31541-31546.

Hamel, B.C., Raams, A., Schuitema-Dijkstra, A.R., Simons, P., van der Burgt, I., Jaspers, N.G. and Kleijer, W.J. (1996) Xeroderma pigmentosum--Cockayne syndrome complex: a further case. J Med Genet, 33, 607-610.

Hanawalt, P.C. (2000) DNA repair. The bases for Cockayne syndrome. Nature, 405, 415-416.

Hanawalt, P.C., Donahue, B.A. and Sweder, K.S. (1994) Repair and transcription. Collision or collusion? Curr Biol, 4, 518-521.

Harbers, K., Muller, U., Grams, A., Li, E., Jaenisch, R. and Franz, T. (1996) Provirus integration into a gene encoding a ubiquitin-conjugating enzyme results in a placental defect and embryonic lethality. Proc Natl Acad Sci U S A, 93, 12412-12417.

Heard, J.M., Herbomel, P., Ott, M.O., Mottura-Rollier, A., Weiss, M. and Yaniv, M. (1987) Determinants of rat albumin promoter tissue specificity analyzed by an improved transient expression system. Mol Cell Biol, 7, 2425-2434.

Hiyama, H., Yokoi, M., Masutani, C., Sugasawa, K., Maekawa, T., Tanaka, K., Hoeijmakers, J.H.J. and Hanaoka, F. (1999) Interaction of hHR23 with s5a. The ubiquitin-like domain of hhr23 mediates interaction with s5a subunit of 26s proteasome. J Biol Chem, 274, 28019-28025.

Hofmann, K. and Bucher, P. (1996) The UBA domain: a sequence motif present in multiple enzyme classes of the ubiquitination pathway. Trends Biochem Sci, 21, 172-173.

Huang, A.J., Tseng, S.C. and Kenyon, K.R. (1991) Change of paracellular permeability of ocular surface epithelium by vitamin A deficiency. Invest Ophthalmol Vis Sci, 32, 633-639.

Kumar, S., Talis, A.L. and Howley, P.M. (1999) Identification of HHR23A as a substrate for E6-associated protein- mediated ubiquitination. J Biol Chem, 274, 18785-18792.

Lombaerts, M., Goeloe, J.I., den Dulk, H., Brandsma, J.A. and Brouwer, J. (2000) Identification and characterization of the *rhp23(+)* DNA repair gene in Schizosaccharomyces pombe. Biochem Biophys Res Commun, 268, 210-215.

Masutani, C., Araki, M., Sugasawa, K., van der Spek, P.J., Yamada, A., Uchida, A., Maekawa, T., Bootsma, D., Hoeijmakers, J.H.J. and Hanaoka, F. (1997) Identification and characterization of XPC-binding domain of hHR23B. Mol Cell Biol, 17, 6915-6923.

Masutani, C., Sugasawa, K., Yanagisawa, J., Sonoyama, T., Ui, M., Enomoto, T., Takio, K., Tanaka, K., van der Spek, P.J., Bootsma, D. and et al. (1994) Purification and cloning of a nucleotide excision repair complex involving the xeroderma pigmentosum group C protein and a human homolog of yeast RAD23. Embo J, 13, 1831-1843.

Mayne, L.V. and Lehmann, A.R. (1982) Failure of RNA synthesis to recover after UV irradiation: an early defect in cells from individuals with Cockayne's syndrome and xeroderma pigmentosum. Cancer Res, 42, 1473-1478.

Mueller, J.P. and Smerdon, M.J. (1996) RAD23 is required for transcription-coupled repair and efficient overrall repair in *Saccharomyces cerevisiae*. Mol Cell Biol, 16, 2361-2368.

Nakane, H., Takeuchi, S., Yuba, S., Saijo, M., Nakatsu, Y., Murai, H., Nakatsuru, Y., Ishikawa, T., Hirota, S., Kitamura, Y. and et al. (1995) High incidence of ultraviolet-B or chemical-carcinogen-induced skin tumours in mice lacking the xeroderma pigmentosum group A gene. Nature, 377, 165-168.

Perry, W.L., Hustad, C.M., Swing, D.A., O'Sullivan, T.N., Jenkins, N.A. and Copeland, N.G. (1998) The itchy locus encodes a novel ubiquitin protein ligase that is disrupted in *a1SH* mice. Nat Genet, 18, 143-146.

Pizzuti, A., Novelli, G., Ratti, A., Amati, F., Mari, A., Calabrese, G., Nicolis, S., Silani, V., Marino, B., Scarlato, G., Ottolenghi, S. and Dallapiccola, B. (1997) *UFD1L*, a developmentally expressed ubiquitination gene, is deleted in CATCH 22 syndrome. Hum Mol Genet, 6, 259-265.

Russell, L.D., Franca, L.R. and Brinster, R.L. (1996) Ultrastructural observations of spermatogenesis in mice resulting from transplantation of mouse spermatogonia. J Androl. 17, 603-614.

Russell, S.J., Reed, S.H., Huang, W., Friedberg, E.C. and Johnston, S.A. (1999) The 19S regulatory complex of the proteasome functions independently of proteolysis in nucleotide excision repair. Mol Cell, 3, 687-695.

Sands, A.T., Abuin, A., Sanchez, A., Conti, C.J. and Bradley, A. (1995) High susceptibility to ultraviolet-induced carcinogenesis in mice lacking *XPC*. Nature, 377, 162-165.

Schauber, C., Chen, L., Tongaonkar, P., Vega, I., Lambertson, D., Potts, W. and Madura, K. (1998) RAD23 links DNA repair to the ubiquitin/proteasome pathway. Nature, 391, 715-718.

Sijbers, A.M., de Laat, W.L., Ariza, R.R., Biggerstaff, M., Wei, Y.F., Moggs, J.G., Carter, K.C., Shell, B.K., Evans, E., de Jong, M.C., Rademakers, S., de Rooij, J., Jaspers, N.G., Hoeijmakers, J.H.J. and Wood, R.D. (1996) Xeroderma pigmentosum group F caused by a defect in a structure-specific DNA repair endonuclease. Cell, 86, 811-822.

Sugasawa, K., Masutani, C., Uchida, A., Maekawa, T., van der Spek, P.J., Bootsma, D., Hoeijmakers, J.H.J. and Hanaoka, F. (1996) hHR23B, a human RAD23 homolog, stimulates XPC protein in nucleotide excision repair *in vitro*. Mol Cell Biol, 16, 4852-4861.

Sugasawa, K., Ng, J.M.Y., Masutani, C., Iwai, S., van der Spek, P.J., Eker, A.P., Hanaoka, F., Bootsma, D. and Hoeijmakers, J.H.J. (1998) Xeroderma pigmentosum group C protein complex is the initiator of global genome nucleotide excision repair. Mol Cell, 2, 223-232.

Sugasawa, K., Ng, J.M.Y., Masutani, C., Maekawa, T., Uchida, A., van der Spek, P.J., Eker, A.P., Rademakers, S., Visser, C., Aboussekhra, A., Wood, R.D., Hanaoka, F., Bootsma, D. and Hoeijmakers, J.H.J. (1997) Two human homologs of RAD23 are functionally interchangeable in complex formation and stimulation of XPC repair activity. Mol Cell Biol, 17, 6924-6931.

van der Horst, G.T., van Steeg, H., Berg, R.J., van Gool, A.J., de Wit, J., Weeda, G., Morreau, H., Beems, R.B., van Kreijl, C.F., de Gruijl, F.R., Bootsma, D. and Hoeijmakers, J.H.J. (1997) Defective transcription-coupled repair in Cockayne syndrome B mice is associated with skin cancer predisposition. Cell, 89, 425-435.

van der Spek, P.J., Eker, A., Rademakers, S., Visser, C., Sugasawa, K., Masutani, C., Hanaoka, F., Bootsma, D. and Hoeijmakers, J.H.J. (1996a) XPC and human homologs of RAD23: intracellular localization and relationship to other nucleotide excision repair complexes. Nucleic Acids Res, 24, 2551-2559.

van der Spek, P.J., Visser, C.E., Hanaoka, F., Smit, B., Hagemeijer, A., Bootsma, D. and Hoeijmakers, J.H.J. (1996b) Cloning, comparative mapping, and RNA expression of the mouse homologs of the Saccharomyces cerevisiae nucleotide excision repair gene *RAD23*. Genomics, 31, 20-27.

van Hoffen, A., Venema, J., Meschini, R., van Zeeland, A.A. and Mullenders, L.H. (1995) Transcription-coupled repair removes both cyclobutane pyrimidine dimers and 6-4 photoproducts with equal efficiency and in a sequential way from transcribed DNA in xeroderma pigmentosum group C fibroblasts. Embo J, 14, 360-367.

Venema, J., van Hoffen, A., Karcagi, V., Natarajan, A.T., van Zeeland, A.A. and Mullenders, L.H. (1991) Xeroderma pigmentosum complementation group C cells remove pyrimidine dimers selectively from the transcribed strand of active genes. Mol Cell Biol, 11, 4128-4134.

Venema, J., van Hoffen, A., Natarajan, A.T., van Zeeland, A.A. and Mullenders, L.H. (1990) The residual repair capacity of xeroderma pigmentosum complementation group C fibroblasts is highly specific for transcriptionally active DNA. Nucleic Acids Res, 18, 443-448.

Verhage, R.A., Zeeman, A.M., Lombaerts, M., van de Putte, P. and Brouwer, J. (1996) Analysis of gene- and strand-specific repair in the moderately UV-sensitive *Saccharomyces cerevisiae rad23* mutant. Mutat Res, 362, 155-165.

Vermeulen, W., Scott, R.J., Rodgers, S., Muller, H.J., Cole, J., Arlett, C.F., Kleijer, W.J., Bootsma, D., Hoeijmakers, J.H.J. and Weeda, G. (1994) Clinical heterogeneity within xeroderma pigmentosum associated with mutations in the DNA repair and transcription gene *ERCC3*. Am J Hum Genet, 54, 191-200.

Watkins, J.F., Sung, P., Prakash, L. and Prakash, S. (1993) The *Saccharomyces cerevisiae* DNA repair gene RAD23 encodes a nuclear protein containing a ubiquitin-like domain required for biological function. Mol Cell Biol, 13, 7757-7765.

Wood, R.D. (1996) DNA repair in eukaryotes. Annu Rev Biochem, 65, 135-167.

Yokoi, M., Masutani, C., Maekawa, T., Sugasawa, K., Ohkuma, Y. and Hanaoka, F. (2000) The xeroderma pigmentosum group C protein complex XPC-HR23B plays an important role in the recruitment of transcription factor IIH to damaged DNA. J Biol Chem, 275, 9870-9875.

Chapter

VI

Stabilization of XPC by DNA Damage and the Ubiquitin Domain Protein RAD23 Reveals a Novel Mechanism of Regulation of DNA Repair

Jessica M.Y. Ng[1], Gijsbertus T.J. van der Horst[1], Wim Vermeulen[1], Kaoru Sugasawa[3,4], Harry Vrieling[2], and Jan H.J. Hoeijmakers[1]

[1]MGC-Department of Cell Biology & Genetics, Centre for Biomedical Genetics, Erasmus University Rotterdam, P.O. Box 1738, Rotterdam, The Netherlands
[2]MGC-Department of Radiation Genetics and Chemical Mutagenesis, Leiden University Medical Center, 2333 AL Leiden, The Netherlands
[3]Cellular Physiology Laboratory, RIKEN (The Institute of Physical and Chemical Research), and [4]Core Research for Evolutional Science and Technology, Japan Science and Technology Corporation, Wako, Saitama 351-0198, Japan

Summary

Primary DNA damage sensing in mammalian global genome nucleotide excision repair (GG-NER) is done by the XPC protein complexed with HR23B, one of the two homologs of the yeast ubiquitin domain repair factor RAD23. Knockout mice for *mHR23A* and *mHR23B* revealed a fully redundant role of both RAD23 homologs in NER, and a partially redundant function in embryonic development. Inactivation of both genes causes embryonic lethality. Analysis of a *mHR23A/B* double mutant cell line led to the discovery that XPC stability depends on HR23 and that NER damage further stabilizes XPC. These findings resolve the main function of RAD23 in repair, reveal a novel level of regulation of GG-NER (explaining the long known phenomenon of enhanced reactivation) and clarify the link between NER and the ubiquitin system. Additional involvement of HR23/RAD23 in other cellular processes such as base excision repair, chromosome segregation, and cell cycle control explains the essential function of HR23 and suggests a damage response mechanism in mammals similar to the SOS system in *E.coli*.

Introduction

A network of DNA repair systems has evolved to protect the genome against the deleterious effects of a wide range of DNA lesions. Nucleotide excision repair (NER) is the primary mechanism for the removal of UV-induced cyclobutane pyrimidine dimers and pyrimidine (6-4) pyrimidone photoproducts, and numerous bulky chemical DNA lesions (Friedberg et al. 1995). Inherited defects in NER are the cause of the severe UV-sensitive syndrome xeroderma pigmentosum (XP). Patients exhibit mainly cutaneous symptoms, including extreme sun sensitivity, sun-induced pigmentation anomalies and a >2000-fold predisposition to skin cancer. XP is a multigenetic disease, comprising *XPA* to *XPG* genes (Bootsma et al. 2001).

NER is a highly conserved, multistep "cut and patch" type reaction involving the concerted and coordinated action of approximately 30 proteins. These act in sequential steps of DNA damage detection, chromatin remodelling, helix opening, damage verification and dual incision of the damaged strand at some distance from the lesion, followed by removal of the damage-containing oligonucleotide, gap filling DNA synthesis and ligation. (de Laat et al. 1999; Wood et al. 2001). Two distinct NER subpathways are recognized, i.e. global genome nucleotide excision repair (GG-NER), operating over the entire genome and transcription-coupled nucleotide excision repair (TC-NER), focussing on transcription-blocking

lesions in the transcribed strand of active genes (Hanawalt et al. 1994; Hanawalt 2000). Most XP genes are implicated in both NER subpathways, but *XPC*-deficient cells are unique in being selectively deficient in GG-NER (Venema et al. 1990 and 1991; van Hoffen et al. 1995).

Previously, we have identified two human homologs of the *Saccharomyces cerevisiae* NER gene *RAD23*, designated *hHR23A* and *hHR23B* (Masutani et al. 1994). All RAD23 homologs are highly conserved and have an ubiquitin-like (UbL) N-terminus and two ubiquitin-associated (UBA) domains, indicating intimate links with the ubiquitin/proteasome pathway (Hofmann and Bucher 1996; van der Spek et al. 1996b; Bertolaet et al. 2001). In yeast, the UbL domain of RAD23 is important for UV survival and for interaction with the 26S proteasome (Watkins et al. 1993, Mueller and Smerdon 1996; Schauber et al. 1998). The *hHR23B* gene product is tightly complexed with the GG-NER specific XPC protein and a recently identified third component centrin 2 (CEN2) (Masutani et al. 1994; Araki et al. 2001). The initial damage-sensing step within GG-NER is performed by this complex, which triggers the subsequent association of NER factors TFIIH, XPG, XPA, and RPA (Sugasawa et al. 1998; Yokoi et al. 2000; Araujo et al. 2001; Volker et al. 2001). *In vitro* repair studies showed that hHR23B stimulates the NER activity of recombinant XPC (Sugasawa et al. 1996). Moreover, the 60-amino-acid XPC-binding domain of hHR23B alone is sufficient for XPC stimulation (Masutani et al. 1997). In whole cell extracts the vast majority of XPC is complexed with hHR23B (van der Spek et al. 1996a) whereas a minor amount copurifies with hHR23A (Araki et al. 2001). Moreover, *in vitro* formed complexes between XPC and hHR23A can substitute for hHR23B in binding and stimulating of XPC, suggesting a possible functional interchangeability between the two mammalian homologs of RAD23 (Sugasawa et al. 1997). Since only a minority of cellular hHR23B and hHR23A is complexed with XPC, whereas the majority exist in a free form *in vivo*, both proteins are thought to have additional functions outside NER (van der Spek et al. 1996a; Sugasawa et al. 1996).

Recently, we have inactivated the mouse RAD23 homolog *mHR23B* by gene targeting in the mouse germ line (Ng et al. submitted). *mHR23B*-deficient cells are not UV-sensitive, which is in agreement with the *in vitro* findings suggesting functional redundancy of the two mammalian RAD23 homologs (Sugasawa et al. 1997; Ng et al. submitted). However, unlike other NER mouse mutants, *mHR23B*-deficient mice show a severe phenotype associated with impaired embryonic development and high rates of intrauterine death. Surviving animals display retarded growth, male

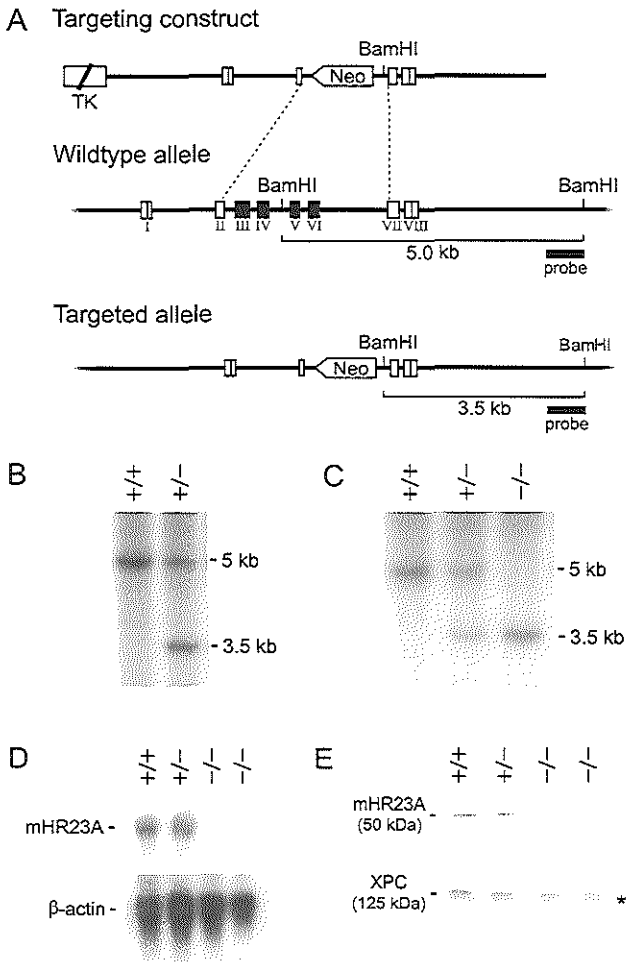

Figure 1. Targeted disruption of the *mHR23A* gene by homologous recombination. **(A)** Genomic organization and disruption strategy for *mHR23A* showing the gene, the targeting construct, and the targeted *mHR23A* allele. Exons III to VI (and part of exon II and VII) were replaced by the dominant selectable neomycin resistance marker transcribed in antisense orientation. **(B)** Southern blot analysis of BamHI digested DNA from ES cells showing the 5.0 kb and 3.5 kb fragment representing the wildtype and the targeted allele of *mHR23A* respectively. **(C)** Southern blot analysis of BamHI digested tail DNA from *mHR23A*$^{+/+}$, *mHR23A*$^{+/-}$, and *mHR23A*$^{-/-}$ mice. **(D)** RNA blot analysis of mHR23A mRNA in cellular extracts from *mHR23A*$^{+/+}$, *mHR23A*$^{+/-}$, and *mHR23A*$^{-/-}$ MEFs using *mHR23A* cDNA as a probe (upper panel). As a loading control for the amount of RNA, the blot was reprobed with β-actin cDNA (lower panel). **(E)** Immunoblot analysis of mHR23A protein in cellular extracts from *mHR23A*$^{+/+}$, *mHR23A*$^{+/-}$, and *mHR23A*$^{-/-}$ MEFs using polyclonal antibodies against the human HR23A protein (upper panel). Polyclonal antibodies against the human XPC protein (lower panel) were used as a loading control. The asterisk indicates an aspecific crossreacting band.

sterility and facial dysmorphology (Ng et al. submitted). These data show that mHR23B is essential for normal development of the mouse, and are indicative for a separate role of mHR23B outside the NER context, which likely involves the ubiquitin/proteasome pathway. Apparently, this role is not or only in part compensated for by mHR23A.

The precise role of the RAD23 proteins in NER has been enigmatic. To investigate the biological impact of the mammalian RAD23 proteins in an XPC-mediated repair mechanism, we generated *mHR23A*$^{-/-}$ mouse mutants by gene targeting. By crossing these animals into a *mHR23B*$^{-/-}$ background, we obtained embryos and a mouse embryonic fibroblast line with a complete *mHR23*-deficiency. Here, we report the application of these double mutant cells to elucidate the function of mammalian RAD23 homologs in NER.

Results

Generation of *mHR23A*-deficient mice and cells

To generate a mouse model for mHR23A, we made a targeting construct in which exons III to VI (and part of exon II and VII) were replaced by the dominant selectable neomycin resistance marker transcribed in antisense orientation. This deletes ~2/3 of the coding region including part of the UbL N-terminus and the entire first highly conserved UBA domain and thus is expected to give rise to a null-allele (Figure 1A). ES cell clones carrying one disrupted *mHR23A* allele (Figure 1B) were obtained, after homologous recombination at a frequency of approximately 16%. Two clones verified for the absence of visible chromosomal abnormalities and additional, randomly integrated constructs were used for blastocyst injections to produce germ line chimeras. Heterozygous offspring from matings between chimeric males and C57BL/6 female mice was intercrossed to generate homozygous mutant *mHR23A* animals (Figure 1C) and day 13.5 embryos (E13.5) for isolation of mouse embryonic fibroblasts (MEFs) of the three expected genotypes. In agreement with the absence of wildtype *mHR23A* mRNA, the 50 kDa wildtype mHR23A protein could not be detected in *mHR23A*$^{-/-}$ MEFs, as shown by RNA and immunoblot analysis respectively (Figure 1D and 1E). We conclude that we have generated *mHR23A* null mice. The two independent mouse lines were biochemically and phenotypically indistinguishable for all parameters tested, indicating that the findings presented in this study are not due to random events that might have occurred in one targeted ES clone, but are the result of genuine *mHR23A* inactivation.

mHR23A$^{-/-}$ animals and MEFs

Because of the role of mHR23A in NER, as suggested by *in vitro* experiments (Masutani et al. 1994) and the *mHR23B* mutant (Ng et al. submitted) we assessed key repair parameters in the *mHR23A*$^{-/-}$ MEFs. As shown by Figure 2, UV survival, UV-induced unscheduled DNA synthesis (UDS), and RNA synthesis recovery after UV-exposure were all in the wildtype range. This indicates that global as well as transcription-coupled NER are unaffected. These data suggest that, in agreement with the *in vitro* repair studies, mHR23A and mHR23B are functional redundant NER proteins *in vivo*.

Crosses between heterozygous mutant *mHR23A* animals yielded *mHR23A*$^{-/-}$ mice in a Mendelian fashion (data not shown). In striking contrast to *mHR23B*$^{-/-}$ animals, *mHR23A*-deficient mice failed to display any detectable abnormalities and appeared indistinguishable from wildtype and heterozygous littermates for all parameters tested, such as morphology, main pathology and growth rate at least up to 16 months. In addition, male and female mice were completely fertile, and their mating activity and litter size were normal. Apparently, mHR23A is not essential for mouse development and mHR23B can compensate for most functions of mHR23A.

Total _mHR23_-deficiency is incompatible with animal life

Inactivation of neither *mHR23A* nor *mHR23B* (Ng et al. submitted) results in a NER defect. In order to investigate the effect of a total *mHR23*-deficiency, double heterozygous matings were set up to generate *mHR23A/B* homozygous double mutant animals (*mHR23A*$^{-/-}$/*B*$^{-/-}$, hereafter referred to as: '*DKO*' for double knockout) and to obtain corresponding MEFs. Remarkably, in the 427 offspring analyzed no *DKO*'s were found (Table 1), indicating that inactivation of *mHR23A* further aggravates the severe developmental defects caused by a *mHR23B*-deficiency to a level incompatible with life. Surprisingly, whereas we obtained *mHR23A*$^{-/-}$/*B*$^{+/-}$ mutant male and female mice at Mendelian expectance (71/427 found and 83/427 expected) that in all aspects were phenotypically indistinguishable from wildtype mice, *mHR23A*$^{+/-}$/*B*$^{-/-}$ mutant animals were not born (0/427). This indicates that loss of even one allele of *mHR23A* in a total *mHR23B* null-background affects embryogenesis and causes lethality. The observed gene dosage effect for mHR23A suggests that both *mHR23* gene products are essential for proper mouse development.

Table 1. Genotype analysis of *DKO* embryos and offspring

Stage	Analyzed	Expected* (if mendelian)	Found
E8.5	43	7	3#
E10.5	14	1.8	0
E13.5	77	9.1	0
Newborn	427	41.4	0

*Derived from different *mHR23A*$^{+/-}$/*B*$^{+/-}$ and *mHR23A*$^{-/-}$/*B*$^{+/-}$ intercrosses; #One cell line established.

To investigate at which embryonic stage a total *mHR23*-deficiency becomes lethal and to attempt to obtain a *DKO* cell line, we isolated embryos from different crossings at various stages of development. Although we did not observe *DKO* embryos at day E13.5 and E10.5, we could isolate *mHR23*-deficient embryos at day E8.5. Importantly, three *DKO* MEF lines were obtained from E8.5 embryos (3/43, see Table 1) which were smaller compared to the heterozygotes and wildtype embryos. These cells displayed severe growth impairment compared to wildtype and double heterozygous mutant MEFs. Although this resulted in the loss of two of the lines, we succeeded in establishing one *DKO* cell line after 30 weeks culturing. This cell line verified for its mHR23 status by genotyping (not shown) permitted characterization of a total *mHR23*-deficiency.

Given the embryonic lethality observed in *mHR23A*$^{+/-}$/*B*$^{-/-}$ mutant mice we also isolated cell lines with only one intact mHR23A allele (using E13.5 embryos, which were also smaller than controls). Unlike *mHR23A*$^{-/-}$/*B*$^{+/-}$ mutant cells which proliferated normally, *mHR23A*$^{+/-}$/*B*$^{-/-}$ MEFs showed poor growth.

Total *mHR23*-deficient cells show an *XPC*-like repair phenotype

Cell survival experiments revealed that *DKO* MEFs are remarkably similar to *XPC*$^{-/-}$ cells in terms of UV survival (Figure 2D), deficiency of UV-induced UDS and proficiency of RNA synthesis recovery after UV-exposure (Figure 2E and F). In contrast, MEFs retaining only one *mHR23A* or *mHR23B* allele were NER competent (Figure 2D). Apparently, one out of four *mHR23* copies is sufficient for normal NER activity.

The striking resemblance to the *XPC*$^{-/-}$ repair phenotype prompted us to examine the status of the XPC protein in the *DKO* MEFs. Interestingly, XPC was undetectable in *DKO* cells by comparative immunofluorescence (Figure 3A-F). In addition, also on immunoblots a strongly reduced steady

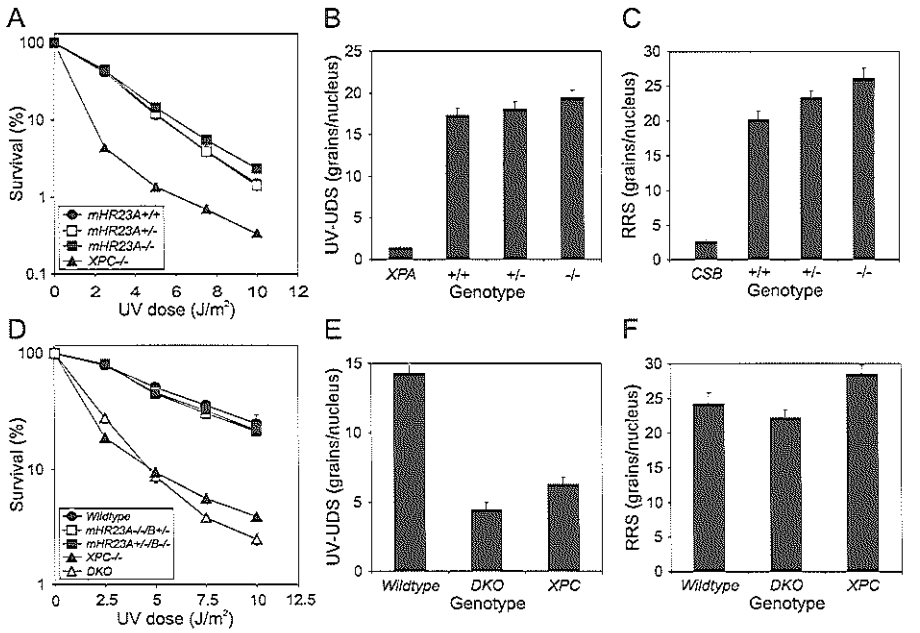

Figure 2. Repair characteristics of *mHR23A* E13.5 primary MEFs (A-C: identical results were obtained for each genotype with three other independent lines (data not shown)) and *DKO* E8.5 (passage 17) MEFs (D-F): (A,D) UV survival curves; (B,E) global genome repair (UDS); (C,F) RNA synthesis recovery (RRS). **(A)** UV survival of $mHR23A^{+/+}$, $mHR23A^{+/-}$, and $mHR23A^{-/-}$ MEFs. $XPC^{-/-}$ fibroblasts were included as negative control. **(B)** UDS in $mHR23A^{+/+}$, $mHR23A^{+/-}$, and $mHR23A^{-/-}$ MEFs. $XPA^{-/-}$ fibroblasts were measured as negative control. **(C)** RRS after UV-exposure of $mHR23A^{+/+}$, $mHR23A^{+/-}$, and $mHR23A^{-/-}$ MEFs. $CSB^{-/-}$ cells were used as negative control. **(D)** UV survival of MEF lines of wildtype, $XPC^{-/-}$, $mHR23A^{-/-}/B^{+/-}$, $mHR23A^{+/-}/B^{-/-}$, and $mHR23A^{-/-}/B^{-/-}$ (*DKO*). **(E)** UDS in wildtype, $XPC^{-/-}$, and *DKO* MEFs. **(F)** RRS after UV-irradiation of wildtype, $XPC^{-/-}$, and *DKO* MEFs.

state level of XPC is observed in whole cell extracts of *DKO* compared to wildtype (Figure 3G and H). Thus, XPC is either hardly expressed at RNA or protein level or unstable in the absence of both mouse RAD23 proteins. In view of the direct physical interaction between HR23 proteins and XPC the latter option seems most plausible.

hHR23B and hXPC-GFP rescue the UV-sensitivity of *DKO* cells

To provide direct evidence that the *XPC*-like phenotype of *DKO* cells is the consequence of the *mHR23* defect we stably transfected human *(h)HR23B* cDNA into double mutant MEFs. hHR23B was able to correct the UV-sensitivity of *DKO* cells, although rescue was incomplete perhaps due to

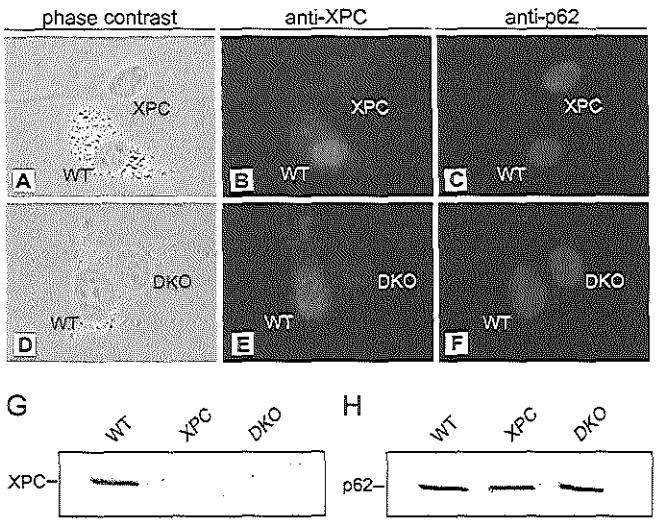

Figure 3. XPC expression in *DKO* E8.5 MEFs. **(A-F)** Phase contrast (A and D) and epifluorescense (B, C, E and F) images of fixed wildtype (*WT*, labeled with latex beads), *XPC*$^{-/-}$ (*XPC*) and *mHR23A*$^{-/-}$*/B*$^{-/-}$ (*DKO*) MEFs. Cells were fixed by paraformaldehyde, permeabilized by 0.1% triton X-100, and subsequently immunolabeled with affinity purified polyclonal antibodies against the human XPC protein (B and E; stained green with goat anti-rabbit Alexa 488-labeled secondary antibody). Monoclonal antibodies recognizing p62 subunit of TFIIH (C and F; stained red with goat anti-mouse Cy3-labeled secondary antibody) were used as an internal control. All images were taken at the same magnification. **(G-H)** Immunoblot analysis of XPC protein in cellular extracts from wildtype, *XPC*$^{-/-}$ and *DKO* E8.5 MEFs using polyclonal anti-human XPC antibodies (G). Monoclonal anti-p62 antibodies were used as an internal reference for the amount of protein in each lane (H).

human-mouse differences (Figure 4A). Importantly, expression of hH23B induced increased levels of the endogenous mXPC, as shown by both immunoblot (Figure 4C, lane 4) and immunofluorescence analysis (Figure 4D and E).

Since the absence of mHR23 causes a strong reduction in mXPC we reasoned that (over)expression of 'exogenous' XPC might bypass the repair defect of *DKO* cells. To that aim, we generated double mutant MEFs that stably express hXPC. To allow direct observation within living cells (Houtsmuller et al. 1999) hXPC was C-terminally tagged with GFP containing an additional His_6-HA double tag (Figure 4B). Functionality of the cDNA encoding hXPC-GFP-His_6HA was demonstrated by microinjection and transfection of the DNA construct in *XP-C* cells (data not shown). Although hXPC-GFP expression was undetectable as assessed by fluorescence microscopy (Figure 4F and H) UV survival revealed that the

stable transformants (verified for the presence of *hXPC-GFP* cDNA by DNA blotting) had largely regained wildtype resistance (Figure 4A), indicating that the repair defect was rescued. Unfortunately, our XPC antibodies (raised against the C-terminus of the protein) failed to recognize the hXPC-GFP because of the presence of the C-terminal tag. Also expression was too low to be detected by the HA-epitope antibody. However, introduction of hXPC-GFP appeared to restore the level of the endogenous mouse XPC as shown by immunoblot (Figure 4C, lane 5) and immunofluorescene analysis (not shown). Apparently, the hXPC-GFP has a trans-effect on mXPC stability.

To investigate the stabilizing effect of mHR23B on XPC we cotransfected *hHR23B* together with *hXPC-GFP* cDNA into double mutant cells. Stably transfected clones exhibited wildtype UV-resistance (Figure 4A) and normalized levels of the endogenous mXPC (Figure 4C, lane 6, and not shown). In contrast to the MEFs expressing only hXPC-GFP, these transfectants displayed in a fraction of cells green fluorescent nuclei, in combination with bright foci dispersed throughout the nucleus (Figure 4G and I). The function of these fluorescent foci is as yet unclear, but they may represent storage loci. These data indicate that the cotransfected hHR23B acts as a stabilizing factor for both hXPC-GFP and endogenous mXPC.

DNA damage causes a dramatic increase of hXPC-GFP

The hXPC-GFP expression was heterogeneous in the XPC-GFP/hHR23B transfected cell population, with only 18 % of cells (88/485) exhibiting fluorescent nuclei (Figure 4G and I). This cell line provided a convenient tool to monitor the effect of DNA damage on XPC steady-state-level in living cells. To our surprise, UV-irradiation (5 and 10 J/m^2) markedly increased the percentage of green cells as well as the intensity of the GFP signal. Kinetic analysis upon UV-exposure (10 J/m^2) showed a time-dependent reversible accumulation of XPC-GFP expression (Figure 5A). To follow the UV-induced increase of hXPC-GFP levels in more detail nuclear expression in living single cells was monitored in time after irradiation with 10 J/m^2. Before UV hardly any fluorescence is detectable (Figure 5C and E), but 6 hours after 10 J/m^2, the same cells and also a vast majority of the entire culture show green nuclei (Figure 5D and F). Increased XPC levels upon UV-irradiation was further corroborated by immunoblotting of whole cell extracts using antibodies against the HA epitope attached to the GFP tag (see Figure 5B, lane 2 for 6 hrs post-UV). UV-induced nuclear accumulation of hXPC-GFP was dependent on hHR23B as no fluorescence was noted in UV-exposed cells transfected with hXPC-GFP alone (results not shown).

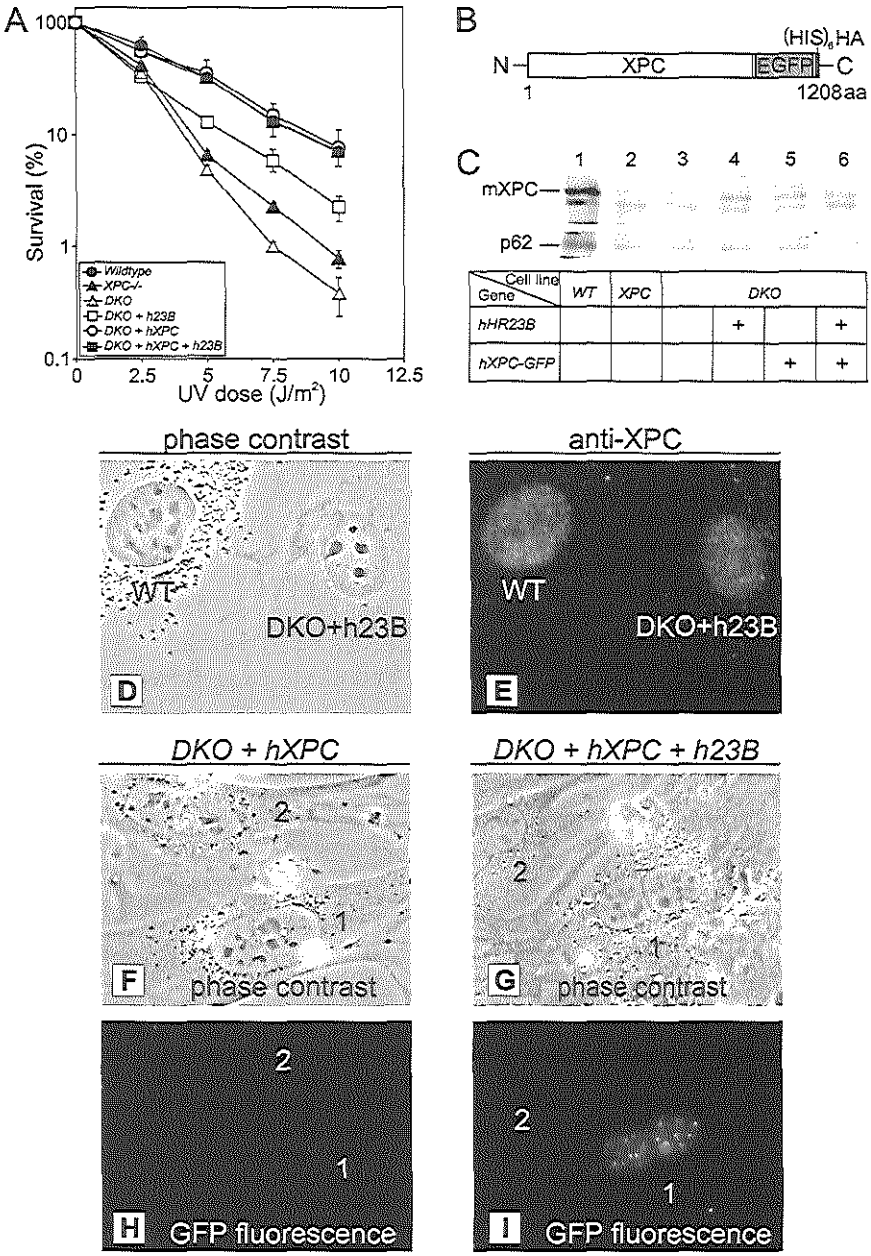
A
100
10
1
0.1
Survival (%)
0
2.5
5
7.5
10
12.5
UV dose (J/m²)
Wildtype
XPC-/-
DKO
DKO + h23B
DKO + hXPC
DKO + hXPC + h23B
B
(HIS)6HA
N
XPC
EGFP
C
1
1208aa
C
1 2 3 4 5 6
mXPC
p62
Cell line
Gene
WT
XPC
DKO
hHR23B
hXPC-GFP
phase contrast
anti-XPC
WT
DKO+h23B
D
E
DKO + hXPC
DKO + hXPC + h23B
2
1
F
phase contrast
G
phase contrast
H
GFP fluorescence
I
GFP fluorescence

Figure 4. Characterization of *DKO* cells expressing hHR23B and XPC-GFP. **(A)** UV survival of wildtype, *XPC*$^{-/-}$, *DKO*, and *DKO* MEFs cotransfected with: *hHR23B* (*h23B*), human *XPC-GFP* (*hXPC*), and *h23B* and *hXPC* cDNAs. Cells were exposed to different doses of UV (254 nm). For each cDNA construct, similar results were obtained with at least two other independent stably transfected cell lines (data not shown). **(B)** Schematic representation of XPC-EGFP-His_6HA-N_3 fusion protein (1208 aa). Indicated are the human XPC protein (940 aa), the enhanced green fluorescent protein tag (EGFP; 238 aa), and the histidine-hemagglutinin epitope tag (His_6HA; 17 aa). **(C)** Immunoblot analysis of XPC expression in cellular extracts of *WT* (lane 1), *XPC* (lane 2), *DKO* (lane 3), and *DKO* MEFs cotransfected with: *h23B* (lane 4), *hXPC* (lane 5), and *h23B* and *hXPC* (lane 6) cDNAs, using a polyclonal anti-human XPC antibody (upper panel). Monoclonal anti-p62 antibodies were used as a loading control (lower panel). **(D-E)** Phase contrast (D) and epifluorescense (E) images of fixed *WT* (labeled with latex beads) and *DKO* cells cotransfected with *hHR23B* cDNA. Cells were fixed by paraformaldehyde, followed by 0.1% triton X-100 permeabilization and subsequently immunolabeled with affinity purified polyclonal anti-human XPC (E; stained green with goat anti-rabbit Alexa 488-labeled secondary antibody). Monoclonal anti-p62 antiserum was used as an internal control (stained red with goat anti-mouse Cy3-labeled secondary antibody; data not shown). All images were taken at the same magnification. Similar results were obtained with *DKO* cells cotransfected with *hXPC-GFP*, and *hHR23B* and *hXPC-GFP* cDNAs (not shown). **(F-I)** Phase contrast (F and G) and epifluorescense (H and I) images of living *DKO* cells cotransfected with: *hXPC-GFP* (F and H), or *hHR23B* and *hXPC-GFP* (G and I) cDNAs. All images were taken at the same magnification. The numbers represent the XPC-GFP expressing cells and the non-GFP expressing cells.

These data indicate that the level of XPC is responsive to UV-irradiation in an HR23-dependent fashion.

To investigate whether XPC accumulation is specific for NER-type DNA damage or just a stress related response cells were exposed to different kinds of genotoxic agents. N-acetoxy-2-acetylaminofluorene (NA-AAF) that induces bulky adducts processed by the NER machinery (Amacher et al. 1977) elicited a very potent UV-like response in all cells within 6 to 8 hrs (Figure 6A-D). In contrast, exposure to γ-rays (6 and 10 Gy) and mitomycin C (MMC, 1.2 and 2.4 μg/ml) inducing mainly double strand breaks and interstrand crosslinks respectively, both of which are dealt with by other repair pathways, failed to provoke any detectable XPC accumulation or enhance the UV effect when combined with UV-irradiation (data not shown). The possibility that UV and NA-AAF evoke a general protein accumulation was ruled out since cells expressing GFP alone do not exhibit a significant increase in fluorescence after genotoxic insults. This indicates that lesions specifically recognized by the NER pathway enhance the level of HR23-dependent hXPC-GFP.

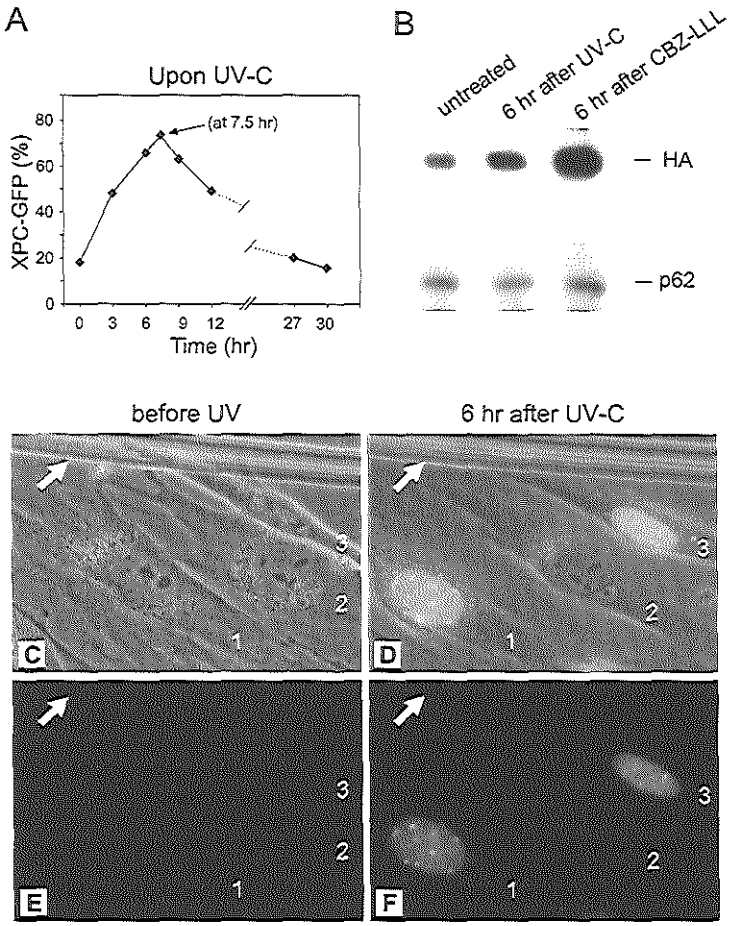

Figure 5. Effect of UV on hHR23B-dependent XPC-GFP level in living *DKO* cells. **(A)** Kinetic analysis of living *DKO* cells expressing XPC-GFP/hHR23B upon 10 J/m^2 UV-C in time over a period of 30 hours. The percentage XPC-GFP was expressed as the number of GFP expressing cells divided by the number of non-GFP expressing cells. **(B)** Immunoblot analysis of *DKO* cells expressing XPC-GFP/hHR23B before exposure to damaging agent (lane 1), 6 hr after exposure to 10 J/m^2 UV-C (lane 2), and 6 hr after treatment with 10 μM CBZ-LLL (lane 3) using monoclonal antibodies recognizing the HA epitope (upper panel). A monoclonal antibody against the p62 subunit of TFIIH (lower panel) was used as a loading control. Similar outcome was obtained with two other independent *DKO* cell lines expressing XPC-GFP/hHR23B (data not shown). **(C-F)** Combined phase contrast (red) and fluorescence (green) images (C and D), and epifluorescence images (E and F) of living *DKO* cells expressing XPC-GFP/hHR23B before UV (C and E) and 6 hr after 10 J/m^2 UV-C (D and F). White arrows indicate the scratch mark on glass coverslips (24 mm Ø). The numbers represent the same living cells before and after UV-exposure. Identical results were obtained with two other independent *DKO* cell lines expressing XPC-GFP/hHR23B (data not shown). All images were taken at the same magnification.

One of the direct consequences of UV- as well as NA-AAF-induced DNA damage is a temporary block of transcription. To investigate whether hXPC-GFP accumulation requires transcription or is induced by blockage of transcription independent of DNA damage, transcription in *DKO* cells expressing hXPC-GFP/hHR23B was arrested by incubation with 5,6-dichloro-1β-D-ribofuranosyl-benzimidazole (DRB, 100 μM) which is able to reversibly inhibit transcription initiation by RNA polymerase II (Chodosh et al. 1989). No induction of XPC-GFP fluorescence was registered after DRB administration. In fact, preincubation with DRB (2-3 hrs) prior to UV treatment prevented UV-induced XPC accumulation, indicating that transcription is required for observing the dramatic increase of XPC. Consistent with this result no enhanced XPC fluorescence was found with translational inhibitor cyclohexamide (30 and 50 μg/ml, data not shown) demonstrating the requirement for *de novo* protein synthesis.

hXPC-GFP is degraded via ubiquitin-dependent proteolysis

To further examine the HR23-dependent XPC stabilization, *DKO* cells expressing hXPC-GFP/hHR23B were incubated with the proteasomal proteolysis inhibitor N-CBZ-LEU-LEU-LEU-AL (CBZ-LLL, Wiertz et al. 1996). Like for UV-irradiation and NA-AAF treatment, all cells displayed a striking XPC-GFP accumulation in time (Figure 6E-H), which was reversible upon drug removal (not shown), and was confirmed by immunoblot analysis using anti-HA antibodies (Figure 5B, lane 3). These data indicate that degradation of XPC-GFP occurs via ubiquitin-dependent proteolysis. Consequently, NER damage together with HR23 protein somehow interfere with this process. This transient stabilization leads to a rapid increase of hXPC-GFP via *de novo* synthesis of mRNA and protein.

Application of local UV damage on hXPC-GFP expressing cells

Two mechanisms may explain the transient stabilization of hXPC-GFP. The binding of XPC to DNA damage *per se* might protect it from proteolysis. Alternatively (or in addition) DNA damage may trigger a specific response, that inhibits degradation of XPC independent of its binding to lesions. To explore the mechanism by which hXPC-GFP is stabilized we employed a recently developed method for induction of DNA damage in a restricted part of the nucleus. For this purpose, monolayer cultures of *DKO* cells expressing hXPC-GFP/hHR23B were covered with an isopore polycarbonate filter with pores of ~5 μm in diameter. Upon UV-irradiation only at the position of pores UV-damage is induced. Cells were fixed at different time points after UV to allow simultaneous immunostaining with antibodies

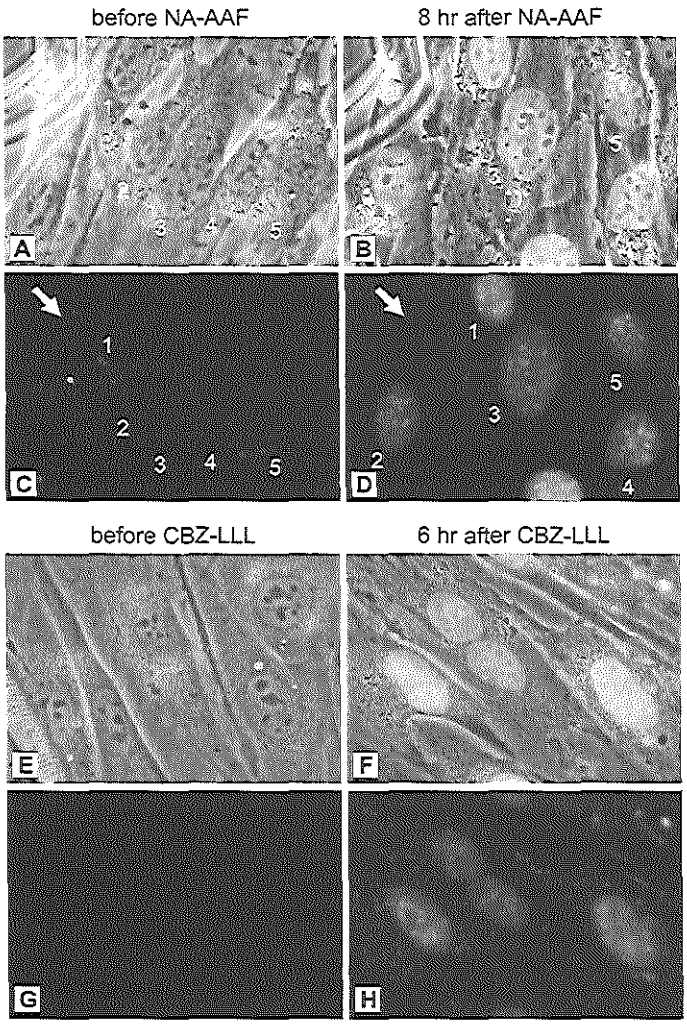

Figure 6. Effect of NA-AAF and proteasome inhibitor on hHR23B-dependent hXPC-GFP level in living *DKO* cells. **(A-D)** Combined phase contrast (red) and fluorescence (green) images (A and B), and epifluorescence images (C and D) of living *DKO* cells expressing XPC-GFP/hHR23B before NA-AAF (A and C) and 8 hr after 50 μM NA-AAF (B and D). White arrows indicate the scratch on glass coverslips (24 mm ∅). The numbers represent the corresponding living cells on coverslips before and after NA-AAF treatment. Identical results were obtained with two other independent *DKO* cell lines expressing XPC-GFP/hHR23B (data not shown). All images were taken at the same magnification. **(E-H)** Combined phase contrast (red) and fluorescence (green) images (E and F), and only epifluorescence images (G and H) of living *DKO* cells expressing XPC-GFP/hHR23B before treatment with proteasome inhibitor CBZ-LLL (E and G) and 6 hr after 10 μM CBZ-LLL (F and H). All images were taken at the same magnification.

against various proteins and GFP fluorescence microscopy (Figure 7). Non-irradiated nuclei and non-damaged regions within partly irradiated nuclei serve as internal controls. Very rapidly (within a few minutes) after UV-exposure GFP fluorescence and anti-HA immunostaining revealed high local accrual of the hXPC-GFP(His_6HA) in part of the nuclei. These XPC-GFP concentrations colocalize with accumulations of other NER proteins, XPA and p62 (subunit of TFIIH) (Figure 7 and not shown). These locations correspond with sites of local UV damage (Volker et al. 2001; Moné et al. submitted) to which all tested NER proteins have been found to specifically migrate (unpublished results). These findings demonstrate that in living cells the GFP-tagged XPC protein translocates very rapidly to sites containing UV lesions. When XPC stabilization occurs only after binding to the damage we expect an increase in fluorescent signal selectively at the damaged sites. On the other hand, with an overall stabilization of hXPC, it is expected that in time a concomittant increase of fluorescence over the entire nucleus (in addition to the damaged area) would be observed in comparison to non-damaged nuclei. The increase of hXPC-GFP (Figure 7A) is initially only at the locally damaged sites, but after two hours also in the remainder of nuclei containing local damage a clearly higher signal is noted when compared to non-exposed nuclei in the vicinity (Figure 7B). These findings suggest that an overall intranuclear stabilization of hXPC-GFP occurs.

Discussion

Involvement and function of HR23A and HR23B proteins in NER

The aim of this work was to shed light onto the enigmatic role of the two HR23 proteins in NER and to reveal the biological impact of both factors by the generation of *mHR23A* and *mHR23B* mutants in the mouse germ line. Since single mutants failed to exhibit any detectable NER defect the most logical interpretation is that these proteins are functionally redundant despite their >40% amino acid sequence divergence and size difference (Masutani et al. 1994). However, definite proof requires the availability of double mutant cells, which we were able to establish notwithstanding early lethality of double mutant embryos and poor growth properties of the cells during adaptation to *in vitro* culturing (see Results). The NER-deficient phenotype exhibited by *DKO* cells and the ability of each of the *HR23* genes to rescue this defect unequivocally established the involvement of mHR23B as well as mHR23A in NER and their fully overlapping functions in repair.

Further characterization of the type of NER defect of the *DKO* cells revealed a selective impairment of the global genome NER subpathway and

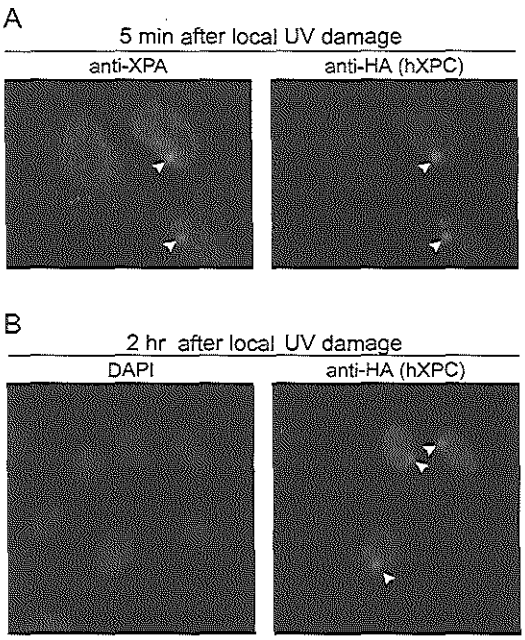

Figure 7. UV-exposure through isopore filter induces locally damaged spots and overall stabilization in the nuclei of *DKO* cells expressing XPC-GFP/hHR23B. *DKO* cells expressing XPC-GFP/hHR23B were exposed to 64 J/m^2 UV-C through 5.0 μm pore filters and fixed 5 min (A) and 2 hours (B) later with paraformaldehyde. Double immunofluorescent labeling using antibodies against XPA (A, left panel: stained green with goat anti-rabbit Alexa 488-labeled secondary antibody) and HA epitope (A, right panel: stained red with goat anti-rat Alexa 594-labeled secondary antibody). DAPI stained (B, left panel) and epifluorescence images without antibody labeling (B, right panel). Arrowheads indicate the site of UV-induced local damage in the nuclei of *DKO* cells expressing hXPC-GFP/hHR23B. Note: Compare the increased fluorescence signal over the entire nucleus of damaged cells to the signal of non-damaged nuclei for overall stabilization of XPC (B).

apparently normal transcription-coupled repair as deduced from the fact that recovery of RNA synthesis after UV-irradiation is unaffected. This is strikingly similar to the repair phenotype of XPC, which hitherto was unique among the NER mutants but deviates from the *S.cerevisiae RAD23* prototype mutant and its *S.pombe* equivalent, which carry a combined GG-NER and TC-NER deficiency (Mueller and Smerdon 1996; Verhage et al. 1996; Lombaerts et al. 2000). This unresolved mammalian-yeast difference is also registered for XPC and its yeast counterpart RAD4, underlining the parallels between HR23 and XPC.

What is the function of HR23 in GG-NER? The remarkable correspondence with *XPC* mutants prompted us to examine the status of

the XPC protein in *DKO* cells. The virtual absence of XPC in immunoblot analysis and in immunofluorescence (Figure 3) provided a direct explanation for the *HR23* phenocopy of *XPC*: in the absence of HR23 the XPC protein is apparently unstable. This resolves the function of HR23, reveals a novel mechanism of regulation of NER and puts a new perspective to the growing number of links emerging between RAD23/HR23 and the ubiquitin system involved in protein turn-over. First, all RAD23 homologs are largely made up of modules found in proteins that are engaged in the ubiquitin process: the UbL N-terminus and two UBA domains (van der Spek et al. 1996b), comprising ~50% of the protein. Second, a number of experimental connections of RAD23/HR23 with the ubiquitin pathway have surfaced during recent years (Schauber et al. 1998; Lambertson et al. 1999; Ortolan et al. 2000; Suzuki et al. 2001). The UBA domains have been shown to interact with ubiquitin (Bertolaet et al. 2001). The UbL domain of RAD23/HR23 provides a platform for direct interaction *in vivo* and *in vitro* with the 19S regulatory complex of the 26S proteasome (Schauber et al. 1998). This domain is required for the *RAD23* NER function in *S.cerevisiae* and can be replaced by the regular ubiquitin sequence (Watkins et al. 1993). However, controversies exist on the functional implications of the RAD23/NER-19S/26S proteasome engagement. Russell (Russell et al. 1999) and Gillette (Gillette et al. 2001) present evidence that the 19S regulatory complex represses NER independent of RAD23 in a manner apparently independent of proteolysis. On the other hand, Ortolan and coworkers (2000) recently reported that the UbL domain of RAD23 negatively regulates proteolysis of (multi-ubiquitinated) protein substrates and proposed that this may inhibit degradation of repair factors to promote NER. Interactions between HR23B and the 26S proteasome were also observed in human cells (Hiyama et al. 1999). In conclusion, a link between NER and the 19S complex of the 26S proteasome mediated by RAD23 seems well established but the functional implications remain obscure.

In mammals, Araki and coworkers (2001) have recently collected evidence for *in vitro* heat lability of recombinant XPC protein, which is partly alleviated by the binding of HR23B. These observations suggest that XPC is intrinsically unstable and that association of HR23B *per se* helps to stabilize its active conformation. In the present work this is extended and applied to the *in vivo* situation: in the absence of HR23 proteins XPC is virtually undetectable, causing an *XPC*-like GG-NER defect, reintroduction of HR23 leads to reappearance of XPC. Indeed we could bypass the HR23 NER defect by overexpression of hXPC, compensating for the short half life by increased synthesis of the protein. The most logical interpretation of the

above findings is that HR23 proteins normally protect XPC from degradation. In view of the severity of the NER defect in *DKO* cells correlating with the low cellular XPC content it appears that this is the main *in vivo* NER function of RAD23/HR23 proteins.

Effect of DNA damage on XPC/HR23

After generation of a cell line stably expressing functional GFP-tagged XPC we were curious to know what would happen when damage is induced in view of the notion that XPC is the first protein to sense DNA injury (Sugasawa et al. 1998; Kusumoto et al. 2001). To our surprise exposure to UV and NA-AAF led to a dramatic further stabilization of the XPC-GFP fusion protein resulting in strong XPC-GFP signals in the nucleus within a few hours. This phenomenon is clearly dependent on induction of helix-distorting lesions that are substrate of the GG-NER subpathway and is not due to a general stress-related response (Figures 5C-F and 6A-D). XPC-GFP induction occurred with largely similar kinetics when proteasome-mediated protein degradation is inhibited providing further proof for the idea, that protein stabilization is responsible for the XPC-GFP increase. Assuming that proteolysis was largely inhibited, the similar kinetics indicate that under conditions of DNA damage hardly any XPC-GFP is degraded.

How is XPC-GFP stabilized? The experiments involving local DNA damage (Figure 7) reveal a very rapid (within minutes), specific accumulation of XPC-GFP in the damaged regions, which is found for all NER factors and is due to actual engagement in DNA repair events (Volker et al. 2001; and our unpublished results). However, on top of this we observed a time-dependent (within 1 or 2 hours) enhancement of XPC-GFP

Figure 8. A novel mechanism of regulation of XPC and GG-NER by HR23 involves the ubiquitin system and other cellular processes. **(A)** In the absence of the HR23 (indicated as 23), XPC is intrinsically unstable and is preferentially targeted for ubiquitin-dependent proteolysis via the 19S regulatory complex of 26S proteasome. As a consequence the steady state level of XPC and thus the GG-NER capacity is decreased. Ubiquitin proteins are depicted as "u". **(B)** HR23 together with CEN2 (C2) stabilize XPC by recruiting the complex to the 19S regulatory complex exploiting its protein refolding capacity. This partly protects XPC from degradation and leads to a higher steady state level of XPC. **(C)** NER-specific DNA damage directly (via enhanced protein stability) and/or indirectly (via stimulation of the 19S salvage route of the proteasome system) results in a further increase in XPC/HR23/CEN2 protein levels, and accordingly GG-NER capacity. This mechanism might also explain the enhanced reactivation phenomena. A comparable HR23 mediated stabilization/refolding mechanism may hold for other proteins (here indicated by "?") and cellular pathways (i.e. cell cycle control, cell division, and other repair pathways), in which HR23 proteins are involved.

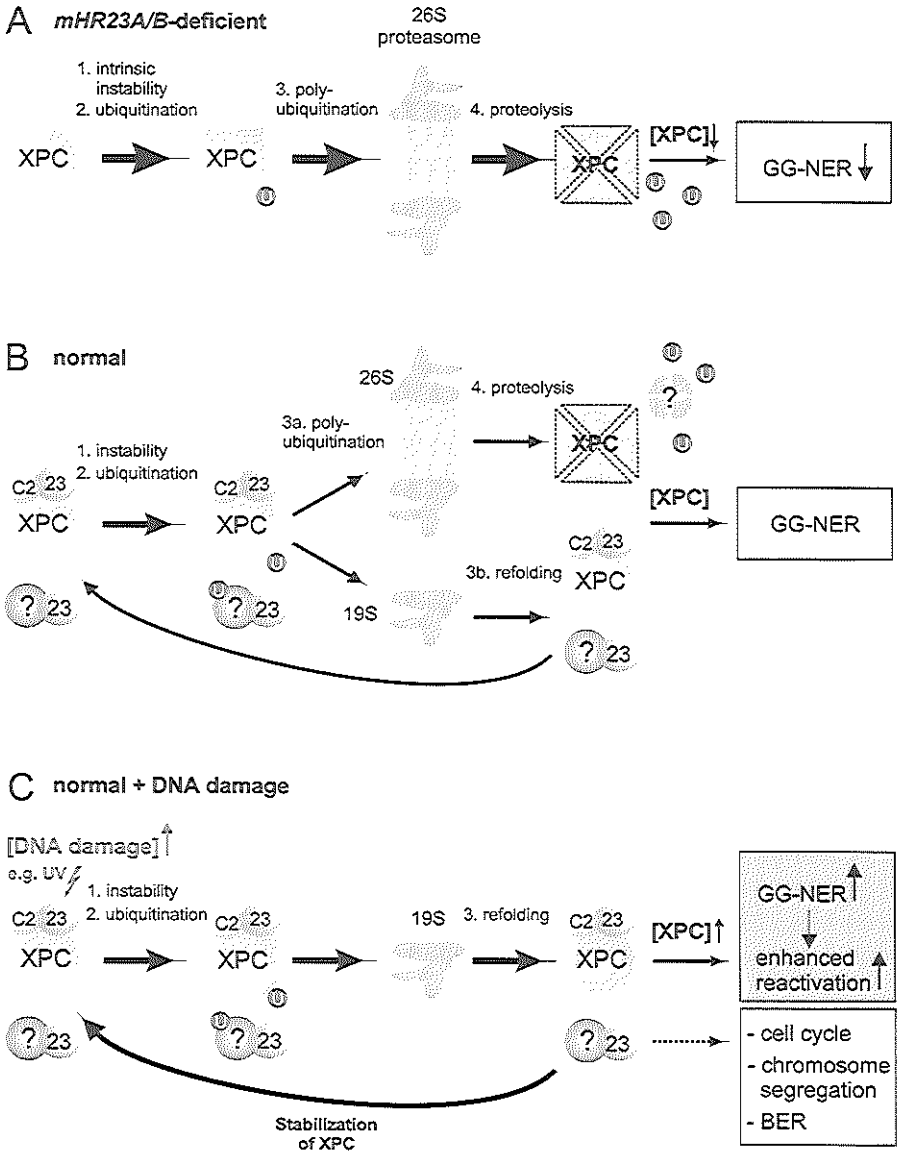
A mHR23A/B-deficient
26S proteasome
1. intrinsic instability
2. ubiquitination
3. poly-ubiquitination
4. proteolysis
XPC
XPC
[XPC]↓
GG-NER ↓
B normal
26S
4. proteolysis
3a. poly-ubiquitination
1. instability
2. ubiquitination
C2 23
XPC
[XPC]
GG-NER
3b. refolding
19S
? 23
C normal + DNA damage
[DNA damage]↑
e.g. UV
1. instability
2. ubiquitination
19S
3. refolding
[XPC]↑
GG-NER ↑
enhanced reactivation ↑
- cell cycle
- chromosome segregation
- BER
Stabilization of XPC

signals over the entire nucleus. This argues in favor of the idea that also XPC-GFP molecules in undamaged parts of the nucleus become transiently more stable and against the possibility that only molecules actually bound to a lesion are protected from proteolysis. It is feasible however, that participation of XPC/HR23 in NER events triggers its stabilization. For instance, dissociation of XPC/HR23 from the damage might involve the 19S regulatory complex that could at the same time refold or otherwise modify the protein into a stable, active state.

A novel mechanism of regulation of NER – parallels with the *E.coli* SOS response.

Figure 8 puts all our observations and other findings on RAD23/HR23 and the ubiquitin system in a unifying model. As the main initiator of global genome NER (Sugasawa et al. 1998) XPC constitutes an ideal focal point for the regulation of the entire pathway. In line with this idea overexpression of RAD4 in yeast confers accelerated rates of NER (Lommel et al. 2000) and here we show that reduction of XPC leads to a corresponding decrease of GG-NER. As suggested by the *in vitro* heat lability it appears that XPC - in the absence of HR23 - is intrinsically unstable (Araki et al. 2001). As a consequence *in vivo* the protein may be preferentially targeted for ubiquitin-dependent proteolysis via the 19S regulatory complex of the 26S proteasome (Figure 8A). This is consistent with the finding that in *rad23Δ* mutants NER is enhanced by additional mutations in the 19S complex, which may affect its role in proteolysis of critical NER factors (Gillette et al. 2001). Similar findings have been made in wildtype *S.cerevisiae* (Lommel et al. 2000). Binding of HR23 to XPC may help stabilize the protein (Araki et al. 2001). In addition we suggest that HR23 enables reactivation of XPC by recruiting the protein refolding capacity of the 19S regulatory complex protecting XPC from degradation and boosting the steady state level (Figure 8B). A protecting role of RAD23/HR23 in relation to NER and other processes *in vivo* was already postulated from various other studies (Schauber et al. 1998; Ortolan et al. 2000). When cells experience a high level of damage the involvement in NER shifts the equilibrium of the XPC complex more to the stable conformation by stimulating the salvage option of the 19S regulatory complex (Figure 8C). This would lead to an up-regulation of XPC protein and consequently the entire GG-NER pathway when cells are subjected to a high level of damage for prolonged periods of time. This rheostat model for adapting the level of XPC to the amount of damage explains the long known phenomenon of enhanced reactivation: increased survival of a UV-irradiated virus when the host cells have been

irradiated before infection (Cornelis et al. 1980; Hagedorn et al. 1985) which likely is due to the fact that the UV challenge up-regulates XPC and GG-NER. The above model is also in agreement with most of the reported observations on RAD23.

Importantly, a number of other proteins have been found to associate with HR23 and - like XPC - may be subject to a similar mechanism of transient stabilization. One interesting HR23 partner is an enzyme at the start of another DNA repair mechanism: 3-Methyladenine (3Me-A) DNA glycosylase that initiates base excision repair of a number of DNA alkylation damages including 3Me-A, 3Me-G, 7Me-G, etheno-adenine, ethenoguanine, and hypoxanthine (reviewed in Memisoglu and Samson 2000). Binding of HR23 *in vitro* elevates the rate of excision of hypoxanthine containing substrates (Miao et al. 2000), which opens the possibility that this branch of base excision repair is regulated in an analogous fashion as is demonstrated here for XPC/GG-NER.

Another intriguing link relevant for genome care-taking is an emerging series of connections of RAD23/HR23 with the cell cycle. RAD23 exerts a partially redundant role together with Rpn10 in the G2/M phase of the cell cycle (Lambertson et al. 1999), together with the RAD23/HR23-like protein Ddi1 in Pds1-dependent mitotic control, spindle assembly and S-phase checkpoints (Clarke et al. 2001) and with Dsk2 in spindle pole duplication (Biggins et al. 1996). In mammals, HR23 was found to interact with the Rpn10 homolog S5α (Hiyama et al. 1999). The link with spindle pole duplication has recently been strengthened by the discovery of the centrosome factor centrin 2 (also designated Caltractin 1), as a third component of the XPC/HR23 complex (Araki et al. 2001). Furthermore, in mammals, the p53 protein is regulated in part by hHR23A via inhibition of CREB (cyclic AMP-responsive element binding) protein that acts a co-activator of p53 transcription (Zhu et al. 2001). In addition, several viral proteins have been found to target the HR23 proteins presumably to influence the cell cycle program (Withers-Ward et al. 1997; Dieckmann et al. 1998; Kumar et al. 1999; Withers-Ward et al. 2000). Finally, HR23 proteins themselves appear to be regulated in a cell cycle dependent manner with specific degradation during S-phase (Kumar et al. 1999). Thus multiple, intimate engagements between RAD23/HR23 and critical stages in the cell cycle are apparent.

It is likely that the principal mechanism for regulation of XPC and GG-NER by HR23 also applies to many of the above mentioned HR23 partners and the corresponding processes. In fact, these processes might well be functionally related to each other via HR23. A potential scenario

putting many of these connections in a functional perspective is depicted in Figure 8C. The HR23 damage-dependent cellular responses could be triggered by primary DNA damage sensors bound by HR23, such as the GG-NER initiator XPC, and 3-Me-A DNA glycosylase and coordinated via the HR23 proteins impinging upon cell cycle progression, S-phase checkpoints and chromosome segregation, possibly including p53 transcription. This system is in its effect reminiscent of the well-known SOS response in *E.coli*, involving the RecA/LexA regulon. In this case DNA damage triggers autocleavage of the LexA repressor stimulated by RecA. As a consequence a specific set of genes with diverse functions in response to DNA injury is up-regulated. This includes genes involved in NER, damage-induced mutagenesis and translesion DNA synthesis and cell division (reviewed by Sutton et al. 2000). In addition, the multiple engagements of the HR23 proteins provide a plausible explanation for the - compared to other NER mutants deviant - phenotype of the *mHR23B*-deficient mice and the embryonic lethality of the *DKOs*.

Down-regulation of XPC

Why are XPC levels not constitutively high? At first sight it would seem highly advantageous to have GG-NER always operating at maximal capacity instead of complex, time-consuming up-regulation as revealed here for XPC. However, several lines of evidence indicate that RAD4 and its mammalian equivalent XPC are highly toxic when expressed at too high levels in homologous and heterologous systems. Even low copy expression of RAD4 in *E.coli* interfered with growth and only defective derivatives of the gene could be propagated (Siede and Eckardt-Schupp 1986; Couto and Friedberg 1989; Wei and Friedberg 1998). This suggests that the protein interferes with some important cellular process. One likely function that may affect the basic DNA machinery is the ability of XPC and RAD4 to bind very strongly to DNA in particular to a wide range of (aberrant) DNA structures. A fundamental dilemma is that some DNA lesions resemble normally occurring functional DNA conformations and the latter may erroneously be considered by the damage sensing machinery as DNA injury. For instance, XPC has recently been shown to detect helix-distortions on the basis of disrupted base-pairing and also to bind to regular mismatches (Sugasawa et al. 2001). This highlights the basic quandary of the twilight zone between specific forms of intact DNA and true DNA damage. Thus, titrating XPC to low levels may reduce abortive or untargeted repair interfering with natural DNA transactions. Intriguingly, by overexpression of exogenous hXPC we observed that at the same time the endogenous mXPC was co-stabilized

(Figure 4). One interpretation of this trans-effect is that the pathway responsible for degradation of mXPC becomes saturated by the high production of exogenous hXPC driven by the strong SV40 promoter. This in turn points to a quite specific proteolysis mechanism that normally keeps XPC concentrations low.

Concluding remarks and future perspectives

The generation of the first mammalian cells deficient in mHR23 starting from *mHR23A* and *mHR23B* single mutants permitted the elucidation of the main NER function of RAD23 revealed a novel level of regulation in the NER pathway and clarified the link between NER and the ubiquitin system. The damage-induced, mHR23-dependent stabilization of XPC provides an explanation for long known phenomena such as enhanced reactivation that lacked an adequate mechanistic basis. The multiple engagements of mHR23 proteins may connect stress response mechanisms including cell cycle control to known damage sensors like XPC paralleling the *E.coli* SOS system. Interestingly, RAD23 transcription is also damage inducible in yeast (Madura and Prakash 1990), although this property appears not preserved in human keratinocytes (van der Spek et al. 1996b). The GFP tagging of XPC will permit *in vivo* analysis of dynamic properties of this crucial NER factor including rapid migration of the XPC-GFP to local damage observed in this study using sophisticated photobleaching techniques (Houtsmuller et al. 1999). Finally, the cell line expressing GFP-tagged XPC will also be useful for screening and detection of genotoxic agents that induce (helix-distorting) lesions recognized by GG-NER.

Experimental Procedures

Construction of *mHR23A* targeting vector

Isogenic mouse genomic DNA was derived from an Ola129 ES cell-derived phage lambda library after probing with human *HR23A* cDNA sequences. An *mHR23A* targeting construct was generated by changing the BglII site of clone pG7M23Ag1 (containing a 4 kb EcoRI fragment) into a ClaI site, which resulted in deletion of sequences downstream the BglII site in exon II (clone pG7M23Ag7). Next, the EcoRI site was removed by filling-in the overhangs with Klenow, resulting in clone pG7M23Ag9. After changing the BstXI site in a SalI site, the 3 kb XhoI-SalI fragment (including the ClaI, HindIII, and BamHI sites in the 3' MCS) was cloned into SalI digested pGEM5, resulting in clone pG5M23Ag17. Next, the 3' arm of the construct, consisting of a Klenow-blunted 1.5 kb SmaI-XbaI fragment starting at the SmaI site in exon VII, was inserted in the blunted NdeI site of pG5M23Ag17 (giving pG5M23Ag20), followed by insertion of a Neo marker cassette in antisense orientation in the ClaI site (giving pG5M23Ag24). Finally, the NotI-NsiI insert of pG5M23Ag24 was

recloned into a pGEM-9Zf(-) based vector containing a 2.8 kb thymidine kinase (TK) marker cassette (giving pG5M23Ag30).

ES cell culture and transfection

The Ola129-derived ES cell line E14 was electroporated with the *mHR23A* targeting construct and cultured on gelatinized dishes as described (van der Horst et al. 1997). G418 (Geneticin, Gibco, final concentration 200 µg/ml) was added 24 hr after electroporation and cells were maintained under selection for 6-8 days. Genomic DNA from G418-resistent clones was digested with BamHI and subjected to Southern blot analysis using a 0.6 kb XbaI-RsaI fragment (3' external to the construct) as a probe. Targeted clones were subsequently screened with a Neo cDNA probe (ClaI fragment) to confirm proper homologous recombination in the 5' arm.

Generation of the *mHR23A*$^{-/-}$ and *mHR23A*$^{-/-}$/*B*$^{-/-}$ *(DKO)* mice and fibroblasts

Targeted *mHR23A* clones were karyotyped and cells from two independent clones with 40 chromosomes were injected into 3.5-day-old blastocysts isolated from pregnant C57BL/6 females (van der Horst et al. 1997). Male chimeric mice were mated with C57BL/6 females to obtain heterozygote animals. Germline transmission was observed in the coat colour of the F1 offspring. Heterozygous males and females for *mHR23A* were interbred to generated *mHR23A*$^{+/+}$, *mHR23A*$^{+/-}$, and *mHR23A*$^{-/-}$ mice. For the generation of double mutant *mHR23A/B* mice, male and female animals heterozygous for both *mHR23A* and *mHR23B* (Ng et al. submitted) were interbred. Genotyping was performed by Southern blot analysis or by PCR analysis (as described below) of genomic DNA prepared from tail biopsies of 10-14-day-old pups.

Primary *mHR23A* MEFs (three independent lines per genotype) were isolated from day 13.5 embryos (E13.5) obtained from matings between *mHR23A*$^{+/-}$ mice. Double mutant *mHR23A/B* MEFs were isolated from day 8.5 embryos (E8.5) derived from different crossings between *mHR23A*$^{+/-}$/*B*$^{+/-}$ and *mHR23A*$^{-/-}$/*B*$^{+/-}$ mice. Part of the embryo was used for genotyping and the remaining tissue was minced using a pair of scissors and immersed in a thin layer of F10/DMEM culture medium (Gibco BRL) supplemented with 15% fetal calf serum, 2mM glutamate, and 50 µg/ml penicillin and streptomycin. Spontaneously immortalized (established) cell lines were obtained by continuous subculturing of primary MEFs.

E8.5 embryos were dissected, and the yolk sacs were used for genotyping as described (Gurtner et al. 1995). In short, the yolk sac of E8.5 embryos was collected in 20 µl of water and frozen in dry ice immediately. Samples were heated for 5 min at 95°C and incubated with 1 µl of proteinase K (10 mg/ml) for 1 hr at 55°C. Proteinase K was heat-inactivated for 5 min at 95°C. PCR analysis was performed using the three-primer sets described below for 30 cycles (93°C, 1 min; 55°C, 1 min; 72°C, 90 sec) using *mHR23A* and *mHR23B* primers (as described below).

Primer set 1: mHR23Ap1 (5'-atg-gga-ctt-ggg-cat-agg-tga-3'), mHR23Ap2 (5'-tct-tca-gcc-agg-cct-ctt-ac-3') and anti-sense neo (5'-atc-tgc-gtg-ttc-gaa-ttc-gcc-aat-g-3') giving 243 and 350 bp PCR fragments from the wildtype and targeted allele respectively. Primer set 2: mHR23Bp1 (5'-gta-aag-gca-ttg-aaa-gag-aag-3'), mHR23Bp2 (5'-cta-cag-tct-tgt-ttc-tga-cag-3') and anti-sense pgk3 (5'-tag-ggg-agg-agt-aga-agg-tg-3') giving 202 and 600 bp PCR fragments from the wildtype and targeted allele respectively.

DNA Repair Assays

UV sensitivity was determined as described (Sijbers et al. 1996). MEF cultures were exposed to different doses of UV-C light (254 nm, Philips TUV lamp) and allowed to grow for another 3-5 days, before reaching confluency. The number of proliferating cells was estimated by scintillation

counting of the radioactivity incorporated during a 3 hr pulse with [^{3}H]thymidine (5 μCi/ml, specific activity (s.a.): 50 Ci/mmole; Amersham). Cell survival was expressed as the ratio of ^{3}H incorporation in irradiated and non-irradiated cells.

UV-induced global genome repair was assayed using the UDS method as described (Vermeulen et al. 1994). Cells were exposed to 16 J/m^2 of 254 nm UV light and labelled with [methyl-^{3}H]thymidine (10 μCi/ml, s.a.: 50 Ci/mmole). Repair capacity was quantified by grain counting after autoradiography. Incorporation of radioactivity was measured by autoradiography and grain counting (average of 50 nuclei per cell line; the standard error of the mean is indicated).

RNA synthesis recovery was measured according to (Mayne and Lehmann 1982). Cells were exposed to 10 J/m^2 of 254 nm UV light, allowed to recover for 16 hr, labelled with [5,6-^{3}H]uridine (10 μCi/ml, s.a.: 50 Ci/mmole), and processed for autoradiography. The relative rate of RNA synthesis was expressed as the quotient of the number of autoradiographic grains over the UV-exposed nuclei and the number of grains over the nuclei of nonirradiated cells (average of 50 nuclei per cell line; the standard error of the mean is indicated).

RNA and protein analysis

Total RNA was isolated from *mHR23A* MEFs using a RNeasy Mini Kit (Qiagen). 20 μg of total RNA was separated on a 0.9% agarose gel and transferred to Hybond-N+ membrane (Amersham Pharmacia Biotech). RNA blots were hybridized using *mHR23A* and β-actin ^{32}P-labeled cDNA probes.

Immunoblot analysis was performed on fibroblast extracts obtained by sonification (5 x 10^6 cells in 300 μl phosphate-buffered saline (PBS)) or extraction. In the latter case, NP lysis buffer (25 mM Tris-HCl (pH 8.0), 1 mM EDTA, 10% glycerol, 0.01% Nonidet P-40, 1 mM dithiothreitol, 0.25 mM PMSF, and protease inhibitor mix (chymostatin, leupeptin, antipain, and pepstatin A)) was added to a monolayer of MEFs. After 30 min on ice the lysate was collected with a cell scraper and clarified by 2 times centrifugation at 4°C. NP lysis buffer containing 0.3 NaCl was added to the cell pellet and homogenized by sonification.

SDS polyacrylamide gel electrophoresis was performed by loading 25-50 μg of total cellular protein per lane on 6-8% gels. Proteins were blotted to nitrocellulose membranes (Schleicher & Schuell) and probed with polyclonal antibodies recognizing human HR23A or XPC, or with monoclonal antibodies recognizing the HA epitope (HA.11, BAbCO) or p62 subunit of TFIIH (C39). Proteins were visualized using alkaline phosphatase-labeled goat anti-rabbit or peroxidase-conjugated goat anti-rabbit or goat anti-mouse secondary antibodies.

Immunofluorescence labeling

Cells were grown on glass coverslips at 60-80% confluency. After washing twice with PBS, cells were fixed with 2% paraformaldehyde in PBS for 10 min at room temperature (RT) and permeabilized with 0.1% Triton X-100 in PBS for 2x 10 min at RT. After extensive washing (three times of 5 min each) with PBS$^+$ (PBS supplemented with 0.15% glycine and 0.5% BSA) cells were incubated with affinity purified primary antibodies in PBS$^+$ in a moist chamber for 1½ hr at RT. After washing five times in PBS$^+$, cells were incubated with the secondary antibodies for 1½ hr in PBS$^+$ in a moist chamber at RT. Following 5 times washes with PBS$^+$ and once with PBS, coverslips were preserved with Vectashield™ Mounting Medium (Vector Laboratories) containing 4'-6-diamino-2-phenylindole (DAPI, 1.5 μg/μl).

Primary antibodies used: affinity purified, rabbit polyclonal anti-human XPC; rabbit polyclonal anti-XPA (a kind gift from Dr. K. Tanaka); mouse monoclonal anti-p62 of TFIIH subunit (3C9); and high affinity, rat monoclonal anti-HA (3F10; Boeringer). Secondary antibodies were:

goat anti-rat Alexa 594-conjugated and goat anti-rabbit Alexa 488-conjugated antibodies (Molecular probes); and goat anti-mouse Cy3-conjugated antibodies (Jackson ImmunoResearch Laboratories).

Generation of *XPC-GFP* fusion cDNA construct and cotransfection studies

Full length *h*uman *XPC* cDNA (ScaI-Asp718I fragment) was cloned in EcoRI-Asp718I digested eukaryotic expression vector pEGFP-N3 (Clontech) containing a 3' histidine-hemaglutinine tag (generated by insertion of a doublestranded oligonucleotide in SspBI-NotI digested pEGFP-N3: kindly provided by D. Hoogstraten). For simplicity, the resulting tagged cDNA construct *hXPC-EGFP-His_6HA-N_3* is referred to as *hXPC-GFP*.

Full length cDNAs of the *hHR23B* (in an pSLM vector, Pharmacia biotech) and *hXPC-GFP* were cotransfected into *DKO* MEFs using puromycin as selectable marker. The transfection was performed using SuperFect Transfection Reagent (Qiagen) and puromycin was added 24 hr after transfection to a final concentration of 1μg/ml, and the cells were maintained under selection for 20-40 days. Stable puromycin-resistant clones were isolated and integration of the cDNA construct was confirmed by DNA blotting (data not shown).

Exposure of cells to DNA damaging agents

Cells stably expressing hXPC-GFP were rinsed with PBS, exposed to UV-C light (254 nm; Philips TUV lamp, dose as indicated in the text) and subsequently cultured at 37 °C for various time periods (as indicated in the text). XPC was detected either by immunoblot analysis or by visualization in living cells using light microscopy. A similar approach was used to study the effect of N-acetoxy-2-acetylaminofluorene (NA-AAF; kindly provided by Dr. van Zeeland; final concentration 50 or 100 μM), mitomycin C (MMC; Sigma; final concentration 1.2 or 2.4 μg/ml), ionizing radiation (γ-rays from a ^{137}Cs source; single dose of 6 and 10 Gy), the proteasome inhibitor N-CBZ-LEU-LEU-LEU-AL (CBZ-LLL; Sigma; final concentration 5 or 10 μM), the transcription inhibitor 5,6-dichloro-1β-D-ribofuranosyl-benzimidazole (DRB; Sigma; final concentration of 100 μM, 2-3 hrs), and the translation inhibitor cyclohexamide (CHX; Boehringer; final concentration 30 or 50 μg/ml, 1-3 hrs.) were added to the culture medium.

Local UV-irradiation was obtained by covering cells grown on glass coverslips with an isopore polycarbonate filter with pores of 5.0 μm diameter (Millipore, TMTP) during UV-irradiation (4 x 16 J/m^2 UV-C). Immediately after exposure, the filter was removed and medium was added back to the cells and culturing was continued. After various time periods (as indicated in the text), cells were processed for immunolabeling.

To identify cells in mixtures of control and mutant fibroblasts, cells were labeled with latex beads (diameter 0.79 μm; Polybead Carboxylate Microspheres, Polysciences) added to fibroblasts cultures 2 days prior to mixing of the cells. Cells were thoroughly washed in PBS (3x) before trypsinization to remove the non-incorporated beads and seeded in a 1:1 ratio on coverslips and cultured for 2 days.

Light microscopy and image analysis

Immunofluorescent microscopy images were obtained with either a Leitz Aristoplan microscope equipped with epifluorescene optics and a PlanApo 63x/1.40 oil immersion lens or a Leica DMRBE microscope equipped with epifluorescene optics and a PL Fluotar 100x/1.30 oil immersion lens. For the detection of GFP-tagged proteins in the living cell, we have used an Olympus IX70 microscope equipped with epifluorescene optics and Olympus PlanApo 60x/1.40 oil immersion lens. GFP images were obtained after excitation with 455-490 and long pass emission filter (>510

nm). Cy-3 images were obtained after excitation with 515-560 and long pass emision filter (580 nm).

References

Amacher DE, Elliott JA, and Lieberman MW (1977). Differences in removal of acetylaminofluorene and pyrimidine dimers from the DNA of cultured mammalian cells. Proc Natl Acad Sci U S A *74*, 1553-1557.

Araki M, Masutani C, Takemura M, Uchida A, Sugasawa K, Kondoh J, Ohkuma Y, and Hanaoka F (2001). Centrosome protein centrin2/caltractin1 is part of the xeroderma pigmentosum group C complex that initiates global genome nucleotide excision repair. J Biol Chem *18665-18672*, 27.

Araujo SJ, Nigg EA, and Wood RD (2001). Strong functional interactions of TFIIH with XPC and XPG in human DNA nucleotide excision repair, without a preassembled repairosome. Mol Cell Biol *21*, 2281-2291.

Bertolaet BL, Clarke DJ, Wolff M, Watson MH, Henze M, Divita G, and Reed SI (2001). UBA domains of DNA damage-inducible proteins interact with ubiquitin. Nat Struct Biol *8*, 417-422.

Biggins S, Ivanovska I, and Rose MD (1996). Yeast ubiquitin-like genes are involved in duplication of the microtubule organizing center. J Cell Biol *133*, 1331-1346.

Bootsma D, Kraemer KH, Cleaver JE, and Hoeijmakers JHJ (2001). Nucleotide excision repair syndromes: xeroderma pigmentosum, Cockayne syndrome, and trichothiodystrophy. *In:* Scriver CR, Beaudet, AL, Sly, WS, Valle, D Vogelstein and Kinzler (eds) The Metabolic and Molecular Bases of Inherited Disease, McGraw-Hill Book Co, New York *1*, 677-703.

Chodosh LA, Fire A, Samuels M, and Sharp PA (1989). 5,6-Dichloro-1-beta-D-ribofuranosylbenzimidazole inhibits transcription elongation by RNA polymerase II *in vitro*. J Biol Chem *264*, 2250-2257.

Clarke DJ, Mondesert G, Segal M, Bertolaet BL, Jensen S, Wolff M, Henze M, and Reed SI (2001). Dosage suppressors of pds1 implicate ubiquitin-associated domains in checkpoint control. Mol Cell Biol *21*, 1997-2007.

Cornelis JJ, Lupker JH, and van der Eb AJ (1980). UV-reactivation, virus production and mutagenesis of SV40 in UV-irradiated monkey kidney cells. Mutat Res *71*, 139-146.

Couto LB, and Friedberg EC (1989). Nucleotide sequence of the wild-type *RAD4* gene of Saccharomyces cerevisiae and characterization of mutant *rad4* alleles. J Bacteriol *171*, 1862-1869.

de Laat WL, Jaspers NG, and Hoeijmakers JHJ (1999). Molecular mechanism of nucleotide excision repair. Genes Dev *13*, 768-785.

Dieckmann T, Withers-Ward ES, Jarosinski MA, Liu CF, Chen IS, and Feigon J (1998). Structure of a human DNA repair protein UBA domain that interacts with HIV-1 Vpr. Nat Struct Biol *5*, 1042-1047.

Friedberg EC, Walker GC, and Siede W (1995). DNA repair and mutagenesis. ASM Press, Washington DC.

Gillette TG, Huang W, Russell SJ, Reed SH, Johnston SA, and Friedberg EC (2001). The 19S complex of the proteasome regulates nucleotide excision repair in yeast. Genes Dev *15*, 1528-1539.

Gurtner GC, Davis V, Li H, McCoy MJ, Sharpe A, and Cybulsky MI (1995). Targeted disruption of the murine *VCAM1* gene: essential role of VCAM-1 in chorioallantoic fusion and placentation. Genes Dev *9*, 1-14.

Hagedorn R, Thielmann HW, and Fischer H (1985). SOS-type functions in mammalian cells. Enhanced reactivation of UV-irradiated SV40 in UV-irradiated CV-1 cells. J Cancer Res Clin Oncol *109*, 89-92.

Hanawalt PC (2000). DNA repair. The bases for Cockayne syndrome. Nature *405*, 415-416.

Hanawalt PC, Donahue BA, and Sweder KS (1994). Repair and transcription. Collision or collusion? Curr Biol *4*, 518-521.

Hiyama H, Yokoi M, Masutani C, Sugasawa K, Maekawa T, Tanaka K, Hoeijmakers JHJ, and Hanaoka F (1999). Interaction of hHR23 with s5a. The ubiquitin-like domain of hhr23 mediates interaction with s5a subunit of 26s proteasome. J Biol Chem *274*, 28019-28025.

Hofmann K, and Bucher P (1996). The UBA domain: a sequence motif present in multiple enzyme classes of the ubiquitination pathway. Trends Biochem Sci *21*, 172-173.

Houtsmuller AB, Rademakers S, Nigg AL, Hoogstraten D, Hoeijmakers JHJ, and Vermeulen W (1999). Action of DNA repair endonuclease ERCC1/XPF in living cells. Science *284*, 958-961.

Kumar S, Talis AL, and Howley PM (1999). Identification of HHR23A as a substrate for E6-associated protein-mediated ubiquitination. J Biol Chem *274*, 18785-18792.

Kusumoto R, Masutani C, Sugasawa K, Iwai S, Araki M, Uchida A, Mizukoshi T, and Hanaoka F (2001). Diversity of the damage recognition step in the global genomic nucleotide excision repair *in vitro*. Mutat Res *485*, 219-227.

Lambertson D, Chen L, and Madura K (1999). Pleiotropic defects caused by loss of the proteasome-interacting factors Rad23 and Rpn10 of Saccharomyces cerevisiae. Genetics *153*, 69-79.

Lombaerts M, Goeloe JI, den Dulk H, Brandsma JA, and Brouwer J (2000). Identification and characterization of the *rhp23(+)* DNA repair gene in *Schizosaccharomyces pombe*. Biochem Biophys Res Commun *268*, 210-215.

Lommel L, Chen L, Madura K, and Sweder K (2000). The 26S proteasome negatively regulates the level of overall genomic nucleotide excision repair. Nucleic Acids Res *28*, 4839-4845.

Madura K, and Prakash S (1990). Transcript levels of the *Saccharomyes cerevisiae* DNA repair gene *RAD23* increase in response to UV light and in meiosis but remain constant in the mitotic cell cycle. Nucleic Acids Res *18*, 4737-4742.

Masutani C, Araki M, Sugasawa K, van der Spek PJ, Yamada A, Uchida A, Maekawa T, Bootsma D, Hoeijmakers JHJ, and Hanaoka F (1997). Identification and characterization of XPC-binding domain of hHR23B. Mol Cell Biol *17*, 6915-6923.

Masutani C, Sugasawa K, Yanagisawa J, Sonoyama T, Ui M, Enomoto T, Takio K, Tanaka K, van der Spek PJ, Bootsma D, and et al. (1994). Purification and cloning of a nucleotide excision repair

complex involving the xeroderma pigmentosum group C protein and a human homolog of yeast RAD23. Embo J *13*, 1831-1843.

Mayne LV, and Lehmann AR (1982). Failure of RNA synthesis to recover after UV irradiation: an early defect in cells from individuals with Cockayne's syndrome and xeroderma pigmentosum. Cancer Res *42*, 1473-1478.

Memisoglu A, and Samson L (2000). Base excision repair in yeast and mammals. Mutat Res *451*, 39-51.

Miao F, Bouziane M, Dammann R, Masutani C, Hanaoka F, Pfeifer GP, and O'Connor TR (2000). 3-methyladenine-DNA glycosylase (MPG protein) interacts with human RAD23 proteins. J Biol Chem *275*, 28433-28438.

Mueller JP, and Smerdon MJ (1996). RAD23 is required for transcription-coupled repair and efficient overrall repair in *Saccharomyces cerevisiae*. Mol Cell Biol *16*, 2361-2368.

Ortolan TG, Tongaonkar P, Lambertson D, Chen L, Schauber C, and Madura K (2000). The DNA repair protein RAD23 is a negative regulator of multi-ubiquitin chain assembly. Nat Cell Biol *2*, 601-608.

Russell SJ, Reed SH, Huang W, Friedberg EC, and Johnston SA (1999). The 19S regulatory complex of the proteasome functions independently of proteolysis in nucleotide excision repair. Mol Cell *3*, 687-695.

Schauber C, Chen L, Tongaonkar P, Vega I, Lambertson D, Potts W, and Madura K (1998). RAD23 links DNA repair to the ubiquitin/proteasome pathway. Nature *391*, 715-718.

Siede W, and Eckardt-Schupp F (1986). DNA repair genes of *Saccharomyces cerevisiae*: complementing rad4 and rev2 mutations by plasmids which cannot be propagated in *Escherichia coli*. Curr Genet *11*, 205-210.

Sijbers AM, de Laat WL, Ariza RR, Biggerstaff M, Wei YF, Moggs JG, Carter KC, Shell BK, Evans E, de Jong MC, *et al.* (1996). Xeroderma pigmentosum group F caused by a defect in a structure-specific DNA repair endonuclease. Cell *86*, 811-822.

Sugasawa K, Masutani C, Uchida A, Maekawa T, van der Spek PJ, Bootsma D, Hoeijmakers JHJ, and Hanaoka F (1996). hHR23B, a human RAD23 homolog, stimulates XPC protein in nucleotide excision repair *in vitro*. Mol Cell Biol *16*, 4852-4861.

Sugasawa K, Ng JMY, Masutani C, Iwai S, van der Spek PJ, Eker AP, Hanaoka F, Bootsma D, and Hoeijmakers JHJ (1998). Xeroderma pigmentosum group C protein complex is the initiator of global genome nucleotide excision repair. Mol Cell *2*, 223-232.

Sugasawa K, Ng JMY, Masutani C, Maekawa T, Uchida A, van der Spek PJ, Eker AP, Rademakers S, Visser C, Aboussekhra A, *et al.* (1997). Two human homologs of RAD23 are functionally interchangeable in complex formation and stimulation of XPC repair activity. Mol Cell Biol *17*, 6924-6931.

Sugasawa K, Okamoto T, Shimizu Y, Masutani C, Iwai S, and Hanaoka F (2001). A multistep damage recognition mechanism for global genomic nucleotide excision repair. Genes Dev *15*, 507-521.

Sutton MD, Smith BT, Godoy VG, and Walker GC (2000). The SOS response: recent insights into umuDC-dependent mutagenesis and DNA damage tolerance. Annu Rev Genet *34*, 479-497.

Suzuki T, Park H, Kwofie MA, and Lennarz WJ (2001). RAD23 provides a link between the Png1 deglycosylating enzyme and the 26S proteasome in yeast. J Biol Chem *276*, 21601-21607.

van der Horst GTJ, van Steeg H, Berg RJ, van Gool AJ, de Wit J, Weeda G, Morreau H, Beems RB, van Kreijl CF, de Gruijl FR, *et al.* (1997). Defective transcription-coupled repair in Cockayne syndrome B mice is associated with skin cancer predisposition. Cell *89*, 425-435.

van der Spek PJ, Eker A, Rademakers S, Visser C, Sugasawa K, Masutani C, Hanaoka F, Bootsma D, and Hoeijmakers JHJ (1996a). XPC and human homologs of RAD23: intracellular localization and relationship to other nucleotide excision repair complexes. Nucleic Acids Res *24*, 2551-2559.

van der Spek PJ, Visser CE, Hanaoka F, Smit B, Hagemeijer A, Bootsma D, and Hoeijmakers JHJ (1996b). Cloning, comparative mapping, and RNA expression of the mouse homologs of the *Saccharomyces cerevisiae* nucleotide excision repair gene *RAD23*. Genomics *31*, 20-27.

van Hoffen A, Venema J, Meschini R, van Zeeland AA, and Mullenders LH (1995). Transcription-coupled repair removes both cyclobutane pyrimidine dimers and 6-4 photoproducts with equal efficiency and in a sequential way from transcribed DNA in xeroderma pigmentosum group C fibroblasts. Embo J *14*, 360-367.

Venema J, van Hoffen A, Karcagi V, Natarajan AT, van Zeeland AA, and Mullenders LH (1991). Xeroderma pigmentosum complementation group C cells remove pyrimidine dimers selectively from the transcribed strand of active genes. Mol Cell Biol *11*, 4128-4134.

Venema J, van Hoffen A, Natarajan AT, van Zeeland AA, and Mullenders LH (1990). The residual repair capacity of xeroderma pigmentosum complementation group C fibroblasts is highly specific for transcriptionally active DNA. Nucleic Acids Res *18*, 443-448.

Verhage RA, Zeeman AM, Lombaerts M, van de Putte P, and Brouwer J. (1996). Analysis of gene- and strand-specific repair in the moderately UV-sensitive *Saccharomyces cerevisiae rad23* mutant. Mutat Res *362*, 155-165.

Vermeulen W, Scott RJ, Rodgers S, Muller HJ, Cole J, Arlett CF, Kleijer WJ, Bootsma D, Hoeijmakers JHJ, and Weeda G (1994). Clinical heterogeneity within xeroderma pigmentosum associated with mutations in the DNA repair and transcription gene *ERCC3*. Am J Hum Genet *54*, 191-200.

Volker M, Moné MJ, Karmakar P, Hoffen A, Schul W, Vermeulen W, Hoeijmakers JHJ, van Driel R, Zeeland AA, and Mullenders LHF (2001). Sequential assembly of the nucleotide excision repair factors *in vivo*. Mol Cell *8*, 213-224.

Watkins JF, Sung P, Prakash L, and Prakash S. (1993). The *Saccharomyces cerevisiae* DNA repair gene *RAD23* encodes a nuclear protein containing a ubiquitin-like domain required for biological function. Mol Cell Biol *13*, 7757-7765.

Wei S, and Friedberg EC (1998). A fragment of the yeast DNA repair protein Rad4 confers toxicity to *E.coli* and is required for its interaction with Rad7 protein. Mutat Res *400*, 127-133.

Wiertz EJ, Jones TR, Sun L, Bogyo M, Geuze HJ, and Ploegh HL (1996). The human cytomegalovirus US11 gene product dislocates MHC class I heavy chains from the endoplasmic reticulum to the cytosol. Cell *84*, 769-779.

Withers-Ward ES, Jowett JB, Stewart SA, Xie YM, Garfinkel A, Shibagaki Y, Chow SA, Shah N, Hanaoka F, Sawitz DG, *et al.* (1997). Human immunodeficiency virus type 1 Vpr interacts with hHR23A, a cellular protein implicated in nucleotide excision DNA repair. J Virol *71*, 9732-9742.

Withers-Ward ES, Mueller TD, Chen IS, and Feigon J (2000). Biochemical and structural analysis of the interaction between the UBA(2) domain of the DNA repair protein hHR23A and HIV-1 Vpr. Biochemistry *39*, 14103-14112.

Wood RD, Mitchell M, Sgouros J, and Lindahl T (2001). Human DNA repair genes. Science *291*, 1284-1289.

Yokoi M, Masutani C, Maekawa T, Sugasawa K, Ohkuma Y, and Hanaoka F (2000). The xeroderma pigmentosum group C protein complex XPC-HR23B plays an important role in the recruitment of transcription factor IIH to damaged DNA. J Biol Chem *275*, 9870-9875.

Zhu Q, Wani G, Wani MA, and Wani AA (2001). Human homolog of yeast RAD23 protein A interacts with p300/cyclic AMP-responsive element binding (CREB)-binding protein to down-regulate transcriptional activity of p53. Cancer Res *61*, 64-70.

Chapter

VII

Concluding remarks and perspectives

The XPC-hHR23B complex (which also includes centrin 2; Araki et al. 2001) is responsible for initiating DNA damage recognition in GG-NER (Chapter IV). The heterotrimer then recruits additional NER factors to the site of damage. *In vitro*, hHR23A and hHR23B are functionally interchangeable in their ability to form a complex with XPC and to stimulate its repair activity in the NER reactions (Chapter III). *In vivo*, the two HR23 homologs are also functionally redundant in NER as witnessed by the observation that *mHR23A*- and *mHR23B*-deficient cells both have a wildtype capacity for DNA repair (Chapters V and VI). However, in the intact organism, the functional redundancy of the homologs is incomplete: *mHR23A* knockout mice have an apparently normal phenotype, whereas in striking contrast, *mHR23B*$^{-/-}$ mice have a very severe phenotype, indicating that mHR23A can not fully substitute for the absence of mHR23B. Unexpectedly, the phenotype of *mHR23B*$^{-/-}$ mice (anticipated to eliminate the GG-NER pathway) is much more severe than the phenotype of mice completely deficient in NER (GG-NER and TC-NER). *mHR23B*$^{-/-}$ mice are born at sub-Mendelian frequency, runted and die prematurely, implying that mHR23B is essential for proper mouse development. This provides irrefutable evidence that the mHR23B protein (and based on homology, likely mHR23A) has additional functions outside of NER which are critical for life.

As might be anticipated on the basis of the *mHR23B*$^{-/-}$ phenotype, *mHR23A/B* double mutant mice are not born (Chapter VI). Characterization of *mHR23A/B*-deficient cells derived from viable mouse embryos of day 8.5 revealed an *XPC*-like NER phenotype (absence of GG-NER). Furthermore, the XPC protein itself is unstable in the *mHR23A/B*-deficient cells, indicating that the mHR23 proteins are required for the stabilization of XPC. The *mHR23A/B*-deficient cells were transfected with fluorescently-tagged XPC (*XPC-GFP*) to allow visualization of the XPC protein in living cells. Treatment of these cells with DNA damaging agents that induce lesions specifically recognized by NER further increases the stability of XPC-GFP, but only if HR23 is also expressed in the double mutant cells. Furthermore, the degradation of XPC in the absence of its binding partner HR23 may occur via ubiquitin-dependent proteolysis. In addition, XPC-GFP rapidly translocates to sites of DNA damage under conditions where only a portion of the nucleus is irradiated with UV. Finally, if the whole cell is irradiated with UV, GFP fluorescence increases over time, indicating a general stabilization of XPC as a result of DNA damage. Both these latter observations were completely HR23-dependent. There are at least two possible mechanisms by which XPC-GFP is transiently stabilized as a result

of DNA damage: (i) binding of XPC-HR23 to DNA damage might protect XPC from proteolysis, or (ii) DNA damage may trigger a secondary response that inhibits degradation of XPC, regardless of whether or not the protein is bound to DNA. Experiments involving induction of local DNA damage in the nucleus suggest that there is a general stabilization of XPC (Chapter VI). Taken together, these findings reveal a novel level of regulation in the NER pathway and clarify the link between NER and the ubiquitin system. The damage-induced, mHR23-dependent stabilization of XPC provides an explanation for long known phenomena such as enhanced reactivation that lacked an adequate mechanistic basis (Cornelis et al. 1980; Hagedorn et al. 1985). The multiple engagements of mHR23 proteins may connect stress response mechanisms including cell cycle control to known damage sensors like XPC paralleling the *E.coli* SOS system (reviewed in Sutton et al. 2000). Interestingly, RAD23 transcription is also damage inducible in yeast (Madura and Prakash, 1990), although this property appears not preserved in human keratinocytes (van der Spek et al. 1996).

One conclusion of this thesis is that DNA damage in the presence of HR23 stabilizes XPC. Continued studies in living cells stably transformed with fluorescently-tagged XPC can further elucidate the roles of HR23 and ubiquitin in NER and other processes. The GFP tagging of XPC will permit *in vivo* analysis of dynamic properties of this crucial NER factor including rapid migration of the XPC-GFP to local damage observed in this study using sophisticated photobleaching techniques (Houtsmuller et al. 1999). For instance, FRAP (fluorescence redistribution after photobleaching) experiments will allow us to determine whether XPC-GFP moves freely throughout the nucleus and then becomes fixed once the DNA is damaged. Furthermore, exploiting (real-time) confocal microscopy and the XPC-GFP, it is possible to determine the turnover rate of XPC-GFP (in concert with immunoblotting), and dynamics of XPC-dependent recruitment of other NER factors to the sites of DNA damage. Moreover, it will be very interesting (although complicating) to transfect the XPC-GFP cell line with other repair genes fused with different fluorescence tags to study the entrance of these essential NER components in the repair complex at the site of DNA injury. Such studies will enable a more precise determination of the steps and proteins involved in DNA damage recognition and processing by NER. Finally, the cell line expressing GFP-tagged XPC will also be useful for screening and detection of genotoxic agents that induce (helix-distorting) lesions recognized by GG-NER.

Further characterization of *mHR23B*$^{-/-}$ mice will permit better predictions as to the additional function(s) of mHR23B outside the context

of NER. However such an analysis is complicated for two reasons: (i) the frequency of *mHR23B*$^{-/-}$ mice born alive is 10-fold lower than expected, requiring large scale breeding protocols to obtain sufficient mutant mice, and (ii) the phenotype is too severe to discriminate between primary effects of a loss of mHR23B and secondary consequences of severe illness. Thus, to comprehensively study the function of mHR23B in specific tissues in the whole organism, a conditional *mHR23B* mutant mouse would be informative and convenient. This approach makes it possible to create a genetically modified mouse in which the gene of interest can be turned off in a time- and/or tissue-specific manner (extensively reviewed in Nagy 2000). Briefly, the insertion of a "*loxP*" recombinase recognition sequence in an intron as well as at the end of the *mHR23B* gene enables the removal of the entire sequence between the *loxP* sites by Cre recombinase. The Cre recombinase transgene can be regulated by a tissue-specific or drug-inducible promoter. This results in conditional knockout of the *mHR23B* gene, thereby preventing elimination of the *mHR23B* gene during critical stages of mouse development or in tissues in which mHR23B is essential for growth. Production of large numbers of conditional *mHR23B*$^{-/-}$ mice that survive until adulthood will also permit direct analysis of the role of mHR23B in carcinogenesis. However, it should be kept in mind that the Cre endonuclease may cause chromosomal aberrations (Loonstra et al. 2001).

Another approach that may lead to increased longevity of *mHR23B*$^{-/-}$ mice is to breed them with *p53* mutant mice. It is known that a *p53*$^{-/-}$ background partially rescues the embryonic lethality of a number of gene defects including *BRCA1*$^{-/-}$ (Welcsh et al. 2000). *BRCA1* encodes a breast cancer susceptibility gene implicated in homologous recombination and double strand break repair (Welcsh et al. 2000). The increased survival on the *p53*$^{-/-}$ background can be explained by the assumption that in *BRCA1*$^{-/-}$ (and perhaps *mHR23B*$^{-/-}$) mice DNA damage persists, which in a p53-proficient background triggers apoptosis. The removal of the p53-dependent apoptotic pathway thereby reduces cell death. Generation of cell lines from *p53*$^{-/-}$/*mHR23B*$^{-/-}$ mice will also permit detailed analysis of the link between GG-NER and apoptosis. Ultimately, if the survival of *mHR23B*$^{-/-}$ mice can be improved, tissues can be isolated for gene expression profiling studies using DNA micro-array technology (reviewed in Lockhart and Winzeler 2000). This technique is being applied to a number of transgenic mouse models, in order to discover the consequence of a highly defined genetic disruption of a particular cellular pathway (such as GG-NER). It is expected that such studies will reveal gene expression patterns that might be predictive of human disease or the specific response to therapeutic intervention. Last

but not least, it will be challenging to find a link between *HR23* gene dysfunction and human disease (e.g. fertility syndromes and developmental disorders).

References

Araki M, Masutani C, Takemura M, Uchida A, Sugasawa K, Kondoh J, Ohkuma Y, and Hanaoka F (2001). Centrosome protein centrin2/caltractin1 is part of the xeroderma pigmentosum group C complex that initiates global genome nucleotide excision repair. J Biol Chem *18665-18672*, 27.

Cornelis JJ, Lupker JH, and van der Eb AJ (1980). UV-reactivation, virus production and mutagenesis of SV40 in UV-irradiated monkey kidney cells. Mutat Res *71*, 139-146.

Nagy A (2000). Cre recombinase: the universal reagent for genome tailoring. Genesis *26*, 99-109.

Hagedorn R, Thielmann HW, and Fischer H (1985). SOS-type functions in mammalian cells. Enhanced reactivation of UV-irradiated SV40 in UV-irradiated CV-1 cells. J Cancer Res Clin Oncol *109*, 89-92.

Houtsmuller AB, Rademakers S, Nigg AL, Hoogstraten D, Hoeijmakers JHJ, and Vermeulen W (1999). Action of DNA repair endonuclease ERCC1/XPF in living cells. Science *284*, 958-961.

Lockhart DJ and Winzeler EA (2000). Genomics, gene expression and DNA arrays. Nature *405*, 827-836.

Loonstra A, Vooijs M, Beverloo HB, Allak AA, van Drunen E, Kanaar R, Berns A, and Jonkers J (2001). Growth inhibition and DNA damage induced by Cre recombinase in mammalian cells. Proc Natl Acad Sci USA *98*, 9209-9214.

Madura K and Prakash S (1990). Transcript levels of the *Saccharomyes cerevisiae* DNA repair gene *RAD23* increase in response to UV light and in meiosis but remain constant in the mitotic cell cycle. Nucleic Acids Res *18*, 4737-4742.

Nagy A (2000). Cre recombinase: the universal reagent for genome tailoring. Genesis *26*, 99-109.

Sutton MD, Smith BT, Godoy VG, and Walker GC (2000). The SOS response: recent insights into umuDC-dependent mutagenesis and DNA damage tolerance. Annu Rev Genet *34*, 479-497.

van der Spek PJ, Visser CE, Hanaoka F, Smit B, Hagemeijer A, Bootsma D, and Hoeijmakers JHJ (1996). Cloning, comparative mapping, and RNA expression of the mouse homologs of the *Saccharomyces cerevisiae* nucleotide excision repair gene *RAD23*. Genomics *31*, 20-27.

Welcsh PL, Owens KN, and King MC (2000). Insights into the functions of BRCA1 and BRCA2. Trends Genet *16*, 69-74.

Summary

Summary

DNA carries the genetic information that ultimately encodes all of the proteins required for proper cellular function. Yet, the integrity of the code is continuously challenged by exposure to substances that are able to chemically modify the DNA. Environmental factors that negatively impact DNA include the UV component of sunlight, ionizing radiation, and chemical compounds present in for example cigarette smoke and industrial pollution. In addition, endogenous products of cellular metabolism such as oxygen radicals can modify DNA. DNA damage can, in turn, perturb vital cellular processes such as transcription, replication, and cell cycle progression. Persistent damage can induce mutations and ultimately lead to cancer (uncontrolled cell growth) and likely contributes to aging, or to (controlled) cell death. In order to maintain the integrity of genetic material, cells have evolved an intricate network of DNA repair mechanisms.

Chapter I provides an overview of the different repair mechanisms that are currently known to function in higher organisms including man. Although overlap in substrate specificity exists, each repair pathway is responsible for the recognition and elimination of a particular class of DNA lesions.

In **Chapter II**, the mechanism of nucleotide excision repair (NER) and the genes encoding the different repair proteins are discussed in more detail. NER is one of the primary DNA repair pathways and is highly conserved from yeast to man. It is responsible for the removal of a wide spectrum of DNA lesions that have in common their ability to distort the DNA helical structure. These lesions include UV-induced photoproducts and bulky chemical DNA adducts. The NER pathway requires the coordinated activity of approximately 30 proteins. The mechanism involves a multistep "cut and patch"-like reaction in which a short segment of the damaged DNA strand is excised and replaced by a copy synthesized from the intact complementary strand.

Furthermore, **Chapter II** describes the clinical consequences of a defect in NER in humans. This is highlighted by three human syndromes: xeroderma pigmentosum (XP, caused by a mutation in one of seven genes: *XPA* to *XPG*), Cockayne syndrome (CS, caused by a mutation in one of two genes: *CSA* or *CSB*; and sometimes occurring in combination with XP) and trichothiodystrophy (TTD, caused by a mutation in one of three genes:

TTDA, *XPB* or *XPD*). Extreme sensitivity to sunlight is the hallmark of all three human disorders. However, the remainder of the clinical picture is very heterogeneous. Only XP patients exhibit the expected predisposition to skin cancer. In contrast, CS and TTD patients suffer severe developmental and neurological abnormalities that are difficult to explain as a consequence of a NER defect. The fairly recent observation that several of the NER proteins are also involved in transcription (XPB, XPD, CSA and CSB) provides an alternative cause of the severe CS and TTD phenotype (i.e. a transcriptional defect instead of a NER defect). This also demonstrated that NER, as well as other repair mechanisms, is closely intertwined with other essential cellular processes. To study the human NER deficiency syndromes, repair-deficient mouse models that may mimic several aspects of the phenotype of XP, CS, and TTD patients were generated.

Two distinct NER subpathways can be distinguished: i.e. global genome repair (GG-NER) operating over the entire genome and transcription-coupled repair (TC-NER) which repairs only the transcribed strand of active genes. Most XP patients have defects in both GG-NER and TC-NER. However, in patients of complementation group C (XP-C) only GG-NER is affected. The XPC protein was found to be in a tight complex with the hHR23B protein. hHR23B is one of two human homologs of the *Saccharomyces cerevisiae* ubiquitin-like DNA repair protein RAD23. Both homologs contain two ubiquitin-associated domains, which is a unique feature amongst the NER proteins. Thus far, no human NER-deficiency syndrome was linked to a mutation in the *hHR23B* gene. This could be because the hHR23A protein is functionally interchangeable with hHR23B. This thesis describes the biological characterization of the XPC-hHR23B complex and the generation of knockout mice for both of the mammalian RAD23 homologs.

Chapter III describes experiments that address the hypothesis that the two hHR23 homologs are functionally redundant. The NER reaction was reconstituted *in vitro* using purified recombinant proteins and this was used to demonstrate that hHR23A and hHR23B are functionally interchangeable in their ability to complex with XPC and to stimulate the DNA repair. This demonstrated for the first time that the hHR23 proteins are directly involved in NER and that their repair function is mediated by interaction with XPC. Within the NER reaction, six (sometimes multimeric) core factors, XPA, XPC-hHR23B, TFIIH, ERCC1-XPF, XPG, and RPA are required for recognition and removal of DNA damage by NER *in vitro*.

Chapter IV describes experiments that explore the role of the XPC-hHR23B complex in NER. Using a DNA damage recognition-competition

assay, the complex was identified as the primary DNA-damage sensor and repair protein-recruitment factor of the GG-NER subpathway. DNAse I footprinting demonstrated that the XPC-hHR23B complex by itself can bind to damaged DNA.

The biological function of the mammalian RAD23 homologs in cells and whole organisms is investigated extensively in experiments described in **Chapters V and VI**. Consistent with *in vitro* results, which showed the RAD23 homologs to be redundant, both *mHR23A* and *mHR23B* single knockout cells have a normal capacity for NER. The picture in the intact organism, however, is different. Both *mHR23A*- and *mHR23B*-deficient mice were generated by standard gene targeting methodologies. The *mHR23A*$^{-/-}$ mouse is phenotypically normal. In striking contrast, *mHR23B*$^{-/-}$ mice have a very severe phenotype. Features include intrauterine death, growth retardation, male sterility, and facial dysmorphology, and are indicative of an essential role for mHR23B in mouse development. We attribute the enormous disparity between the phenotype of *mHR23B*$^{-/-}$ and *mHR23A*$^{-/-}$ mice to the inability of mHR23A to completely compensate for the absence of mHR23B. As might be expected, *mHR23A/B* double knockout mice are not viable. A severe *mHR23B*-like phenotype, including embryonic lethality as observed in the absence of both *HR23* genes, has not been described for any other mouse model carrying specific GG-NER and/or TC-NER defects (i.e. *XPA*, *XPC*, *CSA*, and *CSB* mice) and implies that the mammalian RAD23 proteins have additional functions outside NER. Based on the fact that both proteins contain ubiquitin-associated domains it is likely that the additional functions are related to the ubiquitin/proteasome protein degradation pathway.

Importantly, *mHR23A/B* double knockout cells from day 8.5 embryos are viable, which allowed us to generate a *mHR23A/B*-deficient cell line. Characterization of the cells revealed a NER deficit similar to *XPC*$^{-/-}$ cells. This phenotype was directly linked to the observation that XPC is unstable in the absence of both mHR23 proteins. Stable cotransfections of the mutant cells with cDNAs encoding either a fluorescently-tagged XPC (XPC-GFP) and/or hHR23B rescued the UV-sensitivity and stabilized the fluorescent signal from the XPC in nuclei. The fluorescent XPC was further stabilized by the addition of DNA damaging agents that cause lesions specifically recognized by the NER pathway. Damage-induced stabilization of XPC-GFP was HR23-dependent. Furthermore, in line with the proposed role of the hHR23 proteins in ubiquitin pathways, destabilization of XPC was found to be mediated by ubiquitin-dependent proteolysis. Induction of local UV damage in only one portion of the nucleus of XPC-GFP expressing

cells revealed that the fluorescently-tagged protein translocates very rapidly to sites containing DNA damage. This translocation was also HR23-dependent. In addition, the presence of DNA damage in concert with expression of HR23 causes a gradual increase in the amount of fluorescence in the entire nucleus of UV-irradiated cells compared to non-damaged nuclei, indicating further stabilization of XPC-GFP. At least two mechanisms might explain the transient stabilization of XPC-GFP in the face of DNA damage: (i) the binding of XPC to DNA damage might protect it from proteolysis, or (ii) DNA damage may trigger a specific response, that inhibits degradation of XPC, independent of DNA binding. The results of local DNA damage experiments argue in favor of the latter mechanism of HR23-dependent XPC stabilization. In conclusion, the main findings of this thesis elucidate the primary function of HR23 in NER, and reveal that HR23-dependent XPC stabilization, and likely the entire global genome repair pathway is tightly damage-regulated. In addition, both HR23 proteins are essential for proper embryonic development, pointing to a broader function that (analogous to their role in NER) is expected to involve the ubiquitin/proteasome pathway.

Samenvatting

DNA is de drager van genetische informatie en codeert voor alle eiwitten die noodzakelijk zijn voor het functioneren van de cel en uiteindelijk het hele organisme. Het DNA staat voortdurend bloot aan stoffen, die de chemische structuren kunnen veranderen en zelfs ernstig beschadigen. Omgevingsfactoren die een dergelijk schadelijk effect op het DNA uitoefenen, zijn onder andere: de UV stralen van het zonlicht, ioniserende straling en chemische stoffen die aanwezig zijn in bijvoorbeeld sigarettenrook en industriële vervuiling. Daarnaast kunnen endogene producten die ontstaan tijdens het metabolisme van de cel (zoals zuurstofradicalen) het DNA beschadigen. DNA schade kan op zijn beurt vitale cellulaire processen zoals transcriptie (overschrijven van genen), replicatie (het verdubbelen van het DNA voor iedere celdeling) en voortgang van de celcyclus verstoren. Blijvende DNA schade kan vervolgens leiden tot kanker (mutaties en ongecontroleerde celgroei) en draagt zeer waarschijnlijk ook bij aan veroudering en aan celdood. Om de integriteit van het genetisch materiaal te bewaren, is in de loop van de evolutie een complex netwerk van DNA herstelmechanismen ontstaan.

Hoofdstuk I geeft een overzicht van de verschillende DNA herstelmechanismen die momenteel bekend zijn in hogere organismen, waaronder de mens. Elk herstelmechanisme is verantwoordelijk voor de herkenning en verwijdering van een specifieke categorie van DNA schades, waarbij echter ook enige overlap tussen de verschillende mechanismen bestaat.

In **Hoofdstuk II** worden Nucleotide Excisie Reparatie (NER) en de eiwitten die bij dit proces betrokken zijn, besproken. NER is één van de belangrijkste DNA herstelsystemen en is in de evolutie sterk geconserveerd van gist tot mens. NER is verantwoordelijk voor het verwijderen van een breed spectrum aan schades die over het algemeen de DNA helix sterk verstoren, zoals UV-geïnduceerde fotoproducten. De gezamenlijke activiteit van ± 30 eiwitten is noodzakelijk voor het juist functioneren van NER. Dit mechanisme is te vergelijken met een 'knip en plak' reactie waarbij een aantal stappen is te onderscheiden, waaronder herkenning van de schade, excisie (uitsnijden) van het beschadigde DNA fragment en vervanging van dit fragment door een nieuwe kopie vervaardigd aan de hand van de intacte complementaire streng.

Vervolgens beschrijft **Hoofdstuk II** de klinische gevolgen van een NER defect in patiënten. Deze zijn af te leiden aan de hand van drie ernstige, gelukkig zeldzame syndromen: xeroderma pigmentosum (XP, veroorzaakt door een mutatie in één van de zeven genen *XPA* t/m *XPG*), Cockayne syndroom (CS, veroorzaakt door een mutatie in de genen *CSA* of *CSB*, en soms ook voorkomend in combinatie met XP) en trichothiodystrophy (TTD, veroorzaakt door een mutatie in de genen *TTDA*, *XPB* of *XPD*). Extreme gevoeligheid voor zonlicht is een belangrijk gemeenschappelijk kenmerk van deze drie ziektebeelden. De overige klinische kenmerken zijn erg heterogeen. Alhoewel CS en TTD patiënten ook extreme gevoeligheid voor zonlicht vertonen, hebben alleen XP patiënten een sterk verhoogde kans (>2000x) op huidkanker. CS en TTD patiënten daarentegen lijden aan ernstige ontwikkelingsstoornissen en neurologische afwijkingen, kenmerken die moeilijk te verklaren zijn als gevolg van een defect DNA herstel. De recente bevinding dat verschillende NER eiwitten ook betrokken zijn bij transcriptie (*XPB*, *XPD*, *CSA* en *CSB*) geeft een alternatieve verklaring voor een aantal van de ernstige ziekteverschijnselen van CS en TTD. Tevens geeft dit aan dat NER nauw verbonden is met andere essentiële cellulaire processen. Om de humane syndromen, die voortkomen uit een NER defect te bestuderen, zijn muismutanten gegenereerd die deficiënt zijn in DNA herstel, en die de situatie in XP, CS en TTD patiënten ten dele zouden kunnen nabootsen.

Er kunnen twee duidelijk verschillende routes onderscheiden worden in NER: het zgn. globaal genoom herstel (GG-NER) dat DNA repareert in het gehele genoom, en transcriptie-gekoppeld herstel (TC-NER) dat zich richt op de afgeschreven streng van actieve genen zodat die snel hersteld worden. De meeste XP patiënten hebben een defect in zowel GG-NER als TC-NER, maar er is een groep patiënten waarbij alleen GG-NER is aangedaan. Dit zijn de XP patiënten van de complementatie groep C (XP-C). Het XPC eiwit bevindt zich in een complex met het eiwit hHR23B. hHR23B is één van de twee humane homologen van het ubiquitine-geassocieerde DNA herstel eiwit RAD23, afkomstig uit de bakkersgist *Saccharomyces cerevisiae*. Beide homologen bevatten twee ubiquitine-geassocieerde domeinen, hetgeen een uniek kenmerk is binnen de groep van NER eiwitten. Tot op heden zijn geen patiënten beschreven met een NER syndroom veroorzaakt door een mutatie in het *hHR23B* gen. Een verklaring hiervoor zou kunnen zijn dat de DNA herstel functies van hHR23B overgenomen worden door de andere homoloog hHR23A. Dit proefschrift beschrijft de biologische karakterisering van het XPC-hHR23B complex en

de generatie en de karakterisatie van mutant muizen waarbij één (of beide) RAD23 homologen is uitgeschakeld.

Hoofdstuk III beschrijft experimenten waarmee de hypothese wordt getest dat de beide hHR23 homologen functioneel uitwisselbaar zijn. De NER reactie is *in vitro* nagebootst met gezuiverde recombinante eiwitten. Deze experimenten wezen uit dat hHR23A en hHR23B daadwerkelijk elkaars functie kunnen overnemen wat betreft complexvorming met XPC en stimulatie van DNA herstel. Voor de eerste keer wordt hier aangetoond dat de hHR23 eiwitten direct betrokken zijn bij NER en dat deze betrokkenheid tot stand komt door interactie met XPC. Voor het herkennen en verwijderen van DNA schade door NER *in vitro* zijn 6 factoren van belang: XPA, XPC-hHR23B, TFIIH, ERCC1-XPF, XPG en RPA.

In **Hoofdstuk IV** worden experimenten beschreven waarin de rol van het XPC-hHR23B complex in NER wordt bestudeerd. Met behulp van een DNA schade herkenning-competitie test wordt aangetoond dat het complex de primaire sensor is voor het herkennen van DNA schades. Ook is het complex in staat om andere DNA herstel eiwitten aan te trekken die noodzakelijk zijn voor de uitvoering van GG-NER. DNAse footprinting experimenten tonen aan dat het XPC-hHR23B complex zelf aan DNA schade kan binden.

De biologische functie van de RAD23 homologen in zowel cellen als het gehele organisme is uitgebreid onderzocht en wordt beschreven in de **Hoofdstukken V en VI**. *In vitro* gegevens tonen aan dat de RAD23 homologen elkaars functie kunnen overnemen. In overeenstemming met deze bevinding hebben zowel de *mHR23A* als *mHR23B* knock-out cellen een normale DNA herstel capaciteit. In het intacte organisme is de situatie echter anders. Zowel *mHR23A* als *mHR23B* knock-out muizen zijn gegenereerd door middel van standaard methodes om genen gericht uit te schakelen. De *mHR23A* knock-out muis blijkt een normaal fenotype te hebben. De *mHR23B* knock-out muizen daarentegen vertonen zeer ernstige afwijkingen. Kenmerken van deze muis zijn onder andere intra-uteriene dood, groeiachterstand, onvruchtbaarheid bij de mannetjes en misvorming van het gelaat. Dit ernstige fenotype impliceert een belangrijke rol voor mHR23B in de ontwikkeling van de muis. Het grote verschil tussen het fenotype van *mHR23A* en *mHR23B* muizen kan worden veroorzaakt doordat mHR23A niet in staat is het gebrek aan mHR23B compleet te compenseren. Zoals verwacht op basis van het *mHR23B* knock-out fenotype zijn *mHR23A/mHR23B* dubbel knock-out muizen niet levensvatbaar. Het gegeven dat een knock-out van de *mHR23* genen een veel ernstiger en duidelijk verschillend fenotype vertoont vergeleken met een muis die

deficiënt is in het gehele NER (zowel GG-NER als TC-NER), wijst op andere functies van de RAD23 eiwitten naast een rol in NER. Gezien het feit dat beide eiwitten ubiquitine-geassocieerde domeinen bezitten, is het niet onwaarschijnlijk dat deze andere functies te maken hebben met afbraak van eiwitten via de ubiquitine-proteasoom route.

Het feit dat *mHR23A/mHR23B* dubbel knock-out embyro's van 8.5 dagen nog levensvatbaar bleken te zijn, stelde ons in staat een *mHR23A/mHR23B* deficiënte cellijn te isoleren. Karakterisering van deze cellijn liet een NER defect zien dat sterk vergelijkbaar is met $XPC^{-/-}$ cellen. Een verklaring hiervoor wordt gegeven door de bevinding dat in afwezigheid van beide mHR23 eiwitten XPC instabiel is. Stabiele cotransfectie van deze mutante cellen met hHR23B cDNA en/of fluorescerend XPC (XPC-GFP) leidde tot herstel van de UV gevoeligheid van deze cellen en tot stabilisatie van het fluorescente XPC in de kern. Het fluorescente XPC werd nog sterker gestabiliseerd door blootstelling van de cellen aan stoffen die resulteren in NER specifieke DNA schades. De stabilisatie van XPC-GFP, geïnduceerd door DNA schade, was HR23-afhankelijk. In overeenstemming met de mogelijke rol van hHR23 in ubiquitinering, werd aangetoond dat destabilisatie van XPC veroorzaakt wordt door ubiquitine-afhankelijke eiwitafbraak. Experimenten waarbij lokale DNA schade in slechts een deel van de kern van XPC-GFP cellen wordt geïnduceerd, tonen aan dat het XPC eiwit zich zeer snel verplaatst naar de plek waar DNA schade zich bevindt. Ook deze verplaatsing was afhankelijk van aanwezigheid van HR23. De aanwezigheid van zowel DNA schade als HR23 resulteerde tevens in een toename van fluorescentie in de gehele kern door verdere algehele stabilisatie van XPC-GFP. Concluderend: de bevindingen beschreven in dit proefschrift geven inzicht in de primaire functie van HR23 in NER en laten bovendien zien dat HR23-afhankelijke XPC stabilisatie en dus waarschijnlijk ook het totale GG-NER strikt gereguleerd wordt door DNA schade. Daarnaast zijn de HR23 eiwitten onmisbaar voor embryonale ontwikkeling. Dit duidt op een een bredere functie van deze eiwitten, waarbij (net als voor de NER functie) het ubiquitine/proteasoom systeem betrokken is.

摘要

去氧核糖核酸(DNA = deoxyribonucleic acid)所帶有的遺傳密碼記載著在日常生活中細胞所需要的蛋白. 這密碼的完整、不斷地受到可以把 DNA 結構改變的物質的挑戰, 對 DNA 的完整有負面影響的環境因素包括有太陽光中的紫外光, 輻射, 以及其他化合物如香煙以至工業產生的廢煙. 此外, 細胞因新陳代謝而所產生的氧分子副產品, 也可以使 DNA 改變. 因此, 較高等的生物, 在進化過程發展出可以保持遺傳密碼完整的結構.

本論文的第一章將會簡單地介紹在高等生物中(包括人類)有關 DNA 修正的途徑.

第二章便會更深入地討論切除修正(NER = Nucleotide Excision Repair)的結構. 對於 NER 結構內所需要的蛋白(包括記載著這些蛋白的基因)如 XPC-hHR23B 組合內的 hHR23 蛋白(*h*HR23 代表人類的). 繼會作更深入的討論人類 NER 結構有缺陷的病例, 因而帶出發展一個動物模形的重要性.

第三章介紹有關人類的其中兩個 hHR23(A 和 B)蛋白以及有關實驗佈告.

第四章則探討 XPC-HR23B 組合在 NER 中的角式.

總括來說, 本論文布告 HR23 在 NER 中重要的研究、而帶出 HR23 在控制整個 DNA 完整的可能性. HR23 的重要性是很廣闊的, HR23 在 NER 的研究中只是一個很小微的部份. 在第五章和第六章內會有更長細的討論.

List of publications

Chiurazzi P, de Graaff E, Ng J, Verkerk AJ, Wolfson S, Fisch GS, Kozak L, Neri G, and Oostra BA (1994) No apparent involvement of the *FMR1* gene in five patients with phenotypic manifestations of the fragile X syndrome. *Am J Med Genet 4: 309-314.*

Sugasawa K, Ng JMY, Masutani C, Maekawa T, Uchida A, van der Spek PJ, Eker AP, Rademakers S, Visser C, Aboussekhra A, Wood RD, Hanaoka F, Bootsma D, and Hoeijmakers JHJ (1997) Two human homologs of Rad23 are functionally interchangeable in complex formation and stimulation of XPC repair activity. *Mol Cell Biol 12: 6924-6931.*

Sugasawa K, Ng JMY, Masutani C, Iwai S, van der Spek PJ, Eker AP, Hanaoka F, Bootsma D, and Hoeijmakers JHJ (1998) Xeroderma pigmentosum group C protein complex is the initiator of global genome nucleotide excision repair. *Mol Cell 2: 223-232.*

Neuteboom LW, Ng JMY, Kuyper M, Clijdesdale OR, Hooykaas PJ, and van der Zaal BJ (1999) Isolation and characterization of cDNA clones corresponding with mRNAs that accumulate during auxin-induced lateral root formation. *Plant Mol Biol 2: 273-287.*

Ng JMY, Vrieling H, Sugasawa K, Ooms MP, Grootegoed JA, Vreeburg JTM, Visser P, Beems RB, Gorgels TGMF, Hanaoka F, Hoeijmakers JHJ, and van der Horst GTJ. Developmental defects and male sterility in mice lacking the ubiquitin-like DNA repair gene *mHR23B. Submitted.*

Ng JMY, van der Horst GTJ, Vermeulen W, Sugasawa K, Vrieling H, and Hoeijmakers JHJ. Stabilization of XPC by DNA damage and the ubiquitin domain protein RAD23 reveals a novel mechanism of regulation of DNA repair. *To be submitted.*

Curriculum vitae

The author of this thesis was born on the 2nd of December 1970 in Hong Kong. In 1989, she graduated from high school (HAVO and VWO Gymnasium) at the International College Edith Stein in The Hague. In 1993, she finished the Medical Biotechnology study in Delft. In 1996, she successfully completed the Medical Biology study including the major subject Developmental Genetics at the University of Leiden. From October 1996 till April 2001, she performed the PhD research presented in this thesis, at the Department of Cell Biology & Genetics, Erasmus University Rotterdam, under the supervision of Prof. Dr. Jan Hoeijmakers.

Acknowledgements

Dit proefschrift is het resultaat van viereneenhalf jaar werk van velen, daarom valt het ook niet mee om iedereen specifiek te bedanken, toch wil ik graag een aantal mensen noemen die zeer nauw betrokken zijn bij het onderzoek.

Ten eerste wil ik graag mijn promotoren Prof. Dr. D. Bootsma en Prof. Dr. J.H.J. Hoeijmakers ontzettend bedanken voor hun steun die ze mij de afgelopen jaren hebben gegeven. Het werken onder jullie leiding heb ik als een voorrecht ervaren. Jan, jij bent echt één uit een miljoen! Jouw kennis, inspiratie en gedrevenheid is onmeetbaar groot en is niet in woorden uit te drukken. Ondanks jouw overvolle agenda maak je toch altijd tijd voor me vrij. Met name tijdens het schrijven van mijn boekje. Zowel als promotor en als de "key component" van de DNA repair groep is jouw geestelijke en lichamelijke kracht onuitputtelijk!

To Kaoru, Bert and Wim: I would like to thank you all for the nice and open collaboration. I really learned a lot from you! Kaoru, it was pleasant to work with you. Bert, heel erg bedankt voor jouw enthousiasme én andere dingen. En Wim, zonder jouw bezieling was er geen XPC-GFP en ik heb echt genoten van onze samenwerking (vooral achter de fluorescentie microscoop).

Alle leden van de Kleine en Grote Commissie, wil ik heel erg bedanken voor het lezen van mijn proefschrift, en met name: Anton (ondanks je drukke agenda mag ik je toch altijd storen en jouw "enorme enthousiasme" waardeer ik buitengewoon), en Harry en Harry (gezellig dat jullie in de commissie willen zitten).

Alle mensen van de 5de, 7de en de 10de verdieping wil ik ontzettend bedanken voor hun gezelligheid en hulp, met name: Jan V. (hoi Jan), Marja O. (he Marja), Bas (hey Bassie), Marike (één van mijn favoriete secretaresses), Jasperina (Eden mmmh...), Rita (lieve Rita, word gauw beter, we missen je heel erg!), de lieve mensen van de keuken (Jopie & co.) en van het EDC (Patrick & co.), Annie en Es (bibas, amaretto en wit bier), Jan (kweekkoning JdW), An (brownies), Tom en Ruud (goeie fotografen), Ton Verkerk en Sjozef (Shit, ik zit weer vast, rot PC! Maw, jullie zijn ONmisbaar!), Pim Visser (hoort eigenlijk ook bij Celbio&Gen), Sjaak (docTOR Sjakie Philipsen), Deborah en Vincent (gezellige AIOotjes), Nils en Arjan (stoere jongens), Jeroen en Betty (mijn voormalige en gezellige

labgenootjes in 738), Francis (多謝你的 "excellent" 中文翻譯), Roald (congresmaatje), Theo (dag lieve Theo), Harm (pestpaaltje), Sander (blijft een ukkie), Yvonne (jammer dat je weg bent), Xavier (NICE that you stay for my thesis), Dave (the (non)essence of Aikido), and last but not least Filippo (tequila shots!).

Wetenschap maakt het nog extra leuker en interessanter met het Leidsche triootje: Bert, Leon en Harry. Het is altijd feest met jullie in de buurt! En ik blijf het zeggen: .....bijna had ik beroemd kunnen worden in Savannah met Robert Redford, maar.....

Dit boekje was echter niet tot stand gekomen zonder de essentiële bijdragen, de morale steun en de gezelligheid van mijn dierbare collega's: Laura (Many Thanks for reading of the thesis), Inês (Obrigada por toda a tua ajuda e apoio com a minha tese), Karin (lunch, massages, en nog véél meer...), Hennie (Bedankt voor jouw opbeurende woorden. SF met jou was bijzonder gezellig en onvergetelijk!), en natuurlijk mijn twee lieve en vrolijke steunpilaren, Judith (Beertje) en Ingrid (Pluijmpje): bedankt voor jullie vriendschap! Jullie waren meer dan alleen collega's. Ik had geen betere kunnen wensen dan jullie. Daarom maakt het de wetenschap ondanks zijn ups en downs ook een stuk boeiender!

Naast het werk is er natuurlijk het thuisfront van families en vrienden die al die jaren achter me hebben gestaan, ook al snappen ze vaak niet waar ik mij de afgelopen jaren mee bezig hield (Hé, het is weekend, moet je weer werken, je kan je kindertjes (lees als "muisjes") zeker niet in de steek laten?). Wim & Manja: "Erg jammer dat jullie niet op mijn feestje kunnen komen". En Michael (san): "Eindelijk kunnen we aan onze tequila-marathon beginnen"!

除了在工作上,當然亦得到親戚和朋友的支持及鼓勵,雖然他們(有些)仍然不明白我在研究些什麼,(週末了,還要返工? 捨不得你的老鼠仔嗎?)
在此說聲:多謝你們對我的支持!
爸爸媽媽:這本書終於完成了,真正的挑戰開始了!

And last but the most important person in my life: "Tony, THANKS for being there and for happiness every single day"!

Color Appendix

Figure 7. *mHR23B*$^{-/-}$ males show impaired spermatogenesis and dysfunction of Sertoli cells.

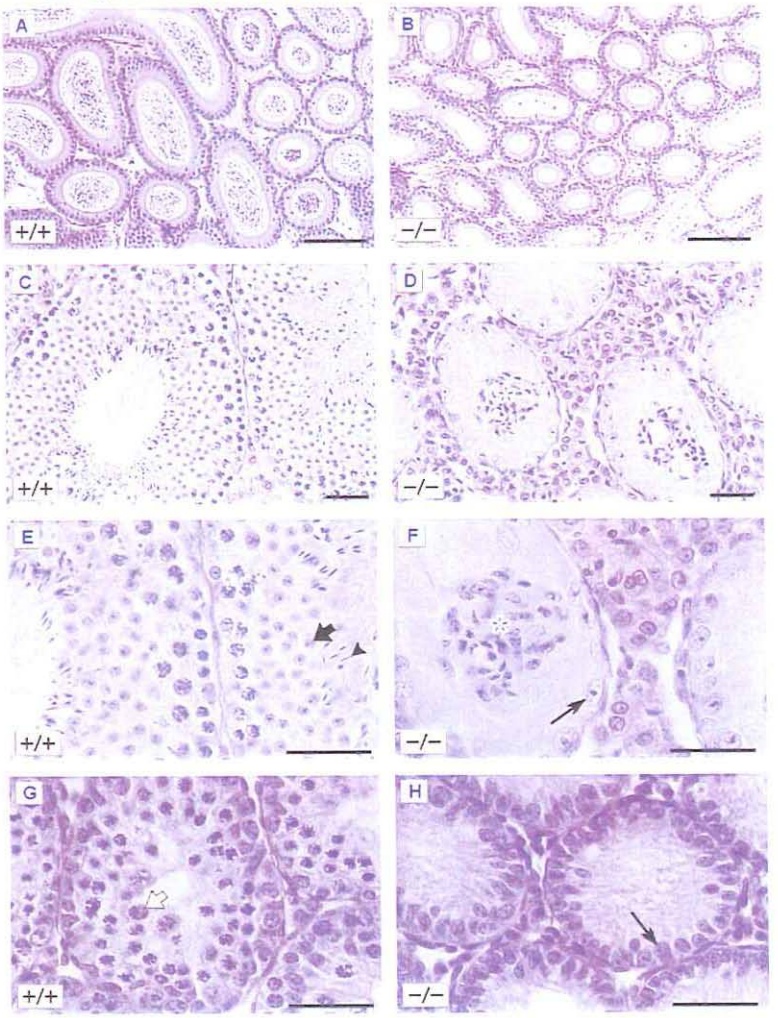

Figure 3. Developmental impairment in *mHR23B*$^{-/-}$ embryos at E15.5.

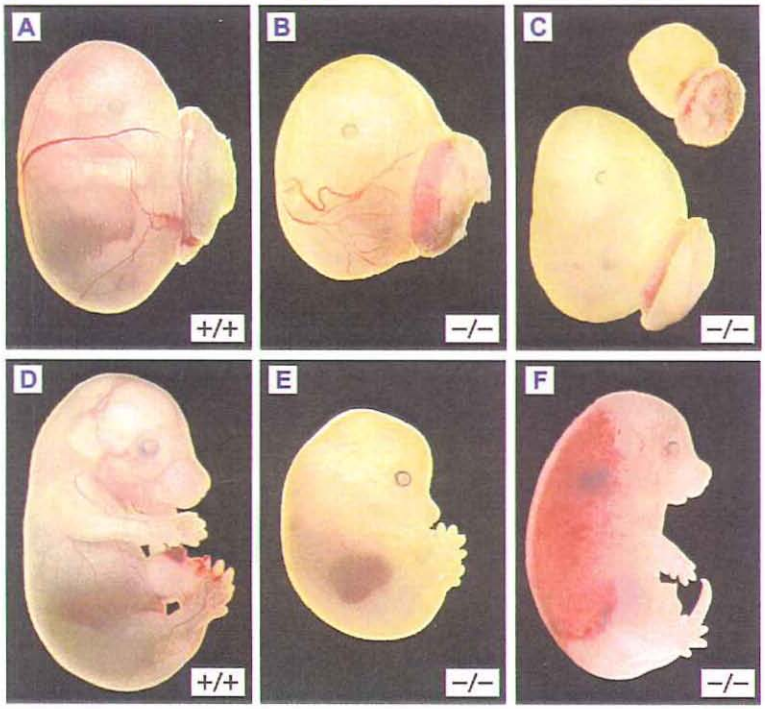

Figure 4. Placental defect in *mHR23B*$^{-/-}$ embryos at E18.5.

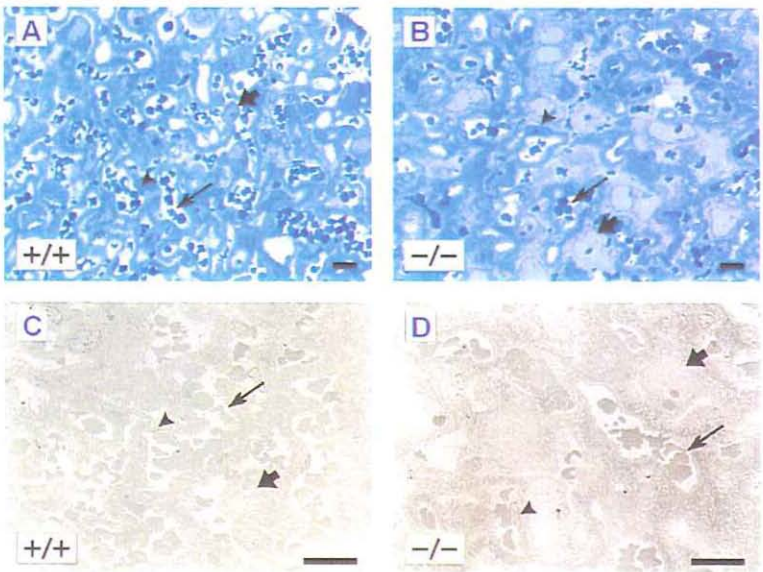

Chapter V

Chapter VI

Figure 5C-F. Effect UV on hXPC-GFP levels (p.152).

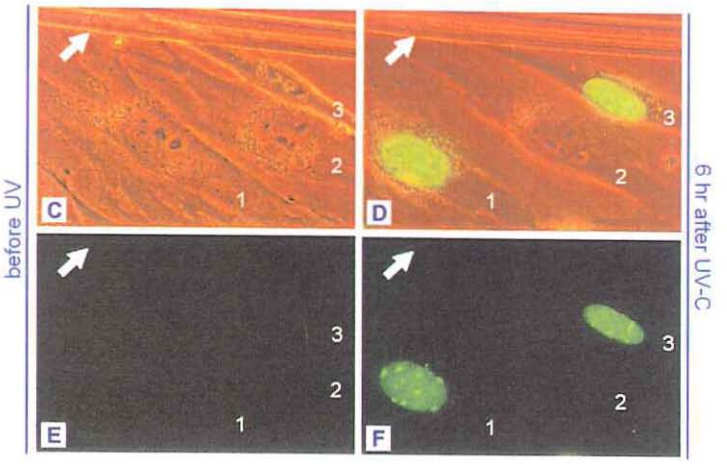

Figure 6. Effect NA-AAF **(A-D)** and proteasome inhibitor **(E-H)** on hXPC-GFP levels (p.154).

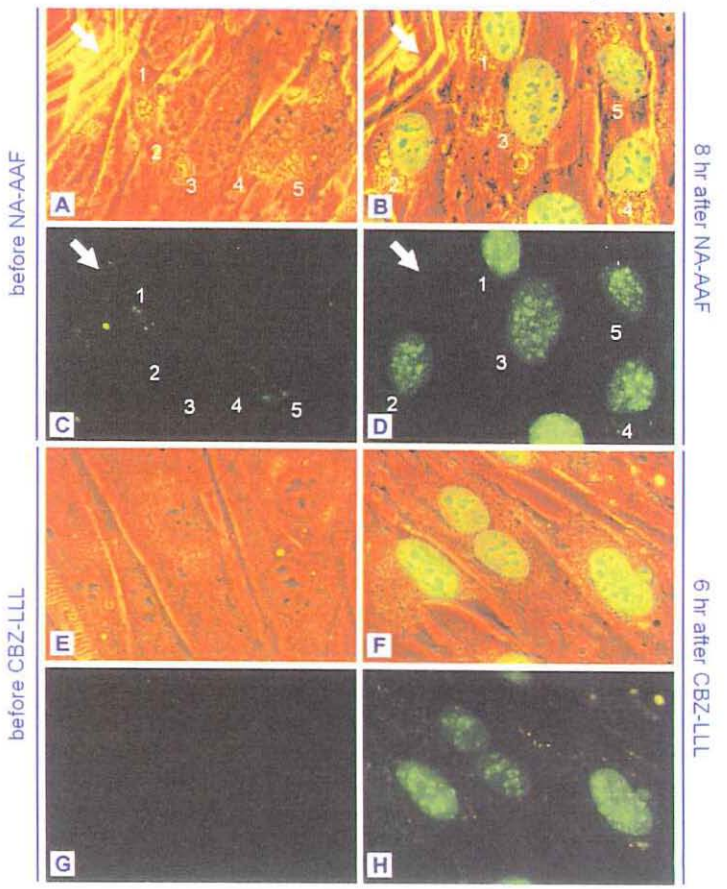

Figure 3A-F. Reduced XPC expression in *DKO* E8.5 MEFs (p. 148).

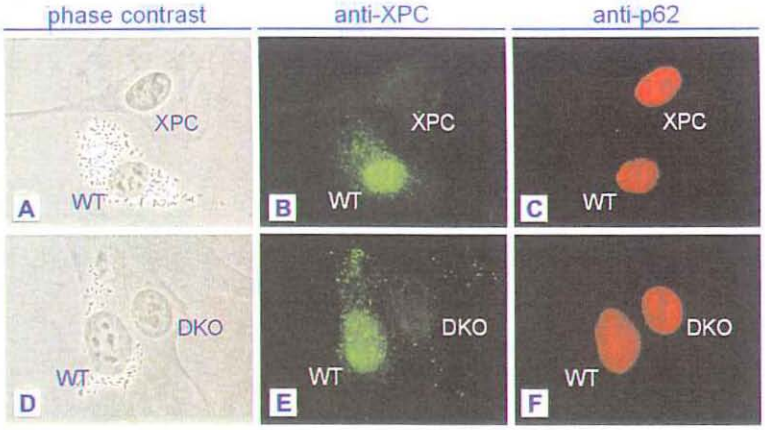

Figure 4D-E. Correction of *DKO* cells by *hHR23B* cDNA (p. 150).

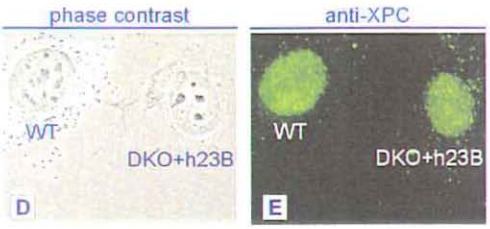

Figure 4F-I. hXPC-GFP is stabilized by hHR23B (p. 150).

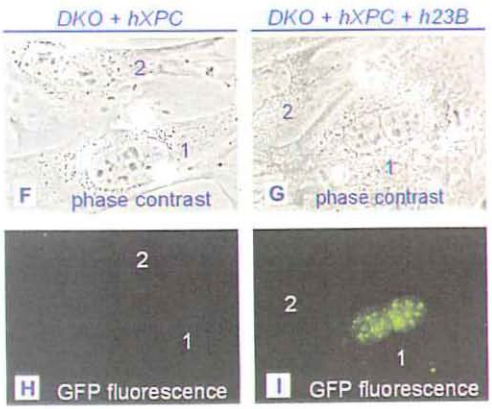

Figure 7A-B. Local UV damage induces overall XPC stablization (p. 156).

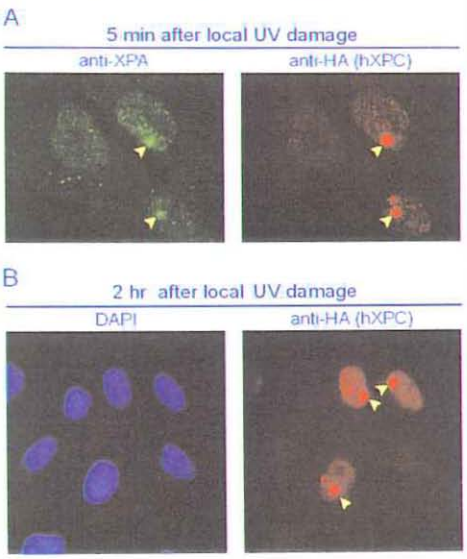

Figure 8. A novel mechanism of regulation of XPC and GG-NER by HR23 - striking parallels with *E.coli* SOS response - (p. 159).